Geochimica et Cosmochimica Acta

JOURNAL OF THE GEOCHEMICAL SOCIETY

UNIVERSITY OF HAWAII LIBRARY
OCT 27 1959

Executive Editors

C. W. CORRENS, *Göttingen.* E. INGERSON, *Austin, Texas.* L. R. WAGER, *Oxford.*

Editors

L. H. AHRENS, *Capetown.* S. R. NOCKOLDS, *Cambridge.* H. C. UREY, *La Jolla, Calif.*
JOHN VERHOOGEN, *Berkeley, Calif.* A. P. VINOGRADOV, *Moscow.*
W. A. WAHL, *Helsingfors.*

CONTENTS VOLUME 17, NOS. 1/2 AUGUST 1959

T. SUDO and M. MATSUOKA: Artificial crystallization of volcanic glass to sodalite and a zeolite structure . . . 1
M. ICHIKUNI: Une considération sur la formation de l'ion sulfate dans les eaux thermales . . . 6
R. J. W. MCLAUGHLIN: The geochemistry of some kaolinitic clays . . . 11
D. S. KORZHINSKII: The advancing wave of acidic components in ascending solutions and hydrothermal acid–base differentiation . . . 17
T. J. CHOW and C. C. PATTERSON: Lead isotopes in manganese nodules . . . 21
J. H. HOFFMAN and A. O. NIER: The cosmogenic He^3 and He^4 distribution in the meteorite Carbo . . . 32
K. K. TUREKIAN: The terrestrial economy of helium and argon . . . 37
H. HAMAGUCHI and R. KURODA: Silver content of igneous rocks . . . 44
D. S. COOMBS, A. J. ELLIS, W. S. FYFE and A. M. TAYLOR: The zeolite facies; with comments on the interpretation of hydrothermal syntheses . . . 53
G. ALLAIS et H. CURIEN: Mesure de la teneur en bore-10 des mineraux . . . 108
H. C. UREY and T. MAYEDA: The metallic particles of some chondrites . . . 113
W. D. EHMANN and J. R. HUIZENGA: Bismuth, thallium and mercury in stone meteorites by activation analysis . . . 125
M. V. WOODLAND: Data of rock analyses—VI. Periodical and serial literature of Scotland . . . 136

Letters to the Editor:

A. M. POMMER: Synthesis of häggite . . . 148
M. HONDA: Cosmogenic potassium-40 in iron meteorites . . . 148
A. J. COHEN: Moldavites and similar tektites from Georgia, U.S.A. . . . 150
H. FAUL, P. L. D. ELMORE and W. W. BRANNOCK: Age of the Fen carbonatite (Norway) and its relation to the intrusives of the Oslo region . . . 153
News and Notes . . . 157
Erratum . . . 158
Papers to be published in future issues . . . 159

QE 351
.4 25

PERGAMON PRESS NEW YORK • LONDON • PARIS • LOS ANGELES

GEOCHIMICA ET COSMOCHIMICA ACTA

EXECUTIVE EDITORS

PROF. C. W. CORRENS (1959) *Sedimentpetrographisches Institut der Universität, Lotzestr.* 13, *Göttingen, Germany*
PROF. E. INGERSON (1959–1960) *Department of Geology, University of Texas, Austin* 12, *Texas, U.S.A.*
PROF. L. R. WAGER, F.R.S. (1959–1961) *Department of Geology and Mineralogy, The University Museum, Oxford, England*

EDITORS

PROF. L. H. AHRENS (1959–1960) *Department of Chemistry, University of Capetown, Rondebosch, Cape Province, South Africa*
DR. S. R. NOCKOLDS (1959) *Department of Mineralogy and Petrology, The University, Cambridge, England*
PROF. H. C. UREY, For. Mem. R. S. (1959) *University of California, La Jolla, California, U.S.A.*
DR. JOHN VERHOOGEN (1959–1961) *Department of Geology, University of California, Berkeley, California, U.S.A.*
PROF. A. P. VINOGRADOV (1959–1961) *Vernadsky Institute, Moscow, U.S.S.R.*
PROF. W. A. WAHL (1959–1961) *Observatoriegaten* 8, *Helsingfors, Finland*

EDITORIAL ADVISORY BOARD

AMERICAN CONTINENT

A. F. BUDDINGTON, *Princeton*
D. GUIMÃRAES, *Belo Horizonte*
G. E. HUTCHINSON, *New Haven*
B. H. MASON, *New York*
F. WHIPPLE, *Cambridge*
R. WILDT, *New Haven*
H. S. YODER, *Washington*

EUROPE

T. F. W. BARTH, *Oslo*
L. CAPDECOMME, *Toulouse*
E. J. CONWAY, *Dublin*
P. ESKOLA, *Helsinki*
P. GALLITELLI, *Modena*
A. HADDING, *Lund*
O. HAHN, *Göttingen*
H. W. HARVEY, *Plymouth*
F. HEIDE, *Jena*
A. HOLMES, *Edinburgh*
W. Q. KENNEDY, *Leeds*
PH. H. KUENEN, *Gröningen*
S. LANDERGREN, *Stockholm*
F. MACHATSCHKI, *Vienna*
A. MUIR, *Harpenden*
J. ORCEL, *Paris*
E. RAGUIN, *Paris*
E. REINHARD, *Basle*
TH. G. SAHAMA, *Helsinki*
C. E. TILLEY, *Cambridge*
T. VOGT, *Trondheim*

FAR EAST

T. WATANABE, *Tokyo*

Publishing Office: Pergamon Press, Inc., 122 East 55th Street, New York 22, N.Y. (Plaza 3-9651)

Four issues per volume, three volumes per year

Subscription *per annum* (including postage) (A) $51.00; (B) For individual subscribers who write directly to the publisher certifying that the Journal is for their private use, $21.50. Members of the Geochemical Society, or non-members who occasionally publish papers in the Journal, $10.00 *per annum*.

Back numbers, $28.00 per volume

Single issues, $7.00 each

Copyright © 1959 Pergamon Press Ltd.

PERGAMON PRESS, INC.

122 EAST 55TH STREET, NEW YORK 22, N.Y. 4 & 5 FITZROY SQUARE, LONDON W.1

PRINTED IN NORTHERN IRELAND AT THE UNIVERSITIES PRESS, BELFAST.

Some PERGAMON PRESS titles in Geology and Geophysics

CLAYS AND CLAY MINERALS

Proceedings of the Sixth National Conference on Clays and Clay Minerals.
Edited by **Ada Swineford, Ph.D.,** *State Geological Survey, University of Kansas*

A most comprehensive source of information on recent advances in clay mineralogy, stress crystal structure of clay minerals, alteration of feldspars, clay mineralogy of soils, morphology of clay particles, water vapor sorption, and diageneses.

60s. net ($8.50)

Proceedings of the Seventh National Conference on Clays and Clay Minerals

In preparation

COALS AND BITUMENS and related fossil carbonaceous substances

Nomenclature and Classification

By **S. I. Tomkeieff, D.Sc., F.R.S.E., F.G.S.,** *University of Durham*

This book (the first of its kind) contains a glossary of terms relating to fossil carbonaceous substances, mainly coals and bitumens. The terms are arranged in two parts:

(a) An alphabetical glossary in which each term is concisely defined, giving, when possible, an etymological definition and references.

(b) Synoptic tables in which the terms are arranged in natural groups and sub-groups.

In this way the book acts as a two-way dictionary. Terms relating to similar substances, grouped together, provide an easy way of finding the required name if the meaning is approximately known. On the other hand, if the name is known the meaning can be found by consulting the alphabetical glossary. The introduction contains a simple and rational classification of fossil carbonaceous substances.

17s. 6d. net ($3)

ECONOMICS FOR THE MINERAL ENGINEER

By **Edmund J. Pryor,** *Royal School of Mines, Imperial College of Science and Technology, London*

Presents the basic principles of company administration and conventional accountancy to show the plant superintendent the overall pattern of organization; later chapters examine the philosophy and technique of mill control, and discuss the testing, building and working up of new plant. A glossary is provided defining the specialized words and phrases used in mining, mineral engineering and in the commercial minerals world. There is a good bibliography and appendices giving specimen illustrations of some common forms in which technical and financial information is circulated.

35s. net ($6)

ALLUVIAL PROSPECTING AND MINING

(Second Edition)

By **S. V. Griffith, A.C.S.M., M.I.M.M.,** *Institution of Mining and Metallurgy*

This is a revision and enlargement of the first edition which was used as a standard textbook by the Camborne School of Mines, Cornwall, and was recommended as a textbook for the Royal School of Mines.

In preparation

ORGANIC GEOCHEMISTRY

Edited by **Irving A. Breger**

This treatise will be the first undertaking in the field, and will assure a complete synthesis between the application of the principles of organic chemistry and geology. Contributions to this book are made by many well known and eminent people on the subject.

In preparation

Please write for fully descriptive leaflets

PERGAMON PRESS

LONDON NEW YORK PARIS LOS ANGELES

4 & 5 Fitzroy Square, London W.1. 122 East 55th Street, New York 22, N.Y.
24 Rue des Écoles, Paris Ve.

A Most Valuable Series of Journals

Annals of the International Geophysical Year

This series is the central record of the International Geophysical Year, and gives readers full information on this vast project. The complete series will indicate the inception, planning, preparations, programmes, progress and main results of the I.G.Y. Amongst the subjects covered will be weather, cosmic rays, glaciers, the form of the earth, natural and man-made radioactivity in the air and the seas, and earthquake waves in remote places.

Already published:

Volume I
- Part 1 - The First International Polar Year
- Part 2 - The Second International Polar Year
- Part 3 - The Inception and Development of the I.G.Y.

Volume IIA (Historical) - Contents;
- The First Meeting of the Special Committee for the I.G.Y. (Brussels)
- The Second Meeting of the Special Committee for the I.G.Y. (Rome)
- The Third Meeting of the Special Committee for the I.G.Y. (Brussels)
- The Fourth Meeting of the Special Committee for the I.G.Y. (Barcelona)

Volume III - Ionosphere

Volume IV
- Parts 1 to 3 - Nuclear Radiation Manual; Aurorae & Airglow; Longitude & Latitude
- Parts 4 to 7 - Manual on Geomagnetism, Parts 1 & 2; Seismology Observations; Cosmic Radiation Manual

Volume V
- Part 1 - Ozone
- Part 2 - Aurorae & Airglow

Volume VI - Manual on Rockets and Satellites

Volume VII - World Days and Communications; CSAGI Guides of World Data Centres

Volume VIII - Geographical Distribution of the I.G.Y. Stations

To be published shortly:

Volume IX - Programmes of Participating Nations

Volume IIB
- First CSAGI Antarctic Conference (Paris)
- Second CSAGI Antarctic Conference (Brussels)
- Third CSAGI Antarctic Conference (Paris)
- Fourth CSAGI Antarctic Conference (Paris)
- CSAGI Arctic Conference (Stockholm)
- CSAGI Western Hemisphere Regional Conference (Rio de Janeiro)
- CSAGI Eastern Europe Regional Conference (Moscow)
- Joint CSAGI/CSA Meeting for the I.G.Y. in Africa, South of the Sahara (Bukavu)
- CSAGI Western Pacific Regional Conference (Tokyo)
- CSAGI Working Group on Oceanography (Göteborg)
- CSAGI Working Group on Nuclear Radiation (Utrecht)
- I.G.Y. World Data Centres Meeting (Uccle)
- CSAGI Rockets and Satellites Conference (Washington, D.C.)

Subscription rates are £6 or $17 per volume

Orders should be placed with

PERGAMON PRESS

LONDON • NEW YORK • PARIS • LOS ANGELES

ORDER FORM

ANNALS OF THE INTERNATIONAL GEOPHYSICAL YEAR

To PERGAMON PRESS
4 & 5 Fitzroy Square, London W.1
or
122 East 55th Street, New York 22, N.Y.

I should like to place a standing order for all volumes of *The Annals of the International Geophysical Year*

Please send me.....copy/copies of each volume as published.

I enclose remittance value.....

Name .....

Address .....

.....

Geochimica et Cosmochimica Acta, 1959, Vol. 17, pp. 1 to 5. Pergamon Press Ltd. Printed in Northern Ireland

Artificial crystallization of volcanic glass to sodalite and a zeolite structure

T. Sudo and M. Matsuoka
Geological and Mineralogical Institute, Faculty of Science,
Tokyo University of Education, Tokyo, Japan

(*Received* 22 *October* 1958)

Abstract—By digesting glassy tuff with alkali solutions on the water-bath, the writers obtained sodalite and a zeolitic material. Studying in detail the products obtained by the reactions of glassy tuff with NaCl and NaOH solutions in various concentrations, the writers confirmed the conditions being favourable for crystallization of these materials. As a result of this, the writers further confirmed that the longer the tuff was warmed in more concentrated solutions, the more sodalite was produced, and crystallization of a zeolitic material is favourable in cases of lower concentrations of these solutions. NaOH solution seems to behave as a catalyst for the crystallization.

Introduction

In the course of the study on clay minerals in Japan, particularly on their colour-forming reactions, the writers noticed that a bluish-green colour-forming reaction easily occurs at room temperature and pressure when one drop of concentrated sodium sulphide solution was dropped on it. This fact led to a suggestion that the formation of such a bluish-green coloured material was related to that of ultramarine, and furthermore, to an anticipation that chemical reactions may occur easily at room temperature and pressure among volcanic glass and various salt solutions containing halogen, or sulphur, or sulphate ions, and they may result in forming sodalite, ultramarine and noselite etc.

This short paper purposes to communicate that the chemical reactions easily occur at room pressure and a temperature less than 100°C by digesting volcanic glass with NaOH and NaCl solutions.

We could notice a considerable number of earlier works; for example, Nagai (1936,1938) obtained base-exchanging permutite by attacking clay minerals with alkali solutions, and discussed permutite from the industrial points of view. Furthermore, many reports have been published concerning the hydrothermal synthesis of zeolites and other related materials. As is well known, the most useful industrial process of the synthesis of ultramarine is to treat metakaolin with alkali salts at a high temperature. The earlier works related to the synthesis of sodalite, ultramarine, zeolites and related materials are well introduced and discussed by Eitel (1954).

Experimental

The original specimen used for this study was selected among white coloured vitric tuff, which is found in widespread occurrence particularly in the north-eastern part of Japan. The chemical composition of the specimen collected from Fukaura-machi, Nishi-tsugaru-gun, Aomori Prefecture is as follows: SiO_2, 69·31 per cent; Al_2O_3, 12·10 per cent; Fe_2O_3, 2·17 per cent; FeO, 0·51 per cent; MgO,

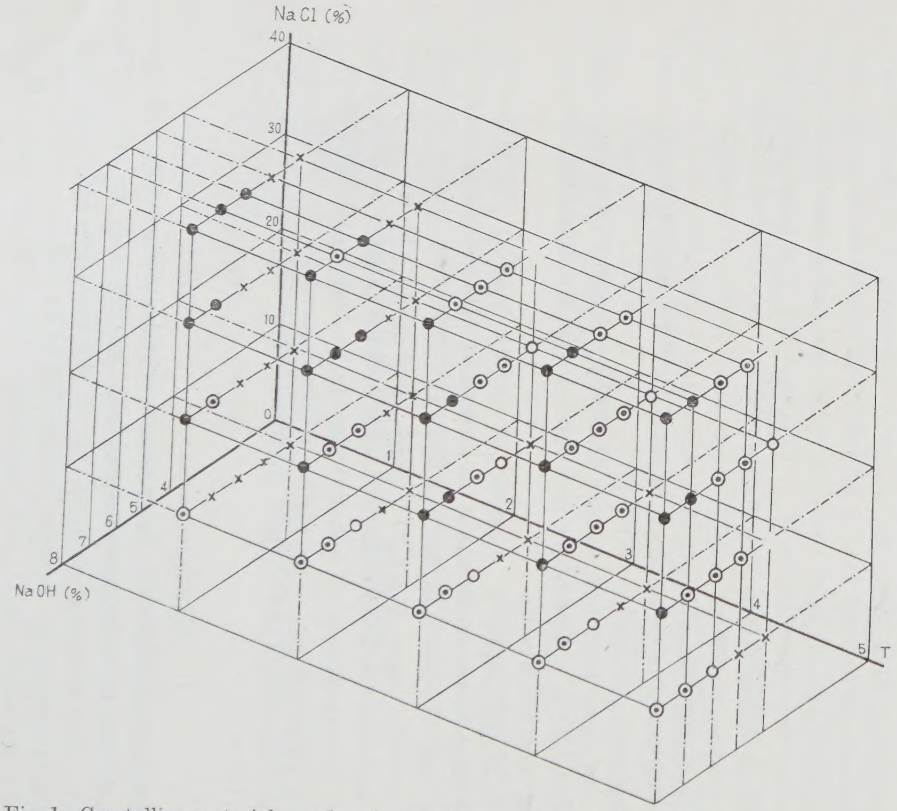

Fig. 1. Crystalline materials produced at various experimental conditions; ×: no crystalline material; ⊙: mixture of sodalite and a zeolite material; ●: sodalite; T, time (hr) for warming on the water-bath.

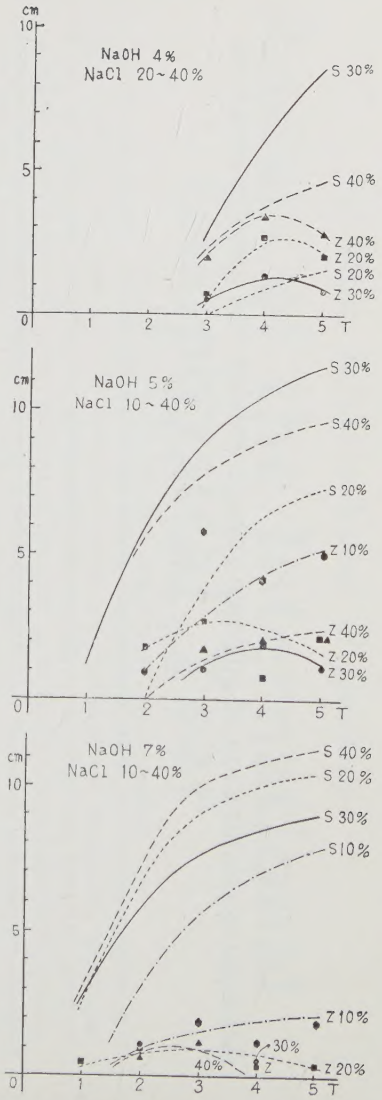

Fig. 2. Peak heights of X-ray reflections of sodalite and a zeolitic material and times (hr) for warming.

0·66 per cent; CaO, 0·45 per cent; Na_2O, 2·50 per cent; K_2O, 4·66 per cent; H_2O (+), 5·25 per cent; H_2O (−), 2·48 per cent; TiO_2, 0·25 per cent; P_2O_5, 0·04 per cent; MnO, 0·01 per cent; Total, 100·39 per cent. The microscopic observation revealed that it entirely consists of glassy fragments showing a low refractive index and a slight anisotropism. The latter optical behaviour along with its considerable content of water suggest that these fragments have effected a slight alteration. However, on the basis of its X-ray diffraction data, it can be said that

Table 1. X-ray powder diffraction data for sodalite (a) and a zeolite material (b)

(a)*		(b)†	
d (Å)	*I*	*d* (Å)	*I*
6·33	30	14·7	85
4·46	8	9·03	30
4·04	3	7·69	17
3·66	100	6·33	14
3·16‡	40	5·79	50
2·81	12	4·87	20
2·57	23	4·46	30
2·37	20	3·83	90
2·10	30	3·36	60
1·99	6	3·16‡	100
1·93‡	20	3·08	14
1·88	6	2·90	50
1·82	6	2·81	20
1·75	6	2·75	20
1·65‡	10	2·68	20
1·63	6	2·56	20
1·57	10	2·09	20
1·53	6	1·93‡	85
1·48	10	1·65‡	30
1·44	10	1·37	20
1·37	5		

* NaOH, 8%; NaCl, 40%; time for warming, 5 hr.
† NaOH 4%, NaCl, 30%; time for warming, 4 hr.
‡ Fluorite used for internal-standard.

this material is still amorphous showing only a very broad band between 3–4 Å, and its base exchange capacity is low: 10·31 me/100 g of a specimen dried at 105–110°C was obtained by the calcium acetate method in 18°C.

This specimen was pulverized to fine powder and was warmed on the water-bath together with NaCl and NaOH solutions of various concentrations during various hours. Evaporation was avoided by attaching cooling tubes. Violent stirring was also avoided except gentle stirring every 20 min. After warming for a definite hour, the residue was filtered off and washed by distilled water until salt solutions

were completely removed. The residue thus obtained was dried up at room temperature and was examined by X-ray diffractometer.

In the case when the specimen was warmed in NaCl solution only for 5 hr, the powder reflections of the residue was substantially unchanged. But in the case when NaCl solution was used along with NaOH solution, crystallization of the original specimen was very rapidly promoted. X-ray powder reflections of the

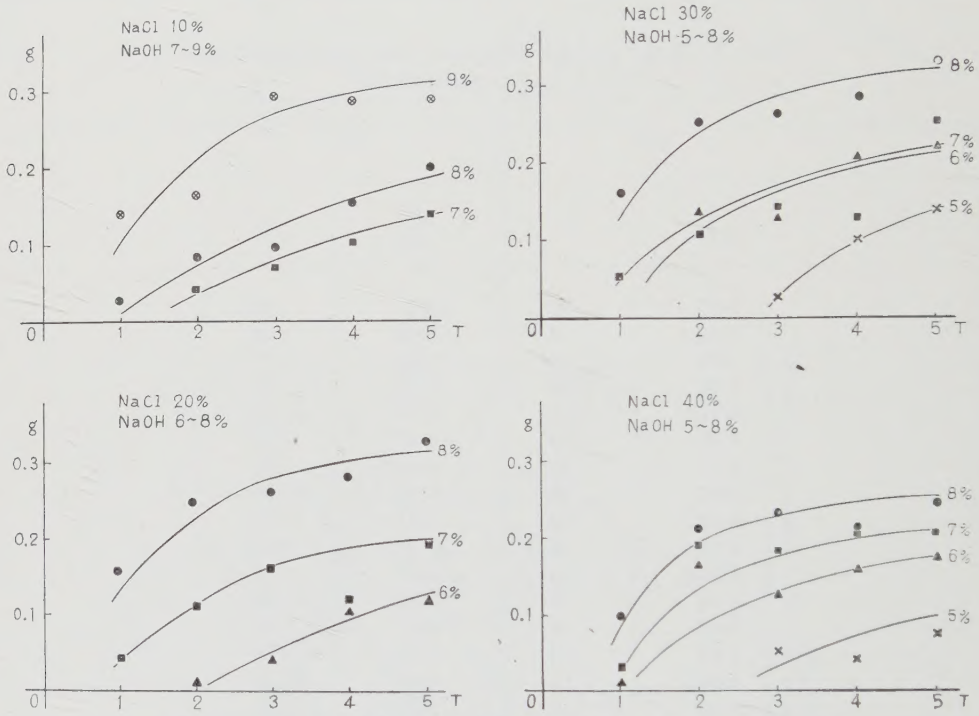

Fig. 3. Amounts of sodalite crystallized and times (hr) for warming (T).

crystalline materials are sharp and can be grouped into those agreeing with natural sodalite reflections (Table 1a), and those of an unknown material (Table 1b). The lattice constant of the sodalite was obtained as $a = 8{\cdot}93$ Å on the basis of the spacing of certain principal reflections. The unknown material may possibly be a zeolite because of its very high base exchange capacity as 198·83 me/100 g (the experimental conditions are the same as in the case of the original specimen). But we could not find out earlier X-ray data for natural zeolites agreeing with those of this unknown material; the X-ray powder reflections of mordenite–ptilolite are near to those of the material now in question, but good agreement has never been shown between these data.

On the basis of confirmation of some characteristic powder reflections of these crystalline materials in the residue, the conditions of the formation of these materials can be illustrated as in Fig. 1. The conditions were denoted by three factors as hours for warming (T, 1–5 hr), concentrations of NaCl solutions (N_1, 10–40%) and of NaOH solutions (N_2, 5–8%). A zeolite was obtained only in the

conditions of small values of T, N_1, N_2. Sodalite was usually obtained in the conditions of large values of T, N_1 and N_2. In the conditions of intermediate ranges, both of these materials were produced.

On the basis of the peak heights of some characteristic powder reflections of these materials, rise and fall of these peak heights shown along with the changes of the conditions were examined (Fig. 2). In the conditions represented by certain definite values of N_1 and N_2 and various hours, the amounts of both of these materials increase in the initial stage, but on passing time the amount of a zeolitic material attains its maximum and gradually decreases in spite of the amount of sodalite still increasing progressively. The larger the concentrations of NaCl and NaOH solutions, the larger the ratio of the peak of sodalite with that of the zeolitic material.

The amount of sodalite was estimated by using fluorite as internal-standard, and the relationship between the amount of sodalite produced with hours for warming is shown in Fig. 3. As shown in this Figure, in the range of small values of N_1 and N_2, the amount of sodalite produced increases in linear relationship against time-change. But in the range of large values of N_1 and N_2, the inclination of the curve is steep in the initial stage, but it grades into a curve with a gentle slope in the successive stage. In general, the larger the values of N_1 and N_2 the steeper the slope of the curve in the initial stage, and the more gentle the slope in the successive stage. This experiment suggests that NaOH seems to behave as a catalyst in the course of crystallization of volcanic glass; probably, it may take an important role to break the network linking of Si(Al)-oxygen in volcanic glass and facilitate the rearrangement of atoms toward new crystalline materials.

Acknowledgements—The writers are greatly indebted to O. Nagashima for supplying a valuable specimen, and Dr. T. Harada and T. Yumoto of the National Institute for Agricultural Science, Tokyo for measuring carefully the base exchange capacities.

References

Nagai S. (1936) *J. Soc. Chem. Ind., Japan* **39,** 252–254.
Nagai S. (1938) *J. Jap. Ceram. Ass.* **46,** 77–83.
Eitel W. (1954) *The Physical Chemistry of the Silicates.* University of Chicago Press.

Geochimica et Cosmochimica Acta, 1959, Vol. 17, pp. 6 to 10. Pergamon Press Ltd. Printed in Northern Ireland

Une considération sur la formation de l'ion sulfate dans les eaux thermales

M. Ichikuni
Laboratoire de chimie, Faculté des Sciences, Université Métropolitaine de Tokio

(*Received* 2 *January* 1959)

Résumé—Etant donné qu'on peut exprimer la concentration de tout composant se trouvant dans les eaux des sources principales de Tamagawa, Japon, sous forme de $a\,[Cl^-] + b\,[SO_4^{2-}]$, on arrive à constater l'indépendance de l'ion chlorure et de l'ion sulfate. Ainsi, on peut assurer au moins trois sortes d'eau qui constitue ces sources: l'une, origine magmatique, contenant de l'acide chlorhydrique, de l'hydrogène sulfuré, de l'anhydride sulfureux, mais pas de sulfate; la deuxième, une eau contenant de l'acide sulfurique, dont la formation est due à l'oxydation de certains composés de soufre qui a lieu dans un endroit peu profond dans la terre; la troisième, une eau souterraine qui contribue simplement à la dilution des eaux acides.

Introduction

La majeure partie de sources thermales acides au Japon contient de l'ion chlorure et de l'ion sulfate comme anions principaux. Cependant on trouve souvent des sources acides dont l'anion consiste presque entièrement en ion sulfate. On attribue leur formation à l'oxydation de l'hydrogène sulfuré et de l'anhydride sulfureux contenus dans un gaz d'origine magmatique, provenant de l'activité volcanique ou thermale, par l'oxygène entrainé par les eaux souterraines. C'est ainsi qu'après la formation de l'acide sulfurique ces eaux émergent à la surface de la terre.

La présence de ces deux sortes de sources acides à la station thermale de Tamagawa, département d'Akita, Japon, nous intéresse énormément. Le long d'un ruisseau, on trouve en bas des sources contenant de l'ion chlorure et de l'ion sulfate, tandis qu'en amont d'elles des fumaroles et des sources acides dont les eaux sont exemptes de chlorure. Noguchi (1952) a supposé que les sources exemptes de chlorure puissent se former par le mécanisme mentionné ci-dessus, et que les autres soient formées par la pénétration du gaz ascendant, d'origine magmatique, dans une eau acide sulfurique d'origine superficielle.

Mais ce n'est qu'une hypothèse admise par la présence des deux sortes de sources, et on ne trouve pas jusqu'ici des preuves méritant notre attention. On ignore encore au cours de quel processus l'ion sulfate a été formé. L'auteur du présent rapport va mettre en évidence le processus de sa formation à l'aide des résultats obtenus par de différents chercheurs et de ceux d'analyse de quelques composants effectuée par lui-même.

Resultats Sommaires des Essais Effectues Jusqu'a Present

Ayant effectué le dosage du gaz spontané de la Grande Source de Tamagawa, Oana (1954) a donné le résultat en Tableau 1.

Tableau 1. Composition du gaz spontané de la Grande Source

Gaz	(% v/v)
H_2S	61,2
SO_2	12,9
CO_2	7,1
O_2	3,8
N_2	15,0

D'après lui, l'azote a été contenu dans les eaux souterraines participant à la formation de la source.

Miura (1956) a nié l'existence de l'oxygène libre en profondeur dans la terre, car celui réagit sur l'hydrogène sulfuré immédiatement à une température supérieure à 200°C. Il a donc attribué l'origine de l'oxygène aux eaux souterraines. Ayant effectué des expériences à son laboratoire, il a montré que la réaction de l'hydrogène sulfuré avec l'oxygène ne donne que le soufre libre en présence du fer, et que la formation de l'acide sulfurique par cette réaction est peu possible, étant donné que la vitesse de réaction de formation de l'acide est extrêmement lente.

Un résultat très intéressant a été obtenu par Sakai (1957) qui a effectué la mesure du rapport isotopique S^{34}/S^{32} dans l'ion sulfate. Il a conclu que l'ion sulfate contenu dans les eaux de Tamagawa s'est formé à la température de 75 à 140°C, et qu'il n'est pas d'origine magmatique.

Les eaux de ces sources étant bouillantes à leur émergence, on pourrait atteindre la température indiquée par Sakai à un endroit peu profond dans la terre. Ce fait souligne que l'oxydation de l'anhydride sulfureux ou d'autres composés de soufre en acide sulfurique a lieu dans une zone superficielle de la terre.

Cependant on n'arrive pas avec ces résultats à différer si l'oxydation d'eux en acide a lieu avec leur séparation d'avec le gaz d'origine magmatique ou sans leur séparation.

D'après l'analyse de quelques composants sur les eaux de la Grande Source et d'autres sources voisines, effectuée par Noguchi (1952), le rapport Cl^-/SO_4^{2-} montre une petite variation d'une source à l'autre. Cette variation de composition a donné à l'auteur du présent rapport l'idée de poursuivre des relations des deux anions avec d'autres composants. Cette étude a ouvert la voie pour la solution du problème.

Interpretation du Resultat d'Analyse

Le Tableau 2 montre le résultat d'analyse des eaux de la Grande Source et des sept sources voisines. Ces sources sont déjà numérotées par Noguchi, et la source A_1 se rapporte à la Grande Source.

En utilisant ces chiffres, on calcule quelques rapports dont le Tableau 3 montre le résultat.

On peut considérer la valeur HBO_2/Cl^- identique pour toutes les sources. De

ce fait on conclut que l'acide borique se comporte de la même façon que l'ion chlorure et qu'ils sont fournis de la même origine.

La valeur Acidité/($Cl^- + SO_4^{2-}$) est d'autant plus petite que celle de Cl^-/SO_4^{2-} est plus petite. Ce résultat n'affirme pas la formation de l'ion sulfate au cours

Tableau 2. Résultat d'analyse des eaux de Tamagawa

Sources	Cl^- (mé/l.)	SO_4^{2-} (mé/l.)	HBO^2 (m-mol/l.)	Acidité (mé/l.)	K^+ (mé/l.)
A_1	71,2	21,1	2,46	65,7	1,38
A_2	82,1	25,7	2,84	76,4	1,64
A_3	81,6	25,7	2,80	75,7	1,63
A_4	87,6	26,5	3,03	81,2	1,74
A_5	83,0	25,9	2,90	76,8	1,68
A_6	88,4	27,5	3,05	81,7	1,77
A_7	76,0	23.2	2,59	70,1	1,54
A_8	74,7	24,7	2,58	69,4	1,55

de l'ascension des eaux souterraines imprégnées du gaz d'origine magmatique, car l'acidité des eaux doit augmenter avec la diminution du rapport Cl^-/SO_4^{2-}, l'oxydation de composés de soufre en sulfate donnant l'acide sulfurique.

En ce qui concerne la valeur $K^+/Cl^- + SO_4^{2-}$, elle est d'autant plus grande que le rapport Cl^-/SO_4^{2-} est plus petit.

Tableau 3. Calcul de quelques rapports

Sources	$\frac{Cl^-}{SO_4^{2-}}$	$\frac{HBO_2}{Cl^-}$	$\frac{\text{Acidité}}{Cl^- + SO_4^{2-}}$	$\frac{K^+}{Cl^- + SO_4^{2-}}$
		($\times 10^{-2}$)		($\times 10^{-2}$)
A_1	3,37	3,46	0,712	1,50
A_2	3,20	3,45	0,708	1,52
A_3	3,18	3,43	0,706	1,52
A_4	3,31	3,46	0,710	1,53
A_5	3,20	3,50	0,706	1,54
A_6	3,21	3,46	0,706	1,53
A_7	3,28	3,41	0,708	1,55
A_8	3,02	3,47	0,698	1,56

La régularité existant entre ces valeurs a fait essayer à l'auteur d'exprimer la concentration d'acidité et de potassium en fonction de $[Cl^-]$ et de $[SO_4^{2-}]$. Il a examiné une équation de combinaison linéaire, c'est-à-dire celle représentée sous forme de $a[Cl^-] + b[SO_4^{2-}]$, où a, b sont constantes valables pour toutes les

sources. Elles sont calculées par la méthode des moindres carrés. On obtient ainsi deux équations suivantes:

$$[\text{Acidité}] = 0{,}865[Cl^-] + 0{,}198[SO_4^{2-}]$$

$$[K^+] = 0{,}0103[Cl^-] + 0{,}0314[SO_4^{2-}]$$

où la concentration s'exprime en mé/l.

En introduisant la valeur trouvée de $[Cl^-]$ et de $[SO_4^{2-}]$, on trouve la valeur calculée d'acidité et de potassium qui colle bien avec leur valeur trouvée dont le Tableau 4 est témoin. Il n'y aurait donc aucune contradiction d'exprimer tout composant en fonction de combinaison linéaire de $[Cl^-]$ et de $[SO_4^{2-}]$.

Tableau 4. Comparaison de la valeur calculée avec la valeur trouvée

Sources	Acidité			Potassium		
	Calculée	Trouvée (mé/l.)	Dif.	Calculé	Trouvé (mé/l.)	Dif.
A_1	65,7	65,7	0,0	1,36	1,38	−0,02
A_2	76,1	76,4	−0,3	1,65	1,64	+0,01
A_3	75,8	75,7	+0,1	1,65	1,63	+0,02
A_4	81,1	81,2	−0,1	1,74	1,74	0,00
A_5	76,9	76,8	+0,1	1,67	1,68	−0,01
A_6	81,9	81,7	+0,2	1,78	1,77	+0,01
A_7	70,3	70,1	+0,2	1,51	1,54	−0,03
A_8	69,3	69,4	−0,1	1,55	1,55	0,00

Pour que tout composant soit représenté par l'équation indiquée ci-dessus, il est nécessaire que l'ion chlorure et l'ion sulfate soient indépendants l'un de l'autre. Cela veut dire que le véhicule de l'ion chlorure n'accompagne pas d'ion sulfate et celui de l'ion sulfate est exempt d'ion chlorure.

L'hypothèse proposée par Noguchi semble favorable pour expliquer ce résultat.

Conclusion

Voici un mécanisme de formation de l'ion sulfate qui conviendra d'éclaircir tous les résultats d'études effectuées à ce sujet: tout d'abord, la séparation de l'hydrogène sulfuré et de l'anhydride sulfureux d'avec le gaz ascendant d'origine magmatique a lieu dans endroit peu profond, le gaz garde pourtant l'acide chlorhydrique et l'acide borique et probablement une partie d'hydrogène sulfuré et d'anhydride sulfureux. L'hydrogène sulfuré et l'anhydride sulfureux séparés sont oxydés en acide sulfurique après leur pénétration dans les eaux souterraines accompagnant de l'oxygène. Ainsi s'explique la formation des eaux acides exemptes de chlorure, d'origine superficielle. Leur minéralisation sera généralement faible, étant donné que leur durée de contact avec les roches n'est pas très longue. Ensuite le gaz d'origine magmatique se mélange avec ces eaux acides formées comme il a été dit. Il faut encore prendre en considération des eaux souterraines de caractère normal qui participent à la dilution de la solution acide.

Ce n'est qu'un exemple de mécanisme de formation de l'ion sulfate dans les eaux thermales et il va sans dire que ce mécanisme ne s'applique pas toujours à d'autres sources.

Remerciements—L'auteur exprime ses remerciements sincères à Monsieur le professeur Noguchi qui lui a donné l'idée de cette étude et à Monsieur le professeur Hanya qui a bien voulu donner des conseils au cours de l'exécution de ce travail. Il remercie également Monsieur le docteur Saijo dont le concours amical ne lui a jamais manqué.

Bibliographie

Miura H. (1956) Vitesse de réaction de H_2S sur O_2 dans les eaux de Shibukuro. *J. Chem. Soc. Japan, Pure Chem. Sec.* **77**, 417.

Noguchi K. (1952) Etudes chimiques sur les eaux de la station thermale de Tamagawa. *Assembl. Soc. Chim. Japon, Séct. Géochim.*

Oana S. (1954) Teneur en hydrogène sulfuré des eaux de Tamagawa. *Rapp. Commém. 10e Annivers. Ass. Etudes Station, Tamagawa.*

Sakai H. (1957) Fractionation of sulphur isotopes in nature. *Geochim. et Cosmochim. Acta* **12**, 150.

Geochimica et Cosmochimica Acta, 1959, Vol. 17, pp. 11 to 16. Pergamon Press Ltd. Printed in Northern Ireland

The geochemistry of some kaolinitic clays

R. J. W. McLaughlin
Geology Department, University of Melbourne, Australia

(*Received* 15 *January* 1959)

Abstract—The major and minor elements of ten kaolinitic clays (kandites) are traced through the various size-fractions (sand, silt and clay). The minerals considered range from dickite through kaolinite to halloysite with also an example of *b*-disordered kaolinite.

Samples ranging from those containing the well crystallized and crystallographically-ordered mineral dickite, through kaolinite and a *b*-disordered kaolinite to halloysite, the least ordered member of the group, have been analysed from the following localities:

Dickite, from South of Ouray, Colorado, U.S.A., on U.S. 550, near Red Mountain pass. (no. 14 of American Petroleum Institute, reference clay samples, Project 49 (Kerr, 1951)).
Dickite, from Bull valley, Washington Co., 40 miles NW of St. George, Utah, U.S.A. (no. 16 of A.P.I., Project 49).
Kaolinite, from Twin Knobs, Murfreesboro, Pike Co., Arkansas, U.S.A. (no. 1 of A.P.I., Project 49).
Kaolinite, from O'Neal pit, 8·8 miles SE Macon railway station, Georgia, U.S.A. (no. 4 of A.P.I., Project 49).
Kaolinite, from W slope of Canada de Camino on Mesaalta, 5 miles NW of Coyote, New Mexico, U.S.A. (no. 9 of A.P.I., Project 49).
Kaolinite, from Carpalla, St. Austell, Cornwall, England.
Kaolinite, from the Pugu Hills, west of Dar-es-Salaam, Tanganyika. (Pugu D. of Robertson, Brindley and MacKenzie (1954)).
Kaolinite, fireclay from Torwood, near Lambert, Stirlingshire, Scotland.
Halloysite, from Huron, S.W. Lawrence Co., Indiana, U.S.A. (no. 12 of A.P.I., Project 49).
Halloysite, from Agnew's Hill, near Larne, Antrim Co., Northern Ireland.

Nacrite, the most highly ordered mineral of the kaolin group, was not investigated owing to the difficulty in obtaining the quantities required in sufficient purity. The $<2\ \mu$ equivalent spherical diameter (e.s.d.) fraction of the dickite samples was not investigated because of the difficulty in obtaining sufficient of this fine grain size for analysis (these dickites both lie largely between 2–20 μ e.s.d.)

The samples were separated into their various fractions after a preliminary treatment with hydrogen peroxide to destroy traces of organic matter. The dispersant used was sodium hexametaphosphate. Separation of sand fraction, $>20\ \mu$ e.s.d., was gravitational; silt, 2 μ–20 μ e.s.d., and clay $<2\ \mu$ e.s.d., were separated by centrifugal means. All samples were thoroughly washed with

Table 1. Major and minor elements (p.p.m.) present

Element	Dickite, Colorado		Dickite, Utah		Kaolinite, Arkansas			Kaolinite, Georgia			Kaolinite, New Mexico		
	Sand	Silt	Sand	Silt	Sand	Silt	Clay	Sand	Silt	Clay	Sand	Silt	Clay
$Si^{4+} \times 10^2$	2319	2124	2129	2132	2489	2221	2080	1923	2122	2113	2198	2340	2076
$Al^{3+} \times 10^2$	1914	1998	2117	2088	1635	2019	2095	*	2065	2015	2022	1916	2103
$Ti^{4+} \times 10^2$	23	11	9	1	54	40	53	*	69	88	32	29	44
$Fe^{3+} \times 10^2$	54	27	17	17	140	52	62	*	74	43	27	57	62
$Mg^{2+} \times 10^2$	28	68	32	60	72	8	13	30	17	22	18	12	11
$Mn^{2+} \times 10^2$	—	—	—	—	—	—	—	—	—	—	—	—	—
$Na^{1+} \times 10^2$	3·2	13	3·7	1·4	15	3·6	2·1	7·2	2·1	2·1	2·6	3·4	2·1
$Ca^{2+} \times 10^2$	47	7	26	10	134	27	27	250	31	16	29	20	17
$K^{1+} \times 10^2$	8·4	28	6·4	4·8	24	14·2	8·4	76	12	6·8	6	9·6	6·4
Ga^{3+}	10	15	—	—	—	7	7	15	7	7	15	7	7
Cr^{3+}	45	45	18	18	10	18	5	100	45	100	4	45	10
V^{3+}	50	95	95	95	10	22	50	95	95	100	22	10	22
Sn^{4+}	—	10	—	—	—	—	—	—	—	10	—	—	30
Li^{1+}	2	—	3	2	2	3	3	40	40	40	6	12	12
Ni^{2+}	22	—	5	—	10	6	6	32	10	10	5	5	—
Co^{2+}	—	—	5	—	—	—	—	—	—	—	—	—	—
Zr^{4+}	10	—	10	—	350	180	350	>1000	20	10	180	45	160
Y^{3+}	—	—	—	—	30	30	55	100	—	—	30	17	30
La^{3+}	—	—	—	—	220	180	320	—	—	—	—	—	—
Sr^{2+}	—	—	20	10	17	20	20	15	—	15	—	—	—
Pb^{2+}	—	100	—	—	30	50	50	100	—	30	—	—	—
Ba^{2+}	650	100	32	—	100	40	32	100	5	5	—	5	—
Rb^{+}	—	—	—	—	—	—	—	—	—	—	—	—	—
Ag^{+}	—	—	*T*	*T*	—	—	—	—	—	—	—	—	—
Si/Al	1·21	1·06	1·01	1·02	1·52	1·10	0·99	*	1·03	1·05	1·09	1·22	0·987
Al/Fe	35·4	74·0	124·4	122·8	11·7	38·8	33·8	*	27·9	46·8	74·9	33·6	33·9
K + Na × 1000/Al	6·07	20·5	4·78	2·97	23·8	8·82	5·02	*	6·83	4·42	4·26	6·80	4·05
K/Na	2·62	2·15	1·73	3·43	1·60	3·94	4·0	10·6	5·72	3·24	2·31	2·82	3·05

distilled water before drying with alcohol and acetone. The results of the analyses are presented in Table 1.

Discussion

Because of the rigorous pre treatment of the various fractions, explanation of any concentration of elements as due to base-exchange or absorption phenomena is precluded. This facet of the geochemistry of these kaolin minerals is therefore not discussed.

The ideal formulae for kaolinite gives $Si^{4+} = 21{\cdot}75$ per cent and $Al^{3+} = 20{\cdot}90$ per cent, with $Si/Al = 1{\cdot}041$. The ideal lattice should contain no extraneous elements (except, of course, hydrogen and oxygen) but such ideal lattices are never realized in nature. The figures in Table 1 show the degree of purity and substitution within the lattice. Thus silicon and aluminium are, generally speaking,

in various size fractions of ten kaolin minerals

Kaolinite, Cornwall			Kaolinite, Stirlingshire			Kaolinite, Tanganyika			Halloysite, Indiana			Halloysite, N. Ireland			S	A
Sand	Silt	Clay	Sand	Silt	Clay	Sand	Silt	Clay	Sand	Silt	Clay	Sand	Silt	Clay		
3711	2312	2310	1972	2031	1626	4582	3865	2074	1848	2037	2012	3493	3628	2242		0·42
639	2056	2067	1990	1797	1692	85	493	2011	1969	2026	2151	897	1733	1868		0·51
19	66	7	19	100	63	14	228	104	69	1	3	36	28	48		0·68
166	5	50	50	188	159	7	57	112	218	8	18	60	70	73		0·64
17	11	13	37	35	24	6	29	12	10	39	4	7	52	11		0·66
—	0·8	0·3	—	—	—	—	—	—	—	—	—	—	I	—		0·80
7·2	65	2·5	12·9	6·2	6·4	4	6	6	11	3·9	2·4	11·6	12	3·6		0·97
37	16	9	36	226*	76	6	69	29	50	6	39	36	20	34		0·99
174	139	64	27·7	29·2	27·7	9·2	20·4	51·8	4·4	5·6	4·9	18·2	6	4·4		1·33
7	7	7	5	7	7	—	—	7	—	—	—	7	5	7	2	0·62
—	—	—	100	120	100	2	70	180	2	2	2	18	5	18	2	0·63
—	—	—	55	110	95	—	50	10	—	—	—	10	22	50	5	0·74
10	10	30	—	—	10	—	—	30	—	—	10	—	—	10	10	0·71
220	65	10	40	100	50	—	2	12	—	—	—	12	12	3	1	0·68
—	—	4	22	50	50	—	50	10	100	100	100	12	10	10	2	0·69
—	—	—	5	10	10	—	—	—	—	—	—	—	—	—	5	0·72
20	20	10	10	45	20	220	>1000	10	—	—	—	>1000	220	60	10	0·79
10	12	17	17	30	17	—	100	—	—	—	—	17	15	10	10	0·92
—	—	—	—	—	—	—	—	—	—	—	—	—	—	—	30	1·14
—	50	80	—	50	220	—	20	50	—	—	—	—	—	—	10	1·12
—	30	65	—	30	30	—	—	65	—	—	30	—	—	30	10	1·20
—	100	300	32	100	300	5	300	5	300	300	32	100	32	100	5	1·34
700	320	140	—	—	—	—	—	—	—	—	—	—	—	—	30	1·47
—	—	—	—	—	—	—	—	—	—	—	—	—	—	—	1	1·26
5·80	1·13	1·12	0·991	1·13	0·96	53·9	7·85	1·03	0·939	1·01	0·936	3·89	2·09	1·20		
3·86	411·2	41·3	39·8	9·56	10·6	12·1	8·67	17·9	9·03	253·3	119·5	14·6	24·9	25·6		
283	99·4	32·2	20·4	19·7	20·2	155	53·5	28·8	7·83	4·68	3·40	33·2	10·4	4·28		
24·2	2·14	25·6	2·15	4·72	4·32	2·30	3·4	8·63	0·40	1·44	2·04	1·57	0·5	1·22		

Size fractions are Sand >20 μ, Silt 2–20 μ, Clay <2 μ. S = Sensitivity. A = Ionic size in angstrom units. All values except ratios are in p.p.m. with major elements $\times 10^2$. * = absence of data. — = below sensitivity. T = Trace. Be^{2+}, $S = 30$; Mo^{4+}, $S = 2$; Cs^{1+}, $S = 15$; Sc^{3+}, $S = 8$ are all below sensitivity.

inversely sympathetic, the general trend being to increase the latter in the finer grain size, a demonstration of increase in purity of this finer fraction. The Si/Al ratios demonstrate this purification but also bring out another interesting facet, namely, that there is in many cases considerable excess of aluminium over that required for the theoretical lattice. The low value for the Indiana halloysite is due to the presence of gibbsite, as also is perhaps that for the Pugu kaolinite. Highly aluminous minerals have not been found, however, in the other samples and the explanation for Utah dickite, Torwood kaolinite, New Mexico kaolinite and Arkansas kaolinite must be looked for elsewhere. All of these are similar in either having very small crystals or irregular crystal outlines, as shown by electron

micrographs. As no highly aluminous materials could be found in these specimens (as judged by X-ray analysis), the only conclusion is that the excess aluminium is either amorphous or within the lattice. Amorphous alumina could well explain all except Arkansas kaolinite, for the ragged crystal outlines of the remainder would point to perhaps some removal of material by leaching. Although Arkansas kaolinite has perfect crystal shape, there is evidence of leaching, for the zirconium and titanium are concentrated in both the sand and clay fraction with a minima in the silt fraction. This points to solution of these latter two elements, presumably originally concentrated in the coarser fraction. On solution they would almost immediately precipitate and, of necessity, would concentrate about the finer particles, for these finer particles would have a stronger adsorption potential. Furthermore, if the excess aluminium were within the lattice, then it must be present subsituted for silicon. Unless substitution occurs of magnesium or lithium for aluminium, then there would be a resultant charge on the lattice which, to maintain electrostatic neutrality, would demand entry of potassium between the sheets in a fashion similar to that obtaining in micas. There is no sympathetic variation of any of these elements to the extent demanded by such an hypothesis, and therefore it would seem that in all cases the excess aluminium is amorphous.

In the case of the other major elements: iron and titanium vary sympathetically and are therefore presumably associated together either as amorphous oxide or as ilmenite. Magnesium and iron do not bear any apparent relation, nor does magnesium seem related to titanium. The trends of the alkalis and calcium are similar, decreasing with finer grain-size, but they do not bear any apparent relation to the other major elements.

Amongst the minor elements there is parallel behaviour in trend between chromium, vanadium, zirconium, yttrium and titanium. The former two are believed to be concentrated in the ferro-titaniferous complex and the Zr and Y in the mineral zircon (except in cases where leaching and precipitation has occurred). Lithium and nickel generally tend to follow the behaviour of magnesium.

The $K + Na \times 1000/Al$ ratios illustrate the increase in purity of the fine fraction. Such ratios are usually used as leaching factors, whereas here they demonstrate the lowering of felspathic and sericitic impurity in the finer fractions and its concentration in the coarser fractions. Thus the ratios generally fall as the grain size becomes finer.

The K/Na ratios demonstrate the rise in potassium, relative to sodium, of the finer grained material. Since base-exchange phenomena have been excluded by the pre-treatment, this must illustrate that even in the finest fractions some sericitic material is present.

In many samples there are exhibited maxima and minima of concentrations in the silt fraction. The elements which illustrate this point to the best advantage are, perhaps, titanium and zirconium, and to a lesser extent iron. This type of concentration has been also observed in soil clays (McLaughlin, 1955) and is believed to illustrate concentrations of heavy minerals (ilmenite and zircon) and also recrystallization. Thus, if considerable comminution has taken place prior to deposition then concentration of heavy minerals is more likely in the silt fraction. Should there be continued leaching of material, especially by solutions rich in

organic matter, then ilmenite and zircon are slowly dissolved but almost immediately precipitated again, first as hydrated oxide and later, on ageing, this alters to the very insoluble oxide. Concentrations effected by this means are in the finest fractions, as in Arkansas and New Mexico specimens (kaolinite–mineral).

The high contents of alkali in the Carpalla, St. Austell, specimen (containing kaolinite) is reflected also in the high lithium and rubidium content. This is due to the presence of considerable amounts of micaceous material which persists even into the finest fraction.

The concentration of zirconium in the silt fraction of the Pugu specimen (contains disordered kaolinite mineral) is due to the very fine nature of the zircon and has been commented on elsewhere (McLaughlin, 1957). The only sample in which lanthanum was detected was the Arkansas specimen. The source is presumably associated with the zirconium in view of the known close geochemical association of this element with yttrium. There is sympathetic variation between all three of these elements, and it is interesting to note that the yttrium : lanthanum ratio remains almost constant throughout the three fractions.

The concentrations of barium observed in the Torwood specimen (kaolinite–mineral) and Indiana specimen (containing halloysite) are believed to be due to precipitation of barium sulphate, for in the former there is present organic matter and some pyrite, while in the latter alunite has been recorded by the A.P.I. Project (1951).

It is difficult on so few samples to be dogmatic about any marked geochemical differences which are dependent upon the degree of lattice order. There are, however, definite trends which are apparent, and generally titanium, sodium, potassium, lithium, zirconium, yttrium and strontium are lower in the dickite-bearing specimens than in either the kaolinite- or halloysite-bearing materials. On the other hand magnesium, lead and barium seem higher in dickite containing specimens than the less ordered members of the group. When the origin of the minerals is considered these variations are explicable. The dickites have arisen from hydrothermal alteration whereas the remainder are sedimentary (except Carpella kaolinite). The higher lead and barium are due directly to the hydrothermal origin, the lead from associated galena veins and the barium from precipitation of the insoluble sulphate. The lower titanium, zirconium and yttrium in dickites is a reflection on the efficiency of sedimentary processes in concentrating these elements in minerals such as ilmenite and zircon, thus the kaolinite bearing specimens are higher in these elements. The lower sodium, potassium, lithium and strontium in the dickite-containing specimens is more difficult to explain, for in both dickite and kaolinite material there is known to be sericitic impurity. It may be that this lower concentration is related to the degree of substitution within the lattice, for the ordered dickite would, being more ordered, be expected to provide small opportunity for any silicon–aluminium replacement, or the resultant strains might well produce disorder. On the other hand this type of postulation is directly contrary to all the evidence adduced in alumino-silicates of larger size-ranges, where it is found that during formation a rise in temperature favours aluminium for silicon substitution and the dickites, being of hydrothermal origin, were certainly probably crystallized at a higher temperature than the kaolinites.

Perhaps the reason lies in relative rate of crystal growth. The dickites, in their hydrothermal environment, could grow and also undergo some re-solution of any extraneous elements laid down with the lattice. The kaolinites, however, would tend to form by precipitation and there would be very little re-solution. Under these latter conditions other extraneous elements could be held within the lattice when the kaolinite structure is finally built.

The halloysite-containing specimens do not seem to display any marked dissimilarity from the kaolinite material, except in perhaps a lower trend in chromium and slightly lower titanium content. This is presumably an effect of sorting during sedimentation.

It will be seen, therefore, that in any geochemical description of kaolin minerals the elements which seem to reveal most of the history of a deposit are titanium and zirconium. Thus by a study of these two and their partition amongst various grain sizes, not only can some estimate of the type of conditions operative during formation be arrived at, but also some idea of the subsequent history as far as leaching and recrystallization is concerned.

References

Kerr P. F. (Editor) (1951) *Reference Clay Minerals.* Research Project 49, American Petroleum Institute.

McLaughlin R. J. W. (1955) *Geochim. et Cosmochim. Acta* **8,** 109–130.

McLaughlin R. J. W. (1957) *Clay Min. Bull.* **3,** 184–88.

Robertson R. H. S., Brindley G. W. and Mackenzie R. C. (1954) *Amer. Min.* **39,** 118–139.

Geochimica et Cosmochimica Acta, 1959, Vol. 17. pp. 17 to 20. Pergamon Press Ltd. Printed in Northern Ireland

The advancing wave of acidic components in ascending solutions and hydrothermal acid–base differentiation*

D. S. Korzhinsky
Institute of Geology of Ore Deposits, Petrography, Mineralogy and Geochemistry, Academy of Sciences, Moscow

(*Received* 8 *November* 1958)

The acidity of ascending solutions changes regularly in the course of postmagmatic processes as is shown by geological evidence. Toward the end of the crystallization of granitic magmas the acidity of the residual solutions increases, which results in the leaching out of rocks which the solutions encounter. The acidity then decreases, which causes the precipitation of bases, including ore, from the solutions (Korzhinsky, 1955).

The leaching process may affect a large volume of rock, while the succeeding precipitation of the bases is substantially confined to fissures, so that fissure vein deposits are formed within the leached rocks.

The regularities in the regimen of acidity of postmagmatic solutions and particularly the close spatial relationship of leaching and successive precipitation cannot be explained by the existing hypotheses.

According to the writer's hypothesis, the postmagmatic leaching and subsequent precipitation depend in essence, not on the fractionation of the solutions in the magma chamber, but on the passage of an "advancing wave of acidic components" along the flow of magmatogeneous solutions (Korzhinsky, 1957). It is assumed that the acidic components (CO_2, HCl, H_2S, etc.) of a solution percolate through the rocks more rapidly than the other components of the solution, a phenomenon which may be designated an "acidic filtration effect". The effects resulting from the filtration of inorganic solutions through inorganic filters were discussed by Mackey (1946) and by Korzhinsky (1947) and experimentally verified by Ovchinnikov and Maksenkov (1949), and Ovchinnikov and Shour (1953). Acidic components in aqueous solutions have on the average higher electrochemical mobilities than basic components and in particular hydrogen ion is more mobile than hydroxide ion. Accordingly we may expect, that in filtration of ascending solutions through rocks the acidic components of the solutions, being more mobile and volatile, will ascend more swiftly than the basic components. In the last stage of magma crystallization the acidic components accumulate in residual solutions. Owing to the filtration effect, they can ascend along the flow of transmagmatic and postmagmatic solutions as an "advancing wave of acidic components". At any given section of the flow in the passing of this wave the acidity of the solution first increases and then decreases.

* Presented at the annual meeting of the Geological Society of America, St. Louis, Missouri, 7 November, 1958.

Some experimental work on the acidic filtration effect has been carried out by Shour (Sverdlovsk). According to Shour (personal communication), in the filtration of aqueous solutions of alkali metal chlorides through a silica filter, an acidic filtration effect was observed. The decrease in the pH of the filtrate in the case of CsCl solutions amounted to 0·4, that is, the concentration of the hydrogen ion was increased 2·5 times.

In freshly opened cavities of minerals the acidity of the liquids enclosed substantially decreases in a fraction of a minute, due to the escape of volatile components, as was shown by Kaluzhnii (1957). In his experiments the increase in pH was as high as 1·0. The importance of the change in the content of volatiles in ore formation has been suggested by Deicha (1956, 1958).

The increasing acidity of postmagmatic solutions first begins to manifest itself in high temperature autometasomatic reactions, for example in the myrmekitization of potassium feldspar. But the maximum acidity of the solutions is always attained at a later stage, usually under conditions of moderate temperature in contact rocks, and in subvolcanic formations at some distance from the magmatic source of the solutions. This relation indicates that the cooling of the postmagmatic solution initially causes an increase in its acidity. This may be explained by the condensation of the solution from gaseous to liquid state. That the condensation should cause the increase of acidity may be seen from the following consideration. If on boiling, a solution separates into two phases, liquid and gaseous, the latter will be enriched in the more volatile acidic components and impoverished in the less volatile bases. Since these two phases are in equilibrium, we have to conclude that the activity coefficients of the acidic components in the gaseous phase will be lower than in the liquid phase and the reverse relationship will hold for the basic components. Therefore in condensation of the solution, its bulk composition being unchanged, the activity of acidic components must increase and that of the basic components must decrease. The less the external pressure, the sharper is the difference between the liquid and gaseous phases, and therefore the more the increase in acidity in the condensation. Consequently, the maximum acidity attained by postmagmatic solutions must be higher for shallow depths than for abyssal conditions. Indeed, under abyssal conditions of leaching, alkaline feldspars are replaced by muscovite or sericite, but further leaching with the formation of andalusite, kaolinite or even zunyite, takes place only under conditions of shallow depths.

The structural difference displayed by the acidic and subsequent basic stages is not necessarily dependent on the difference in tectonic conditions. With the advancing wave of acidic components setting in, dissolution predominates over precipitation, which results in the widening of the pores of the rocks, and therefore favours the even percolation of solutions through the rocks. After the passage of the wave of acidic components, precipitation predominates over dissolution. Therefore the pores of the rocks are stopped, the percolation of solutions through the rocks is hampered and the ascension of the solutions with precipitation of bases is confined to fissures.

As the acidic components pass away, the solution grows oversaturated with bases. The precipitation of the components of the solution proceeds in order of

increasing basicity, the actual order depending also on the concentration of the components in the supersaturated solution, that is, on the bulk composition of the leached out rocks. In this manner a peculiar "acid–base differentiation" takes place in the rocks in the sense that bases, leached out from large volumes of rocks, are concentrated in veins or veinlets among the leached rocks (KORZHINSKY, 1958). Along with bases, leached from wallrocks, the magmatogeneous bases, including ores, may precipitate as well, because their solubility is lowered by the enrichment of the solutions in the strong bases of the wallrocks.

The most striking instances of acid–base differentiation are furnished by massifs of "secondary quartzites", that is, massifs of strongly leached out, substantially alumina–silica rocks in volcanic formations. In secondary quartzites which have replaced liparitic rocks, poor in alkaline-earths, the high-alumina veins and veinlets (corundum–andalusitic, monomineralic sericitic, alunitic, kaolinitic, etc.) are universally present. In secondary quartzites, which have replaced the rocks of the spilite–keratophyre series, in addition to sericitic, chloritic, calcitic and baritic veinlets, lodes of copper pyrite are common. Thus in secondary quartzites the dependence of the precipitated vein minerals on the composition of the enclosing rocks is clearly expressed. Among greisenized rocks of initial granitic composition, monomineralic muscovite, topaz or alkali feldspar veins are typical. Among partly leached propylitized andesitic rocks, veins of monomineralic or adularia epidosite are always abundant. In quartz veins and their leached wallrocks, veinlets of sericite, chlorite, carbonate, albite, adularia, pyrite, etc., are common. All these cases may be considered as examples of hydrothermal acid–base differentiation.

Owing to acid–base differentiation, ore veins may be formed at the expense of the ore components which were scattered through the rocks and then leached out and redeposited. This is particularly evident in the case of the alumina of high-alumina veins, and the iron of pyritic lodes among secondary quartzites. Some copper ore veins associated with series of basic effusives, are likely to have had the same manner of origin. The concentration of metals from wall rocks into veins was long ago suggested by the lateral-secretion theory, but the latter failed to explain the causes of the concentration.

The wave of acidity generated by the crystallization of magma attains maximum acidity at some point in its ascent and then gradually fades, owing to the diffusion of the acidic components into the wallrocks and the fixing of these components by the replacement reactions. Owing to the flow of the solutions, the passing of the acidity wave results in the general displacement of the leached components in the direction of flow. Therefore in rocks, altered by the flow of ascending solutions the following vertical zoning should evolve (from bottom to top):

(1) The zone of increasing acidity of the advancing wave. The leaching out of the rocks increases upwards, the subsequent precipitation being insignificant or even almost lacking. This is essentially the zone of autometasomatic alteration of the magmatic rocks.

(2) The zone of maximum leaching. Leaching is accompanied by subsequent precipitation, mainly of weak bases (minerals of aluminium, iron, titanium, etc.). On the average, in this zone the leaching out of bases sharply predominates over their precipitation.

(3) The zone of fading acidity of the advancing wave. Leaching decreases upwards whereas the subsequent precipitation of bases increases. In telethermal ore veins (carbonate, fluoritic, baritic) the precipitation sharply predominates over the preceding leaching. The latter may even be absent.

The above suggested hypothesis is, of course, only a tentative rough scheme depicting a very complicated natural process.

References

Deicha G. (1956) Variation de la constitution des solvants et dépôts métallifères. *C.R. Soc. Géol. Fr.* 46–47.

Deicha G. (1958) Differentiation des fluides géochimiques d'origine profonde et dépôts métallifères. *C.R. Soc. Géol. Fr.* **7-8,** 157.

Kalyuzhny V. A. (1957) On the results of determinations of the pH of the solutions in liquid inclusions. *Geokhimiya* **1,** 77–79. (In Russian).

Korzhinsky D. S. (1947). Filtration effect in solutions and its significance in geology. *Izv. Akad. Nauk SSSR, Ser. Geol.* No. 2. (In Russian).

Korzhinsky D. S. (1955) *Outline of metasomatic processes. Symposium on fundamental problems of magmatic processes of ore formation.* Academy of Sciences, Moscow, U.S.S.R. (In Russian).

Korzhinsky D. S. (1957) On the character of the acidity of postmagmatic solutions. *Izv. Akad. Nauk SSSR, Ser. Geol.* No. 12. (In Russian).

Korzhinsky D. S. (1958) Hydrothermal acid-alkaline differentiation. *Dokl. Akad. Nauk SSSR* **122,** No. 2. (In Russian).

Mackay R. A. (1946) The control of impounding structures on ore deposition. *Econ. Geol.* **41,** No. 1, 13–46.

Ovchinnikov L. N. and Maksenkov V. G. (1949) Experimental investigation of the filtration effect in solutions. *Izv. Akad. Nauk SSSR, Ser. Geol.* No. 3. (In Russian).

Ovchinnikov L. N. and Shour A. C. (1953) On the filtration effect during the seepage of solutions through mineral filters. *Proceedings of the Fourth Conference on Experimental Mineralogy and Petrology* No. 2. Academy of Sciences, Moscow, U.S.S.R. (In Russian).

Geochimica et Cosmochimica Acta, 1959, Vol. 17, pp. 21 to 31. Pergamon Press Ltd. Printed in Northern Ireland

Lead isotopes in manganese nodules

Tsaihwa J. Chow and C. C. Patterson
Division of Geological Sciences, California Institute of Technology, Pasadena, California*

(*Received* 7 *December* 1958)

Abstract—The isotopic compositions of leads which were isolated from manganese nodules of the Atlantic and the Pacific Oceans were determined. The Atlantic leads were more radiogenic than those of the Pacific. The Pacific samples showed a trend of increasing radiogenic leads from the north-west toward the south-east Pacific. The relationship between the collecting sites and the isotopic compositions of leads can be used to trace the circulation patterns of deep-water masses. The oceanic leads originated from rock systems whose uranium and lead contents have differentiated at various times appreciably later than $4{\cdot}5 \times 10^9$ years.

Introduction

The evolution of lead can be used as a tracer for studying the relationships of sedimentary and igneous rock systems in space and in time. Changes in relative abundances of lead isotopes within rock systems depend upon the uranium, thorium and lead contents, and the ages of the systems. The nature of this dependency together with a knowledge of these variables makes it possible to infer past relationships of these elements which serves the purpose of defining or restricting mechanisms which describe geological phenomena. This approach has become important to problems concerning the age of the earth, the genesis of the continental platforms, and the origin and relationship of igneous and sedimentary rocks. Oceanic lead is an essential link in these studies since the oceans serve as collecting and mixing reservoirs for leads which are derived from vast land areas, and thus provide samples of leads which reflect geochemical relations among uranium, thorium and lead within large continental segments. The change in isotopic composition of oceanic lead is recorded and preserved in marine sediments and therefore such materials can be used for the studies of oceanic leads deposited in the past. Lead isotopes can also be used as tracers for the study of circulation and mixing patterns in the oceans when more information concerning lead in rivers and lead precipitating mechanisms in the oceans becomes available.

When studies are made on lead isolated directly from sea water, difficulties of possible contamination are encountered owing to its low lead content. However, lead may be readily obtained from manganese nodules without contamination because these ocean-bottom concretions contain appreciable amounts of it. Pertinent information on the geochemistry of lead in the oceans is rather meagre. Boury (1938) has published some spectrophotometric measurements of a preliminary nature on lead concentrations in sea water. Murray and Renard (1891) discovered that manganese nodules contained high concentrations of lead, and this was later substantiated by Goldberg and Arrhenius (1958). Patterson *et al.* (1953) made a preliminary investigation of the isotopic composition of lead isolated from a manganese nodule and a red clay sample. Buser and Grütter (1956, 1957)

* Contribution No. 899.

have determined the gross structural features of the important minerals in manganese nodules. Goldberg and Arrhenius (1958) have discussed some aspects of the origin of lead in the nodules. Wickman (1948) has discussed possible geochronological applications of oceanic leads, and Pettersson (1943) has made nodule growth-rate studies.

The material in this report consists of three parts: first a description of the methods of comparing isotopic analyses; second, a tabulation of the manganese nodule data; and third, an interpretation of the data in terms of geochemical models.

1. Calibration of Mass Spectrometer

We tried to obtain reasonable limits of measurement error which would allow us to consider differences among the isotopic compositions of leads isolated from manganese nodules. These limits, which allowed us to compare isotopic analyses on a relative basis, are termed "random errors". These random errors were determined by preparing a standard lead nitrate solution (CIT shelf standard no. 1) and then analysing a series of ten aliquots of this solution as individual samples. Each isotopic analysis consisted of an independent set of measurements satisfying the criteria of ion beam intensity, stability and duration described by Chow and McKinney (1958) The results of ten analyses are given in Table 1. The correction factors for these analyses are discussed later.

Table 1. Analyses of CIT shelf standard lead No. 1

Date of analyses	No. of ratios	$\frac{Pb^{206}}{Pb^{204}}$	Standard deviation	$\frac{Pb^{206}}{Pb^{207}}$	Standard deviation	$\frac{Pb^{206}}{Pb^{208}}$	Standard deviation
10/20/56	34	16·763	0·057	1·0693	0·0029	0·4530	0·0015
10/22/56	37	16·790	0·031	1·0684	0·0020	0·4529	0·0010
10/24/56	20	16·739	0·046	1·0699	0·0025	0·4544	0·0012
10/25/56	45	16·787	0·049	1·0683	0·0024	0·4532	0·0012
10/28/56	44	16·703	0·044	1·0699	0·0022	0·4538	0·0011
10/31/56	46	16·752	0·056	1·0690	0·0023	0·4531	0·0008
11/ 1/56	48	16·803	0·043	1·0688	0·0020	0·4532	0·0010
11/ 2/56	45	16·751	0·048	1·0690	0·0020	0·4536	0·0011
11/11/56	48	16·755	0·051	1·0700	0·0015	0·4539	0·0009
11/16/56	40	16·715	0·061	1·0698	0·0027	0·4540	0·0009

If it is assumed that the performance of our mass spectrometer over a long time has been adequately sampled during the time interval represented in Table 1 and that the data are normally distributed, then an approximation of random error is given by the spread of the data. At the present time the effort required to justify these assumptions is so great that we have abstained in favour of more urgent problems. On the basis of these assumptions, a statistical analysis of the data was made for the purpose of using conventional procedures for the assignment of random errors. A statistical study of the data in Table 1 showed that analyses of individual aliquots gave significantly different results on different days. Such effects can

result from drifts of signal or mass discrimination in the spectrometer or from fluctuation of operator bias in translating chart information. For isotope ratios of about unity, the effects of signal discrimination and operator bias are essentially absent and random differences among ratios are minimal for these ratios compared to all others. From the data given in Table 1, the following 90 per cent confidence interval limits were assigned to the lead isotope ratios of the manganese nodules: $\pm 0{\cdot}3$ per cent of the Pb^{206}/Pb^{204} ratio; $\pm 0{\cdot}1$ per cent of the Pb^{206}/Pb^{207} ratio; and $\pm 0{\cdot}2$ per cent of the Pb^{206}/Pb^{208} ratio. These errors define an interval about a single analysis such that if this sample were analysed nine more times, the mean of the ten analyses should lie within this interval. Two lead samples were considered to be different if the differences between their isotopic compositions were outside the intervals defined by these limits.

We also attempted to make a reasonable approach to the problem of differences between the isotopic compositions of leads analysed in our laboratory and the isotopic compositions of leads analysed by other investigators. The differences which exist between the observed and known isotopic compositions of an absolute standard are termed "systematic errors". Such systematic errors and their associated correction factors were determined by analysing absolute standards consisting of known mixtures of uranium isotopes. We exercised great care in the preparation of these standard mixtures, especially in the preparation of the gravimetric form of the isotopes. Repeated analyses of different mixtures were made. The final result of such experiments performed on our instrument was:

$$\left(\frac{U^{238}O_2^{16}}{U^{235}O_2^{16}}\right)_{\text{expected}} \Big/ \left(\frac{U^{238}O_2^{16}}{U^{235}O_2^{16}}\right)_{\text{observed}} = 1{\cdot}0136 \pm 0{\cdot}002$$

Our instrument utilizes an electron multiplier. Inghram and Hayden (1954) have pointed out that a correction proportional to the square root of the ion mass should be applied when a multiplier is used. We have assumed that this suggestion is correct and further that there is a residual mass discrimination factor,

$$\frac{1{\cdot}0136}{(U^{238}O^{216}/U^{235}O^{216})^{1/2}},$$

which is directly proportional to the fractional change of the magnetic field. Shunt circuits of the electrometer were calibrated by conventional means. The lead isotope ratios were therefore subjected to three corrections: (a) a correction proportional to the square root of the mass ratio; (b) a correction proportional to the fractional change of magnetic field as determined from uranium; and (c) an electrometer scale calibration factor. The corrections for each of the lead ratios listed in this paper are:

corrected ratio	observed ratio	correction factor (a)	(b)	(c)
Pb^{206}/Pb^{204}	$= Pb^{206}/Pb^{204} \times$	1·0049	× 1·0069	× 0·9996
Pb^{206}/Pb^{207}	$= Pb^{206}/Pb^{207} \times$	0·9976	× 0·9966	× 1·0000
Pb^{206}/Pb^{208}	$= Pb^{206}/Pb^{208} \times$	0·9952	× 0·9932	× 1·0007

Systematic errors and their correction factors exceeded random errors and, as a consequence, defined absolute uncertainties. Since the use of these correction

factors has not been unequivocally justified, an estimate of the absolute uncertainty in the lead ratios of about unity might be half the value of the corrections, i.e. about one part in two hundred. The absolute uncertainties associated with isotope ratios appreciably different from unity are probably much greater than one part in two hundred.

II. Manganese Nodule Data

Isotopic analyses were made of leads isolated from thirty-four manganese nodules dredged from the floors of the Pacific and Atlantic oceans. Analyses were carried out using chemical techniques and spectrometer conditions described by Chow and McKinney (1958). Specimens were dried at 110°C. The average loss in weight, or the moisture content, was 15 per cent. Lead concentrations were calculated for the dried material. Each sample was composed of material originating from 10 to 15 mm of concentric growth layers.

Results of the analyses were compared using the criteria described in the previous section. Gradational and essentially continuous differences in Pb^{206}, Pb^{207} and Pb^{208} abundances relative to Pb^{204} were found to exist among different lead samples. In general, the abundances of Pb^{206}, Pb^{207} and Pb^{208} increased or decreased simultaneously, but not congruently, when different samples were compared. Considering all samples, the difference between extreme values of the ratio Pb^{207}/Pb^{204} was twice the allowed random error interval, or a factor of 2. This factor was 3 for the Pb^{208}/Pb^{204} ratio, 4 for the Pb^{208}/Pb^{207} ratio, 6 for the Pb^{206}/Pb^{204} ratio and 14 for the Pb^{206}/Pb^{207} ratio. We made a statistical study of the abundance trends of Pb^{206}, Pb^{207} and Pb^{208} in the samples. Because it was necessary to make qualifying and perhaps erroneous assumptions regarding sample population distributions we used the results only for rough guides. The Pb^{207}/Pb^{204} vs. Pb^{206}/Pb^{204} regression of these data was considered not to be useful for interpretation of the geochemistry of lead and uranium, because measurement errors were too large compared to differences among samples. Owing to this, geochemical inferences were made only from the Pb^{206} abundance trend.

The linear regression of Pb^{206}/Pb^{204} vs. Pb^{206}/Pb^{207} was determined as shown in Fig. 1, and this prominent feature of the data was used for sample classification. The lead samples were arranged according to the order in which they fell on the regression line. The validity of this convenient procedure can be judged by considering the replicate analyses of the standard given in the insert of Fig. 1. Our spectrometer introduced a bias which did not appreciably affect the regression. The overall abundance trend of Pb^{206} is clearly outside experimental error. The lead isotope analyses are listed in Table 2 arranged in the order of increasing Pb^{206} abundance. The abundance trend of Pb^{208} was also considered to be significant and useful. The Pb^{208}/Pb^{204} vs. Pb^{208}/Pb^{207} regression line is shown in Fig. 2.

Another feature of these leads is the relationship between their collecting sites and their isotopic compositions. This is illustrated in Fig. 3, where ordinal sample numbers which are related to the Pb^{206} abundances in the samples are located near their respective collecting stations on an ocean chart. It can readily be shown that a typical lead sample in the Atlantic has distinctly more Pb^{206} than a typical lead sample in the Pacific. The grouping of Pacific and Atlantic samples is natural, so that it is not necessary to consider whether such a grouping might occur by random

chance. It can also be shown in a less rigorous way that there is a significant tendency for the Pb^{206} abundance in manganese nodule leads to increase from north-west to south-east down across the Pacific. A calculated direction of the Pb^{206} concentration gradient in the Pacific Ocean is indicated by the arrow in Fig. 3.

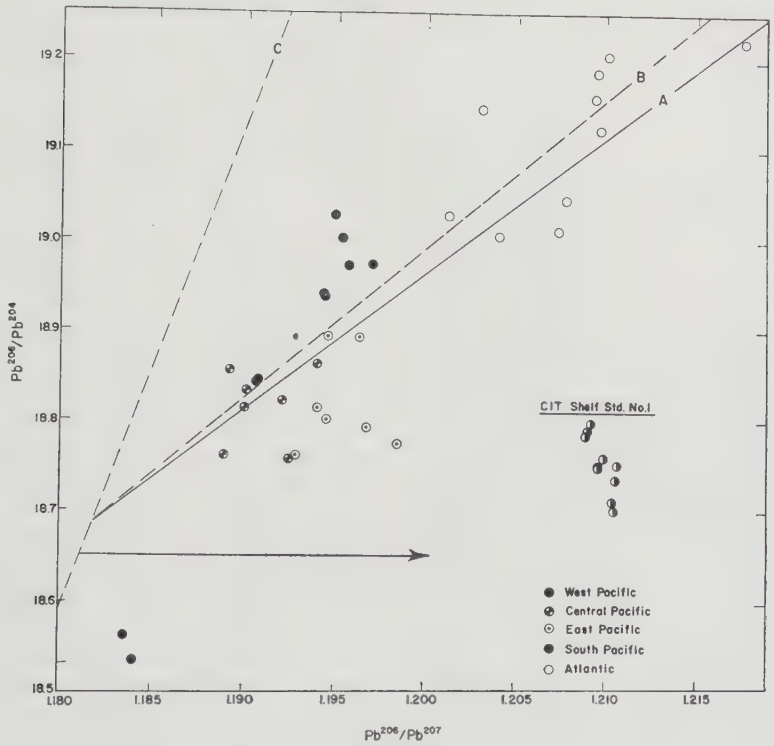

Fig. 1. The Pb^{206} abundance trend. The Pb^{206} regression is given by A. The scales for the co-ordinates of the standard lead analyses are equal to those of the sample analyses, but the origin has been translated. A primary growth curve ($\mu = 9{\cdot}0$, $T_0 = 4{\cdot}55 \times 10^9$ years, $Pb_{primordial}$ = that in iron meteorites) is given by B. A primary isochron of zero age ($T_0 = 4{\cdot}55 \times 10^9$ years, $Pb_{primordial}$ = that in iron meteorites) is given by C.

III. Discussion

Leads in the manganese nodule samples were accumulated during time intervals which probably exceeded 10^3 years but which may not have exceeded 10^6 years. Pettersson (1943) observed a regular decrease of Ra^{226} from the surface to the centre of a manganese nodule and estimated a growth rate of about 1 mm per 10^3 years. Goldberg and Arrhenius (1958, personal communication) found Th^{230} in large excess of equilibrium in some manganese nodules. They suggest that Pettersson's estimates on growth rate may be too high if the Ra^{226} in the specimen was Th^{230} supported. Goldberg and Koide (1958) also found that when there is a Th^{230} excess in manganese nodules, it is usually discontinuous, occurring within a thin outermost layer. These investigators suggest that the concentric layered structure of the nodules may be produced by a succession of short periods of

Table 2. The isotopic composition of manganese nodule leads

Ordinal number	Specimen	Location Lat.	Location Long.	Depth (m)	Pb concn. (p.p.m.)	$\frac{Pb^{206}}{Pb^{204}}$	$\frac{Pb^{206}}{Pb^{207}}$	$\frac{Pb^{206}}{Pb^{208}}$
1	Japan No. 2	34°N	140°E	2600	21	18·533	1·1842	0·4749
2	Japan No. 1	34°23′N	139°05′E	260	167	18·561	1·1838	0·4758
3	Horizon nodule	40°14′N	155°15′W	5500	1120	18·759	1·1890	0·4795
4	MP-26-A3	19°23′N	171°08′W	—	2440	18·755	1·1925	0·4789
5	MP-25-F2	19°40′N	168°32′W	1740	2180	18·812	1·1901	0·4769
6	GA-3 dredge-7	50°15′N	145°20′W	—	1500	18·759	1·1929	0·4805
7	MP-37-C	17°04′N	177°15′W	2000	2080	18·831	1·1902	0·4773
8	MP-43-A	12°09′N	164°44′E	2000	2050	18·853	1·1893	0·4793
9	MP-33-K	17°54′N	174°16′W	1790	1940	18·840	1·1907	0·4789
10	MP-5 core-2 top	13°45′N	133°05′W	—	560	18·842	1·1908	0·4777
11	Chubasco 34-92	6°12′N	125°27′W	4500	27	18·819	1·1922	0·4774
12	MP-3 #3	20°45′N	127°20′W	—	720	18·799	1·1946	0·4799
13	MP-3 #11	20°45′N	127°20′W	—	980	18·811	1·1941	0·4799
14	PAS-19121	19°N	121°W	—	1000	18·790	1·1968	0·4809
15	MP-43-D	11°57′N	164°59′E	2000	1680	18·860	1·1941	0·4798
16	Wigwam-5	27°38′N	124°25′W	4000	576	18·772	1·1985	0·4803
17	Henderson nodule	25°15′N	119°40′W	—	1910	18·891	1·1947	0·4785
18	Jasper sea mount	30°32′N	122°42′W	—	1180	18·889	1·1964	0·4795
19	Downwind HD-15	15°23′S	136°18′W	4480	300	18·935	1·1945	0·4806
20	Downwind HD-72	25°31′S	85°14′W	920	2400	18·938	1·1944	0·4799
21	Downwind HD-16-B	16°29′S	145°33′W	1270	2350	18·969	1·1958	0·4801
22	Downwind HD-16-A	16°29′S	145°33′W	1270	2300	19·000	1·1954	0·4806
23	Downwind HD-47	42°00′S	102°01′W	4200	300	18·971	1·1971	0·4825
24	Downwind BD-7	46°44′S	123°01′W	4100	700	19·026	1·1950	0·4810
25	V-3-27	23°58′N	86°02′W	1765	2500	19·020	1·2013	0·4817
26	V-9-22	8°09′S	18°39′W	4000	385	19·002	1·2041	0·4838
27	Theta trawl #4 Scripps	29°18′N	57°20′W	5400	1020	19·009	1·2074	0·4817
28	V-9-4	3°26′S	35°02′W	995	1800	19·144	1·2031	0·4796
29	Swedish expd-270	31°51′N	30°19′E	160	828	19·043	1·2078	0·4821
30	Theta trawl #4 Lamont	29°18′N	57°20′W	5400	800	19·122	1·2097	0·4803
31	A-180-50 core	27°48′N	94°00′W	366	500	19·177	1·2094	0·4823
32	A-150-8 dredge	31°49′N	43°25′W	3700	930	19·185	1·2095	0·4824
33	A-160-1 core	30°08′N	57°53′W	5090	1020	19·204	1·2101	0·4832
34	C-25-4	39°50′N	66°17′W	1790	300	19·222	1·2178	0·4842

relatively rapid growth separated by longer intervals of quiescence. The total interval probably approaches 10^6 years.

Such an accumulation interval is long compared to ocean water turnover rates, but equal to or less than the time of stability of oceanic circulation patterns. The very low C^{14} activity recently observed in waters at intermediate depths in the South Pacific suggests turnover rates of the order of 10^3 years (Ferguson, 1958). Goldberg and Koide have also found that the pelagic areas of the Pacific may be divided into zones, each with a characteristic Th^{230}/Th^{232} ratio at the sediment surface. In most instances the ratios appear to decrease regularly with depth to a limiting value in the sediments. If the decrease is due to radioactive decay, the sediments have been incorporating thorium of a fixed isotopic composition which suggests that pelagic zonal circulation has been stable for minium periods of about 10^6 years.

The ages of the manganese nodules which are now available for study probably do not exceed 10^6 years. It is possible that a few may have a Tertiary age. The nodules cease growing after they are buried by sediments, and the recovery of a

nodule that had been buried and then exposed later by slumping or erosion may be a rare event. Uranium decay cannot appreciably affect the isotopic composition of lead in manganese nodules, since the lead to uranium ratio in them is of the order of 10^3.

Two major constituents of manganese nodules are ferric and manganese manganite (Buser and Grütter, 1956, 1957). It has been suggested that lead is situated in the disordered layers of the manganites. The lead in manganese nodules is probably water-born, originating from shallow areas where high sedimentation rates prevail. Goldberg and Arrhenius (1958) have shown that lead is one of a family of trace elements that are highly concentrated in pelagic deposits and have presented convincing arguments for a land origin for these elements. The lead to silicon ratio in red clay is over ten times that in igneous rocks. They have suggested that a large portion of the lead in red clay is contained within scattered manganite minerals which, in fact, are incipient manganese nodules. It seems clear that the lead in manganese nodules has undergone an extraction process while being transported to pelagic areas, which implies additional mixing above and beyond that obtained by a simple mixing of fine clay particles which might otherwise serve as carriers for transport.

The lead in manganese nodules is probably representative of that in a very large volume of sea water. There is some uncertainty regarding the concentration of lead in sea water. Boury (1938) found about 5 μg of lead per litre of water while Chow (1959) found only 0·1 μg/l. The amount of water sampled by a manganese nodule depends upon the efficiency with which lead is removed from the water. Manganese nodules probably do not remove lead from sea water efficiently during growth if one considers that lead concentrations are low, that lead isotopic compositions are uniform throughout relatively large water volumes, and that water currents are rapid relative to nodule growth rates.

All of the foregoing information suggests that leads in manganese nodules are derived from land by means of streams, rivers and ocean currents, and that the lead in each nodule is a composite of leads from a very large area of land. The transport process involves extensive mixing which in this case is further enhanced by concentration processes, prolonged sampling periods, and low extraction efficiencies. Zonal circulation in the oceans tends to restrict the land area represented by each nodule. Since we cannot measure isotopic evolution in common leads during intervals as short a time as 10^6 years, the leads were collected essentially during the present, or they have zero age.

The leads which were analysed in this study could not have originated from any source except manganese nodules. Although some of the samples may have contained as much as 2 per cent biogeneous or terrigeneous material, the concentration of lead in manganese nodules is 10^2 times that in red clay and 10^4 times that in calcareous tests of marine organisms. The amount of lead isolated from each nodule was about 50 μg and was contaminated with 0·1 μg of common lead originating from the laboratory.

The leads show a trend in isotopic composition similar to that shown by most post-Tertiary lead ores, except that isotopic variations are very small and isotopic regressions are much more distinct in oceanic leads than in post-Tertiary lead ores.

Some investigators have contended that the range in isotopic compositions of most young lead ores cannot be explained either by age differences or by uranium–lead differentiation at the time the earth was formed, i.e. the use of a primary growth curve is forbidden and a primary isochron of zero age will not describe such ore lead data. The oceanic lead data clearly and strongly fortify the above view. Although the oceanic Pb^{206} abundances could be described by a primary growth curve such as that represented by the dashed line *B* in Fig. 1, we cannot seriously consider such a relationship because the range in ages of about 2×10^8 years required by the data is too large. If a zero age is assigned to the leads most abundant in Pb^{206}, then intermediate leads have assigned ages of 10^8 years and some of these intermediate leads originate from nodules which contain Th^{230} in large excess of equilibrium.

The oceanic Pb^{206} abundances cannot be described by a primary isochron of zero age such as that represented by the dashed line *C* in Fig. 1 because the slope of the regression curve *A* is considered to be significantly less than the slope of the function *C*. Thus, oceanic leads originate from rock systems which have experienced uranium-lead differentiation at times appreciably later than $4{\cdot}5 \times 10^9$ years ago. We cannot calculate with confidence the extent or time of uranium–lead differentiation from these data without more information because of the possibility of multiple differentiation at various times.

The parameters of the function that describes the primary isochron of zero age for the earth are known from meteoritic data. These parameters are derived from the fixed Pb^{206}/Pb^{204} and Pb^{207}/Pb^{204} ratios in meteoritic troilite lead and the fixed Pb^{206}/Pb^{207} ratio obtained from the difference between any two meteoritic leads (Patterson, 1956). Line *C* in Fig. 1 is the primary isochron located by these data, but measurement error would allow it to be displaced (without appreciable change in slope) to the right or left by an amount indicated by the length of the arrow at the bottom of Fig. 1. Although this uncertainty of location of the primary isochron is too large for our purposes here, there is independent evidence which suggests that this position relative to the oceanic leads may be correct. The igneous rocks, associated sediments and meta-sediments of the drainage areas leading to the Pacific Ocean are distinctly younger than those of the Atlantic Ocean. In addition the abundance of exposed basic rocks is greater in the Pacific drainage areas. Consequently the younger and less differentiated drainage areas of the Pacific should produce leads falling closer to the primary isochron than those from the Atlantic, which is in accord with the data as presented in Fig. 1.

The Pb^{208} abundance trend given by line *A* in Fig. 2 clearly shows that the thorium–uranium ratio is higher in the source areas of the Atlantic leads than in those of the Pacific leads, but there is no indication whether this thorium–uranium differentiation occurred at the time the earth was formed or later. The Pacific leads fell in a geographical sequence on the thorium -lead differentiation curve illustrated by line *C* in Fig. 2, but measurement errors are so large that they do not allow further consideration of thorium–lead differentiation in the source areas of these samples.

The systematic relationship between the location of the collecting sites of the manganese nodules and the isotopic compositions of their leads indicates that sea

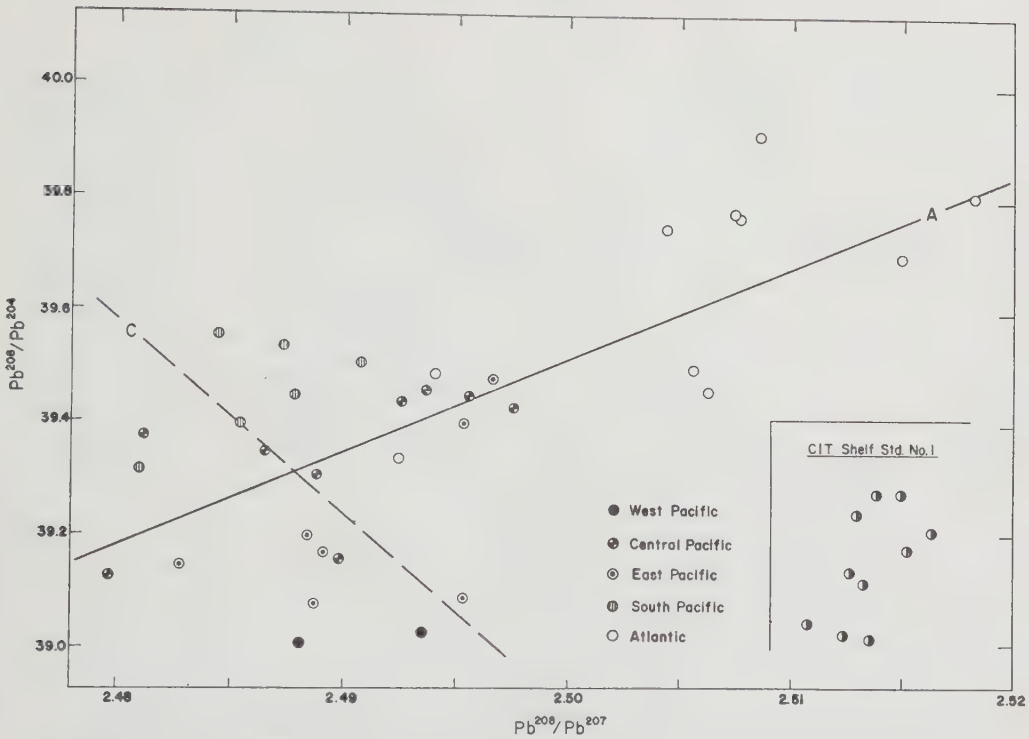

Fig. 2. The Pb^{208} abundance trend. The Pb^{208} regression is given by *A*. A primary isochron of zero age ($T_0 = 4{\cdot}55 \times 10^9$ years, $Pb_{primordial}$ = that in iron meteorites, $K = 4{\cdot}0$) is given by *C*.

water leads are incompletely mixed in pelagic areas. These observations are in accord with the distribution of Th^{230} and Th^{232} in pelagic sediments (Goldberg *et al.*, 1958). The residence time of lead in the oceans, about 10^4 years, is appreciably long compared to the rate of deep water mass movement. Therefore the restriction of bottom water circulation to zones is a major factor in determining the degree of mixing. We cannot estimate the extent of mixing of oceanic lead because there is insufficient information concerning deep-water circulation. The observed differences in isotopic compositions therefore may not reflect the maximum differences in land source areas. The source areas of either the Atlantic or the Pacific can be demarked with some confidence because of obvious drainage paths and land barriers, but the source areas of the significantly different leads within the Pacific cannot be so demarked. Investigations of lead isotopes in shelf areas and in rivers waters should aid both in the identification of source areas and in the estimation of degrees of mixing.

The arithmetic mean of the isotopic compositions of all the manganese nodule leads is: $Pb^{206}/Pb^{204} = 18{\cdot}92$, $Pb^{207}/Pb^{204} = 15{\cdot}80$, $Pb^{208}/Pb^{204} = 39{\cdot}40$. This composition can only approximate the average sea water lead, since the samples were not weighted according to the mass of water they might represent. Oceanic leads are derived from uranium-enriched rocks which have as their counterparts

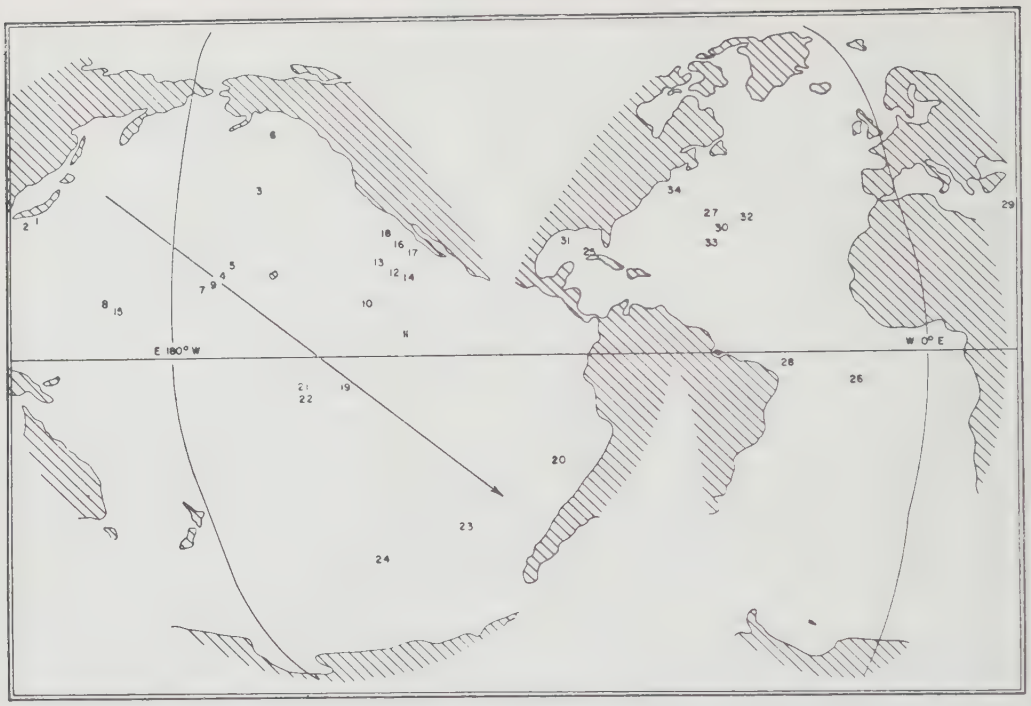

Fig. 3. Map showing the collecting sites of the manganese nodules. The numbers indicate the relative abundance of Pb^{206} in the lead samples.

uranium-deficient rocks. Together, these two rock systems can be classified as a super system. The average isotopic composition of lead derived from this super system would better represent the lead in the outer part of the earth's crust. We can only crudely estimate the isotopic composition of such lead, but on the basis of arguments made previously, it should lie near the lower part of the primary isochron illustrated in Fig. 1. The approximate upper limits of its isotopic composition would be: $Pb^{206}/Pb^{204} = 18{\cdot}5$, $Pb^{206}/Pb^{207} = 1{\cdot}18$.

Acknowledgement—We are indebted and sincerely grateful to many of our colleagues at the California Institute of Technology and elsewhere for their helpful advice and criticism. Fortunately, we can make specific references to aid provided by a few. F. Spitzer, now at the University of Minnesota, suggested a test for significance of homogeneity of means, which took into account non-equal variances that could be applied to the analyses of the standard lead. C. McKinney rescued us from several inadvertent arithmetical errors and gave helpful advice. B. Kamb pointed out a test for significance of the regression plane of Pb^{206} concentration in the Pacific. He also derived tests for significance of covariance which took into account the covariance introduced by the mass spectrometer. E. Goldberg, of the Scripps Institution of Oceanography, not only contributed the Pacific samples, but also provided information regarding the origin of manganese nodules. He is responsible for much of the recent progress in this matter which is of special importance to the geochemistry of lead isotopes. D. Ericson, of Columbia University, provided the Atlantic samples. F. Houtermans, Physikalisches Institüt der Universität, Bern, Switzerland, engaged in fruitful and encouraging discussions. The American Petroleum Institute provided the major financial support for this investigation through API Project 53 and the U.S. Atomic Energy Commission provided equipment, facilities and supplemental support through Contract AT(11-1)-208. We are grateful to the members of the Advisory Committee of Project 53 and the U.S. Atomic Energy Commission for this support.

References

Boury M. (1938) Le plomb dans le milieu marin. *Rev. Trav. Off. Pêches Marit.* **11,** 157–166.

Buser W. and Grütter A. (1956) Über die Natur der Manganknollen. *Schweiz. min. petrogr. Mitt.* **36,** 49–62.

Chow T. J. (1959) Lead isotopes in sea water and marine sediments. *J. Mar. Res.* In press.

Chow T. J. and McKinney C. R. (1958) Mass spectrometric determination of lead in manganese nodules. *Analyt. Chem.* **30,** 1499–1503.

Ferguson G. J. (1958) Reduction of atmospheric radiocarbon concentration by fossil fuel carbon dioxide and the mean life of carbon dioxide in the atmosphere. *Proc. Roy. Soc.* A**243,** 561–574.

Goldberg E. D. and Arrhenius G. O. S. (1958) Chemistry of Pacific pelagic sediments. *Geochim. et Cosmochim. Acta* **13,** 153–212.

Goldberg E. D. and Koide M. (1958) Ionium-thorium chronology in deep sea sediments. *Science* **128,** 1003.

Goldberg E. D., Patterson C. C. and Chow T. J. (1958) Ionium-thorium and lead isotope ratios as indicators of oceanic water masses. *Proc. 2nd Int. Conf. on Peaceful Uses of Atomic Energy,* Geneva, Switzerland.

Grütter A. and Buser W. (1957) Untersuchungen an Manganseditmenten. *Chimia* **11,** 132–133.

Inghram M. G. and Hayden R. J. (1954) Mass Spectrometry, *Nat. Res. Coun. Nat. Acad. Sci. (U.S.), Nucl. Sci. Ser. Rep.* No. 14.

Murray J. and Renard A. F. (1891) Report on deep-sea deposits based on the specimens collected during the voyage of H.M.S. *Challenger* in the years 1872–1876. *Challenger Rep.* p. 525.

Patterson C. C., Goldberg E. D. and Inghram M. G. (1953) Isotopic compositions of Quaternary leads from the Pacific Ocean. *Bull. Geol. Soc. Amer.* **64,** 1387–1388.

Patterson C. C.(1956) Age of meteorites and the earth. *Geochim. et Cosmochim. Acta* **10,** 230–237.

Pettersson H. (1943) Manganese nodules and the chronology of the ocean floor. *Göteborgs Vetensk-Samh. Handl.* Ser. 2, No. *8.*

Wickman F. E. (1948) Isotopic ratios: A clue to the age of certain marine sediments. *J. Geol.* **56,** 61–66.

Geochimica et Cosmochimica Acta, 1959, Vol. 17, pp. 32 to 36. Pergamon Press Ltd. Printed in Northern Ireland

The cosmogenic He^3 and He^4 distribution in the meteorite Carbo*†

J. H. Hoffman and A. O. Nier
School of Physics, University of Minnesota, Minneapolis 14, Minnesota

(*Received* 2 *February* 1959)

Abstract—The cosmogenic He^3 and He^4 distribution in a cross-section of the iron meteorite, Carbo, has been made with a mass spectrometer. The He^3/He^4 ratio is approximately constant throughout most of the cross-section and has a value of 0·239. The amount of He^3 varies between the approximate limits of 3·2 and 4·6 $\times 10^{-6}$ std. cm^3/g of meteorite. Contours of constant He^3 and He^4 were plotted. These are open curves indicating the meteorite was either split in half late in its lifetime or eroded away on one side since its fall to earth.

When a high energy proton strikes a nucleus such as of iron, the nucleus will become highly excited and dissipate its energy by evaporating light nuclei including He^3 and He^4. In an attempt to gain a quantitative understanding of this process, studies are being made of the rare gases found in iron meteorites. These gases are produced by the interaction of cosmic rays (principally protons) with the meteorite nuclei.

Since cosmic rays are attenuated as they pass through matter and also produce secondary particles in an interaction, a "depth effect" in the He^3 and He^4 contents should be observed in a meteorite. Paneth *et al.* (1953) studied the isotopic composition as well as the absolute amount of helium found in drillings taken from two holes bored in the iron meteorite Carbo and found a depth effect. Martin (1953) made a theoretical analysis of the problem. More recently Ebert and Wänke (1957) and Vinogradov *et al.* (1957) have discussed similar problems. Hoffman and Nier (1958) have reported in detail on the H^3 and He^4 distribution in a cross-section of the $\frac{1}{2}$ ton iron meteorite, Grant.

The present paper is a report on an investigation of the He^3 and He^4 of the Carbo meteorite. This meteorite, a medium octahedrite weighing 1000 lb and found in 1923 on the Almo Ranch 40 miles west of Carbo, Mexico, was cut in half and a slice approximately 1 cm thick was removed (parallel to the cut surface) from one of the halves.‡ The slice was cut into a number of parallel bars (see Fig. 1). Mass spectrometric analyses were made of the helium content of samples from various points along each of these bars in the same manner as for the Grant meteorite (Hoffman and Nier, 1958). The results for a typical bar, bar *J*, are shown in Table 1 and are plotted in Fig. 2. Distances are referred to a line scribed

* Supported by joint program of U.S. Office of Naval Research and U.S. Atomic Energy Commission.
† Preliminary report, *Bull. Amer. Phys. Soc.* Ser. II, **2**, 349 (1957).
‡ The authors are indebted to Dr. E. L. Fireman of the Astrophysical Observatory of the Smithsonian Institution, Cambridge, Massachusetts, and Professor C. Frondel of Harvard University, Department of Mineralogy, for providing the material used in this research. The Watertown Arsenal, Watertown, Massachusetts, did the cutting of the meteorite.

Table 1. Helium concentrations in bar J of meteorite Carbo. L and R in position column refer to distances left or right from reference line scribed on slice (see Fig. 3).

Position (cm) L or R	He^3 ($\times 10^{-6}$ std. cm^3/g)	He^4 ($\times 10^{-6}$ std. cm^3/g)	Total He ($\times 10^{-6}$ std. cm^3/g)	Ratio He^3/He^4
17·3 L	3·73	15·54	19·27	0·240
17·2 L	3·71	15·59	19·30	0·238
16·5 L	3·66	15·28	18·94	0·238
15·0 L	3·59	14·87	18·46	0·242
13·5 L	3·64	14·80	18·44	0·245
12·0 L	3·44	14·05	17·49	0·244
11·0 L	3·31	14·02	17·33	0·236
10·5 L	3·31	14·08	17·39	0·235
9·0 L	3·33	14·01	17·34	0·238
7·2 L	3·29	13·78	17·07	0·238
4·0 L	3·24	13·46	16·70	0·241
2·0 L	3·28	13·67	16·95	0·239
0·5 L	3·26	13·57	16·83	0·239
1·5 R	3·21	13·33	16·54	0·241
3·0 R	3·24	13·39	16·63	0·242
4·4 R	3·24	13·58	16·82	0·238
5·0 R	3·18	13·36	16·54	0·238
5·4 R	3·01	12·96	15·97	0·232
5·5 R	2·72	12·23	14·95	0·222

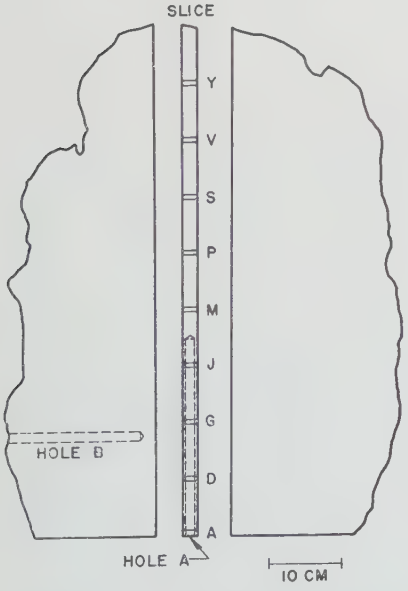

Fig. 1. Exploded cross-sectional view of meteorite Carbo showing edge view of slice from which bars were cut. End views of bars A, D, G, J, M, P, S, V, and Y used in present investigation shown. Diagram also shows location of holes A and B referred to by Paneth *et. al.* (1953) in their depth variation study.

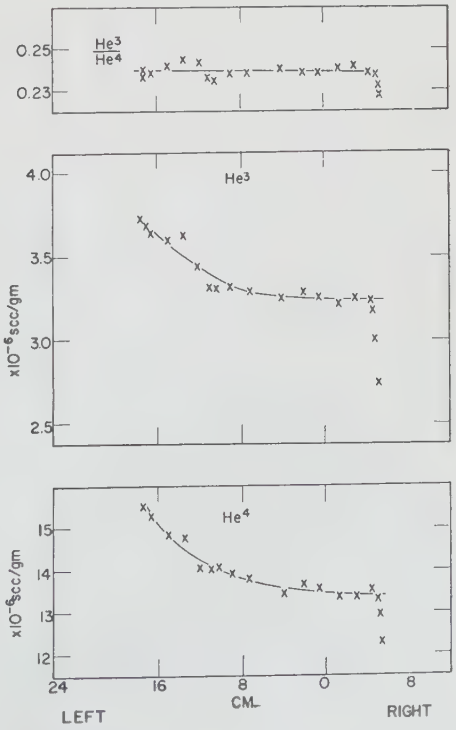

Fig. 2. Helium concentration in bar J. Distances are with respect to reference line inscribed on slice (see Fig. 3).

on the slice perpendicular to all the bars. (See Fig. 3 for reference line and bar positions.)

Contours of constant He^3 and constant He^4 were drawn from the helium content data, the results for He^3 being the contour map shown in Fig. 3. It was found that the He^3/He^4 ratio remained constant at approximately 0·239 except

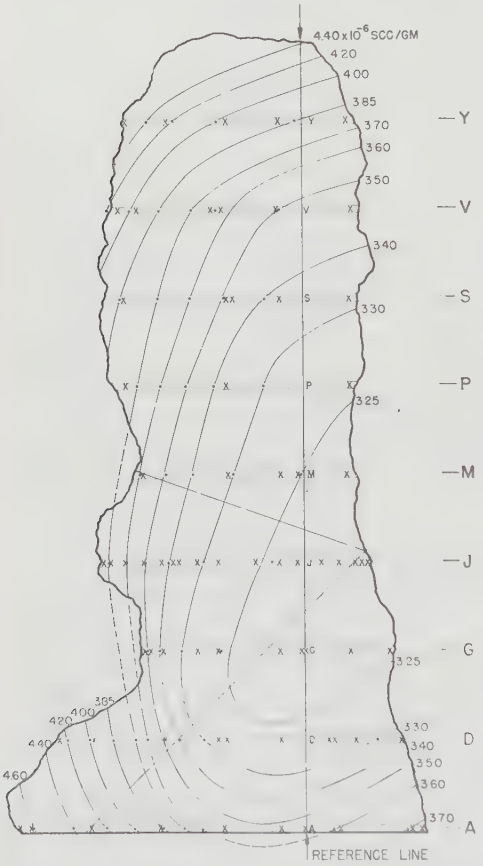

Fig. 3. Contours of constant He^3 in meteorite slice. Sets of horizontal lines indicate bars into which slice was cut. Crosses (×) are points at which helium analyses were actually made. Dots (·) are interpolated helium concentrations taken from graphs such as shown in Fig. 2.

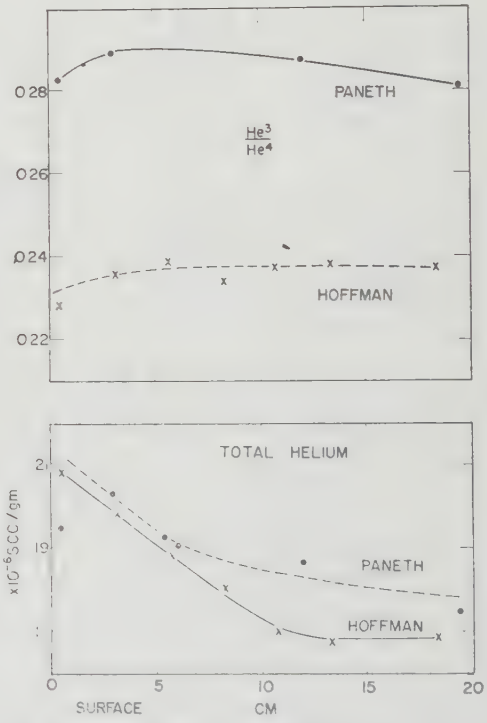

Fig. 4. He^3/He^4 ratio and total helium content of drillings from hole *B* (see Fig. 1 for location) plotted against distance from present surface of meteorite. Both Paneth's (Paneth *et. al.*, 1953) and present measurements shown.

near the left end of bars *V* and *Y*, where it rose to about 0·257. These numbers are believed accurate to within 3 per cent. Therefore, the contours of constant He^4 look essentially the same as those of He^3 and will not be reported separately.

Fireman (1958) has reported the He^3 distribution in a set of bars adjacent to ours. His work was done by neutron activation of the samples and counting the H^3 formed. The results are in reasonably good agreement with those presented here.

Helium analyses also were made on drillings from holes *A* and *B* in Carbo.

These results for *B*, together with those of PANETH *et al.* (1953) appear in Fig. 4. It should be noted that there is a 25 per cent difference in the He^3/He^4 ratio between the two sets of data. This is outside the errors quoted in the two investigations. The total helium content curves would have similar shapes if the first point of PANETH's data were discarded, yielding the dashed curve. In the comprehensive study of bar *J* reported here, material taken from the very end contained up to 50 per cent less helium per gramme of meteorite than samples in the body of the meteorite. The corroded appearance of the iron at the surface suggested that helium was lost from this more porous structure. It appears likely that PANETH's first sample contained such oxide contamination.

Data from samples from hole *A* agree with the subsequent data from the slice and will not be reported separately. It is difficult to make a comparison with PANETH's data for hole *A* because an unknown amount of material is missing from the bottom of Carbo and the positions of PANETH's samples are not accurately known.

From the nature of the helium production mechanism by cosmic rays, one would expect that the contours of constant helium should be closed loops as for the Grant meteorite (HOFFMAN and NIER, 1958). Since this is not the case for Carbo, the open contours indicate that the meteorite either was split in half late in its lifetime (since there is no helium increase near its right hand surface), or else eroded away while on earth. FIREMAN's (1958) A^{39} measurements on Carbo indicate it fell at least 1500 years ago.

The results from hole *B* combined with the contour map indicate that the rather flat section near the right centre of the meteorite is actually a three dimensional region of constant helium content. This suggests that Carbo was irradiated as part of a somewhat larger body.

In the investigation of the Grant meteorite, HOFFMAN and NIER (1958) attempted to formulate a quantative explanation of the helium distribution in a meteorite in terms of a model based on present-day knowledge of the interaction of high energy protons with matter. It is of some interest to use the parameters obtained from applying this model to the Grant helium contours in an analysis of the Carbo helium distribution. If one considers the Carbo meteorite to be approximately a sphere (a very rough approximation) and uses the measured central He^3/He^4 ratio of 0·239, and applies the Grant analysis, one finds a value of 64 cm for the pre-atmospheric radius of Carbo. It should be pointed out that this analysis is based on a spherical model of a meteorite and thus the radius calculation yields an average value. The average radius, taken along the diagonal lines shown in Fig. 3, is 28 cm or thus according to this analysis the radius decreased to slightly less than half of its initial value during passage of the meteorite through the earth's atmosphere.

The model predicts a definite increase in the radial He^3 and He^4 content from the centre of the meteorite toward the surface, whereas the measured distribution shows a region of constant He^3 and He^4 content too large and too flat to be consistent with the model predictions. A possible explanation for this seemingly anomalous behaviour might be that this meteorite had been heated sometime during its lifetime causing the helium to diffuse from regions of high to regions

of lower concentration. This process would have the effect of causing the central portion of the meteorite to have a more nearly constant helium content and the surface to lose helium, with the result that the helium content would be less near the surface than at some intermediate depth. Unfortunately, the interesting region near the surface where such diffusion effects could have been observed has been lost during passage of the meteorite through the earth's atmosphere and thus this hypothesis cannot be verified.

It is to be emphasized that any attempt at a quantitative explanation of the results offered here must be taken with a great deal of reservation until such time that other meteorites can be analysed and the helium production model further tested.

Acknowledgement—The authors are indebted to Dr. E. L. Fireman for co-operation in providing meteorite samples and for a number of stimulating conversations. They further wish to acknowledge the interest and suggestions of their colleagues, particularly Professors E. P. Ney and J. R. Winckler. Finally, special thanks are due to Mr. R. B. Thorness whose shop built the mass spectrometer and who is responsible for many design features which made the apparatus effective.

References

Ebert K. H. and Wänke H. (1957) The interaction of cosmic rays on iron meteorites. *Z. Naturforsch.* **12a,** 766

Fireman E. L. (1958) Distribution of helium–3 in the Carbo meteorite. *Nature, Lond.* **181,** 1725.

Hoffman J. H. and Nier A. O. (1958) Production of helium in iron meteorites by the action of cosmic rays. *Phys. Rev.* **112,** 2112.

Martin G. R. (1953) The origin of meteorite helium and the age of meteorites. *Geochim. et Cosmochim. Acta* **3,** 288.

Paneth F. A., Reasbeck P. and Mayne K. I. (1953) Production by cosmic rays of helium–3 in meteorites. *Nature, Lond.* **172,** 200.

Vinogradov A. P., Zadorozhnyi I. K. and Florenskii K. P. (1957) Content of the inert gases in the sikhote–alin iron meteorite. *Geokhimiya* **6,** 443–448.

Geochimica et Cosmochimica Acta, 1959, Vol. 17, pp. 37 to 43. Pergamon Press Ltd. Printed in Northern Ireland

The terrestrial economy of helium and argon

K. K. Turekian
Department of Geology, Yale University, New Haven, Conn.

(*Received* 17 *October* 1958)

Abstract—Using a model of continuous degassing of the earth and recent data on the chemical composition of chondritic meteorites, a "degassing constant," α, is determined from the argon-40 economy of the earth. The value of α, assuming an earth $4{\cdot}55 \times 10^9$ years old, is $2{\cdot}81 \times 10^{-11}$ year^{-1}. On the assumption that α is constant for all volatiles escaping from the earth, the helium economy of the earth is discussed. On the same premise the primordial water concentration of the solid earth, devoid of a hydrosphere, is determined to be 2300 p.p.m. which compares favourably with 2650 p.p.m. for chondrites. The small size of α indicates that the rate of water release from the earth has been sensibly constant over the past $4{\cdot}55 \times 10^9$ years.

In a recent paper, Damon and Kulp (1958) using an estimated cosmic ray production rate of He^3 and its abundance in the atmosphere calculated the rate of loss of He^4 from the atmosphere. Assuming that the steady state condition has been established, this can be equated with the rate of He^4 entry into the atmosphere from the solid earth. If this is used to calculate the rate of entry of argon-40 into the atmosphere from the crust, a value is obtained which is too small, according to Damon and Kulp, to account for the amount of argon-40 in the atmosphere at the present time. Hence they postulated a major degassing of the interior of the earth, perhaps as a result of radioactive heating approximately 3500 million years ago.

Because of the uncertainties in the estimates of the He^3 entry rate into our atmosphere as the result of cosmogenic phenomena as well as in the estimates of the abundances of uranium, thorium and potassium in the earth, the following discussion of the economy of H^3, He^4 and A^{40} will be presented here from another perspective than that of the above authors, namely using a simple model of A^{40} outgassing from the earth similar to that suggested by Shillibeer and Russell (1955).

The Argon-40 Economy of the Earth

The following assumptions are used to develop the manner of production and distribution of argon-40 with time in the earth:

(1) Two phases are considered only, namely the solid earth and the combined hydrosphere and atmosphere. The model does not concern itself with the internal constitution of the earth.

(2) The constants chosen are those given in Table 1. The potassium concentration of chondrites is accepted as the abundance in the earth as a whole, following the considerations of Suess and Urey (1956), and MacDonald and Knopoff (1958), not for the mantle only. The potassium value for chondrites was taken from isotope dilution analyses of seven chondrites by Geiss and Hess (1958). Their values on chondrites also analysed by Edwards and Urey (1955) by a distillation technique agree very well although less agreement was found for achondrites. Other possible values for chondrites may be gained from the averages of analyses

presented by Edwards and Urey (1955), 850 p.p.m. (twenty-one samples); or Edwards (1955), 870 p.p.m. (twenty-one samples). Urey (1955) used 880 p.p.m. in an early paper and revised this downward to 823 p.p.m. in a later paper (Urey, 1956). I have chosen the higher value for this development.

Table 1. Constants used in this paper for the argon-40 argument

Abundance of potassium in chondrites (p.p.m.)	880
Abundance of K^{40} in chondrites (p.p.m.)	0·10472
Abundance of K^{40} in chondrites $4{\cdot}55 \times 10^9$ years ago (p.p.m.)	1·280
Mass of earth (g)	$5{\cdot}976 \times 10^{27}$
Total primordial K^{40} in earth assuming chondritic composition at $4{\cdot}55 \times 10^9$ years ago (K'_0) (g)	$7{\cdot}65 \times 10^{21}$
Branching ratio $\lambda_{E.C.}/\lambda_{\beta-} = R$	0·124
Number of A^{40} atoms in present-day atmosphere (a_2)	$9{\cdot}85 \times 10^{41}$
$K_0 = \frac{R}{1+R} K'_0$ (g)	$8{\cdot}44 \times 10^{20}$

(3) The earth is $4{\cdot}55 \times 10^9$ years old.

(4) There was very little primordial argon-40 when the earth was formed (Brown, 1952).

Using these assumptions and a degassing model the economy of argon-40 in the solid earth as a function of time can be evaluated. There will be two processes operative: (a) the production of argon-40 by the decay of potassium-40, and (b) the loss of argon-40 by escape to the atmosphere and hydrosphere. If we assume for a degassing model that the loss of argon from the solid earth obeys the equation of a first-order reaction, we can set up the differential equation describing how the argon content of the solid earth varies with time:

$$\frac{dA}{dt} = \lambda K_0 e^{-\lambda t} - \alpha A \tag{1}$$

where: A is the amount of argon in the solid earth at any time t
t is measured from the beginning of the earth ($t_0 = 0$)
λ is the decay constant for K^{40}

K_0 is equal to $\frac{R}{1+R} K'_0$

where K_0 is the primordial abundance of K^{40} in the earth and R is the branching ratio of K^{40} ($\lambda_{E.C.}/\lambda_{\beta-}$)
α is the "degassing" constant

Solving equation (1)

$$Ae^{\alpha t} = \frac{K_0}{\alpha - \lambda} e^{\alpha t} e^{-\lambda t} + C \tag{2}$$

The constant C can be evaluated since we have assumed that at $t = 0$, $A = 0$. Hence:

$$C = \frac{\lambda K_0}{\alpha - \lambda}$$

Equation (2) then becomes:

$$A = \frac{\lambda K_0}{\alpha - \lambda}(e^{-\lambda t} - e^{-\alpha t}) \tag{3}$$

It is possible now to evaluate α, the "degassing" constant since equation (3) can be evaluated for the present time. However, the method of solution is graphical and it is most convenient to express equation (3) in the following manner:

$$\frac{A}{K_0} = \frac{1}{\alpha/\lambda - 1}(e^{-\tau} - e^{-(\alpha/\lambda)\tau}) \tag{4}$$

where $\tau = \lambda t$.

Table 2 lists the values of A/K_0 determined for different values of α/λ for the present time ($t = 4{\cdot}55 \times 10^9$ years). Since the present value of A/K_0 is known to be 0·8411 (from our assumption and the abundance of argon-40 in the atmosphere), the value of α/λ is determined graphically to be 0·051. This results in a value of $\alpha = 2{\cdot}81 \times 10^{-11}$ year^{-1}.

Table 2

α/λ	A/K_0
0·01	0·9024
0·05	0·8426
0·10	0·7741
0·20	0·6533

Present day value of A/K_0, as determined from the constants of Table 1, is 0·8411 which corresponds to $\alpha/\lambda = 0{\cdot}051$.

It is now possible to determine for any desired time the argon content produced in the whole earth (a_1), the argon content of the solid earth (A), and the argon content of the atmosphere (a_2). The results of these calculations are given in Table 3.

Table 3. The abundance and distribution of A^{40} in the earth with time, "degassing constant," $\alpha = 2{\cdot}81 \times 10^{-11}$year^{-1}

Time after beginning (in 10^9 years)	a_1 (total A^{40} produced in earth $\times 10^{42}$ atoms)	A (amount of A^{40} in solid earth $\times 10^{42}$ atoms)	$a_2 = (a_1 - A)$ (amount of A^{40} in atmosphere $\times 10^{42}$ atoms)
0·5	3·078	3·059	0·019
1·0	5·418	5·338	0·078
1·5	7·192	7·028	0·164
2·0	8·540	8·270	0·270
2·5	9·564	9·172	0·392
3·0	10·342	9·817	0·525
3·5	10·932	10·267	0·665
4·0	11·382	10·569	0·813
4·5	11·722	10·761	0·961
4·55	11·752	10·773	0·979
5·0	11·982	10·869	1·113

The rate of supply of argon to the atmosphere at the present time may now be calculated. The rate of entry of A^{40} into the atmosphere at any time t is given by:

$$\frac{da_2}{dt} = K_0\lambda\left(\frac{\alpha/\lambda}{\alpha/\lambda - 1}\right)[e^{-\lambda t} - e^{-\alpha t}] \tag{5}$$

for $t = 4{\cdot}55 \times 10^9$ years

$$\left(\frac{da_2}{dt}\right)_{\text{present}} = 3{\cdot}02 \times 10^{32} \text{ atoms/year}$$

The Helium Economy of the Earth

Having obtained a value for α it is possible to make an estimate of the rate of entry of He^4 into the atmosphere at the present time. For He^4 this can be equated to the rate of loss of He^4 from the atmosphere to outer space, assuming that a steady state of entry and escape for He has been established.

The equations for the helium economy are completely analogous to the argon equations and are given below:

$$H = \frac{8\lambda_{238}U_0^{238}}{\alpha - \lambda_{238}}[e^{-\lambda_{238}t} - e^{-\alpha t}] + \frac{7\lambda_{235}U_0^{235}}{\alpha - \lambda_{235}}[e^{-\lambda_{235}t} - e^{-\alpha t}] + \\ - \frac{6\lambda_{232}\,Th_0^{232}}{\alpha - \lambda_{232}}[e^{-\lambda_{232}t} - e^{-\alpha t}] \tag{6}$$

where: H is the amount of He^4 in the solid earth at time t

$\left.\begin{matrix}\lambda_{238}\\ \lambda_{235}\\ \lambda_{232}\end{matrix}\right\}$ = the decay constants of U^{238}, U^{235}, and Th^{232}, respectively.

$\left.\begin{matrix}U_0^{238}\\ U_0^{235}\\ Th_0^{232}\end{matrix}\right\}$ = the abundance of these nuclides in the earth at the beginning of earth history.

α = degassing constant $= 2{\cdot}81 \times 10^{-11}$ year^{-1}

Similarly it is possible to write the equation for the rate of degassing of the solid earth at the present time:

the rate of degassing of He^4 from the solid earth =

$$\frac{dh_2}{dt} = 8\lambda_{238}U_0^{238}\left(\frac{\alpha/\lambda_{238}}{\alpha/\lambda_{238} - 1}\right)[e^{-\lambda_{238}t} - e^{-\alpha t}] + \\ + 7\lambda_{235}U_0^{235}\,\frac{\alpha/\lambda_{235}}{\alpha/\lambda_{235} - 1}[e^{-\lambda_{235}t} - e^{-\alpha t}] + \\ + 6\lambda_{232}Th_0^{232}\,\frac{\alpha/\lambda_{232}}{\alpha/\lambda_{232} - 1}[e^{-\lambda_{232}t} - e^{-\alpha t}] \tag{7}$$

Table 4 lists the critical values necessary to solve the above equation. The uranium and thorium values used for the total earth are those given by HAMAGUCHI *et al.* (1957) and BATE *et al.* (1957) for chondrites.

It is seen that the above calculation gives a rate of degassing for He^4 of $0{\cdot}866 \times 10^{32}$ atoms/year compared to a degassing rate for A^{40} of $3{\cdot}02 \times 10^{32}$ atoms/year.

Table 4

	Abundance $4{\cdot}55 \times 10^9$ years ago (10^{41} atoms)	(using $\alpha = 2{\cdot}81 \times 10^{-11}$ years^{-1}) present rate of degassing (atoms/year)
U^{238} $0{\cdot}1541 \times 10^{-9}$ year^{-1}	3·33	$0{\cdot}415 \times 10^{32}$
U^{235} $0{\cdot}9722 \times 10^{-9}$ year^{-1}	1·01	$0{\cdot}179 \times 10^{32}$
Th^{232} $0{\cdot}4987 \times 10^{-10}$ year^{-1}	8·38	$0{\cdot}272 \times 10^{32}$
total rate of loss at present		$0{\cdot}866 \times 10^{32}$
U content of chondrites $= 1{\cdot}1 \times 10^{-8}$ g/g		
Th content of chondrites $= 4{\cdot}3 \times 10^{-8}$ g/g		
$U^{238}/U^{235} = 137{\cdot}7$ at the present time.		

The half-life of escape of He^4 then may be calculated:

$$T_{\frac{1}{2}}(He^4) = \frac{0{\cdot}693 \times 5{\cdot}3 \times 10^{38}}{0{\cdot}866 \times 10^{32}} = 4{\cdot}24 \times 10^6 \text{ years.}$$

According to the graph used by DAMON and KULP, based on SPITZER's (1952) model, this corresponds to a "temperature" of the exosphere of 2200°K and a $T_{\frac{1}{2}}$ for He^3 of about $2{\cdot}6 \times 10^5$ years. The rate of entry of He^3 then into our atmosphere (by cosmic ray production, meteoritic accumulation, etc.) assuming a steady state is:

$$He^3 \text{ production rate} = \frac{0{\cdot}693 \times 6{\cdot}4 \times 10^{32}}{2{\cdot}6 \times 10^5} = 1{\cdot}71 \times 10^{27} \text{ atoms/year.}$$

This value may be too high, but the information on the rate of entry (by cosmic ray production in our atmosphere and meteorite accumulation) of He^3 is not good enough to decide this conclusively at present, nor is the exact manner of escape of the light gases from the earth known with certainty. Undoubtedly the accumulating rocket and satellite data will shed a great deal of light on both these processes. NICOLET (1957) discusses this point but his assumptions seem no more valid, at present, than those based on SPITZER's model because the data are not as yet sufficient to decide unequivocally. Perhaps the calculation presented may assist in eliminating or modifying one or another of several models.

It is not necessary, using the above argument, to postulate any major degassing of the earth at some remote time as suggested by DAMON and KULP (1958). With the present uncertainties in the data available, it is reasonable to postulate a continuous degassing of the earth with a calculated degassing constant of $2{\cdot}81 \times 10^{-11}$ year^{-1} by the above model.

Application to the History of the Oceans

The relationship between argon escape from the interior and the accumulation of water on the surface of the earth has been explored in an interesting paper by Kulp (1951). With the relatively poor data at his disposal at that time, Kulp was able to show that it would be possible to account for the water on the surface of the earth by the same mechanism of degassing that brought the argon-40 to the surface.

Since water at high pressures and temperatures has different properties than argon, any argument relating the two must be grossly qualitative.

Assuming, however (as is probably not the case) that argon and water have similar mobilities at the high temperatures and pressures encountered in the earth, then α for water would be the same as that calculated for argon, namely $2{\cdot}81 \times 10^{-11}$ year^{-1}.

Using this constant and the present amount of water on the surface of the earth, in the hydrosphere, atmosphere and sediments, calculated by Poldervaart (1955) to be 1644×10^{21} g, we can estimate the water concentration of the earth $4{\cdot}55 \times 10^9$ years ago by the equation:

$$W_0 = \frac{W_H}{(1 - e^{-\alpha t})}$$

where

$W_H = 1644 \times 10^{21}$

$\alpha = 2{\cdot}81 \times 10^{-11}$ year^{-1}

$t = 4{\cdot}55 \times 10^9$ year

$W_0 =$ the amount of water at $t = 0$ in the earth.

Solving this equation $W_0 = 1370 \times 10^{22}$ g. To get this in terms of parts per million water in the entire earth, it is necessary to divide by the mass of the earth (from Table 1). This gives a primordial water concentration of the solid earth equal to 2300 p.p.m. This number can be compared with the average water content of chondrites from Wiik (1956) which is 2650 p.p.m.

The small size of α indicates that on the above assumption the earth has been releasing water to the hydrosphere at an approximately slow constant rate for the last $4{\cdot}55 \times 10^9$ years.

Summary

(1) On the basis of a model of a continuously degassing earth, using the potassium content of chondrites as representative of the total earth and an age of the earth of $4{\cdot}55 \times 10^9$ years, the "degassing" constant, α, for the earth has been calculated to be $2{\cdot}81 \times 10^{-11}$ year^{-1}.

(2) The above assumptions lead to a present day rate of argon loss from the solid earth to the atmosphere of $3{\cdot}02 \times 10^{32}$ atoms/year.

(3) Assuming that α is applicable to helium as well as argon and using the current values of uranium and thorium in chondrites as representative of the total earth, the present-day rate of He^4 degassing is calculated as $0{\cdot}866 \times 10^{32}$ atoms/year.

(4) The corresponding He^3 entry rate into the atmosphere is calculated to be $1{\cdot}71 \times 10^{27}$ atoms/year, using SPITZER's model of gas loss at the base of the exosphere.

(5) Assuming that α holds as well for water loss from the solid earth to the hydrosphere, the primordial water concentration of a solid earth devoid of a primitive hydrosphere is 2300 p.p.m. This is similar to the current value for the water content of chondrites (2650 p.p.m.).

(6) The small size of α also postulates an approximately constant rate of water supply to the hydrosphere over the last $4{\cdot}55 \times 10^9$ years.

References

BATE G. L., HUIZENGA J. R. and POTRATZ H. A. (1957) Thorium content of stone meteorites. *Science* **126**, 612–614.

BROWN H. (1952) Rare gases and the formation of the Earth's atmosphere. *The Atmospheres of the Earth and Planets* (Edited by KUIPER G. P.) pp. 258–266. Chicago.

DAMON P. E. and KULP J. L. (1958) Inert gases and the evolution of the atmosphere. *Geochim. et Cosmochim. Acta* **13**, 280–292.

EDWARDS G. (1955) Sodium and potassium in meteorites. *Geochim. et Cosmochim. Acta* **8**, 285–294.

EDWARDS G. and UREY H. C. (1955) Determination of alkali metals in meteorites by a distillation process. *Geochim. et Cosmochim. Acta* **7**, 154–168.

GEISS J. and HESS D. C. (1958) Argon-potassium ages and the isotopic composition of argon from meteorites. *Astrophys. J.* **127**, 224–236.

HAMAGUCHI H., REED G. W. and TURKEVICH A. (1957) Uranium and barium in stone meteorites. *Geochim. et Cosmochim. Acta* **12**, 337–347.

KULP J. L. (1951) Origin of the hydrosphere. *Geol. Soc. Amer. Bull.* **62**, 326–329.

MACDONALD G. F. J. and KNOPOFF L. (1958) On the chemical composition of the outer core. *Geophys. J.* **1**, 284–297.

NICOLET M. (1957) The aeronomic problem of helium. *Ann. Geophys.* **13**, 1–21.

POLDERVAART A. (1955) *Chemistry of the Earth's Crust.* Geol. Soc. Amer. Spec. Paper 62, 119–144.

SHILLIBEER H. A. and RUSSELL R. D. (1955) The argon-40 content of the atmosphere and the age of the earth. *Geochim. et Cosmochim. Acta* **8**, 16–21.

SPITZER L., JR. (1952) The terrestrial atmosphere above 300 km. *The Atmospheres of the Earth and Planets* (Edited by KUIPER G. P.) pp. 211–247. Chicago.

SUESS H. E. and UREY H. C. (1958) Abundances of the elements. *Rev. Mod. Phys.* **28**, 53–74.

UREY H. C. (1955) The cosmic abundances of potassium, uranium, and thorium and the heat balances of the Earth, the Moon, and Mars. *Proc. Nat. Acad. Sci., Wash.* **41**, 127–130.

UREY H. C. (1956) The cosmic abundances of potassium, uranium, and thorium and the heat balances of the Earth, the Moon, and Mars. *Proc. Nat. Acad. Sci., Wash.* **42**, 889–891.

WIIK H. B. (1956) The chemical composition of some stony meteorites. *Geochim. et Cosmochim. Acta* **9**, 279–289.

Geochimica et Cosmochimica Acta, 1959, Vol. 17, pp. 44 to 52. Pergamon Press Ltd. Printed in Northern Ireland

Silver content of igneous rocks

H. Hamaguchi and R. Kuroda
Department of Chemistry, Faculty of Science, Tokyo University of Education, Tokyo, Japan

(*Received* 8 *December* 1958)

Abstract—The following averages of silver for various types of Japanese igneous rocks have been obtained (in p.p.m.): granites 0·037, granodiorites 0·050, liparites 0·049, quartz diorites and diorites 0·053, silicic andesites and andesites 0·080, basalts 0·11, diabases 0·12, gabbros 0·11 and ultramafic rocks 0·060. The crustal abundance of silver is estimated to be 0·08 p.p.m.

Introduction

At present no reliable value for the average content of silver in various types of igneous rocks is available. The present paper supplies data on the silver contents of igneous, some sedimentary and some metamorphic rocks to supplement the scant available data. In classic papers Lunde (1927) and Lunde and Johnson (1928) reported up to 2·1 p.p.m. Ag in dunite, 9·4 p.p.m. Ag in peridotite and 0·3 p.p.m. Ag in eclogite. According to Clarke (1924), Wagoner found the following values for silver in some types of igneous rocks collected at points remote from known deposits of heavy metals:

	(p.p.m.)
3 granites, California	7·66, 1·22, 0·94
granite, Nevada	5·59
syenite, Nevada	15·43
basalt, California	0·55
diabase, California	7·44

These classic data are remarkably high probably because, in part, of some defect in the analytical methods used.

Goldschmidt (1926) found an average value of 0·12 p.p.m. Ag for the alkalic igneous rocks of the Oslo province. Goldschmidt and Peters (1932) also reported 0·5 p.p.m. Ag for a norite. Recently, Fairbairn *et al.* (1953) have reported the trace elements contents of fifty nine Ontario diabases and detected silver only in thirty-two Nipissing type diabases, the silver contents of which ranged from 0·9 to 7·6 p.p.m., averaging 4 p.p.m. Since the Nipissing type diabases are accompanied with high-grade silver veins in the Cobalt district, the figure given by them for the diabases may not be considered as the representative of common mafic rocks.

The average of silver in igneous rocks was estimated to be 0·1 p.p.m. by Goldschmidt (1937).

Analytical Method

The procedure for silver in silicate rocks has been described in detail (Hamaguchi and Kuroda, 1957). It consists in decomposition of 1 g of sample with perchloric-hydrofluoric acids, precipitation of silver by stannous chloride from

2 N hydrochloric acid solution in the presence of tellurium as a collector and final spectrochemical determination using indium as an internal standard. An Adam Hilger E_2 spectrograph was used. The analysis line pair was Ag 3280·68/In 3256·09. According to a careful check of the procedure, both the precision and the accuracy of the method were estimated to be ±18 per cent. The average sensitivity limit was 0·02 p.p.m. Ag with respect to 1 g of sample.

Analytical Results

The results of the analyses appear in Tables 1 to 5, expressed in parts per million to two significant figures.

Table 1. Silver in silicic rocks

Rock mark	Sample	Ag (p.p.m.)
DA 59	Granite, Dando, Aichi Prefecture	0·030
JO 1	Granite, Numata, Joetsu district	0·036
SO 94	Granite, Soma, Abukuma district	0·034
ER 21	Granite, Kashio, Nagano Pref.	0·032
Okada	Granite, Chuai Tunnel, Miyako, Fukuoka Pref.	0·042
Okada	Granite, Matsuyama, Ehime Pref.	0·042
Okada	Granite, Kabe, Hiroshima Pref.	0·040
SH 139	Aplite, Hidaka, Hokkaido	0·00
JO 98	Granodiorite, Shimizu Tunnel, Gumma Pref.	0·040
SO 172	Granodiorite, Soma, Abukuma district	0·050
HT 95	Granodiorite, Hitachi, Abukuma district	0·034
SH 124	Granodiorite, Hidaka, Hokkaido	0·054
SH 126	Granodiorite, Hidaka, Hokkaido	0·040
SH 140	Granodiorite, Hidaka, Hokkaido	0·066
SH 138	Granodiorite, Hidaka, Hokkaido	0·060
DA 23	Granodiorite, Dando, Aichi Pref.	0·080
DA 43	Granodiorite, Dando, Aichi Pref.	0·046
DA 57	Granodiorite, Dando, Aichi Pref.	0·060
DA 41	Granodiorite, Dando, Aichi Pref.	0·042
SO 106	Granodiorite, Soma, Abukuma district	0·040
FT 89	Granodiorite, Futaba, Abukuma district	0·047
FT 70	Granodiorite, Futaba, Abukuma district	0·070
HT 96	Granodiorite, Hitachi, Abukuma district	0·040
ER 38	Granodiorite, Takato, Nagano Pref.	0·046
	Granodiorite, Takato, Nagano Pref.	0·046, 0·046, 0·040
ER 59	Granodiorite, Takato, Nagano Pref.	0·060
ER 60	Granodiorite, Takato, Nagano Pref.	0·050
ER 185	Granodiorite, Middle basin of the Tenryu River	0·054
ER 123	Granodiorite, Middle basin of the Tenryu River	0·062
Hananoki	Granodiorite, Middle basin of the Tenryu River	0·090, 0·090
UD 30	Granodiorite, Ueda, Nagano Pref.	0·040
UD 39	Granodiorite, Ueda, Nagano Pref.	0·042
Okada	Granodiorite, Matsuyama, Ehime Pref.	0·020
Okada	Granodiorite, Kabe, Hiroshima Pref.	0·056
Okada	Granodiorite, Sachiyama, Miyako, Fukuoka Pref.	0·030
JO 117	Liparite, Joetsu district	0·040
N 14	Liparite, Nijosan, Nara Pref.	0·025
G 1034	Liparite, Tobishima, Yamagata Pref.	0·090
G 1256	Liparite, Naruko, Miyagi Pref.	0·042

Table 2. Silver in intermediate rocks

Rock mark	Sample	Ag (p.p.m.)
TK 72	Quartzdiorite, Tanakura, Abukuma district	0·034
ER 18	Quartzdiorite, Kashio, Nagano Pref.	0·060, 0·050
GT 127	Diorite, Takanuki, Abukuma district	0·050
GT 148	Diorite, Takanuki, Abukuma district	0·020
ON 44	Diorite, Ononiimachi, Abukuma district	0·055
SO 95	Diorite, Soma, Abukuma district	0·050
SO 149	Diorite, Soma, Abukuma district	0·085
18	Diorite, Hidaka, Hokkaido	0·070
MT 132	Pitchstone, Uchimura district, Nagano Pref.	0·054
MT 484	Silicic andesite, Uchimura district, Nagano Pref.	0·050
White	Silicic andesite, Tsuchizukayama, Nara Pref.	0·040
MT 213	Silicic andesite, Uchimura district, Nagano Pref.	0·090
OM 13	Dacite, Ohmachi, Nagano Pref.	0·034
47121401a	Garnet–biotite–dacite, Nijosan, Nara Pref.	0·066
East	Dacite, Mt. Amagi, Shizuoka Pref.	0·060
	Dacite, Myojin Reef, Izu Islands	0·070
G 1025	Pyroxene dacite, Kamitaga, Shizuoka Pref.	0·042
G 1061	Dacite, Mizunami, Gifu Pref.	0·19
G 1062	Dacite, Mizunami, Gifu Pref.	0·090
Akagi	Hyalodacite, Mt. Akagi, Shizuoka Pref.	0·040
15249	Pitchstone, Shikine Isle, Izu Islands	0·15
G 1021	Pitchstone, Horaijisan, Aichi Pref.	0·15
	Obsidian, Wada pass, Nagano Pref.	0·030
MT 506	Andesite, Uchimura, Nagano Pref.	0·10, 0·094, 0·094
N 144	Garnet–biotite–andesite, Nijosan, Nara Pref.	0·050
MT 256	Andesite, Uchimura, Nagano Pref.	0·12
MT 264	Andesite, Uchimura, Nagano Pref.	0·085
N 147	Andesite, Nijosan, Nara Pref.	0·093
	Hornblende–hypersthene–andesite, Nijosan, Nara Pref.	0·090
G 1036	Andesite, Tobishima, Yamagata Pref.	0·050
G 1194	Andesite, Mt. Yatsugatake, Nagano Pref.	0·055
G 1195	Andesite, Mt. Yatsugatake, Nagano Pref.	0·12

Discussion

There is a scarcity of reliable information on the silver content of igneous rocks. Because of the extremely low concentrations of silver in common igneous rocks, it is usually impossible to determine this element directly in a variety of igneous rocks even with sensitive spectrochemical procedures. It is sometimes asserted that silver can be detected spectrochemically in mafic rocks. However, such information may be restricted to special types of rocks of some silver-rich provinces (e.g. Ishikawa and Kuroda, 1958), and furthermore, careful attention must be given to the electrode purity or accidental contamination to ensure the detection of traces of silver in spectrographic analyses.

In the present work, silver in rocks was first enriched five hundred times and

Table 3. Silver in mafic and ultramafic rocks

Rock mark	Sample	Ag (p.p.m.)
	Basalt, Mt. Miharayama, Oshima Island	0·15, 0·17
G 1032	Basalt, Kiyosegawa, Aomori Pref.	0·10, 0·11
G 1030	Basalt, Otose, Aomori Pref.	0·19
G 1099	Basalt, Matsue, Shimane Pref.	0·15
G 1031	Basalt, Takao-san, Nagano Pref.	0·050, 0·070
G 1023	Basalt, Ajiro, Izu, Shizuoka Pref.	0·050, 0·042
G 1033	Basalt, Aomori Pref.	0·090, 0·070
HK 51122003	Olivine basalt, Shibayama, Nara Pref.	0·070
TZ 17	Diabase, Tanzawa, Kanagawa Pref.	0·11
TZ 29	Diabase, Tanzawa, Kanagawa Pref.	0·14
TZ 48	Diabase, Tanzawa, Kanagawa Pref.	0·13
TZ 31	Diabase, Tanzawa, Kanagawa Pref.	0·12
G 1265	Diabase, Shimizu Tunnel, Gumma Pref.	0·080
GT 149	Gabbro, Takanuki, Abukuma district	0·12
Mikabu	Gabbro, Takanuki, Abukuma district	0·14
TK 58	Gabbro, Tanakura, Abukuma district	0·12
G 1120	Gabbro, Miyamori, Iwate Pref.	0·068
SH 135	Picrite Gabbro, Hidaka, Hokkaido	0·11
G 1009	Serpentinite, Tosayama, Kochi Pref.	0·060
G 1119	Peridotite, Miyamori, Iwate Pref.	0·080
SH 178	Peridotite, Hidaka, Hokkaido	0·054
SH 176	Peridotite, Hidaka, Hokkaido	0·080
TA 4	Cortlandite, Miharu, Abukuma district	0·030

then determined spectrographically, so that a satisfactory sensitivity was obtained for traces of silver in a variety of rocks.

Individual samples have been analysed to obtain average figures of silver in common igneous rock types. Averages for silicic rocks are summarized as follows:

	(p.p.m.)
granites (7 samples)	0·037
granodiorites (27 samples)	0·051
liparites (4 samples)	0·049
all silicic rocks (39 samples*)	0·046

* Aplite included

Although the distinction between granite and granodiorite is rather obscure, granitic rocks having colour indices less than 10 per cent were conventionally classified as granite, and those whose colour indices range from 10 to 24 per cent as granodiorites.

The granite and granodiorite averages (0·037 and 0·051 p.p.m.) do not differ from their volcanic equivalent liparite, average 0·049 p.p.m.

Table 4. Silver in miscellaneous rocks

Rock mark	Sample	Ag (p.p.m.)
44	Slate, Okaya, Nagano Pref.	0·060
Okada	Slate, Kesen-gun, Iwate Pref.	0·060
5	Contact slate, Yanai, Yamaguchi Pref.	0·033
SH 150	Hornfels, Hidaka, Hokkaido	0·11
SH 115	Hornfels, Hidaka, Hokkaido	0·12
Okada	Hornfels, locality unknown	0·060
SH 162	Coarse migmatite (granodioritic), Hidaka, Hokkaido	0·026
O–257	Coarse migmatite (granodioritic), Hidaka, Hokkaido	0·065
SH 164	Fine migmatite (quartzdioritic), Hidaka, Hokkaido	0·064
SH 159	Fine migmatite (granodioritic), Hidaka, Hokkaido	0·066
	Composite of 6 samples of migmatitic intrusive type of granite, Ryoke metamorphic region, Nagano Pref.	0·040, 0·050
DA 29	Granitized diabase, Dando, Aichi Pref.	0·060
DA 47	Granitized diabase, Dando, Aichi Pref.	0·050
	Composite of granitized diabases, Dando, Aichi Pref.	0·033
ER 172	Granite vein in the Ryoke–biotite–gneiss, middle basin of the Tenryu River	0·040
ER 179	Granite vein in the Ryoke–biotite–gneiss, middle basin of the Tenryu River	0·028
ER 171	Granite vein in the Ryoke–biotite–gneiss, middle basin of the Tenryu River	0·034
ER 182	Concordant aplitic thin sheet in the Ryoke gneiss, middle basin of the Tenryu River	0·034
GT 113L	Granitic vein in banded gneiss, Abukuma district	0·020
ER 79L	Granitic vein in banded gneiss, Takato, Nagano Pref.	0·070
ER 101L	Granitic vein in banded gneiss, Takato, Nagano Pref.	0·090

Table 5. Silver in marine sediments

	Location		Depth (m)	Ag (p.p.m.)
composite of blue mud	41°24·0′N	131°53·0′E	3394	0·10
	41°11·6′N	132°4·2′E	3417	
	39°49·5′N	133°15·6′E	1622	
	38°34·0′N	133°41·7′E	1350	
blue mud	38°45·2′N	134°11·0′E	1605	0·15

Average figures for intermediate rocks are as follows:

	(p.p.m.)
quartzdiorites and diorites (8 samples)	0·052
silicic andesites and andesites (24 samples)	0·080
all intermediate rocks (32 samples)	0·073

There is some indication that the intermediate volcanic rocks tend to show somewhat higher value than their plutonic equivalents. Mafic and ultramafic rocks give the following averages:

	(p.p.m.)
basalts (8 samples)	0·10
diabases (5 samples)	0·12
gabbros (5 samples)	0·11
all mafic rocks (18 samples)	0·11
ultramafic rocks (5 samples)	0·060

Ultramafic rocks seem to be a little lower in silver than the mafic rocks. In each rock type, the variations of silver content are relatively small. Silver seems to show preference for mafic rocks (average 0·11 p.p.m.). As mentioned above, the Nipissing type Ontario diabases are extremely high in silver (average 4 p.p.m.), and this is probably due to silver mineralization.

The frequency distributions of silver in granitic, intermediate, and mafic rocks are shown in Figs. 1 to 3. The distribution patterns of silver for granitic and intermediate rocks show a sign of positive skewness, whereas that for mafic rocks does not show any skewness, although the number of analyses is comparatively small.

Judging from the distribution of silver in magmatic rocks, it may be reasonably stated that silver concentrates preferentially into early crystallizates during magmatic differentiation. A trace element in a series of magmatic rocks is usually present either in independent minerals, or at a lattice site of the principal rock-forming minerals. Ringwood (1955) postulated a diadochy between silver and potassium, and expected from the stand-point of electronegativity that silver must be concentrated in later differentiates during magmatic crystallization as compared with potassium. For the following discussions some physical constants are summarized below:

Ion	Radius (Å)	Electronegativity	Ioniz. potential (eV)	F-value (I/R)
Ag^+	1·26	1·8	7·57	6·0
K^+	1·33	0·8	4·34	3·3

According to the Ringwood's rule, where diadochy occurs between Ag^+ and K^+ ions, K^+ ion with the lower electronegativity will be preferentially incorporated because K^+ ion forms a stronger and more ionic bond than Ag^+ ion. Evidently this situation is entirely contrary to the present information on the distribution

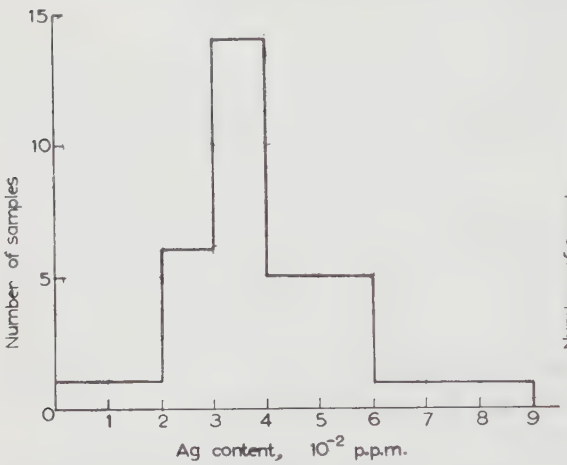

Fig. 1. Frequency distribution of silver in granitic rocks (including one aplite).

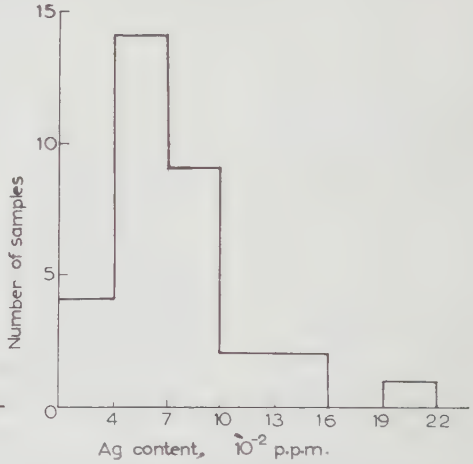

Fig. 2. Frequency distribution of silver in intermediate rocks (all rocks listed in Table 2 included).

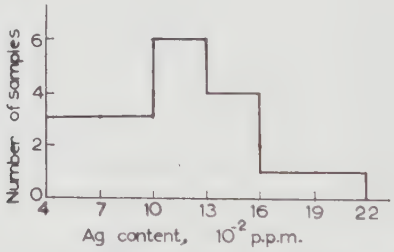

Fig. 3. Frequency distribution of silver in mafic rocks (basalt, diabase and gabbro).

behaviour of silver in magmatic rocks. On the other hand, the well-known Goldschmidt's rule suggests that Ag ion with smaller radius must be preferentially incorporated in the early crystallizates. According to the Field Function Concept of Ahrens (1953), when Ag^+ and K^+ ions, which have the same valence and similar radii, compete for a given structure site in a growing crystal Ag^+ ions with the greater electric intensity should arrive first. The latter two rules fit well the the actual behaviour of silver in igneous rocks. The Ringwood's rule, however, takes account of the chemical bond factor and may be regarded as a more general one than Goldschmidt's rules, which are usually applicable when diadochy occurs between the elements possessing similar electronegativities. Ahrens' rule has also some restriction, as indicated by Ringwood (1955). Thus, the discrepancy met in the explanation of the actual behaviour of silver in igneous rocks may be considered as due to the assumption that the Ag^+ ion is incorporated in the structural site of silicate crystals. A strong possibility may be suggested that silver is not

incorporated in silicate minerals, but exclusively in sulphide minerals or precipitates as independent sulphide minerals. Forland and Weyl (1949) have already pointed out that highly polarizing cations possessing non-noble gas electron configurations will combine preferentially with any sulphur in silicate melts, forming either discrete non-polar molecules, or precipitating as separate sulphide crystals. Although the sulphur content of magmas is relatively low, usually nearly all of the sulphur combines with highly polarizing abundant Fe^{2+} ions. Thus, pyrite (FeS_2) is the most abundant sulphide mineral of normal igneous rocks. The small amount of sulphur must be preferentially taken up with Cu^{2+} and Ag^{+} ions, both of which possess higher affinity for sulphur. Apparently, this process should occur during early stages of magmatic differentiation, and thus effective concentration of copper and silver must decrease toward the later stages of the differentiation. In fact, high silver content of composite of 57 magmatic sulphides (10 p.p.m. Ag) has been reported by Noddack and Noddack (1931). According to Rankama (1950), Joensuu (1948) also found that 79 accessory chalcopyrites from different igneous and metamorphic rocks of the Pre-Cambrian formations in Finland contain, as an average, about 200 p.p.m. Ag. From these figures the strong sulphophile character of silver is also indicated.

Table 4 lists the silver contents of miscellaneous materials. Migmatites listed have granite-like appearance and have been considered as the products of granitization; their silver content does not differ much from those of the intrusive granitic rocks listed in Table 1. The average silver content of one blue mud composite representing four individual samples and one individual blue mud from the Japan Sea are 0·10 and 0·15 p.p.m., respectively. As the present analytical method is not applicable to manganese-rich materials, red clays were not analysed. Averages by Goldschmidt (1926) for deep-sea sediments and terrigenous sediments, western coast of South Africa, are 0·11 and 0·66 p.p.m., respectively. Goldschmidt and Peters (1932) found 1 p.p.m. of Ag in a manganese nodule. From these values it may be pointed out that marine sediments tend to be rich in silver compared to igneous rocks.

Finally, a computation is carried out to obtain an approximate figure for the crustal abundance of silver. It must be noted that in the present work the available samples were completely restricted to Japanese igneous rocks. The averages presented here may not be representative for the corresponding types of igneous rocks elsewhere. Therefore, it must be assumed that there is no marked difference between averages for the same type of igneous rocks from different regions, so long as silver mineralization does not accompany the rocks. Furthermore, the crustal composition differs much for the continental and oceanic regions, but it may be of interest to obtain an approximate value of silver by assuming again that the average crust is composed of equal portions of the continental and oceanic crusts. The continental crust is estimated to consist of five parts of granitic (and granodioritic) and one part of basaltic rocks. Thus an average of 0·058 p.p.m. Ag is obtained for the continental crust. The figure for the oceanic crust is assumed to be the same as the value for the basaltic average, i.e. 0·10 p.p.m. Ag. The mean crustal abundance of silver is calculated as

$$(0{\cdot}058 + 0{\cdot}10) \times 1/2$$

giving 0·079 p.p.m. Ag. This tentative value is somewhat lower than the average for igneous rocks given by Goldschmidt (1937).

Acknowledgements—We are indebted to Professor Dr. M. Gorai, Geological Institute, Tokyo University of Education, for placing numerous rock samples at our disposal and invaluable suggestions during the course of the study. Our thanks are also due to Dr. H. Onishi, Japan Atomic Energy Research Institute, for useful discussions, and to Dr. H. Ishikawa, Kagoshima University, and Dr. S. Okada, Atomic Fuel Corporation, for a number of Japanese igneous rocks.

References

Ahrens L. H. (1953) Anion affinity and geochemistry. *Geochim. et Cosmochim. Acta* **3,** 1–29.

Clarke F. W. (1924) *The Data of Geochemistry* (5th Ed.); *U. S. Geol. Survey Bull.* 770, 657.

Fairbairn H. W., Ahrens L. H. and Gorfinkle L. G. (1953) Minor element content of Ontario diabase. *Geochim. et Cosmochim. Acta* **3,** 34–46.

Forland T. and Weyl W. A. (1949) Distribution of heavy metal ions in silicates containing several ions of different sizes. *J. Amer. Ceram. Soc.* **32,** 267–272.

Goldschmidt V. M. (1926) Probleme und Methoden der Geochemie. *Gerlands Beitr. Geophys.* **15,** 38.

Goldschmidt V. M. (1937) Die Mengenverhältnisse der Elemente und der Atom-Arten. *Skr. Norske VidenskAkad. Mat.-Nat. Kl.* No. 4, 1–148.

Goldschmidt V. M. and Peters C. L. (1932) Zur Geochemie der Edelmetalle. *Nachr. Ges. Wiss. Göttingen, Mat.-Phys. Kl. III,* **24;** *IV,* **26,** 377–401.

Hamaguchi H. and Kuroda R. (1957) Determination of traces of silver in silicate rocks. *Nippon Kagaku Zasshi* **78,** 1668–1671.

Ishikawa H. and Kuroda R. (1958) Die Verteilung des Silbers in den umgewandelten Zonen der Nebengesteinen von einiger "Schwarzerz"-Lagerstätten in Japan. *J. Soc. Min. Geol. Japan* **8,** 82–83.

Lunde G. (1927) Über das Vorkommen des Platins in norwegischen Gesteinen und Mineralen. *Z. anorg. Chem.* **161,** 1–20.

Lunde G. and Johnson M. (1928) Vorkommen und Nachweis der Platinmetalle in norwegischen Gesteine. II. *Z. anorg. allgem. Chem.* **173,** 167–195.

Noddack I. and Noddack W. (1931) Die Geochemie des Rheniums. *Z. phys. Chem.* A **154,** 207–244.

Rankama K. and Sahama T. G. (1950) *Geochemistry* p. 99.

Ringwood A. E. (1955) The principles governing trace element distribution during magmatic crystallization. *Geochim. et Cosmochim. Acta* **7,** 189–202.

Geochimica et Cosmochimica Acta, 1959, Vol. 17, pp. 53 to 107. Pergamon Press Ltd. Printed in Northern Ireland

The zeolite facies, with comments on the interpretation of hydrothermal syntheses

D. S. Coombs, A. J. Ellis,* W. S. Fyfe and A. M. Taylor
Departments of Geology and Chemistry, University of Otago, New Zealand

(*Received* 20 *September* 1958)

Abstract—Field, petrographic and experimental evidence is presented on assemblages involving Ca–Al and Na–Al silicates, warranting recognition of a zeolite facies. This facies largely bridges the gap between diagenesis and conventional metamorphism. The metamorphic geology of the New Zealand Geosyncline is reviewed and zeolite facies rocks are shown to be of regional extent. They include lower grade heulandite–analcime–quartz assemblages and higher grade laumontite–albite–quartz in tuffs and volcanic greywackes. Thomsonite is found in basic igneous rocks of the Otama Complex. Separating the zeolitic rocks from typical greenschists is a broad belt with quartz–prehnite and quartz–pumpellyite assemblages.

The significance of zeolite sequences in amygdales is often a matter of doubt, but zeolite occurrences in sedimentary rocks, active thermal areas, alkaline igneous rocks and miscellaneous joints and cavities lend some support to two broad generalizations: firstly the water content relative to $(Ca,Na_2)O.Al_2O_3$ tends to increase for lower temperatures of formation in accordance with theoretical expectations based on entropy; secondly zeolites can be divided into three groups based on silica content: those whose occurrence is favoured by an environment supersaturated in silica, those that often coexist with quartz, and those favoured by silica-deficient environments.

The common species in the Wairakei thermal area are mordenite and wairakite, both of which are readily synthesized whereas laumontite and heulandite, typical of regional metamorphism, are not readily synthesized. This fact, together with the profound influence of starting materials on reaction products in hydrothermal syntheses, emphasizes the lack of equilibrium in our experiments, even in runs of 30 days. The field of high-silica phases such as mordenite is extended when the silica activity is higher than that of quartz. The effect of differing P_{load} and P_{H_2O} on important transitions such as analcime + quartz = albite + water is explored on theoretical grounds. Experiments place the reaction temperature at 280°C at 1000 bars water pressure, but the equilibrium temperature may be much lower. Preliminary solubility work indicates a reaction temperature near 200°C at saturated water vapour pressure. Under conditions where load pressure equals three times the water pressure the temperature may be lowered by about 200°C. The upper limit of the zeolite facies is believed to be about 300°C, when water and load pressures are approximately equal.

Fields of synthesis are given for the following: analcime–wairakite series, Na–Ca mordenite series, epistilbite, prehnite and an unidentified phase *Z*. Phillipsite was synthesized from chabazite. The upper limit of thomsonite is considered to be near 300°C where it breaks down to anorthite.

The range of composition and density of naturally-occurring zeolites is reviewed. New analyses and optical data are given for heulandite from Cape Blomidon, Nova Scotia, and for prehnite from Prospect Quarry, New South Wales.

1. Introduction

(W. S. F., D. S. C.)

The writers consider that mineral assemblages in which zeolites are characteristic are of such widespread occurrence that a new mineral and metamorphic facies, the zeolite facies, should be recognized, as has recently been proposed by Turner (in Fyfe *et al.*, 1958). Field and laboratory studies indicate that the range of conditions under which the mineral assemblages of this facies form are at least as extensive as for other recognized major facies. The zeolite facies bridges a wide gap between sedimentary processes and the hitherto recognized metamorphic facies and it allows a more complete model of the evolution of metamorphic rocks in progressive regional metamorphism to be developed.

* Now at Dominion Laboratory, D.S.I.R., Wellington.

Turner wrote as follows: "Eskola (1939, p. 345) discussed the possibility of erecting a zeolite facies to include the many and varied assemblages of zeolites and associated minerals formed by deuteric and hydrothermal processes at low pressures and relatively low temperatures. He rejected the idea, however, on the supposition that such assemblages do not represent systems in equilibrium. He noted, moreover, that because of their hydrothermal origin, their nature 'depends largely upon the composition, reaction and concentration of the introduced solution'." Largely on the basis of field and petrographic studies in southern New Zealand (Coombs, 1954) Turner then proceeded to revive the "zeolitic facies" (hereinafter referred to as the zeolite facies) "to cover only regionally developed zeolitic assemblages that largely replace the pre-existing rocks and conform to the mineralogical and chemical requirements of a metamorphic facies as specified in Chapter I."

The purpose of this paper is to present field and laboratory evidence bearing on this problem, to explore the extent to which equilibrium is attained, and to suggest that the facies concept can justifiably be extended to the zones of diagenesis and low grade metamorphism.

Irrespective of the exact definition that is used for a metamorphic facies, in our view the stimulus and long-range value of the facies concept rests in the belief that, in time, the physicochemical conditions under which a rock of given bulk composition forms a given assemblage of minerals will be determined within definite limits.

If we wish to follow, say, the complete evolution of a granulite from an unmetamorphosed sediment, we must be prepared to examine each stage in the process and to recognize as markers each observable change of phase. This has been done in some detail for transitions from greenschist assemblages onwards, but lower grades have not been widely recognized.

Fyfe (1955a) suggested that it was unlikely that greenschists would form much below 300°C. If there is any substance in this view, then, for so long as we ignore this gap of 300°, we are ignoring about one-third of the possible thermal range of normal regional metamorphism. Field and laboratory evidence, imperfect as they may be, indicate that this neglect is not justifiable and that a large number of important phase changes may occur in this temperature interval. Zeolites are sometimes major rock-forming minerals and show a significant number of such phase changes.

In considering any facies covering the lowest grades of metamorphism it is obvious that certain difficulties will arise which may be less apparent in higher grades. First, at low temperatures, the replacement of pre-existing minerals will tend to be a slow process and may not reach completion.* The second difficulty arises from the fact that in low-temperature environments metastable phases may have a considerable chance of formation and survival. In the task of reconstructing

* Partly for this reason it is convenient to consider some zeolitic rocks in terms of the mineral facies concept (Eskola, 1920, pp. 145–146), rather than in terms of metamorphic facies, the assemblage of coexisting minerals concerned forming perhaps an interstitial microaggregate in a sediment or a single zone in an amygdale. On the other hand some of the rocks described can appropriately be considered metamorphic in the sense that they are extensively or even completely reconstituted.

a history it may often be possible to draw interesting conclusions from the occurrence of a metastable phase, but kinetic factors must lead to a large degree of uncertainty. For the correlation of physical environment with mineral assemblage to be approached with any certainty, some assurance that equilibrium has been approached is necessary. In the review that follows it will become apparent that similar zeolite-bearing assemblages do in fact appear to form in similar environments. It also appears probable that in some circumstances metastable growth takes place in nature under conditions that may be comparable with those produced in the laboratory.

On the basis of widespread occurrence of zeolitic cements in Russian sedimentary rocks (reviewed below) RENGARTEN (1950) proposed a "geochemical zeolite facies." It was suggested that rather special chemical conditions including the presence of alkaline, colloidal solutions of silica and alumina and a high oxygen potential were necessary for zeolitization to occur. The oxygen potential was believed to distinguish the zeolite facies from a glauconite facies although zeolites and glauconite have subsequently been shown to coexist (BUSHINSKY, 1950; VASIL'EV, 1954). We do not believe that RENGARTEN's views were justified.

2. The Zeolite Facies in the New Zealand Geosyncline and the Transition to the Greenschist Facies
(D. S. C.)

2.1. *Geological setting: the New Zealand Geosyncline* (Fig. 1)

The dominant structural features of New Zealand geology are those related to the New Zealand Geosyncline (WELLMAN, 1956), in which deposition proceeded from pre-Permian times well into the Jurassic. In Otago, early greywackes, siltstones and occasional volcanics of the geosyncline have been metamorphosed into the extensive chlorite-zone schists, made well-known through the work of TURNER (1938) and HUTTON (1940). These schists continue northwards as a narrow belt, the "Alpine Schists," on the western flanks of the Southern Alps. At the south end of this belt, TURNER (1933) established chlorite, biotite and oligoclase zones, while further north in the Franz Josef–Copland River sector LILLIE and MASON (1955) have mapped chlorite, biotite and garnet zones. Boulders of kyanite gneiss in Paringa River and at Hunts Beach to the west have been collected by ODELL (personal communication), and suggest that kyanite-zone conditions were attained at least locally. The Alpine Schists grade progressively eastwards into "unmetamorphosed" (prehnite-zone) greywackes described below.

In the southern part of the South Island, the schist belt strikes south-east and is flanked on its south-west side, and apparently overlaid, by folded and steeply-dipping Upper Paleozoic greywackes, siltstones and some volcanics, the thickness of which is given by WOOD (1956) as being greater than 36,500 ft. The Upper Paleozoic rocks are in turn overlaid by Triassic and Jurassic beds in the Southland Syncline which includes at Taringatura the area that prompted TURNER's re-erection of the zeolite facies. The Triassic sediments vary in thickness along the north limb of the syncline from about 10,000 to 30,000 ft (COOMBS, 1950), but they are much thinner where exposed on the south limb (WOOD, 1953). The thickness

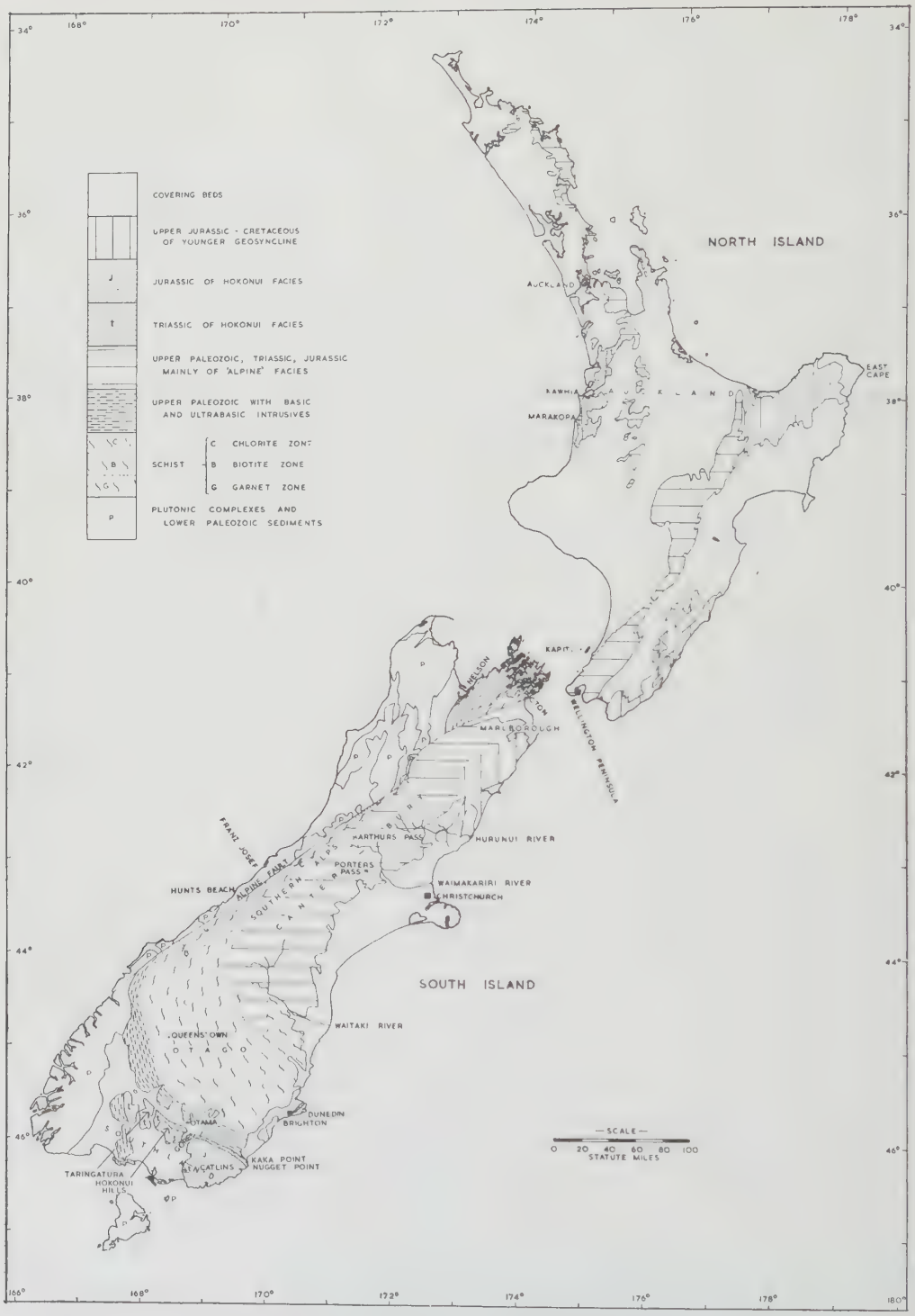

Fig. 1. Geological sketch map showing rocks of the New Zealand Geosyncline (Based on Wellman, 1956, and on the 1 : 2,000,000 geological map of New Zealand, N.Z. Geological Survey, 1958).

of the Jurassic beds is commonly about 10,000 ft. Petrographically, the Lower and Middle Mesozoic rocks of the Southland Syncline consist almost entirely of volcanic greywackes, siltstones and tuffs with scattered lenses of conglomerate. They belong to the "Hokonui Facies" of WELLMAN (1952), which is also preserved near Nelson and in the coastal regions of the south-west part of Auckland province.

On the north flank of the Otago Schists (MACKIE, 1936), as on the east of the Alpine Schists (WELLMAN, GRINDLEY and MUNDEN, 1952), are semi-schists that locally contain Triassic fossils, followed by an extensive belt of "greywacke" of WELLMAN's "Alpine Facies,"* largely Mesozoic in age, but including elements containing the Permian fossil *Atomodesma* sp. in South Canterbury. This belt forms the main mountain ranges of Canterbury and Marlborough, and reappears to the north as the basement of much of the North Island. Thicknesses are largely unknown, although WELLMAN *et al.* (1952) consider that for part of the Triassic at least they are greater than in the Hokonui Facies. Graded, greywacke-type sandstones and siltstones are dominant. The volcanogenic fraction is less conspicuous than in the Hokonui Facies, and detrital quartz, potash feldspar and muscovite are correspondingly more abundant. Occasional interbedded volcanics are mostly spilitic pillow lavas, in contrast to tuffs of andesite–dacite–rhyolite affinities and rare andesitic intrusions which occur in the Hokonui Facies.

The concept has grown among New Zealand geologists of a progressive metamorphism consequent upon increasing depth of burial, depth being held to be the main factor controlling temperature. The absence of major intrusives in the New Zealand Geosyncline and, at least in the case of rocks of the zeolite facies, the sequence of mineralogical changes are both compatible with this view. At least three factors may modify this simple conception. First, the geothermal gradient may have varied in different parts of the geosyncline, the gradient being likely to have been lowest where sedimentation was thickest and most rapid. Secondly, structural evidence (GUNN, 1956; LILLIE *et al.*, 1957; ROBINSON, 1958) indicates the possibility that in the higher grade rocks important folding preceded the metamorphic maximum. Thirdly, it is conceivable that internal deformation, which in the schists is often intense, may have affected the position of mineralogically-determined isograds by promoting reactions or by causing slight rises in temperature.

Opinions differ as to the date of the "main" metamorphism and as to whether sedimentation was essentially continuous in the axial regions of the geosyncline. MUTCH (1957) and WELLMAN (1956) have suggested that there is a continuous thickening of formations from the Southland Syncline towards the Otago schist axis, and consider that the maximum grade of metamorphism was attained in the axial region of the geosyncline where these and Lower Jurassic formations were assumed to have achieved their greatest thickness. If this is so, there is a continuous gradation from the zeolite facies through a broad transitional belt into the greenschist and higher grade facies. In two columns, MUTCH indicates 50,000 and 95,000 ft of pre-Jurassic cover for the schists down to the Chl.2 subzone. Evidence of metamorphic grade in the Otama and Kaka Point areas does not altogether

* Named from the Southern Alps of New Zealand.

support the concept of continuous thickening, and it is conceivable that in Lower Mesozoic times in southern New Zealand there were more or less separate troughs of deposition for the two sedimentary facies.

An upper limit to the date of metamorphism and of erosion deep enough to expose chlorite-zone schists is provided by the deposition of the Kyeburn and Henley formations, the basal members of which may be as old as Upper Jurassic and Lower Cretaceous, respectively (Harrington, 1955). By this time, according to the concept of Wellman (1956, pp. 13, 31), new geosynclines were forming on the east side of the North Island and in the north-east part of the South Island to the east of the now firmly indurated welt of older geosynclinal sediments. Pebbles and grains of quartz–sericite–pumpellyite semi-schist in conglomerates and greywackes of probable Lower Cretaceous age (D. Hamilton, personal communication) in the Hurunui Gorge area are evidence that in North Canterbury the older geosynclinal sediments were providing low grade metamorphic material to a trough in which younger greywacke suites were being deposited.

Similarly, low-grade metamorphics such as actinolitic metavolcanics and quartz–sericite semi-schists are not uncommon as fragments in the Triassic and Jurassic greywackes and conglomerates of Southland. Wood (1953, 1956), has given evidence from northern Southland for at least three "marginal unconformities" (i.e. marginal to the New Zealand Geosyncline), which exposed successively younger members of the Permo-Triassic sequence to erosion. None of these breaks can be correlated with a general orogeny and metamorphism, but, at least in the case of the break between the Waipahi and Arthurton groups (Permian), the effects extended far from the margins of the geosyncline as is shown by the emplacement at Otama of an igneous complex (described later) which is interpreted as a crudely sheet-like mass nearly 4 miles thick.

Difficulties in unravelling the history of the New Zealand Geosyncline arise from the monotonous uniformity of extraordinarily thick and sparsely fossiliferous greywacke suites, known to range in age from Permian to Cretaceous and commonly preserving general uniformity of strike. The present writer considers that evidence for unrest throughout the mobile belt of the New Zealand Geosyncline is likely to increase with the passage of the years and that the concept of continuous sedimentation, with thickening towards the axis of the geosyncline, is likely to prove at best an over-simplification. It is suggested that the locus of most rapid sedimentation may have migrated repeatedly, as indeed it has during New Zealand's later history, and that the metamorphic maximum was not reached simultaneously at all points. The main significance of this interpretation, as far as the present paper is concerned, is that an unchallengable transition from the zeolite facies to typical greenschist facies rocks cannot yet be demonstrated for any one section, nor is it yet possible to state with any great accuracy the depths of cover under which chlorite-zone and higher grade metamorphism occurred. Nevertheless numerous sections of vast thickness are available for study as described below, some of them uncomplicated by unconformities, igneous intrusions or structural disturbance, and from these the general trend of a metamorphic sequence from the zeolite facies through a very broad zone characterized by prehnite and pumpellyite, to the greenschist and hence to higher facies, seems clear.

2.2. *Mesozoic sediments of the Hokonui Facies*

2.2.1. *Taringatura.* In the northern part of the Taringatura district on the north limb of the Southland Syncline is a steeply dipping sequence, approximately 30,000 ft thick, of Hokonui Facies sediments ranging from about Lower to Uppermost Triassic in age (Coombs, 1950). The area is free from any vents or intrusions of Triassic or later age, and deformation is confined primarily to the simple folding of the syncline, adjustment to which has been accomplished by slip on widely-spaced bedding planes. The amount of post-Triassic overburden that may have been removed is unknown, but it is unlikely to have been more than 10,000 to 15,000 ft, and it may have been much less.

Coombs (1954) showed that glass in ash beds in the upper part of the section has been completely replaced by heulandite* or less commonly by analcime. Both zeolites coexist with quartz and fine-grained phyllosilicates. The great majority

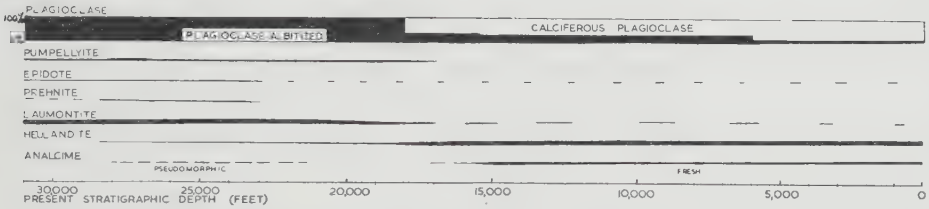

Fig. 2. Mineralogical features in relation to stratigraphic depth below the highest beds at present exposed, Taringatura, Southland, New Zealand (after Coombs, 1954).

of rocks here contain fresh detrital lime-bearing plagioclase as a major constituent, but from successively lower horizons it is found to be missing from more and more specimens. In its place are pseudomorphs of dusty albite with sericite inclusions, although some "islands" rich in relict andesine persist almost to the base of the section. Simultaneously with the albitization of plagioclase, analcime and heulandite disappear. Analcime has not been observed in rocks from lower than about 17,000 ft below the top of the section, its place being taken mainly by albite, but also in some cases by pseudomorphs of adularia or laumontite. Heulandite persists to greater depths, but it appears to give way to laumontite plus quartz and the lower part of the section contains numerous beds of altered ash, some of them very thick, in which laumontite is the dominant constituent. First pumpellyite, then prehnite appear as accessory minerals. In some cases at least, notably in quartz–albite–adularia–pumpellyite metasomatites, the pumpellyite has clearly formed at the expense of laumontite, magnesium and iron being provided by celadonite and chloritic minerals. Tiny granules of epidote that appear to have grown in place are seen in thin sections from most stratigraphic levels, but they are always quite subordinate in quantity. Stilbite is occasionally found in joints of late formation. It is to be emphasized that with this exception the zeolites occur as essential constituents of the rocks and not as the fillings of veins or joints, although laumontite does occur as a replacement of fossils.

Chemical analyses, including spectrographic data on trace elements, are

* Including clinoptilolite.

compatible with the conclusion that although the altered rocks deviate notably from their original composition, the metasomatism is complementary and it is unlikely that material was brought in from outside the sedimentary pile.

The sequence of mineralogical changes (Fig. 2) may be summarized as follows:

(1) Alteration of glass in tuffs to heulandite or analcime.
(2a) Replacement of the assemblage analcime–quartz by albite–quartz.
(2b) Replacement of heulandite by laumontite, and of detrital calciferous plagioclase by albite and laumontite.
(3) Substitution of pumpellyite and prehnite for laumontite.
(4) Post-tectonic precipitation of stilbite in joints.

It is not possible in the Taringatura district to map sharply-defined zones dependent on the stage of alteration, although beds above the present 17,000 ft level are dominantly in a *heulandite–analcime stage* whereas those below 17,000 ft are dominantly in a *laumontite stage*, while a *prehnite–pumpellyite stage* appears spasmodically towards the base. Observed assemblages of coexisting non-detrital minerals from Taringatura include the following. In each case scaly phyllosilicates of various shades from green to brown and of moderate to high birefringence are further possible phases.

Stage 1 (heulandite–analcime stage):

heulandite–montmorillonoid–quartz
heulandite–quartz–celadonite
analcime–quartz–celadonite
heulandite–quartz–celadonite–sphene.

Stage 2 (laumontite stage):

laumontite–albite–quartz–celadonite–sphene
laumontite–albite–adularia–quartz–celadonite
quartz–albite–adularia–montmorillonoid–sphene.

Stage 2 *or* 3:

albite–quartz–chlorite–sphene
albite–chlorite–calcite–sphene.

Stage 3 (prehnite–pumpellyite stage):

quartz–albite–adularia–pumpellyite
albite–chlorite–pumpellyite–sphene
albite–chlorite–prehnite–quartz.

Discussion. The relation of alteration to depth and hence by inference to temperature, seems clear, although the gross overlapping of zones is to be emphasized. The sequence heulandite, laumontite, pumpellyite, prehnite, epidote is one of decreasing hydration accompanied by release of silica as indicated in Fig. 3, although in the case of the non-zeolites dehydration is complicated by changes in the alumina content which must involve reactions with aluminous minerals such

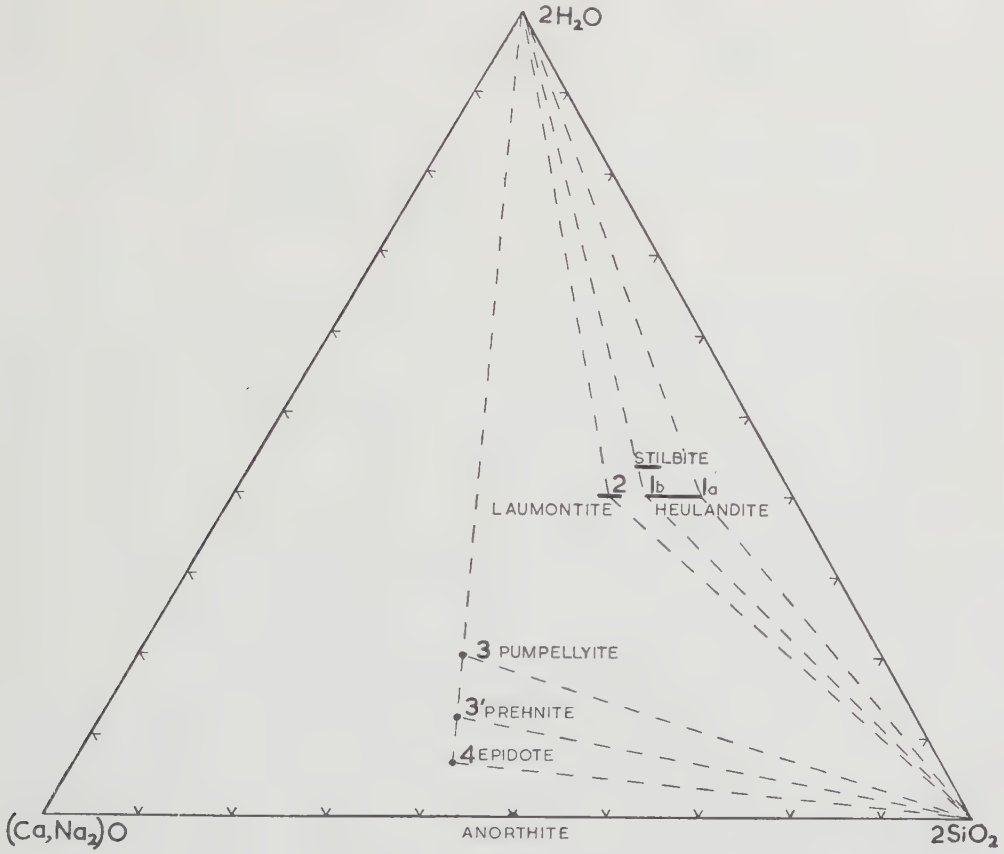

Fig. 3. The sequence of Ca–Al silicates 1, 2, 3, 3′, 4 coexisting with quartz and water under regional conditions in southern New Zealand. 1a and 1b are the siliceous and aluminous extremes of the heulandite series.

as clays, micas and chlorites. Using conventional formulae, we have:

$$\underset{\text{heulandite}}{CaAl_2Si_7O_{18}.6H_2O} \rightarrow \underset{\text{laumontite}}{CaAl_2Si_4O_{12}.4H_2O} + \underset{+\ \text{quartz}}{3SiO_2} + \underset{+\ \text{water}}{2H_2O}$$

$$\text{laumontite} + \text{celadonite} \rightarrow \underset{\substack{\text{pumpellyite}\\ +\\ \text{aluminous silicates + quartz + water}}}{Ca_4MgAl_5Si_6O_{23}(OH)_3.2H_2O}$$

or

$$\text{laumontite} \rightarrow \underset{\text{prehnite}}{Ca_2Al_2Si_3O_{10}(OH)_2} + \text{aluminous silicates (+ quartz) + water}$$

Epidote, $Ca_2(Al,Fe)_3Si_3O_{12}(OH)$, is characteristic of the greenschist facies of Otago and it may be produced from pumpellyite and prehnite by further dehydration reactions. The final step in the series is the well-known decomposition of epidote in the amphibolite facies, anorthite entering the plagioclase and excess alumina being taken up by such minerals as amphiboles. Dehydration is also involved in the formation of albite from analcime and quartz.

Heulandite exists over a wide range of silica content (Appendix 2) and high-silica heulandite (1a in Fig. 3) could theoretically be dehydrated into high-alumina heulandite (1b), thus:

$$\underset{\text{clinoptilolite (1a)}}{5(Ca,\ Na_2)_3Al_6Si_{30}O_{72}.24H_2O} \rightarrow \underset{\text{heulandite (1b)}}{3(Ca,\ Na_2)_5Al_{10}Si_{26}O_{72}.24H_2O} + \underset{\text{quartz}}{72\ SiO_2} + \underset{\text{water}}{48\ H_2O}$$

This reaction is complicated by the fact that clinoptilolite tends to be richer in alkalis than typical heulandite and the chemical nature of the parent ash may well provide the main control over the composition of the phase found. Stilbite is chemically equivalent to a normal or high-alumina heulandite plus additional water. Its position as a low-temperature, post-orogenic joint-filling is therefore not incompatible with the suggestion that temperature exercises a major control over zeolite occurrence in the Taringatura area.

2.2.2 *Hokonui Hills and south-east Otago.* Equivalents of the Triassic beds of the Taringatura Hills, as well as overlying Jurassic formations, outcrop almost continuously for 100 miles to the south-east, where they reach the sea. Scattered observations indicate similar alteration phenomena to those described above, but it may be noted that laumontite replaces plagioclase in certain Jurassic beds of the Hokonui Hills (Coombs, 1952, p. 813) that can hardly have been buried as deeply as the vaguely defined laumontite zone of Taringatura.

In about 4000 ft of the lower Middle Triassic siltstones exposed on the coast near Kaka Point, over 300 thin, water-laid ash beds have been altered to bentonite containing heulanditized (clinoptilolitic) glass relicts, to aggregates of heulandite, microcrystalline quartz and clay minerals, or to analcime and quartz sometimes partially replaced by albite. Celadonite is often present. Detrital calciferous plagioclase and ferromagnesians are largely unaltered both in the tuffs and in the associated siltstones in which occasional glass shards are heulanditized. This part of the section is thus dominantly in the heulandite–analcime stage of alteration as defined for Taringatura.

At Nugget Point, several miles to the south-east, Kaihikuan (Middle Triassic) ash is in part heulanditized or bentonitic but is mostly altered to laumontite in beds which are locally metasomatized to albite rock. Plagioclase in the tuffs and associated volcanic greywackes and arenites is often albitized, but relict andesine is sometimes found. Laumontite occurs in minor crush zones. This part of the section is dominantly in the laumontite stage of alteration, but its structural relation to the area of less altered Lower Triassic beds to the north of it is not yet fully elucidated.

Speden (1956) has described both zeolitic and quartz–albite–prehnite assemblages from Jurassic beds in the Catlins district still further to the south. A significant phenomenon noted by Speden is the direct replacement of calciferous plagioclase by heulandite or analcime, indicating that in the analcime–heulandite stage these zeolites are stable relative to plagioclase plus water, even though this alteration seldom proceeds far, presumably due to slow reaction rates or lack of sufficient water at the grain boundaries. The Catlins section described by Speden, 11,700 ft thick, is dominantly in the laumontite stage, although anomalously it is in one of the upper formations that both the prehnite and heulandite–analcime assemblages were observed.

2.2.3. *Nelson and south-west Auckland.* Andesitic volcanic greywackes, tuffs and siltstones of the *Mytilus* beds (Otamitan stage, Carnian) at Wairoa Gorge, Nelson (O.U. 15822–15827) show heulandite–analcime stage alteration, much as described for Taringatura, apart from the abundance of calcite accompanying one or other of these zeolites in the matrix. Near Marakopa in south-west Auckland (O.U. 11426 *et seq.*), Middle to Upper Triassic beds (Campbell, 1955) form the lower 11,000 ft of the west limb of a Triassic and Jurassic synclinal section

estimated by Marwick (1946) to be 28,000 ft thick. Several hundred thin beds of vitric tuff altered to impure laumontite rock are exposed along the coast. Plagioclase is in part replaced by laumontite and in part is either albitized with sericite inclusions or remains as relict oligoclase or andesine. Subordinate spongy prehnite is not uncommon in laumontitized vitric tuffs, in the groundmass of crystal tuffs and volcanic greywackes, and in tuffaceous siltstones. Calcite–laumontite veins are a feature of crush zones, especially along the bedding planes. Biotite tends to be chloritized, and secondary quartz, calcite, chlorite and sphene occur. Rocks in the heulandite stage were noted but appear to be rare.

2.3. *The Otama Igneous Complex and associated Permian sediments*

2.3.1. *Geological setting.* Four miles north-eastwards across the strike from the lowest Triassic beds of the Hokonui Hills, is the Late Paleozoic Otama Intrusive Complex of which about 16 square miles are exposed. It consists dominantly of metagabbros and albite micro-granites, associated with keratophyric and spilitic volcanics, some of which are hornfelsed by the intrusives. Although individual members are not all stratiform in arrangement the mass is roughly concordant with the enclosing sediments and is interpreted by Wood as having been overturned through an angle of 110°. On its north side, the complex is in steeply dipping thrust-contact with prehnite-bearing greywackes which, as far as is known, grade northwards through progressively more metamorphosed rocks of the Tuapeka Group into the typical schists of Central Otago type.

Permian volcanic greywackes and associated dacitic tuffs immediately south of the complex are partly in the heulandite stage of alteration and partly in the laumontite stage, and it was from this area that Hutton (1949b) first drew attention to the metamorphic significance of laumontite.

2.3.2. *Alteration of the Otama Complex.* At least two types of alteration are represented: contact metamorphic effects produced during the emplacement of successively younger intrusions; and subsequent low-grade alteration of a more regional nature that has affected the igneous complex and sedimentary rocks alike. For example the conversion of keratophyres into plagioclase–hornblende–epidote and plagioclase–hornblende–diopside hornfelses belongs to the first type; albitization of the plagioclase and veining of the same rocks with prehnite and sometimes laumontite belongs to the second type. The later alteration has undoubtedly been promoted by intense crushing almost throughout the complex. This has allowed free access to a vast surface-area of rock, of the water essential for the formation of those minerals diagnostic of zeolite facies conditions, and without which a high-temperature igneous mineral assemblage will be preserved at low temperatures virtually throughout geological time. In both the basic and more acidic rocks calciferous plagioclase is something of a rarity, its place being taken by cloudy albite and/or a variety of other secondary minerals including epidote, pumpellyite, prehnite, laumontite, thomsonite and analcime. Crush-zone laumontite associated with prehnite has already been described (Coombs, 1952).

The more basic rocks are of particular interest in showing the effects of zeolite facies metamorphism in an environment devoid of free silica. The most typical Ca–Al–silicate in these rocks is thomsonite.

An unusually fresh, basic noritic gabbro, no. 946, from 125 chains NE of Otama Hall, consists of bytownite An_{83}, augite and hypersthene sometimes mantled with hornblende, minor

iron ore and rare pseudomorphs after olivine. The plagioclase shows minor alteration to feathery wisps and films of thomsonite. Such alteration is more advanced in a slightly crushed anorthositic segregation, no. 950, from the same area, having bytownite An_{81} as its major primary phase. It is riddled with flecks of thomsonite which are especially abundant near irregular criss-crossing bands of almost pure zeolite, from which innumerable angular embayments extend into the feldspar. Rosette-like clusters of prehnite are often enclosed within the thomsonite and there are also a few threads of an epidote-group mineral, chloritic films and traces of other zeolites. Variable refractive indices such as α 1·527, γ 1·538 indicate aluminous members of the thomsonite series (Hey, 1932a, p. 79). To a first approximation, such alteration of calcic bytownite to thomsonite can be regarded as a simple hydration to $CaAl_2Si_2O_8.2.4H_2O$. In the most crushed rocks plagioclase is completely replaced by thomsonite with nests of prehnite, minor laumontite and tiny veinlets of unidentified fibrous zeolite. There is much relict augite, some hornblende and chloritic material.

Another hypersthene gabbro, 588, from 29 chains downstream from Pyramid Bridge, shows labradorite An_{50} net-veined and partially replaced by thomsonite, pools and later veins of analcime, minor laumontite and occasional nests of prehnite within the thomsonite. In some associated metagabbros feldspar has been completely destroyed. The earlier analcime is penetrated by needles of thomsonite and is likely to have coexisted in equilibrium with it. The analcime presumably represents excess sodium over that taken up by the thomsonite. Replacement of the albite component of plagioclase by analcime would result in the release of silica. A small amount of this could be taken up by an increase in the Si : Al ratio of the thomsonite and it is tempting to consider that the remaining excess silica has caused the formation of the more silica-rich zeolite, laumontite.

A still less basic differentiate, 1581, an apatite-bearing hornblende hypersthene gabbro from about $2\frac{1}{2}$ miles NE of Otama Hall has An_{36} for its plagioclase and shows incipient alteration to laumontite. Another specimen, 1584, which may initially have been rather similar, has had its calciferous plagioclase completely replaced by albite, laumontite and prehnite. These rocks are associated with hornblende and pyroxene andesinites, as well as albitites (e.g. 1587) veined and riddled with laumontite, prehnite, and epidote, suggesting that they were produced by the alteration of andesinites or oligoclasites under conditions transitional between the zeolite facies and the greenschist facies. In some cases the prehnite appears to be replacing earlier laumontite.

The Otama albite microgranites, hornblende microgranites and granophyres are remarkable for near-universal signs of cataclasis, for the uniformly purely albitic plagioclase which is usually somewhat cloudy and flecked with sericite, for their liberal sprinkling and veining along crush-bands with prehnite, epidote and in some cases pumpellyite and for the paucity of potash feldspar. Chloritic minerals and secondary sphene are widespread. Zeolitization is rare both in these and in the albite–hornblende–epidote–sphene hornfelses, and except for a late vein of stilbite (9728) and an occurrence of analcime in a mylonite (9683) the only zeolite noted so far in these quartz-bearing rocks is laumontite. In one case (9741) this appears to be in the process of replacement by pumpellyite and prehnite.

The usual mineral assemblage in the unhornfelsed keratophyric and spilitic volcanics is albite–epidote–chlorite–sphene(–quartz). In other cases pumpellyite (9735), or prehnite and pumpellyite (9734), largely take the place of epidote.

Summarizing the above observations on the Otama rocks it may tentatively be concluded:

(1) At some time subsequent to consolidation, the Complex was subjected to regional cataclasis and alteration under conditions ranging from those of the zeolite to the greenschist facies, quartz–albite–epidote–chlorite–sphene assemblages being typical of the latter.

(2a) Calciferous plagioclase in the microgranites, hornfelses and spilitic volcanics was replaced by assemblages of albite plus prehnite, pumpellyite

or epidote, together with chlorite and sphene derived from the ferromagnesians.

(2b) In a few cases in these rocks the prehnite and pumpellyite appear to replace earlier laumontite.

(3a) In the most basic noritic gabbros thomsonite is the characteristic zeolitic alteration product, and in some cases is itself in process of replacement by prehnite.

(3b) In the less basic gabbros, thomsonite is accompanied by varying amounts of analcime and laumontite, also sometimes partially replaced by prehnite.

(4) Laumontite is the only early-metamorphic zeolite recorded from quartz-bearing members, but analcime and stilbite occur in addition in late veinlets and crush-zones.

2.4. *Greywackes and associated volcanics of the "Alpine Facies"*

2.4.1. *Mid-Canterbury.* The main highway from Christchurch to the west coast of the South Island via Arthurs Pass provides a discontinuous section about 30 miles long from the edge of the Canterbury Plains to Arthurs Pass on the Main Divide. The basement rocks throughout this distance are monotonous, steeply dipping greywackes and associated rocks of WELLMAN's "Alpine Facies." Their general trend is transverse to the line of section, but their structure remains to be elucidated.

Near the east end of the section, little altered greywackes (15711–15714) containing the annelid *Terebellina mackayi*, of probable Triassic age, are exposed at the upper Kowai River bridge. Detrital grains include unaltered andesine and plentiful biotite which shows incipient bleaching and loss of birefringence, as well as quartz, muscovite, orthoclase, accessory minerals and a variety of rock fragments. Very fine-grained reconstituted chloritic material and calcite are disseminated through the groundmass. Joints are filled with calcite. Boulders (15708–15710) from the Kowai River, which has its source in the Torlesse Range about 5 miles north of the bridge, include prehnite-bearing greywackes, variolitic spilite with veins of quartz–pumpellyite and calcite–prehnite–pumpellyite(–epidote), and radiolarian metachert with pumpellyite–chlorite–quartz(–epidote) veins.

Three miles to the north-west at Porters Pass, the greywackes (15715–15719) are distinctly more altered than at Kowai Bridge although in some cases oligoclase–andesine survives amongst the otherwise albitic detrital plagioclase. Prehnite is a variable but often plentiful constituent, occurring as spongy undulose grains or as better-formed groups of crystals in the groundmass, as inclusions in plagioclase and sometimes even as plates separating the cleavage planes of biotite, which shows marked lowering of birefringence (cf. KOSSOVSKAYA and SHUTOV, 1955). Epidote is not abundant and is in part detrital. The rocks are copiously traversed by quartz–prehnite veins varying from a fraction of a millimetre to two centimetres or more in thickness and apparently controlled by early-formed shatter systems, as is commonly the case in rocks of this metamorphic condition in New Zealand. Several episodes of crushing and recementation of the same vein are often apparent. In some cases a quartz–pumpellyite zone occurs near the walls of the vein, the pumpellyite being an iron-poor, pale-green variety. Porters Pass is on the trace of a major active fault and a younger shatter system has been imposed on the older, some of the younger fractures being filled with laumontite.

Rather similar prehnite-stage greywackes, freely traversed by quartz–prehnite or quartz–prehnite–pumpellyite veins, may be collected at numerous points between Porters Pass, the Waimakariri River and the Main Divide. A particularly instructive specimen (15707) from near the bridge over Craigieburn River has the assemblage quartz–albite–prehnite–chlorite–sphene(–epidote) amongst its reconstituted minerals, together with the usual relict detrital minerals, including orthoclase which appears to persist unaltered under prehnite-stage conditions.

The rock is traversed by numerous quartz–prehnite veins which are cut by later fractures cemented by laumontite or lined with dusty analcime, and by still later joints filled with stilbite.

The prehnite from the above rocks appears to be rather uniformly iron-poor. Optical properties of better-crystalline material are α 1·615, β 1·624, γ 1·644 $\pm$ 0·002, $2V_\gamma$ 67 $\pm$ 2°, dispersion imperceptible; suggesting about 1 per cent Fe_2O_3.

2.4.2. *Wellington Peninsula.* Reed (1957) has described the petrology of the greywackes, argillites, spilites and jasperoids of Wellington Peninsula. He briefly records secondary calcite, laumontite and prehnite as coatings and veins in crush zones and considered them to be the product of shearing (Reed, 1957, p. 18). Pumpellyite is recorded from the spilites. The present notes supplement these observations on the basis of an examination of specimens (14951–14974) from the 15,000 ft south-coast section from Houghton Bay to Sinclair Head (Brodie, 1953). Quartz–prehnite veinlets, with or without calcite, sericite, albite and chlorite are here magnificently developed in tension fractures and shatter-planes in greywackes and to a less extent in argillites throughout the section. The prehnite may be coarse (>1 mm) or fine, spongy or well crystallized. Representative specimens do not vary significantly in their optical properties from those recorded above for Canterbury prehnites. In most cases detrital plagioclase is uniformly albitic and prehnite is often thinly disseminated through the matrix of the rock, but in some cases with sparse film-like veinlets of calcite–prehnite instead of quartz–prehnite, unaltered detrital oligoclase–andesine was observed. At Island Bay, laumontite was observed to replace plagioclase in some cases. In the more altered rocks, biotite shows marked loss of birefringence. Specimens (14975–14979) from Worser Bay on the west shore of Wellington Harbour were found to be less altered. They lack quartz veins or prehnite, calciferous plagioclase remains and detrital biotite has almost normal colour and birefringence. The range of alteration phenomena on Wellington Peninsula thus closely parallels that in mid-Canterbury.

2.4.3. *Other occurrences.* Brothers (1956) showed prehnite to be important both in the matrix and in quartz–prehnite veins in tension fractures of greywackes from North Auckland, and Hutton (1949a) has reported prehnite and minor pumpellyite from greywackes of Kapiti Island.

2.4.4. *Discussion.* Pumpellyite and prehnite, especially the latter, are clearly of key importance in the metamorphic history of vast tracts of Wellman's "Alpine Facies." They are here interpreted as having been derived mainly from the breakdown of detrital calciferous plagioclase and perhaps in part from calcite and clay minerals or earlier zeolites.

The following alteration stages may tentatively be recognized for the lowest grades of metamorphism of the Alpine Facies, three of them being progressive and one retrogressive:

(1) Little visible mineralogical change apart from some loss of birefringence of biotite and the formation of very fine-grained chloritic or clay minerals in the matrix. Zeolites in the matrix are rare.

(2a) Detrital plagioclase partly or completely altered to albite commonly accompained by prehnite. Associated volcanics (spilites) have mineral assemblages containing albite–calcite–pumpellyite–chlorite, and less characteristically epidote and/or prehnite and sometimes minor quartz.

(2b) Prehnite is concentrated in monomineralic veinlets and prehnite–calcite veins, without much quartz.

(3) Greywackes heavily veined with quartz–prehnite with or without pumpellyite.

(4) Fracture planes produced subsequent to the metamorphic maximum are filled by a sequence of minerals that is one of increasing hydration, namely prehnite, laumontite, stilbite, with analcime also possible before stilbite.

The first stage corresponds in part at least to the zeolite facies of Southland, zeolites being rare largely on account of the scarcity of suitable reacting materials. It is also conceivable that sedimentation was more rapid and the geothermal gradient even less steep in the Alpine Facies than in the Hokonui Facies. This could have caused water to have been expelled and porosity lost by compaction before zeolites could form at an appreciable rate. Stage 2 corresponds directly to the prehnite–pumpellyite stage as defined for Taringatura although osmotic or water-deficient conditions could conceivably cause the formation of prehnite at lower temperatures than in Taringatura (see 4.5, 4.10). The appearance of plentiful vein quartz in stage 3 (zone of quartz–prehnite veins) may well indicate a higher temperature and is not readily compatible with any suggestion of water-deficient conditions. Wellman *et al.* (1952) have stressed the importance of "quartz" veins as a metamorphic indicator in New Zealand, and although this is a criterion to be used with great caution, the veins being promoted by shattering or the opening of tension fractures, the abundant incoming of quartz-bearing veins is here accepted as being of potential metamorphic significance, as further discussed on theoretical grounds in a later section.

The sequence of vein fillings noted in stage 4 is a reversal of the trend recorded for progressive metamorphism under increasing load and temperature although with stilbite taking the place of heulandite, and it can be correlated with the filling of fractures under conditions of progressively decreasing load and temperature during denudation. Laumontite in minor faults in chlorite-zone schists at Five Mile Creek, and in joints in greenschists near Shotover Bridge, both near Queenstown, Central Otago, has a similar retrogressive significance. Apart from the possible effects of differing rock pressure and vein-water pressure as discussed later, and in the absence of the incoming of newly heated solutions, the metamorphic significance of a late zeolite- or prehnite-bearing vein is that the rock it cuts has passed through a metamorphic maximum with P–T conditions at least as severe as those of which the vein mineral assemblage is diagnostic.

2.5. *Later Mesozoic geosynclinal sediments*

Analcime and heulandite in Lower Cretaceous greywackes, in part tuffaceous, collected by D. Hamilton from the Hurunui Gorge above Ethelton in North Canterbury, veinlets with laumontite and calcite and laumontite replacement of plagioclase in the Cretaceous Taitai sandstone from Motu Falls, Poverty Bay, show that zeolitic alteration also occurs in thick sedimentary sequences of New Zealand younger than those of the main New Zealand Geosyncline.

2.6. *A prehnite–pumpellyite zone*

The above descriptions show that prehnite-bearing rocks are of regional extent in New Zealand. They appear to grade continuously into chlorite-zone schists, and prehnite-bearing assemblages are also found in the more altered members of the zeolite facies. Turner and Hutton (see Turner, 1948, p. 38) have divided the "chlorite zone" of metamorphism in Southern New Zealand into four *texturally* defined subzones, these being progressively more reconstituted from subzone Chl. 1 to Chl. 4. Robinson (1958) shows that pumpellyite occurs freely in semischists of subzones Chl. 1 and 2 on the east Otago coast south of Brighton, but

disappears at about Chl. 3 beyond which epidote is the only Ca–Al silicate apart from actinolite. Pumpellyite is now known to be a characteristic Ca–Al silicate of semi-schists of similar metamorphic grade described by Mackie (1936) from his traverse south of the Waitaki River, although epidote is also present. It is also common, for example, in the lower grade schists of north-west Otago (Hutton, 1937) in the Kakanui Ranges (Turner, in Williamson, 1939; Amies, 1952) in South Canterbury (Amies, 1950), and in Upper Paleozoic spilites, greywackes and tuffs of about Chl. 1 grade from northern Southland (Reed, 1950).

Mutually associated minerals in the Alpine Facies greywackes include quartz, albite, prehnite, pumpellyite, chlorite, sphene and detrital orthoclase: and in typical Chl. 2 rocks from East Otago there is some combination of the following: quartz, albite, chlorite, sphene, actinolite, muscovite, stilpnomelane, pumpellyite and epidote. An extremely broad zone can thus be mapped in New Zealand characterized by prehnite and/or pumpellyite. The incoming of actinolite and stilpnomelane in rocks of appropriate composition, the conversion of orthoclase to mica, and the disappearance of prehnite represent possible isogradic markers within the zone. Beyond a zone of transition, zeolites disappear and the rocks are not to be placed in the zeolite facies. We suggest that it may prove convenient to erect a new facies or low-grade subfacies of the greenschist facies to accommodate these rocks but that further field work on their subdivision is desirable before this is done. It will be recalled that Miyashiro and Banno (1958) have recently shown that pumpellyite occurs in the lowest grade schists of the Sanbagawa–Mikabu zone in Japan and that de Roever (1950, 1955) has already suggested that pumpellyite-bearing assemblages belong to a special subfacies, perhaps of the greenschist facies. His further suggestion that it represents a very low-grade equivalent of the glaucophane schist facies is hardly applicable to the New Zealand occurrences in which glaucophane is almost unknown.

2.7. *Distribution of the lower metamorphic grades in New Zealand*

As far as is known, all Lower Mesozoic formations of the Hokonui sedimentary facies (Fig. 1) show zeolite facies alteration although, as recorded above, transitions occur to prehnite–pumpellyite assemblages. At least some of the sediments of the Later Mesozoic geosyncline are to be included and probably also some of those of the Alpine sedimentary facies, as well as part of the belt of Late Paleozoic rocks, including the Otama Igneous Complex, which separates the Lower Mesozoic rocks of Southland from the Otago schists. The remainder of this belt, a corresponding belt to the west of the higher grade schists of Marlborough and almost certainly most of the Alpine Facies rocks belong to a prehnite-pumpellyite zone as described above.

3. Review of Other Zeolite Occurrences

(D. S.C., A. J. E.)

In the following section, the principal types of zeolite occurrence as reported in the literature will be briefly reviewed to test their bearing on the facies concept and on the conditions of zeolite formation.

3.1. *Zeolites in sedimentary rocks*

3.1.1. *U.S.S.R.* Analcime, "mordenite" and laumontite have been reported as authigenic cements in a wide variety of sediments of Permian to Tertiary age coming from vast areas of Russia and Siberia (e.g. Rengarten, 1940, 1945, 1950; Boldyreva, 1953; Dzotsenidze and Skhirtladze, 1953; Bur'yanova, 1954, 1956; Vasil'ev, 1954; Kolbin and Pimburgskayn, 1955; Kossovskaya and Shutov, 1955; Vasil'ev, Kolbin and Krasnova, 1956). According to Bushinsky (1950) associated authigenic minerals in Upper Jurassic and Cretaceous clays, sandstones, marls and chalk of the Russian platform include glauconite, opal, chalcedony, quartz, montmorillonite, nontronite, calcite, pyrite or marcasite, hydromica and the phosphates kurskite and francolite.

On the basis of its refractive indices and platy habit as figured by Bushinsky and in the absence of X-ray data, the present writers believe that much of the "mordenite" of the above authors is likely to be clinoptilolite, the silica-rich variety of heulandite. Vasil'ev (1954) gives a table of crystallographic measurements of crystals isolated from the phosphorites of Kashpur, and shows that they compare closely with those of Dana (1892) for "mordenite." Dana's crystallographic data were obtained from material from Hoodoo Mts., Wyoming, which was subsequently taken by Schaller (1932) as his type clinoptilolite, and shown by Hey and Bannister (1934) to be silica-rich heulandite. Crystallographically this is quite distinct from true mordenite.

The Russian authors do not appear to have recognized any zoning in the occurrence of the above zeolites; in fact in two cases (Rengarten, 1950; Kolbin and Pimburgskayn, 1955), analcime and laumontite occur together, whereas in southern New Zealand they are characteristic of, though not confined to, two distinct depth zones. Significant to the concept of mineralogical zoning with depth is the work of Kossovskaya and Shutov (1955) who recognize a progressive sequence of changes in the alteration of clastic biotite to chlorite at varying depths in more than 5000 m of Permian, Jurassic and Cretaceous sediments of the Verkhoyansk geosyncline in north-east Siberia. Laumontite is recorded as occurring as a cement in the Lower Cretaceous members, whereas the cement in the Upper Permian consists of quartz and albite with new-formed limonite and rutile, and in the Lower Permian of quartz and muscovite. Subsequently (1956) the same authors reported authigenic epidote in the same pile of sediments.

3.1.2. *U.S.A.* The work of Bradley (1928, 1929), Ross (1928, 1941) and Keller (1951, 1952, 1953) on very low temperature sedimentary analcime is well known. Heady (1952) has detected the mineral in a Colorado oil shale while Foster and Feicht (1946) and Rozendal (1957) have found it in coal. Similarly Bramlette and Posnjack (1933) and Kerr and Cameron (1936) have demonstrated the common occurrence of clinoptilolitic heulandite partly preserving glass shards in bentonites, while Gilbert and McAndrews (1948) have described authigenic heulandite cement in Miocene sandstone from Santa Cruz Co., California.

Laumontite cements have been reported by Gilbert (1951) from Mendocino Co., California, by Kaley and Hanson (1955) from Miocene feldspathic sandstone at a depth of 11,000 ft in a well in San Joaquin Valley, California, and by Heald

(1956) from the fluviatile New Haven arkoses of Connecticut. The aggregate maximum thickness of the Triassic of Connecticut is given as rather more than 15,000 ft and the laumontite is reported to occur sporadically in the lower part of the section. Cements of authigenic albite and potash feldspar are abundant throughout the column, although they occur in traces only in the laumontite-bearing rocks. There is minor secondary quartz in the cement and sporadic sericite. Heald considers that since the laumontite occurs as interstitial fillings, part of its material, as of the secondary albite, must have been introduced. Derivation from the Triassic diabases was suggested. It may be pointed out, however, that the alteration of calcic plagioclase to laumontite involves an equation such as:

$$\underset{101\ cm^3}{CaAl_2Si_2O_8} + \underset{45\ cm^3}{2SiO_2} + \underset{72\ g}{4H_2O} \rightarrow \underset{207\ cm^3}{CaAl_2Si_4O_{12}.4H_2O}$$

Hence, if this type of alteration occurs, some of the laumontite constituents must migrate from an altered plagioclase crystal at least as far as the nearest pore space (cf. Antun, 1953, p. 69). Such a cement does not require an outside derivation. Whatever the chemical origin of the laumontite or of the authigenic albite, the assemblage of interstitial minerals, albite, potash feldspar, laumontite and quartz, suggests conditions very similar to those prevailing in the middle and lower parts of the Taringatura section of southern New Zealand as reviewed above.

More recently Ross (1958) has described laumontitized tuffs from wells in Clinch County, Georgia, which are remarkably similar in texture and mineral assemblage to those of Taringatura. The alteration of celadonite to chlorite and its association with saponite are to be noted.

3.1.3. *Australia.* Gill (1957) has recently reported laumontite replacing wood in richly feldspathic Jurassic arkoses from East Gippsland, Victoria, and observations by one of us (D. S. C.) show that the mineral occurs in the groundmass and as a replacement product of plagioclase in the same series of rocks. Gill (personal communication) suggests an original cover of about 3000 ft for the rocks concerned. Coombs (1958) has shown that glass in Carboniferous volcanic ashes of the Kuttung Series, near Seaham, New South Wales, has been altered to clinoptilolite coexisting with quartz, celadonite and sphene. Joints in the same rocks are coated with stilbite, but sometimes contain laumontite as well.

3.2. *Formation of zeolites in active thermal areas*

3.2.1. *Wairakei, North Island, New Zealand.* At Wairakei, a hot-spring and fumarole area in the volcanic region of New Zealand, numerous wells have been drilled to provide steam and hot water for electric power generation. These wells provide an unusual opportunity for studying the mechanism and properties of an active hydrothermal system. From drill cores and cuttings, Steiner (1953, 1955a, b) has demonstrated the following zones of hydrothermal alteration (Fig. 4) caused by the action of steam and hot solutions on a sequence of rhyolite tuffs and breccias interbedded with minor mudstones and claystones. The hot solutions are saturated in silica which precipitates at all levels.

(a) Surface acid leached zone: The characteristic minerals are kaolinite, alunite and opal.

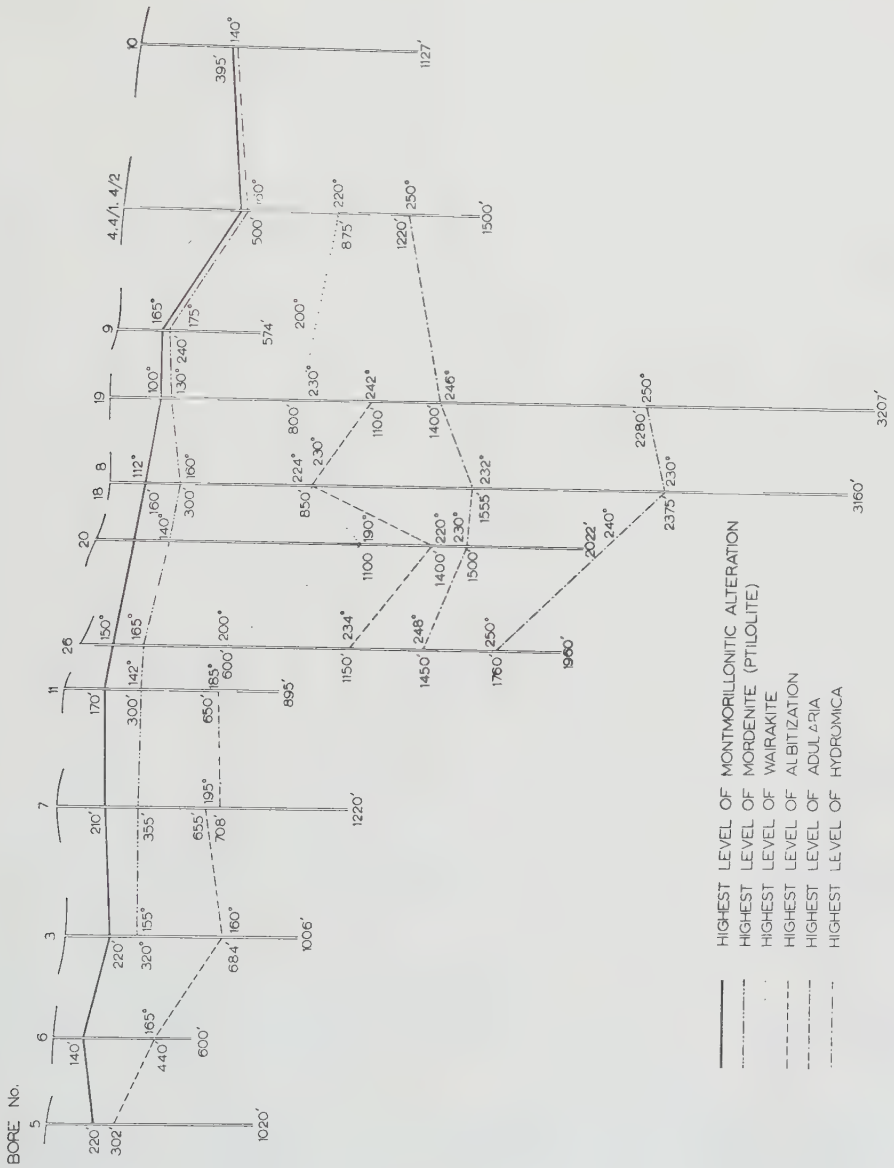
BORE No.
HIGHEST LEVEL OF MONTMORILLONITIC ALTERATION
HIGHEST LEVEL OF MORDENITE (PTILOLITE)
HIGHEST LEVEL OF WAIRAKITE
HIGHEST LEVEL OF ALBITIZATION
HIGHEST LEVEL OF ADULARIA
HIGHEST LEVEL OF HYDROMICA

Fig. 4. Alteration zones at Wairakei, North Island, New Zealand (after Steiner, 1955a) with temperature data (T°C) for some zone boundaries added from Banwell *et al.* (1957). Depths in feet.

(b) Zone of argillization: Rhyolite glass is changed to montmorillonitic clays. Plagioclase crystals are sometimes unaltered but are sometimes replaced by calcite.

(c) Zone of zeolitization: This is superimposed on the zone of argillization and is subdivided into an upper and a lower zone. In the upper zone the lime-soda zeolite "ptilolite", structurally indistinguishable from mordenite, is characteristic, and fills vesicles in pumice. In some cases it is associated with minor heulandite. Plagioclase phenocrysts are practically unaltered. In the lower zeolite zone wairakite (calcium analcime) replaces andesine and also fills veins and cavities by direct crystallization from solution.

Laumontite has subsequently been found by Steiner (personal communication) in a zone between ptilolite and wairakite at a depth between 500 and 900 ft where temperatures ranging from 195 to 220°C have been measured. It has also been found at greater depth below the wairakite zone in a deep drill-hole where a reversal of the temperature gradient appears to occur.

(d) Feldspathization zone: An upper subzone is characterized by albitization, and a lower one by adularia replacing plagioclase. Secondary sphene (titanomorphite) is scattered through the rocks and in bore no. 11 adularia and sphene are accompained by prehnite through a short vertical range. Calcite is locally precipitated, and the alteration of plagioclase to calcite and albite was observed.

(e) Zone of hydromica: In this zone, which exists below about 2000 ft, primary plagioclase is replaced by a hydromica as a result of leaching of alkalis by carbon dioxide solutions entering the zone from below.

The concentrations of sodium, potassium and calcium in the waters collected from bores at various depths (Ellis and Wilson, 1955; Ellis, 1958) correlate very well with this sequence of alteration. The hot solutions in the deepest zones tapped have a high concentration of potassium, which is progressively lowered by the formation of adularia from the original plagioclase. The concentrations of sodium and calcium are increased correspondingly until in the zone of zeolite formation some of these ions are again precipitated. By this stage the atomic ratios Na/K and Ca/K have increased from about 9 and 0·06 in the hydromica zone, to 20 and 0·15, respectively. The pervading solutions are approximately 0·05 N in sodium chloride, saturated with silica, and their pH is controlled by the bicarbonate-carbon dioxide system. Under pressure deep within the area the waters contain sufficient carbon dioxide to make them slightly acid with respect to pure water at the same temperature, e.g. at 250°C, pH = 5·0 (approx.) and for pure water pH = 5·7 (approx.). At lower pressures towards the surface the carbon dioxide is lost from solution and the waters become slightly alkaline with bicarbonate.

3.2.2. *Other active thermal areas.* The recent recognition of wairakite from The Geysers, California (Steiner, 1958) may be noted.

Some data from drill cores from the Upper Basin, Yellowstone National Park (Fenner, 1936) are included in Table 1. The introduction of potash feldspar in the lower levels is noteworthy, as at Wairakei.

Weed (1900) described a close association of quartz, stilbite, calcite and a little opal in veins from which the Boulder hot springs, Montana, now issue at temperatures up to 73°C. Similarly the Hunters hot springs (Weed, 1904) containing

abundant CO_2 and some H_2S, issue at 64°C from a vein-system of gypsum seamed by stilbite. In both cases WEED relates deposition of the stilbite to the present as well as ancestral waters, but WHITE (1955) considers the evidence inconclusive.

SAKURAI and HAYASHI (1952) have described the silica-rich lime zeolite yugawaralite from andesitic tuff which has been much metamorphosed by hot-spring action about 300 miles from the present Yugawara hot spring, Japan. Coexisting minerals are quartz, and minor laumontite, chabazite and mordenite (ptilolite). Epistilbite, heulandite and stilbite are also reported (SAKURAI, 1953).

It is well known that chabazite, christianite (phillipsite), rarer mesotype (natrolite) and possibly other zeolites have been deposited in the wall-work of Roman baths at Plombières and elsewhere (DAUBRÉE, 1879) where hot spring water emerges at a maximum temperature of 70°C. The zeolites occur both within the pores of old tiles and in the mortar, and are accompanied by opal, chalcedony, plombierite, calcite and apophyllite.

3.3. *Michigan copper deposits*

BRODERICK (1929, 1931; esp. 1929, Figs. 4, 7, 8) has described a crude zoning related to depth in the copper-bearing amygdaloids of Keweenaw Point. Successive zones in downward order are characterized by zeolitization (with laumontite, analcime, natrolite, stilbite, datolite, apophyllite); prehnitization overlapping on to the zeolitization zone and characterized by abundant adularia as well as prehnite; and sericitization and propylitization in which sericite takes the place of adularia, and sulphides and ankerite are introduced. Persistent in all zones are epidote, pumpellyite, calcite, quartz, chlorite and native copper, and late veins and vug-fillings of laumontite, prehnite and datolite. Assemblages typical of the deeper, higher-temperature zones penetrate upwards in the neighbourhood of fissures suggesting invasion by heated solutions. Apart from the presence of such minerals as apophyllite, datolite, copper and sulphides, the zoning is broadly analogous to that of the greywackes and semischists of southern New Zealand, natrolite and thomsonite, which are rarer than laumontite and analcime (BUTLER and BURBANK, 1929), possibly being indicative of local silica-deficient conditions. The vesicles are considered by BUTLER and BURBANK to have been filled after accumulation and tilting of the whole lava sequence and overlying sedimentary formations.

3.4. *Zeolites in amygdales, joints and other cavities*

The larger part of zeolite literature refers to occurrences in amygdales and to fillings of other cavities, especially in igneous rocks. Yet such occurrences are particularly difficult to interpret from a physicochemical point of view. It has been customary for authors to publish paragenetic sequences based largely on textural considerations which are often questionable, and furthermore the sequences have often been pieced together from incomplete series in separate cavities (e.g. NIGGLI *et al.*, 1940, Fig. 242), a procedure of doubtful significance unless composition of the depositing solutions can be equated. An observed sequence of cavity fillings may be a function either of changing composition of the depositing solutions or of changing P–T conditions, or both.

In the case of amygdale descriptions, there is often an underlying assumption that the zeolites have been deposited from magmatic solutions with falling temperature during initial cooling of a lava flow. It may well be that minor coatings of zeolites on the walls of cavities in some massive flows may have this origin but zeolites are rare or absent in the vesicles of newly cooled lavas. Walker (1951) has shown convincingly that zeolite deposition in the Garron plateau of Ireland post-dates effusion and cooling of a pile of some forty to fifty flows, in all about 1000 ft thick. It is in a sense metamorphic, as has also been shown for the Keweenaw amygdaloids.

The present writers consider that sequences in cavities may be related to falling temperatures during initial cooling of a thick lava flow or intrusion, to rising temperatures and pressure following burial, to rising temperature resulting from new intrusions of magma or new influxes of hot gases or solutions, or to falling temperature when these conditions are relaxed. Thus McLintock (1915) has clearly described a consistent sequence epidote–prehnite–scolecite in olivine basalts of Ben More, Mull, which he attributes to increasing hydration with falling temperature in agreement with Cornu's "rule" (1908), followed by a reverse sequence of dehydration culminating in garnet, and promoted by the thermal metamorphic effects of a subsequent intrusion.

Published zeolite sequences often show no obvious consistent trend. Nevertheless in view of the difficulties outlined above, we do not consider that this fact should outweigh the evidence from well-studied hydrothermal and regionally altered areas where with increasing temperatures progressively less hydrous zeolites tend to form.

A general correlation also emerges between the silica content of zeolites and the availability of free silica. Thus descriptions given above, together with observations of many other writers, show that the typical zeolites in veins and joints of quartz-bearing rocks are stilbite, heulandite, laumontite and analcime. Other zeolites in such environments appear to be quantitatively insignificant, although scolecite and chabazite are reported by Niggli *et al.* (1940) in "Alpine cleft" localities in quartzose rocks such as gneisses and the Aar granite. The amygdale sequence mordenite, heulandite, chabazite, stilbite, accompanied by quartz, chalcedony or opal reported by Mason and Greenberg (1953) from southern Brazil is one of increasing hydration in silica-rich zeolites, except for chabazite which is rare and was generally found to occur alone. Observations at Wairakei and Yugawara show that mordenite is typical of active thermal areas where silica activity is particularly high, although it also occurs in tholeiitic basalt amygdales.

In contrast, the main lime zeolites of the Garron Plateau olivine basalts are chabazite, levyne, thomsonite, natrolite, mesolite and phillipsite (Walker, 1951), all these tending to be low in silica, and similar assemblages have been reported from many other undersaturated rocks. In considerations of phase equilibria, it is much more important to know the phases which actually coexist with each other than the inferred order of their crystallization. We believe that the grouping of zeolites in Fig. 5 illustrates their general tendency to occur in immediate environments. A supersaturated with respect to quartz, i.e. coexisting with opal,

cristobalite or silica-rich glass, B saturated, C undersaturated with respect to quartz. Many exceptions which could be inferred from published paragenetic sequences seem to be more apparent than real, although exceptions undoubtedly do exist. In particular chabazite, which is chemically equivalent to

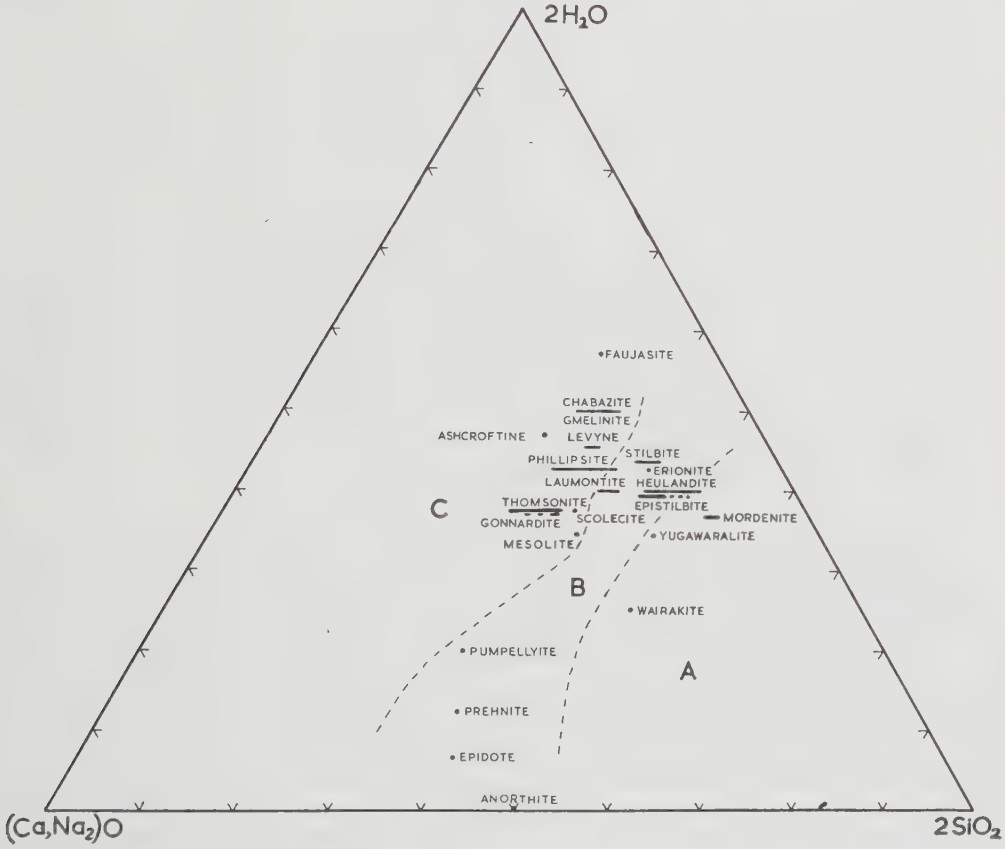

Fig. 5. Composition in molar proportions of lime-rich zeolites (see Appendix 2) and of certain other Ca–Al silicates. For the zeolites and anorthite, (Ca, Na_2)O is numerically equal to Al_2O_3. A. Field of phases favoured by supersaturation in silica. B. Field of phases which can commonly coexist with quartz (erionite coexists with opal). C. Field of phases favoured by a silica-deficient environment.

stilbite with less silica and to laumontite with additional water, falls in the field of the less siliceous zeolites yet has often been reported in association with quartz (e.g. in the Nova Scotia traps, Walker and Parsons (1922) p. 42), although not necessarily in equilibrium with it. Similarly it has been synthesized with quartz (see Table 14).

3.6. *Groundmass zeolites in igneous rocks, pegmatoids and glasses*

It is well known that analcime and other zeolites are common in the groundmass and pegmatoids of basic, alkaline lavas and shallow intrusives. Apart from the fact that they are characteristically silica-poor zeolites, they provide little direct

evidence on zeolite stability. It is known (Yoder, 1953) that analcime is stable to about 570°C at 2000 bars in the absence of free silica and may thus form at much higher temperatures than in the presence of quartz (see later). Experimental evidence is inadequate to interpret the occurrence of phillipsite in the mesostasis of apparently fresh basanites (Coombs in Brown, 1955, p. 370) but thomsonite appears to break down to anorthite near 300°C (Fyfe, 1955) and can be interpreted as either metamorphic, as in the Otama metagabbros, or low-temperature, late stage hydrothermal as in the case of groundmass thomsonite in the Waihola theralite (Hutton, in Benson, 1942). Povarennykh (1954) has discussed how the relative proportions of nepheline, albite and anorthite in feldspathoidal rocks control the proportions of natrolite, analcime and thomsonite in their zeolitic alteration products.

In the later hydrothermal stage in pegmatites of quartzose rocks on the other hand, the typical zeolites are the laumontite–heulandite–stilbite group (e.g. Richmond, 1937; Whitehouse, 1937), while Harris and Brindley (1954) have described an interesting case of the natural devitrification of a highly siliceous pitchstone glass to mordenite. Similarly Hayashi and Sudo (1957) have recognized mordenite and opal in the bentonitic hydrothermal alteration products of Japanese rhyolite tuffs. Such examples provide further evidence for the silica-content correlation described above.

3.7. *Conclusion*

Similar recurring assemblages in a variety of environments of widely differing age support the validity of the zeolite facies concept and we consider that it may be extended, in the form of mineral facies rather than of metamorphic facies, to the zone of diagenesis with its heulandite–quartz–montmorillonoid assemblages as well as to the fillings of many veins and amygdales. Nevertheless as stated above low-temperature conditions are probably particularly conducive of non-equilibrium and some of the parageneses, especially those with phases such as mordenite and epistilbite, are probably to be regarded as metastable.

Occurrences in hydrothermal areas, like that of phillipsite in marine sediments (Murray and Renard, 1891; Goldberg and Arrhenius, 1958), provide some information on actual temperatures and pressures of formation. These data are summarized in Table 1.

4. Theoretical Considerations on Zeolite Stability
(A. J. E., W. S. F.)

The broad pattern of progressive regional metamorphism is one of increasing dehydration as the mineral assemblages of low grade rocks pass to the less hydrated high grade assemblages. Coupled with this dehydration is a tendency for phases to increase in density, even more than is implied by dehydration. The general features are consistent with those which would be deduced if the rocks were subjected to increasing temperatures at steadily increasing pressures.

On grounds of entropy, the stable mineral assemblage at low temperatures must be the one with the maximum possible hydration and it will consist largely of clay minerals and zeolites. That such assemblages are commonly developed, at

Table 1. Temperatures of occurrence of some natural zeolites and related minerals (data derived from references given in text)

Mineral	Occurrence	Temperature (T°C)	Depth (m)
Phillipsite	Deep sea sediments	0°	4000–5000
Chabazite, phillipsite, natrolite	Masonry, Roman baths	40–70°	Surface
Clinoptilolite, analcime	Diagenesis	Low	?
Stilbite	Hunters, Boulder Hot Springs	?64°, ?73°	Surface
Clinoptilolite	Yellowstone	125°	19–26
Analcime	Yellowstone	125–155°	26–60
Mordenite	Wairakei	150–230°	73–300
Heulandite	Wairakei	within range of mordenite	
Laumonite	Wairakei	195–220°	150–275
Wairakite	Wairakei	200–250°	180–600
Prehnite	Wairakei	~200°	~100
Albite	Wairakei	160–240°	100–600
Adularia	Wairakei	230–250°	385–650
Zeolite and adularia	Steam Boat Springs*	170°	52

Note: (1) The maximum temperatures recorded for the Wairakei boreholes are 250–260°C.
(2) The appearance of albite and other minerals at abnormally low temperatures and shallow depths in some Wairakei holes suggest that in these cases they may have been deposited under an earlier regime of higher temperatures.
* See White (1955).

least partially, has been demonstrated in the previous survey. Further, the recurrence of simple assemblages suggests that equilibrium is often approached.

4.1. *The importance of silica activity*

In the low temperature regional environment where zeolite facies minerals are formed, equilibrium with silica normally implies equilibrium with quartz. But in some of the environments where zeolites are formed on a large scale, less stable modifications of silica, such as opal or cristobalite, may be present. This commonly occurs in active hydrothermal areas and also in shallow sediments where opaline silica may be a cement. A solution which is actively precipitating opaline silica must be supersaturated with respect to quartz, and experimental data indicate that the silica activity could be greater than in equilibrium with quartz by a factor of .10 (Ellis and Fyfe, 1957). Experiments described later suggest that a change of environment from one saturated with cristobalite to one saturated with quartz must change the maximum temperature of stability of a mineral assemblage. Natural zeolite assemblages reported above support this conclusion.

In any reaction of type:

$$A_xB_yC_z \rightleftarrows A_xB_yC_{z-w} + C_w$$

phase $A_xB_yC_z$ will form over a wider range of conditions if the state of C is not the stable form at the given pressure and temperature, and if other factors such as nucleation do not interfere. This effect, which is not restricted to silica may be large. Consider, for instance, the reaction:

$$A(SiO_2)_4 + 2SiO_2 \rightarrow A(SiO_2)_6$$

at equilibrium at 25°C where $\Delta G = 0$ and the stable silica phase is quartz. As the free energy of vitreous silica is 3 kcal more positive than that of quartz at this temperature (Latimer, 1952) if silica is added as glass, ΔG at 25°C will now become —6000 cal and the field of $A(SiO_2)_6$ will be expanded. The silica (or any other component) may be added in an experimental run in an amorphous state and at the end of the run may be recovered partly or entirely as quartz. Nevertheless, phases may have grown while the silica activity was high and may persist in the final products.

Consider the effect this silica activity has on a typical hydrate boundary. Data from synthetic studies indicate that the reaction:

$$\underset{\text{wairakite}}{CaAl_2Si_4O_{12}.2H_2O} \rightarrow \underset{\text{anorthite}}{CaAl_2Si_2O_8} + \underset{+\text{ quartz}}{2SiO_2} + \underset{+\text{ water}}{2H_2O}$$

may be at equilibrium around 350°C and 1000 bars. Solubilities (Kennedy, 1950a) indicate that the free energy of amorphous silica is about 1500 cal/mole above that of quartz. Thus with amorphous silica the above process will have a ΔG of +3000 cal. The ΔS of dehydration may be of the order of 10–15 cal/water molecule and the equilibrium temperature with respect to amorphous silica may be 100–150°C higher. This is well demonstrated both in direction and magnitude by the data in Table 3.

4.2. *Relative importance of silica content and water content*

In this paper attention is focused on silica-rich systems. On the basis of entropy it would be expected that the least hydrated phase would also be the high temperature phase. Further, if two assemblages have different amounts of silica bound in silicates it might be anticipated that the assemblage with the greater amount of bound silica would be the more stable. It is a fact that assemblages such as nepheline–quartz, thomsonite–quartz, olivine–quartz are not stable. It might therefore be suggested that the larger silica content of sodium mordenite relative to analcime could conceivably increase its stability and hence make it the higher temperature phase. However, the reaction:

$$NaAlSi_5O_{12}.3{\cdot}5H_2O \rightarrow NaAlSi_2O_6.H_2O + 2{\cdot}5H_2O + 3SiO_2$$

must have a positive entropy change due to the large entropy of free water in the gas or liquid state. This implies that analcime becomes more stable at high temperatures relative to mordenite. Analcime need not be stable at all, but it would be most remarkable if analcime was stable at lower temperatures than mordenite.

The silica-deficient zeolite natrolite ($Na_2Al_2Si_3O_{10}.2H_2O$) is unlikely to occur with free quartz for although its formula suggests intermediate hydration between mordenite and analcime, on the basis of its Na/H_2O ratio it is hydrated to the same extent as analcime but has less silica. Natrolite would be expected to occur only in silica-deficient environments.

The situation with the calcium zeolites is more complex owing to the great number of possible phases. Further, the range of composition of a single phase (e.g. heulandite and its possible polymorph epistilbite) is often considerable (see Appendix 2). In Table 2 some of the possible compositions of calcium end members are listed in order of decreasing water content in relation to anorthite and quartz.

The entropy argument used above would lead one to suggest that the order of

Table 2

Zeolite	Composition
Heulandite (var. clinoptilolite)	An + $8SiO_2$ + $8H_2O$
Chabazite	An + $3{\cdot}2SiO_2$ + $7{\cdot}2H_2O$
Mordenite	An + $8SiO_2$ + $7H_2O$
Stilbite	An + $5SiO_2$ + $7H_2O$
Heulandite	An + $5SiO_2$ + $6H_2O$
Chabazite	An + $2SiO_2$ + $6H_2O$
Stilbite	An + $3{\cdot}2SiO_2$ + $5{\cdot}6H_2O$
Heulandite	An + $4SiO_2$ + $5{\cdot}3H_2O$
Epistilbite	An + $4SiO_2$ + $5{\cdot}3H_2O$
Chabazite	An + $1{\cdot}3SiO_2$ + $5{\cdot}3H_2O$
Levyne	An + $2SiO_2$ + $5H_2O$
Heulandite	An + $3{\cdot}2SiO_2$ + $4{\cdot}8H_2O$
Yugawaralite	An + $3SiO_2$ + $4H_2O$
Laumontite	An + $2SiO_2$ + $4H_2O$
Gismondine	An + $0SiO_2$ + $4H_2O$
Scolecite	An + $1SiO_2$ + $3H_2O$
Thomsonite	An + $0{\cdot}8SiO_2$ + $3H_2O$
Thomsonite	An + $0SiO_2$ + $2{\cdot}4H_2O$
Wairakite	An + $2SiO_2$ + $2H_2O$

stability would be basically controlled by water content. Further, one might anticipate that, given equal water content, the most stable species at any temperature would be that with the most silica. Field data indicate that this latter suggestion is not generally valid; for example yugawaralite should be stable relative to laumontite, but the latter is the common zeolite. Laboratory and field studies suggest that although the silica content of zeolites reflects the silica activity, the silica effect does not override the water effect; with respect to water content (calculated relative to (Ca, Na_2) O. Al_2O_3, contrast Cornu, 1908), the order of stability is normal.

4.3. *Dehydration reactions at high pressures*

The experimental boundaries between zeolites and feldspars are normally steep but as they are ill-defined it is a matter of difficulty actually to measure the slope. Changes in slope of zeolite–feldspar boundaries must occur at high pressures owing to the large molar volumes of zeolites. At very high water pressures some zeolites should be dehydrated to anhydrous phases (cf. Griggs and Kennedy, 1956). In

general, successive dehydration boundaries tend to become steeper at low temperatures, a result of the increasing departure of water from ideal behaviour at low temperatures (Ellis and Fyfe, 1957).

The following examples will illustrate such effects. From the data of Appendix 2 the ΔV's of reaction for the following have been calculated at 25°C.

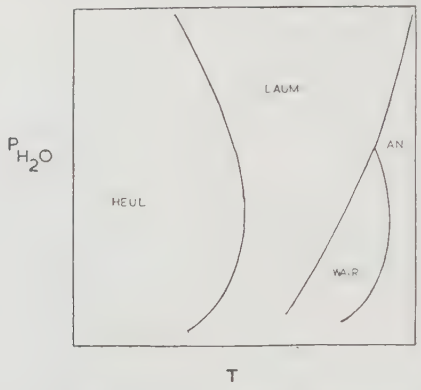

Fig. 6. Possible form of phase relations between heulandite, laumontite, wairakite and anorthite based on volume relations.

(1) $$\underset{\text{heulandite}}{CaAl_2Si_6O_{16}.5{\cdot}3H_2O} \rightarrow \underset{\text{laumontite}}{CaAl_2Si_4O_{12}.4H_2O} + \underset{\text{quartz}}{2SiO_2} + \underset{\text{water}}{1{\cdot}3H_2O}$$
$$\Delta V = -6 \text{ cm}^3$$

(2) $$\underset{\text{laumontite}}{CaAl_2Si_4O_{12}.4H_2O} \rightarrow \underset{\text{wairakite}}{CaAl_2Si_4O_{12}.2H_2O} + \underset{\text{water}}{2H_2O}$$
$$\Delta V = +22 \text{ cm}^3$$

(3) $$\underset{\text{wairakite}}{CaAl_2Si_4O_{12}.2H_2O} \rightarrow \underset{\text{anorthite}}{CaAl_2Si_2O_8} + \underset{\text{quartz}}{2SiO_2} + \underset{\text{water}}{2H_2O}$$
$$\Delta V = -10 \text{ cm}^3$$

(4) $$\underset{\text{laumontite}}{CaAl_2Si_4O_{12}.4H_2O} \rightarrow \underset{\text{anorthite}}{CaAl_2Si_2O_8} + \underset{\text{quartz}}{2SiO_2} + \underset{\text{water}}{4H_2O}$$
$$\Delta V = +13 \text{ cm}^3$$

These values assume a water density of unity; as equilibrium occurs at low temperatures, the values so calculated could be meaningful at moderate pressure. In a normal dehydration series ΔV is positive for each step. This is obviously not the case in the above series and examples of negative boundary slopes and restricted low pressure fields (e.g. wairakite) are to be expected (Fig. 6).

Experimental studies are usually limited at low temperatures to pressures equal to or higher than the vapour pressure of liquid water. As boundaries pass through the two-phase region of water the slopes must change rapidly, but above this region they will be steep over a wide range of pressure.

4.4. *Entropy of analcime*

Fyfe *et al.* (1958) have discussed some general features of entropies of silicates

with emphasis on the limitations of the assumption that entropies of constituent oxides are additive. To the writers' knowledge, the entropy of only one zeolite has been determined, namely analcime for which KING (1955) reports a value of 56·0 cal/deg mole. This entropy is very high compared with the sum of the entropy of the oxides, 44·6 cal/deg mole. However, a large entropy is to be expected since the molar volume of analcime is large. Following the arguments used in FYFE *et al.* (1958) we estimate an entropy of 57·0 cal/deg mole which includes a volume correction and a correction for randomness in the Al–Si arrangement (BEATTIE, 1954). Similarly wairakite would be expected to have a large entropy which is in accord with its ready nucleation and growth (cf. cristobalite). Further, the apparent molar volume of water in analcime is much larger than with most hydrates. The large entropy of analcime leads to some unusual features of its breakdown. At 25°C, the ΔS of the reaction: analcime + quartz → albite + water (liquid) is +0·95 cal/deg mole, a value very near zero. For most dehydration reactions removal of one water molecule to give liquid water at 25°C is accompanied by an entropy increase of 7 cal/deg mole (an average of twenty-four cases). The small change noted above indicates the danger of using average figures with zeolites. In fact it could be possible to have negative entropies of dehydration at low temperatures and pressures.

4.5. *Osmotic conditions*

Data indicate that zeolites will be stable minerals in a low temperature environment or under conditions of moderate depth of burial. In these environments open pores must be common. In hydrothermal areas such as Wairakei, New Zeland, the pressure measured in fissures is often that of the water column and is therefore related to rock pressure in the ratio of water density to rock density. It is thus necessary to consider conditions where the pressure on the solid phases is greater than the pressure in the fluid phase and in particular conditions where $P_{H_2O} \simeq \frac{1}{3} P_{load}$. For this to be relevant it is necessary that alteration produces a zeolitized rock which is still porous yet in which the zeolites support the load of overburden. In contrast the zeolites in a cavity in a basalt grow in an environment where clearly $P = P_{H_2O}$. At great depths continuous pore systems must become unstable unless some fluid can support them. If the porosity is low and water is being expelled on a large scale by dehydration reactions the most likely conditions are $P_{H_2O} \simeq P_{load}$.

For phase changes in hydrate systems where density relations are "normal", if the pressure on the solid phases is greater than the pressure in the gas phase the vapour pressure of the solid will be increased (FYFE *et al.*, 1958). If molar volumes of all phases are known the extent of the effect can be estimated.

Consider the effect on the analcime–albite boundary. In Fig. 7 curve A is our boundary based on synthesis for the experimental conditions that $P = P_{H_2O}$. At 1000 atm it passes through 280°C ± 10°. If at the equilibrium temperature at 1000 atm we add 2000 atm rock load ($P_{load} = 3P_{H_2O}$) then the free energy of the reaction:

$$\text{analcime} + \text{quartz} \rightarrow \text{albite} + H_2O$$

becomes

$$2000 \times \Delta V_{solids} \times 0{\cdot}024 \text{ cal}$$

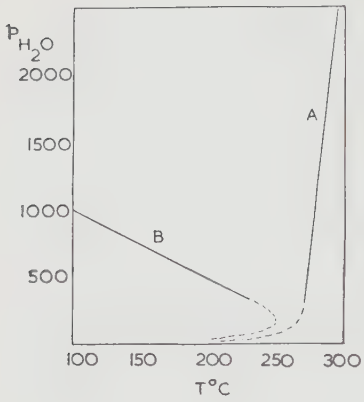

Fig. 7. Equilibrium vapour pressure of the reaction: analcime + quartz = albite + water. Curve A is that suggested by synthesis. Curve B is that estimated for the conditions that $P_{total} = 3\,P_{H_2O}$. The dotted extensions are schematic and illustrate the behaviour expected at low pressures.

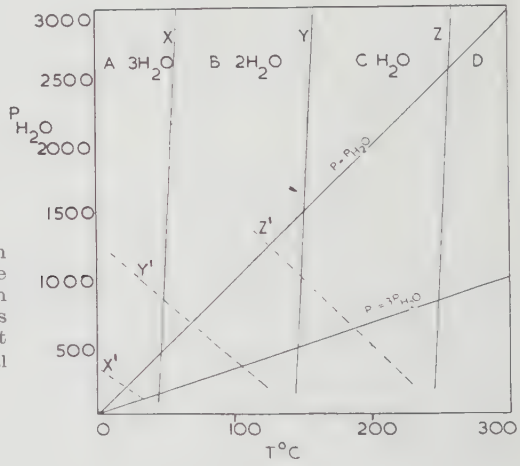

Fig. 8. Diagram illustrating the difference in reaction temperatures in areas where $P_{total} = P_{H_2O}$ and where $P_{total} = 3P_{H_2O}$. X, Y and Z represent the equilibrium vapour pressures for successive dehydration reactions when $P_{total} = P_{H_2O}$, and X', Y', and Z' represent vapour pressures for the same reactions when $P_{total} = 3P_{H_2O}$. A gradient of 30°/km is assumed.

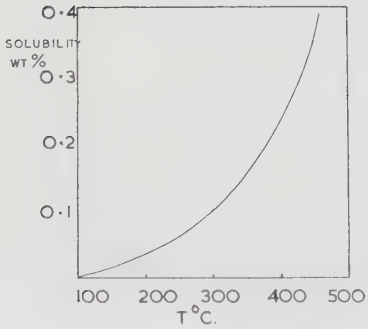

Fig. 9. General form of the 1750 bars solubility curve of quartz in water (after Kennedy, 1950a).

To regain equilibrium, the temperature must be lowered at constant pressure such that a term $\Delta T \Delta S$ equals the above $\Delta P \Delta V$ term. In this region the ΔS of the above reaction will be of the order of 5 cal/mole and $\Delta V_{solids} = 19$ cm^3 so the new equilibrium temperature will be 150–200°C below the experimental value. The result is that of curve B (Fig. 7). Yoder (1954) has reported failure to produce the expected differential pressure effect with analcime. The subject warrants further investigation (see also Harker, 1958).

From the above we conclude that at shallow depths the experimental curves will suggest transition temperatures that are too high, the discrepancy being small at very shallow depths but being considerable at depths of more than 1 km. At great depths the free pore condition probably no longer applies so that the experimental results will apply more closely to the natural conditions.

If the rocks are well sealed and a fissure opens we may have in the rock that $P_{H_2O} = P_{load}$ while in the fissures $P_{H_2O} \simeq \frac{1}{3}P_{load}$, so that analcime might grow in the rock while albite grows in the fissure. But if the conditions in the rock are osmotic, i.e. $P_{load} \simeq 3P_{H_2O}$, and a fissure forms and is held open for free growth, then where albite grows in the rock, analcime could grow in the fissure.

The above effects appear to provide a possible explanation for overlapping of zeolite zones at Taringatura. In particular, the relict heulandite assemblages low in the section characteristically occur in non-porous, well cemented beds, where a closer approach to the condition $P_{load} = P_{H_2O}$ may be expected than in some of the coarser beds which have been converted to laumontite. Variation in composition is another major factor to be considered.

It should be noted that at high temperatures the osmotic correction will be smaller as the entropy of dehydration is larger.

As the apparent molar volume of water in most hydrates is in the range 14–20 cm^3, the high value being typical of low density zeolites, the term ΔV_{solids} in most zeolite reactions will be similar to that for the analcime–albite reaction, and the differential pressure effect will be similar in magnitude. Nevertheless the thermal gradient in natural systems operates to restrict the effect. In Fig. 8 an attempt is made to summarize the type of effects anticipated in an environment where $P_{H_2O} = P_{load}$ (full lines) and where $P_{H_2O} = \frac{1}{3}P_{load}$ (dashed lines) in an area with a temperature gradient of 30°C/km. The crossing points on the gradient lines are changed by about 10–60°C. If the thermal gradient was less, the adjustment would be larger and conversely. In thermal areas such as Wairakei where gradients may be as large as 200°C/km the osmotic corrections should be small.

4.6. *The significance of quartz veins*

In New Zeland the appearance of quartz veins on a large scale is typical of rocks near the zeolite–greenschist facies transition and these veins continue into the greenschists. Where they first appear they commonly carry prehnite and/or pumpellyite. In a very broad sense these veins may serve as an indication of the temperatures in the prehnite zone. KENNEDY'S work (1950a) indicates that high pressure solubility isobars have the form shown in Fig. 9. In the region of liquid water, i.e. at temperatures below the critical temperature, pressure has little effect on solubility. Above the critical temperature the isobars steepen rapidly with increasing temperature.

If water is moving out from high temperature areas at a pressure of 2000 bars then between 250 and 350°C 100g of water would deposit about 0·12g of silica. In the range 250–150°C the amount deposited is only 0·04g. It is apparent that the extent of solution and deposition falls off rapidly below the 300°C region. Experimental data (see Figs. 17 and 18) indicate that the incoming of prehnite relative to zeolites should occur at similar temperatures.

4.7. pH *variation*

In natural systems the principal agent responsible for changes in pH must be carbon dioxide; changes in its concentration will affect relative solubilities of silicates and hence the position of phase boundaries. Experiments designed to test this effect will be discussed later. An increase in alkalinity accelerates the formation of quartz from amorphous silica so that variation in silica activity is a complicating factor.

The significance of pH variation on high level occurrences of calcite–laumontite veins and of laumontite replacement of shell material in fossils is a matter for future investigations.

4.8. *Water content*

The total zeolitization of a feldspathic rock requires a large quantity of water (around 10 per cent) and in many cases this may not be available. Thus in many regions subjected to the P–T conditions of the zeolite facies alteration may be incipient only. This in no way invalidates the recognition of zeolite facies conditions. Boundaries between hydrates will occur at the same temperatures and pressures as in a system with sufficient water, allowing of course, for possible osmotic conditions. Thus, as far as thermal history is concerned, traces of zeolitization as in some rocks of the Alpine Facies of New Zealand will be just as significant as complete alteration. In the partially altered Taringatura rocks the assemblage heulandite + detrital plagioclase does not represent equilibrium. Nevertheless the heulandite is followed by laumontite, and laumontite by still less hydrous phases. Providing successive dehydration transitions such as heulandite → laumontite are observed with increasing temperature it may be inferred that P_{H_2O} has been fixed by external conditions, notably depth, and the reasons for persistence of relict plagioclase (or other water-poor phases) are either kinetic or the result of lack of access by water to grain boundaries. Such conditions are not those of true water deficiency. On the other hand some high-level occurrences of laumontite could be due to water deficiency.

4.9. *Phase rule relationships*

At equilibrium in either the system Na_2O-Al_2O_3-SiO_2-H_2O or CaO-Al_2O_3-SiO_2–H_2O up to two tectosilicates may coexist with an aqueous solution at any arbitrary temperature and pressure and hence there will be only one zeolite in the presence of a silica phase. In the mixed sodium calcium system three tectosilicates may coexist and two in the presence of quartz. The occurrence of three-phase zeolite assemblages such as thomsonite–laumontite–analcime at Otama, does not therefore necessarily imply disequilibrium. In cases of variable alkali–alumina ratios or under conditions where non-tectosilicates such as garnet, epidote or prehnite may form, yet another phase will be possible.

4.10. *Significance of experimental data*

If data on stability fields of minerals are to be applied in petrogenetic interpretation, the actual reactions involved in mineral formation need to be known (note the effects of coupled reactions, Fyfe *et al.*, 1958). In some cases these appear

to be clear cut, as in the conversion of analcime to pseudomorphs of albite. If calcic heulandite alters to calcic laumontite the interpretation is simple but if sodium is present its distribution between the phases will be important and this factor has not yet been examined experimentally. Similarly the experimental reaction: prehnite → anorthite + wollastonite + vapour does not occur when prehnite breaks down in regional metamorphism and it will certainly not take place under the same P–T conditions.

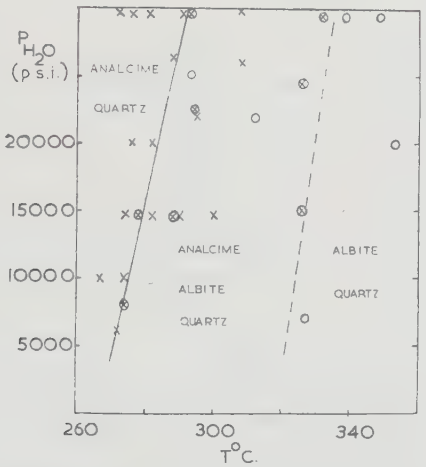

Fig. 10. Results of crystallization of oxide mixes of composition: albite + SiO_2. The full line represents the lower limit of albite and is considered to be nearer the equilibrium boundary than the upper dashed line which represents the upper limit of analcime. Run times vary from 4 to 340 hr.

5. Fields of Synthesis and Stability of Zeolites and Related Phases (A. J. E., W. S. F.)

5.1. *General*

In large part this must be considered a progress report on work which has already occupied about 3 years and a revision of some previous work by one of the writers (Fyfe, 1955). The present position is not one of finality; in fact it abounds in problems which are incompletely solved. Experimental data are recorded in Appendix 1.

The majority of experiments reported here involve the crystallization of glasses or oxide mixes. Gels were not used for reasons outlined below. Mixes were made mainly from calcium oxide, sodium hydroxide solution, active chromatographic alumina, and Mallinckrodt A.R. silicic acid. It became clear as work proceeded that these mixes favoured products high in silica, so in later mixes ground quartz was used with little apparent change in the times necessary for reaction. Many experiments were conducted using minerals as starting materials.

A wide range of apparent phase boundaries have been recorded for the same phase using different starting materials. Although in many cases no satisfactory conclusion can be drawn about the true equilibrium boundary, it is certain that if attainment of equilibrium is desired the worst possible starting materials are the most reactive, i.e. gels, mixes and glasses. These are so unstable that a large number

of metastable intermediates may form and persist. However, with less unstable starting materials reaction rates are commonly too slow for recrystallization to be achieved.

It must be stressed that the field of synthesis of a given phase need bear no relation to the field in which this phase is stable. Equilibrium is indicated only if a reaction is reversible or, less decisively, if a number of different starting materials produce the same results. This has not been demonstrated for any of the hydrothermal syntheses described in this paper.

5.2. *The system albite–silica–water*

There is a wide field (Fig. 10) in which both analcime and albite appear from compositions within this system containing excess silica, a type of behaviour typical of many of the systems studied. The following conclusions are drawn from the experimental data.

(1) The apparent upper stability limit of analcime in the presence of quartz, as established by synthesis, is 280°C ± 10° at 1000 bars. The boundary is steep. This is in reasonable agreement with observations of Fyfe (1955b), Sand *et al.* (1957), and Barrer and White (1952).

(2) The fact that analcime alone appears in short runs above 280°C and that albite appears in longer runs (Valpy, 1957) suggests that analcime grows readily in regions where albite is the stable phase, and that the figures in (1) above represent a higher temperature than that for true stability of analcime.

(3) Preliminary experiments by Campbell (1958) on the solubility of albite in the presence of natural analcime and quartz indicate that the analcime + quartz = albite + water equilibrium temperature is near 200°C at saturated water vapour pressure.

(4) The possibility of synthetic high silica analcimes suggested by Mackenzie (1957) is supported by the absence of a silica phase in the recrystallization of albite glass to analcime. Analyses of natural analcimes (Appendix 2) do not indicate a wide variation of composition.

(5) In experiments using amorphous silica and glasses mordenite appears at temperatures below 230–245°C at 2000 bars. Fyfe (1955b) found that analcime was replaced by mordenite below 220°C at 300 bars.

(6) When quartz is used in place of amorphous silica analcime, not mordenite, appears at temperatures as low as 115°C (Table 9).

(7) Lowering the pH by addition of sodium bicarbonate in runs with amorphous silica raises the temperatures at which mordenite appears. This effect can be correlated with the influence of pH on silica activity since high pH increases the rate of formation of quartz.

5.3. *The system anorthite–silica–water*

The following main conclusions are drawn from the experimental data (Appendix 1).

(1) From all starting materials used in experiments in this system wairakite is the highest temperature calcic zeolite to form. The temperature up to which it forms is greatest when amorphous silica is used in the starting materials. A summary of

apparent field boundaries is given in Table 3. The fact that anorthite appears as low as 340°C in the presence of quartz suggests that wairakite is not stable above this temperature. AMES and SAND (1958) and KOIZUMI and ROY (1958) have produced wairakite from reactive materials at higher temperatures.

(2) Calcium mordenite replaces wairakite at lower temperatures when the silica activity is high in the same way as sodium mordenite replaces analcime (Figs. 11

Table 3

Starting materials	Pressure (bars)	Upper limit of wairakite	Lower limit of anorthite
Oxide mixes	335	440°C	440°C
Glass	2000	450°C	420°C
Glass	5000	450°C	450°C
Oxide mix with quartz	w.v.p.	375°C	340°C
Xonotlite + quartz	2000	380°C	360°C
Stilbite	5000	403°C+	not determined
Chabazite	w.v.p.	310°C+	not determined
Laumontite (amorphous) + quartz	2000	380°C+	not determined
Laumontite + quartz	2000	400°C+	not determined
Lawsonite + silica	3000	440°C	440°C
Lawsonite + quartz	2000	400°C+	390°C
Heulandite (amorphous)	2200	410°C	
Heulandite (amorphous)	w.v.p.	370°	370°C
Prehnite + SiO_2 (glass)	2000	440°C	390°C

Table 4

Starting materials.	P (bars)	Lower limit of wairakite (°C)	Upper limit of epistilbite (°C)
Glass	2000	325	360
Glass	5000	not det.	350+
Oxide mix with quartz	w.v.p.	285	285
Xonotlite + quartz	2000	310	320
Stilbite	5000	ca. 390	ca. 390
Prehnite glass + SiO_2	5000	(missing)	360

and 18). When the silica activity is reduced by the use of quartz, calcium mordenite does not appear even at 212°C. Its field of synthesis is thus lowered by at least 200°C by reducing silica activity.

(3) With many starting materials epistilbite appears as the common low temperature calcium zeolite. A summary of upper limits of synthesis for epistilbite is given in Table 4. Its ready synthesis contrasts with its comparative rarity in nature.

(4) The naturally important zeolite heulandite appeared as only a minor phase in a few runs. It is doubtful if these represent equilibrium (see A.1.6.8). As heulandite

and epistilbite are chemically similar and may be polymorphs with rather similar structures the nucleation of either phase may inhibit the formation of the other. (5) Laumontite was not synthesized although on the basis of water content it might be expected to form at temperatures intermediate between those of epistilbite and wairakite. This contrasts with its copious occurrence in nature. Our failure to synthesize laumontite (and that of Koizumi and Roy, 1958) is a clear indication

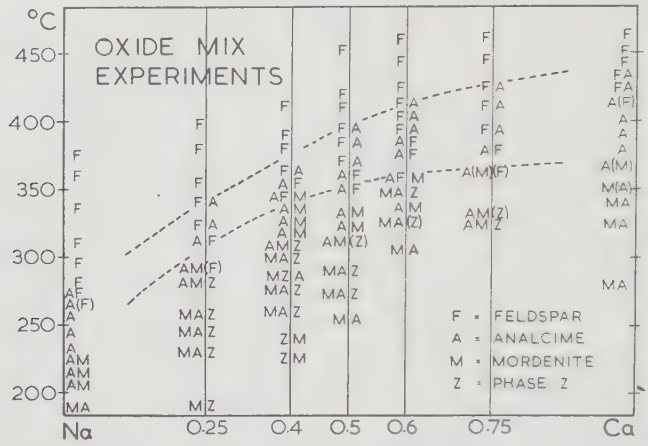

Fig. 11. Phases formed by hydrothermal crystallization of oxide mixes of feldspar compositions. (For pressure data see Appendix I).

of the lack of equilibrium in the synthetic results. On the basis of water content, it is possible that a field of scolecite could occur between laumontite and wairakite. (6) Fyfe (1955b) found that in short runs laumontite and heulandite formed readily over a wide range of temperatures from their "amorphous" dehydration products. Longer runs have shown that such materials appear to retain a nucleating memory and tend to form the parent phase over too wide a range. Data in Table 15, however, indicate that laumontite could be stable relative to wairakite near 300°C for, while at 310–323°C only laumontite was observed in the products, above this temperature wairakite was observed in long runs and in one run at 240°C chabazite was observed.

(7) Our suggestion that the true analcime + quartz → albite boundary is near 200°C and the sequence at Taringatura (Fig. 2) indicate that heulandite should also be stable to about 200°C, and laumontite at rather higher temperatures.

5.4. *Plagioclase–silica–water compositions*

Phases synthesized from compositions within the above system are indicated in Figs. 11 and 12. The lack of a field of synthesis for calcium zeolite + albite, a common assemblage in zeolitized rocks, is strong evidence that equilibrium was not established. It appears that a continous series of analcimes are formed. Epistilbite was formed only from calcium-rich glasses. Refractive index data suggest that mordenites tend to be calcium-rich and feldspars sodium-rich compared with the starting material. Natural plagioclases and synthetic anorthite produced no zeolites in 60 day runs in the range 250–350°C.

5.5. *Synthesis of prehnite*

From glass of its own composition there was little difficulty in growing prehnite at pressures above 2000 atm. Below this pressure, a range of metastable phases appears at low temperatures. Prehnite also formed readily from glasses of epidote composition. In runs with glasses high in silica prehnite was much more reluctant

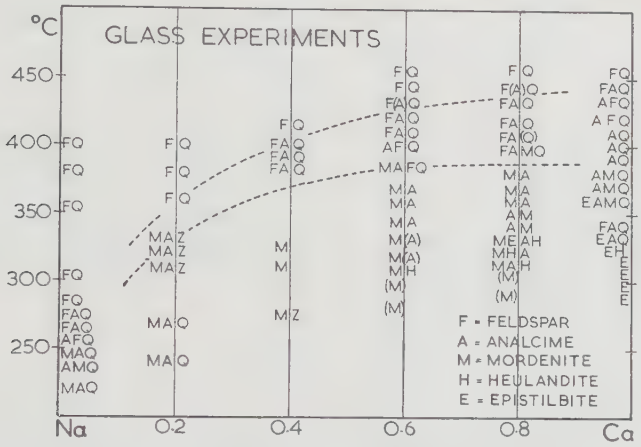

Fig. 12. Phases formed by hydrothermal crystallization of plagioclase plus silica glasses at 2000 bars.

to grow but appeared as a major phase in runs at 5000 bars. The following conclusions emerge. Experiments with three different starting materials (Figs. 13, 14, 15) indicate that prehnite passes to anorthite plus wollastonite at about 450°C at 5000 bars. At temperatures below 300°C (Fyfe, 1955) we consider thomsonite to be the stable phase in silica-deficient environments as is also suggested by the thomsonitic alteration of the Otama gabbros. In these earlier experiments although thomsonite and anorthite grew readily, prehnite was most reluctant to form. Data found previously are summarized in Fig. 16. With more siliceous glasses as starting materials prehnite is cut off in the low temperature and pressure regions by the zeolites wairakite and epistilbite.

The recrystallization of epidote glass indicates that prehnite and vesuvianite form readily.

6. Correlation of Field and Experimental Data
(W. S. F., D. S. C.)

In active hydrothermal areas such as Wairakei zeolite-forming reactions occur in an area of steep thermal gradient, and solutions moving upwards tend to be supersaturated with silica. At Wairakei the principal zeolites are wairakite and mordenite, phases readily formed in the laboratory by using amorphous silica in the starting materials. However, laboratory data suggest a higher temperature for the metastable transition from mordenite to wairakite than is observed at Wairakei. Three factors may contribute to this lack of temperature correlation. There is evidence that the degree of silica supersaturation at Wairakei is small (Ellis and Wilson, 1955; Ellis, 1958) even though amorphous silica is deposited in bores.

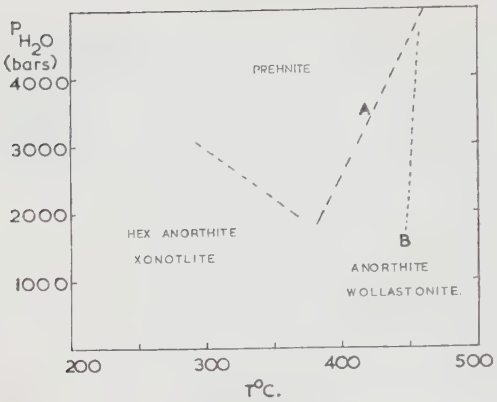

Fig. 13. Phases formed by crystallization of a glass of prehnite composition. Line *A* represents the upper limit of strong prehnite growth. Small amounts of prehnite persist up to line *B*. Boundary lines represent limits of major fields and changes in assemblage are transitional.

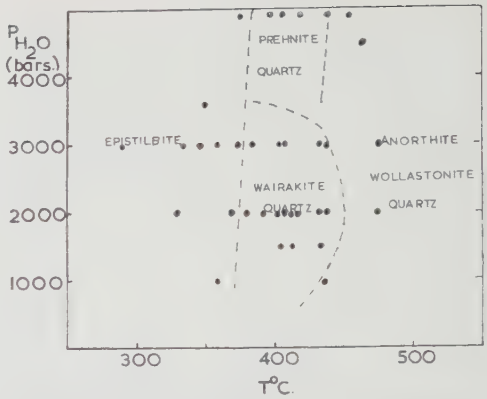

Fig. 14. Phases formed by crystallization of a glass of composition: prehnite + 4 silica.

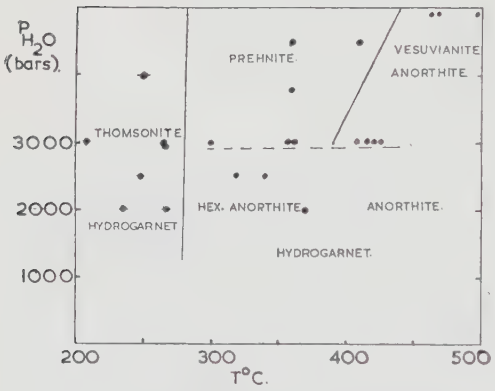

Fig. 15. Phases formed by crystallization of a glass of epidote composition.

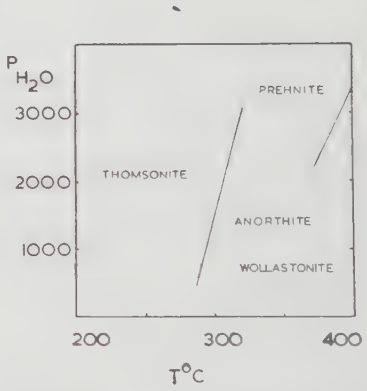

Fig. 16. Phases formed on crystallization of a glass of prehnite composition after Fyfe (1955b) (cf. Fig. 13).

This will tend to diminish the field of mordenite with respect to that determined experimentally. Also, the conditions at these shallow depths may be to some extent osmotic as discussed above, and finally it is possible that the thermal gradient has been steeper in the past.

In the large scale regional zeolitization of sediments, a process consequent upon increasing temperature and pressure caused by depth of burial, a different succession of zeolites occurs. Heulandite, analcime and laumontite are dominant. In the Taringatura section described earlier the transition analcime + quartz → albite + water, occurs about half-way down the section. Assuming a thermal gradient no steeper than average it is unlikely that the temperature at this depth could exceed 240°C and a lower value is more likely. Data from Wairakei and Yellowstone are also compatible with an analcime + quartz → albite transition in

the range 150–240°C (Table 1), and hence with our suggested figure of 200°C. The relation of the heulandite field to that of analcime has been discussed above (5.3).

There is a suggestion (Table 15) that laumontite may be stable near 300°C. Steiner has reported its formation at 195–220°C at Wairakei. Incoming of laumontite above 200°C and gradual transition to a prehnite assemblage at temperatures around 300°C seems possible and is compatible with its main field occurrences in the New Zealand Geosyncline. Nevertheless, a number of occurrences have been noted (e.g. Jurassic of Hokonui Hills and Victorian arkoses) where laumontite would appear to have been formed at lower temperatures.

Wairakite has so far been described only from active thermal areas. The sequence at Taringatura suggests that zeolitization under regional metamorphic conditions could be terminated at the laumontite stage by the coupling effect of other reactions leading to prehnite. Further, it is possible that wairakite is not stable at high pressure as shown in Fig. 14 and hypothetically in Fig. 6.

7. Conclusions
(W. S. F., D. S. C.)

(1) Recurrent formation of similar, zeolite-bearing mineral assemblages in rocks varying in age from Upper Paleozoic to Tertiary justifies the recognition of a zeolite facies. This facies largely bridges the gap between diagenesis and conventional metamorphism.

(2) As certain zeolites are stable in a silica-deficient environment to temperatures at least as high as 550°C, we propose that the zeolite facies should be defined to include at least all those assemblages produced under physical conditions in which the following are commonly formed: quartz–analcime, quartz–heulandite, quartz–laumontite.

(3) In sedimentary rocks the characteristic minerals include heulandite and analcime with quartz in a low grade stage, and laumontite, albite and quartz in a higher grade stage; together with adularia, celadonite, saponite, montmorillonoids, chlorite, calcite and sphene. In silica-deficient environments thomsonite is considered to represent an equivalent stage of metamorphism.

(4) In well-studied areas, there is a general tendency for less hydrated zeolites to occur at higher temperatures in conformity with experimental results and thermodynamic prediction.

(5) There is a tendency for zeolites to fall into three groups according to their mode of occurrence: silica-poor zeolites favoured by an environment lacking free silica; zeolites which coexist with quartz; and highly siliceous zeolites which may only be stable in solutions supersaturated in silica with reference to quartz.

(6) Where zeolitization is confined to the cements in sediments, or to cavity fillings in other rocks the assemblages of new-formed minerals may be considered in terms of Eskola's mineral facies concept. In this respect we are extending the range of the zeolite facies proposed by Turner for metamorphic assemblages only.

(7) Between the rocks of the zeolite facies and typical greenschist facies in New Zealand, there is a very extensive zone characterized by prehnite and/or pumpellyite. There appears to be justification for the erection of a distinct subfacies

of the greenschist facies (or possibly a new facies) to accommodate the rocks concerned.

(8) Extensive laboratory studies on systems related to zeolites have emphasized limitations of synthetic methods of establishing equilibrium phase relations. Change of starting materials has been shown to change apparent phase boundaries by more than 200°C even when run times exceed 30 days.

(9) The determination of phase boundaries by measurement of solubility may provide a sounder approach to the study of some silicate equilibria. Preliminary work on analcime appears promising and suggests that the analcime $-$ quartz $\rightarrow$ albite $+$ water transition occurs near 200°C at low pressures.

(10) The state of silica in starting materials appears critical where the phases on opposite sides of a phase boundary have different silica contents. The field of high-silica phases such as wairakite and mordenite is extended when the silica activity is higher than that of quartz. Observed effects of silica activity can be correlated with thermodynamic expectations and with natural occurrences. Similar conclusions could be drawn for other components in other systems.

(11) We consider that in quartz-bearing systems sodium and calcium zeolites are not stable above temperatures of about 320°C although they may be synthesized readily at temperatures as high as 450°C.

(12) We consider that the prehnite subfacies, transitional between the zeolite facies and greenschist facies, may come in at temperatures around 300°C ($\pm$50°) in regions where water and load pressures are approximately equal and at lower temperatures if osmotic conditions occur.

Acknowledgements—Appreciation is expressed to all those individuals who have assisted the above project. Included among these are Mr. J. D. Campbell, Dr. M. Gage, Mr. D. Hamilton, Dr. H. W. Wellman and Dr. A. J. R. White who have discussed some of the problems and portions of the manuscript. Mr. A. Steiner has provided unpublished data on Wairakei and specimens for examination. Other specimens have been provided by Professor S. Bonatti, Mr. E. D. Gill, Mr. D. Hamilton, Professor B. Mason, Dr. B. Nashar, Dr. N. E. Odell, Professor A. Pabst, Dr. S. C. Robinson, Dr. C. S. Ross, Dr. K. Sakurai, Professor L. W. Staples, and Dr. G. P. L. Walker. Dr. D. A. Brown and Mrs. A. G. Coombs have assisted with translations. Two chemical analyses by Mr. J. A. Ritchie were provided by the Dominion Laboratory.

In particular we wish to express our gratitude for University of New Zealand research grants towards field expenses, and for the purchase of apparatus including a Philips X-ray diffractometer which was regularly used for identification of phases in both the experimental and petrographic parts of the work. The experimental work was also greatly assisted by the Mellor Fund. Valuable technical help was provided by Messrs. G. Clarkson, L. Seeuwen, V. Tyrrell and L. Wylie.

Appendix I

Experimental

(A. J. E., W. S. F., A. M. T.)

A1. 1. *Apparatus*

A great number of experiments were conducted in small closed vessels of capacity 2–10 cm^3. Two features of these should be noted. Firstly they are most satisfactory in the water liquid–vapour range, i.e. at small degrees of filling and temperatures below the critical temperature of water. At supercritical temperatures the density of the fluid was maintained at approximately 0·33 and pressures were calculated from the data of Kennedy (1950b). Secondly, the initial

materials and water must be loaded in the cold bomb and the possibility exists of crystallization during the heating-up period which was normally about 3 hr. However, in runs where the same materials were kept dry during initial heating and were then pumped to pressure at the final temperature, identical results were produced and hence the objection does not appear serious. The other types of vessels used were hot-seal bombs and test-tube bombs 14 in. long with cold seals. All these were pumped to pressure at temperature. Samples were normally enclosed in silver capsules (unsealed) and neither leaching nor corrosion caused concern.

Table 5. X-ray powder pattern of phase Z

d (Å)	I	*d* (Å)	I	*d* (Å)	I
9·52	16	3·65	10	2·474	4
8·32	1	3·52	16	2·397	2
7·78	1	3·46	16	2·344	1
6·98	4	3·13	6	2·305	1
5·73	4	3·040	6	2·105	1
4·08	20	2·95	4	1·988	1
3·96	18	2·711	2	1·919	1
3·93	10	2·641	1	1·897	2
3·84	8	2·541	1	1·767	1
				1·705	1

Errors in temperature, involving control, measurement, and allowance for gradients in vessels are within ±5°C and in most cases ±3°C. Pressures were measured with Bourdon tube gauges calibrated against a manganin coil gauge and results are believed to be accurate to ±5 per cent.

A1.2. *Notes on phases synthesized*

Phases were identified by direct comparison of X-ray diffractometer patterns. The identification of the full assemblage of phases produced was often a matter of great difficulty, and in general the phases reported are those which constitute the major products. The identifications of heulandite and tobermorite are somewhat doubtful. Only three lines of heulandite were not masked by other phases. The patterns of synthetic epistilbite compared closely with epistilbites from Yugawara hot spring, Japan and from Krossanes, Iceland. Hydrogarnets had refractive indices in the range 1·666-1·725 indicating a considerable water content (Yoder, 1950).

There is evidence (Ellis, 1958) from refractive indices that a complete range of synthetic analcimes from sodium to calcium end-members may have been formed. This is not in accord with observations of Steiner (1955) or Barrer (1950). Synthetic wairakite like the natural material (Coombs, 1955) clearly shows the 200 reflection which is absent in strictly cubic analcime and weak in natural non-cubic analcimes. The 400 reflection, although broadened, was not clearly resolved into a doublet. Oxide mixes yielded the closer approach to the cubic modification. With mordenite also a considerable range of intermediate compositions appeared to have been formed between sodium and calcium end-members. Feldspars all tended towards the high temperature forms (Mackenzie, 1957).

A crystalline phase of unknown composition, "phase Z" was found up to temperatures of about 330° from both glasses and oxide mixes, but mainly from the latter. It was found only from mixed sodium–calcium compositions, and was present usually as small thin rectangular plates, or sometimes as larger irregular tablets. The birefringence was very weak, extinction straight, and the R.I. ranged from 1·473–5 at composition 0·75 Ab to 1·484–6 at 0·25Ab. The X-ray spacings are given in Table 5.

The following abbreviations are used:

A	analcime	Ph	phillipsite
Ab	albite	Pr	prehnite
An	anorthite	Q	quartz
Ch	chabazite	S	stilbite
C	cristobalite	T	thomsonite
E	epistilbite	W	wairakite
H	heulandite	Wo	wollastonite
Hg	hydrogrossular	Xo	xonotlite
Hx	hexagonal anorthite	Z	phase Z
L	laumontite		
M	mordenite		

A1.3. *Experiments using oxide mixes*

Over 200 experiments were carried out at s.w.v.p. or at a vapour density of 0·33 in closed bombs on compositions in the plagioclase series. The mixtures were made from calcium oxide, sodium hydroxide, active alumina and silicic acid. The normal run time was 4 weeks, although duplicate runs indicated that products after 2 weeks were probably the same. On the other hand, short runs of 24 hr or less produced different results from those of a month's duration. At the soda-rich end final solutions were always alkaline (pH c. 10).

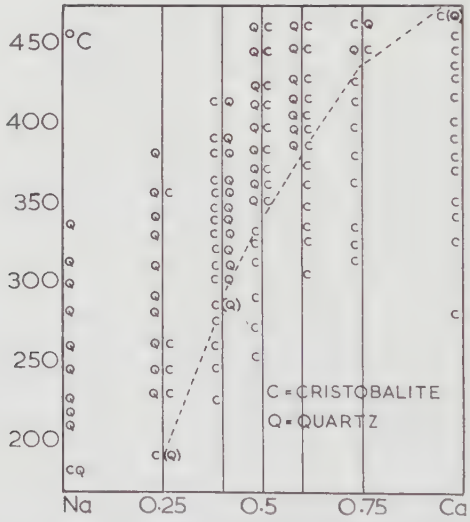

Fig. 17. Variation of silica phases formed during crystallization of oxide mixes of feldspar compositions with excess silica.

Seven compositions were used corresponding to the following: Ab + $6SiO_2$, 3Ab. An. $24SiO_2$, 3Ab. 2An. $30SiO_2$, Ab. An. $12SiO_2$, 2Ab. 3An. $30SiO_2$, Ab. 3An. $24SiO_2$, An + $6SiO_2$.

The basic results are summarized in Fig. 11. Quartz was always produced in runs from albite composition. The formation of quartz seems to be strongly retarded by the presence of calcium and the time for the appearance of quartz is approximately inversely proportional to the calcium content. It appears possible that a film of calcium silicate may protect the cristobalite which first appears. The data are summarized in Fig. 17. A more detailed study of the crystallization of oxide mixes of the sodium system was carried out by G. W. Valpy (1957). A greater variety of run times was used and mixes were pumped to pressure at the proper temperature. These experiments are significant in indicating that analcime tends to persist above its true stability field and to grow rapidly. The results are summarized in Fig. 10. The position of the boundary at low pressures is very close to that indicated by the data of Fig. 11.

A1.4. *Experiments with glasses*

Experiments were carried out on 130 glass samples having the following compositions and refractive indices:

	Composition	*R.I.*
A	Ab + 4·25 SiO_2	1·472
B	0·8Ab + 0·2An + 4·25 SiO_2	1·484
C	0·6Ab + 0·4An + 4·25 SiO_2	1·490
D	0·4Ab + 0·6An + 4·25 SiO_2	1·502
E	0·2Ab + 0·8An + 4·25 SiO_2	1·508
F	An + 4·25 SiO_2	1·515

The lower silica content of the glasses is reflected in the lack of free silica in some end products. The crystallization was conducted at 2000 bars for 14 days in each case. Calcium-rich glasses react readily above 300°C, but with increasing soda content the tendency to crystallize falls off. The sodium glass would not crystallize in 2 weeks at 300°C even at a water pressure of 5000 bars. To obtain results from this glass, sodium fluoride was added as a flux ($\frac{1}{2}$ mole of NaF per mole of $NaAlSi_3O_8$). With calcium members NaF could not be added as insoluble calcium fluoride would form. The crystallization of the soda-rich members was erratic and it appears that small amounts of impurities may have an influence.

Pure calcium glasses did not react rapidly below 275° at 3000 bars but at 5000 bars crystallization was fairly rapid at least down to 212°C. The major results are summarized in Fig. 12. In Table 6 results at 5000 bars are summarized.

Table 6

Glass	T°C	Products
F	212	E
	450	W, An, Q
	460	An, Q
	470	An, Q
D	250	E
	335	M + E
	350	M + E

Some separate experiments (Table 7) were conducted on the crystallization of albite glass at 2000 bars. The glass (R.I. 1·488) was made by melting the very pure albite from Amelia, Virginia. Once more sodium fluoride was added to facilitate crystallization.

Table 7

T(°C)	220	240	255	270	298	310
Products	A	A	A	A	Ab	Ab

The boundary indicated is close to that of Valpy, using oxide mixes, but as found by Mackenzie (1957) a silica phase was not obtained in sufficient quantities to produce an X-ray pattern. In the presence of fluoride the significance of this observation must be treated with caution as some silica may be held in solution as SiF_6^{2-} or sodium silicate.

A1.5. *Mixes with quartz in place of silica*

Results for the pure calcium system (corresponding to anorthite + 8 quartz) are summarized in Table 8. The crystallization was carried out in closed vessels at water vapour pressure or density of 0·33.

Table 8

T(°C)	400	385	375	363	340	330
Products	An	An	An.W	W.An	W(An)	W
	285	265	220			
	E.W	E	E			

The results of a similar series of experiments with the sodium system and quartz are listed in Table 9.

Table 9

T(°C)	335	303	279	267	265	260	160	115
Products	Ab,Q	Ab,Q	A,Ab,Q	A,Q	A,Q	A,Q	A,Q	A,Q

A1.6. *Mixes with sodium carbonate and bicarbonate*

A series of experiments was conducted with mixes of composition Na_2O, Al_2O_3, $18SiO_2$ where the soda was added as bicarbonate or carbonate. The pH of these solutions is lower than that of mixes using sodium hydroxide. At 250°C the pH of molar $NaHCO_3$ is about 9·0 and of an equimolar solution of carbonate–bicarbonate, about 10·8 (Ellis and Fyfe, 1957). The results are summarized in Table 10.

Table 10

Sodium compound	T (°C)	Products
$NaHCO_3$	255	M.A.C.Q
$NaHCO_3$	258	A.M.Q
$NaHCO_3/Na_2CO_3$	258	(A.).(M).Q
$NaHCO_3$	265	A.M.Q
$NaHCO_3/Na_2CO_3$	265	A.Ab.Q
$NaHCO_3$	262	M.A.C.Q
$NaHCO_3$	275	M.A.Q
$NaHCO_3$	280	Ab.Q
$NaHCO_3/Na_2CO_3$	280	Ab.Q

A1.7. *Experiments using minerals as starting materials*

A1.7.1. *Xonotlite.* In a further attempt to reduce the activity of the starting materials the mineral xonotlite was used as a source of calcium and was mixed with quartz and active alumina. The composition used corresponded to calcium mordenite. Results are summarized in Table 11.

Table 11

T(°C)	390	380	380	365	360	320	315	310	265
P(bars)	5000	2000	s.w.v.p	2000	s.w.v.p	s.w.v.p	5000	2000	4000
Products	An.Q	W.An.Q	W.An.Q	W.An.Q	W.An.Q	E.W.Q	W.E.Q	W.E.Q	E.Q

A1.7.2. *Nepheline.* A study was made of the reaction of nepheline from the Haliburton–Bancroft area, Ontario, with natural quartz, Table 12.

Table 12

T(°C)	396	385	380	360	346	338	335	310	250
P (bars)	2000	2000	2000	2000	2000	2000	2000	2000	w.v.p.
Products	Ab.Q	Ab.Q	Ab.Q	Ab.A.Q.	A(Ab)Q	A.Q	A.Q	A.Q	A.Q

A1.7.3. *Stilbite.* A few experiments were conducted on the breakdown of stilbite from an unknown locality (Table 13).

Table 13

T(°C)	315°	350	370	403
P (bars)	s.w.v.p.	5000	5000	5000
Products	S	S (E)	E	W + Q

A1.7.4. *Chabazite.* In Table 14 results are given for the breakdown of chabazite from Richmond, Victoria, a locality that has yielded highly aluminous, alkali-rich specimens such as $(Ca_{3\cdot3}Na_{5\cdot2}K_{1\cdot2})\,Al_{13}Si_{23}O_{72}\cdot36H_2O$ with variable Ca : Na : K ratios, (Doelter, 1921, pp. 75–77).

Table 14

T(°C)	310	285	255	245	250	240	230	220	180
P	s.w.v.p	s.w.v.p	s.w.v.p	s.w.v.p	s.w.v.p	s.w.v.p	5000	s.w.v.p	s.w.v.p
Products	W	W	W + Ph	W + Ph	W + Ph	W + Ph	Ph + W + C	Ph + W + Ch	Ch

A1.7.5. *Laumontite.* Laumontite, shown by analysis to be almost alkali-free (Pabst, personal communication) from Pine Creek Mine, Inyo County, California, with quartz produced wairakite at 400°C, and 380°C, at 2000 bars.

A1.7.6. *Dehydrated laumontite.* When laumontite is heated to 800°C it passes into a state which gives no X-ray pattern (Koizumi and Kiriyama, 1953). This material was used in a number of 30-day runs (Table 15) which were much longer than those of previous experiments by one of the authors (Fyfe, 1955b).

Table 15

P (bars)	s.w.v.p	s.w.v.p	2000	2000	s.w.v.p	s.w.v.p	2000	600
T(°C)	240	310	310	323	330	344	380	380
Products	Ch + Q	L	L + Q	L + Q	W	W.L.(H)	W + Q	(L + W)
Remarks	Q added	100%	Q added	Q added	100%	Heul. doubtful	Q added	3 days

A1.7.7. *Lawsonite.* Lawsonite from Valley Ford, California, with natural quartz gave products indicated in Table 16.

Table 16

P (bars)	2000	2000	2000
T(°C)	400	395	382
Products	An,W,Q	An,W,Q	W,Q

These results may be compared with results on lawsonite and amorphous silica obtained previously by Fyfe (1955b) (Fig. 18). Unfortunately the reaction could not be followed to temperatures much lower than the range shown as the rate of reaction is too slow.

A1.7.8. *Dehydrated heulandite.* The amorphous phase formed by heating heulandite

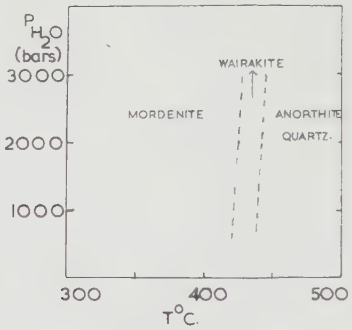

Fig. 18. Phases formed by reaction of lawsonite with amorphous silica.

(Appendix 4) was used in some long runs of more than 30 days. The results (Table 17) differ considerably from those of Fyfe (1955b) from short runs on the same material in which 100 per cent crystallization to heulandite was observed. The appearance of wairakite in the long runs implies that it is more stable than heulandite in the range studied.

Table 17

P (bars)	2000	2600	2200	w.v.p	2200
T (°C)	280	340	360	370	410
Products	H + W	H + W	H + W + M	An + (W)	M + W + An
Remarks	Q added				

A1.7.9. *Thomsonite.* Natural thomsonite from Otama, New Zealand, mixed with quartz, produced wairakite in the range 280–316°C at pressures from s.w.v.p. to 4000 bars. The reaction could not be studied at lower temperatures as 30-day runs produced no detectable alteration.

A1.8. *Experiments involving glasses of prehnite composition*

The results of crystallization of glass formed by fusing a natural prehnite (Appendix 3) are summarized in Table 18 and in Fig. 13.

A series of thirty-six runs was carried out on a glass formed from the same prehnite as above but with silica added to give a molar ratio of prehnite : silica of 1 : 4. The reluctance of prehnite to form except at high pressures is an indication of metastable crystallization (Taylor, 1957). The results are summarized in Fig. 14.

A1.9. *Experiments with epidote glass*

A glass was produced by fusion of a deep green epidote (6·2 per cent Fe_2O_3) and the results of crystallization (Taylor, 1957) of twenty-five samples are summarized in Fig. 15. These results differ from those of Ehlers (1953) who found no field of prehnite or vesuvianite.

Appendix 2

Composition and Density of Zeolites

(D. S. C.)

Basic data on composition, density and structure of zeolites are in many cases inadequate for a proper consideration of mutual relationships and stability fields and a tendency remains

Table 18

Temp. (°C)	Pressure (bars)	Time (days)	Products
270	3000	14	Hx(s) Tb(s)
295	2000	10	Hx(s) Pr(s)
300	3000	9	Hx(s) Tb(s)
320	3000	18	Pr(s)
330	2000	1	Pr(s) Hx(s) Xo(s)
338	1000	9	Pr(s) Hx(s)
340	3000	14	Pr(s)
347	1000	8	Hx(s) Xo(s)
350	1700	4	Hx(s) Xo(s)
353	4000	6	Pr(s) An(w)
357	2000	17	Pr(vs)
357	2000	2	Pr(s) An(w) Wo(w)
360	2000	9	Hx(s) An(w) Pr(w)
377	2000	10	Hx(s)
380	2000	1	An(s) Hx(s) Xo(s)
380	3000	10	Pr(s)
386	2000	12	Pr(s) An(s) Wo(s)
400	3000	9	Pr(s) An(s) Wo(s)
400	3000	3	Pr(s)
405	3000	4	An(s) Wo(s)
409	4000	3	Pr(s) An(vw)
415	4000	5	Pr(s) An(s) Wo(s)
415	4000	1	An(s) Wo(s) Pr(w)
425	3000	9	An(s) Wo(s)
425	5000	3	Pr(s)
427	3000	15	An(s) Wo(s) Pr(vw)
430	3000	7	An(s) Wo(s) Pr(w)
440	5000	7	Pr(s) An(s) Wo(s)
442	2000	6	An(s) Wo(s)
445	4000	6	Pr(s) An(s) Wo(s)
448	2000	11	An(s) Wo(s)
450	2000	17	An(s) Wo(s)
450	3000	9	An(s) Wo(s) Pr(w)
453	3860	3	An(s) Wo(s)
455	4000	3	An(s) Wo(s)
455	5000	5	An(s) Wo(s)
457	5000	4	An(s) Wo(s) Pr(w)
469	3000	9	An(s) Wo(s)
475	4500	2	An(s) Wo(s)
490	4000	5	An(s) Wo(s)
490	4000	5	An(s) Wo(s)
492	4000	2	An(s) W0(s)
516	4700	3	An(s) Wo(s)

for some workers to express compositions in terms of "ideal" formulae which can obscure relationships rather than clarify them. Considerable confidence can be placed in the view that the number of oxygen atoms within the framework of linked $(Si,Al)O_4$ tetrahedra is virtually constant for the unit cell of each species. This number must be even, is commonly a multiple of 8, and can be determined unambiguously from reasonably precise chemical, X-ray and density data. Following Hey (1932a) and others, unit cell contents on the basis of this ideal number of structural oxygens have been calculated by the writer for a large number of zeolite analyses. More attention has been given to variations in the Si : Al ratio than to variations in the other cations, as the latter are subject to secondary, base exchange effects and are therefore less fundamental in reflecting conditions of formation. Nevertheless as the various lime zeolites appear to accept such elements as Na, K and Sr into their lattices to varying degrees, the concentration of these latter elements in the environments of formation must influence stability fields. The Mg-bearing species ferrierite and the barium zeolites are not here considered.

It will be found convenient to describe the range of composition of certain zeolites not only in terms of the familiar isomorphic substitutions: (i) NaSi for CaAl; and (ii) Na_2 for Ca, or more generally $(Na, K)_2$ for (Ca, Sr, Ba) but also in terms of the substitution: (iii) Al for Si within the tetrahedral framework with additional W group cations (Na, K, $Ca_{\frac{1}{2}}$) occupying otherwise vacant lattice sites. This results in a marked variation in the number of W group cations per unit cell and is equivalent to simultaneous operation of the other two types of replacement.

The ranges of composition tentatively accepted for valid species are listed below together with estimates of the specific gravity for some of the compositions listed. Specific gravity is not significantly affected by the substitution of Na_2 for Ca (compare analcime and wairakite), but it does vary markedly with the other types of substitution. The values given have been selected, averaged or interpolated from previously published determinations and in some cases are capable of considerable refinement. Only a few leading references have been cited; many others have been considered.

In Fig. 5 compositions of the calciferous zeolites are plotted in molecular proportions on the triangle $(Ca, Na_2, K_2)O : 2H_2O : 2SiO_2$, the component $(Ca, Na_2, K_2)O$ being numerically equal to Al_2O_3 for zeolites and for other true tectosilicates such as anorthite. Horizontal lines therefore represent the range of variation in Si : Al ratios through each series. Prehnite, pumpellyite and epidote have been plotted for comparison and in these the Al_2O_3 content is not directly related to the other components. The water content has been plotted arbitrarily at the value which is judged to best reflect the chemical analyses and structural data. In several cases it is open to question. Compositions plotted are based on analyses of apparently good quality of natural zeolites. Laboratory crystallization from highly reactive and unstable starting materials such as glasses is likely to lead to a greater range of metastable compositions than in the case of the natural materials.

Analcime. $Na_{17}Al_{17}Si_{31}O_{96}.16H_2O$ to $Na_{14}Al_{14}Si_{34}O_{96}.16H_2O$, with minor substitution of $(K,Ca_{\frac{1}{2}})$ for Na; commonly near $NaAlSi_2O_6.H_2O$; $Z = 16$ (e.g. Hartwig, 1928; Coombs, 1955); $D = 2{\cdot}265 \pm 0{\cdot}01$. Saha (1957) has indicated that synthetic analcimes may range from $NaAlSi_3O_8.nH_2O$, to $NaAlSiO_4.mH_2O$, presumably with $Z = 12$ and $Z = 24$ respectively.

Ashcroftine. $40(KNaCaAl_4Si_5O_{18}.8H_2O)$; $D = 2{\cdot}61 \pm 0{\cdot}05$ (Hey and Bannister, 1933).

Chabazite. $(Ca,Na_2,K_2)_5Al_{10}Si_{26}O_{72}.36H_2O$ to $(Ca,Na_2,K_2)_{6\cdot75}Al_{13\cdot5}Si_{22\cdot5}O_{72}.36H_2O$. Alkalis sometimes exceed Ca. Strunz (1956) gives $(Ca,Na_2)Al_2Si_4O_{12}.6H_2O$; $Z = 6$; $D = 2{\cdot}082$.

Epistilbite. Strunz and Tennyson (1956) give $CaAl_2Si_6O_{16}.5H_2O$; $Z = 3$. In eight out of fifteen analyses considered by the present writer, there are 15·7 to 16·3 H_2O per unit cell, the others showing rather less. We tentatively accept 16 H_2O per unit cell, which would make epistilbite a true, higher density, polymorph of heulandite with the approximate range $(Ca,Na_2)_{2\cdot85}Al_{5\cdot7}Si_{18\cdot3}O_{48}.16H_2O$ to $(Ca, Na_2)_{3\cdot5}Al_7Si_{17}O_{48}16H_2O$; D typically 2·25 ± 0·03. Ca is dominant over alkalis.

Dachiardite is shown by X-ray powder diffraction to be structurally related to epistilbite. It has a higher alkali content with about $Si_{19-19\frac{1}{2}}$ for 48 O.

Erionite. $(Na_2,K_2,Ca,Mg)_{4\cdot5}Al_9Si_{27}O_{72}.27H_2O$; D (calc.) = 2·07 (Staples and Gard, 1958).

Faujasite. Near $(Na_2,Ca)_{1\cdot75}Al_{3\cdot5}Si_{8\cdot5}O_{24}.16H_2O$; $Z = 16$; $D = 1{\cdot}92$ (cf. Strunz, 1955).

Gismondine. $CaAl_2Si_2O_8.4H_2O$; $Z = 8$ (Kraus, 1939) to $Ca_{0.92}Al_{1.84}Si_{2.16}O_8.4H_2O$ with moderate substitution of $(K,Na)_2$ for Ca.

Gmelinite. According to Strunz (1956), polymorphous with Na-rich chabazite, and often containing chabazite in lamellar intergrowth; $(Na_2,Ca)Al_2Si_4O_{12}.6H_2O$; $Z = 4$; $D = 2{\cdot}028$.

Gonnardite. Polymorphous with thomsonite and mostly near $(Ca,Na_2)_{4{\cdot}3}Al_{8{\cdot}6}Si_{11{\cdot}4}O_{40}.12H_2O$ (Meixner *et al.*, 1956) but can also have higher ratios of Al:Si (Mason, 1957). $D = 2{\cdot}27 \pm 0{\cdot}02$.

Heulandite. Normally in the range $(Ca,Na_2)_{4{\cdot}8}Al_{9{\cdot}6}Si_{26{\cdot}4}O_{72}.24H_2O$; $D = 2{\cdot}21 \pm 0{\cdot}03$; to $(Ca,Na_2)_4Al_8Si_{28}O_{72}.24H_2O$; $D = 2{\cdot}18 \pm 0{\cdot}03$. There is often appreciable K and/or Sr. In the silica-rich variety clinoptilolite, the composition approaches $Ca(Na,K)_4Al_6Si_{30}O_{72}.24\ H_2O$; $D = 2{\cdot}14 \pm 0{\cdot}03$.

Laumontite. $Ca_{4{\cdot}25}Al_{8{\cdot}5}Si_{15{\cdot}5}O_{48}.16H_2O$ to $Ca_{3{\cdot}75}Al_{7{\cdot}5}Si_{16{\cdot}5}O_{48}.16H_2O$ with minor replacement of Ca by Na_2, i.e. near $CaAl_2Si_4O_{12}.4H_2O$; $Z = 4$; $D = 2{\cdot}29 \pm 0{\cdot}02$ (Coombs, 1952). Leonhardite is a partially dehydrated variety with about 14 H_2O.

Levyne. Perhaps $CaAl_2Si_4O_{12}.5H_2O$ to $Ca_{1{\cdot}1}Al_{2{\cdot}2}Si_{3{\cdot}8}O_{12}.5H_2O$ with moderate replacement of Ca by $(Na,K)_2$. Strunz (1956) suggests polymorphous and structural relationships with chabazite and gives 6 H_2O; $Z = 9$; $D = 2{\cdot}140$. The few available analyses appear to indicate 5 H_2O rather than 6 H_2O.

Mesolite. Essentially $Na_2Ca_2Al_6Si_9O_{30}.8H_2O$; $Z = 8$; $D = 2{\cdot}26$; minor Na_2 for Ca (Hey, 1933).

Metascolecite. Higher temperature polymorph of scolecite (Hey, 1936).

Mordenite (*ptilolite*). $(Na_2,K_2,Ca)Al_2Si_{10}O_{24}.7H_2O$; $Z = 8$ (e.g. Waymouth *et al.*, 1938). with alkalis usually dominant over Ca. $D = 2{\cdot}12 \pm 0{\cdot}03$. First-class analyses (as defined by Hey, 1932a) show variations of no more than 0·15 Al and Si. Synthetic mordenites range from pure Ca to pure Na members (Barrer, 1948 and Appendix 1 of this paper).

Natrolite. $Na_2Al_2Si_3O_{10}.2H_2O$; $Z = 8$; $D = 2{\cdot}24$. Up to 1 in 16 Na replaced by K and 1 in 4 Na replaced by $Ca_{\frac{1}{2}}$ (Hey, 1932b).

Phillipsite. $(Ca,K_2)_{2{\cdot}5}Al_5Si_{11}O_{32}.12H_2O$ to $(Ca,K_2)_{3{\cdot}5}Al_7Si_9O_{32}.12H_2O$ with Na usually subordinate (cf. Wyart and Chatelain, 1938). $D = 2{\cdot}20 \pm 0{\cdot}02$ for typical intermediate members of the series.

?*Pseudonatrolite.* Near $(Ca,Na_2)Al_2Si_6O_{16}.5H_2O$ (Hey, 1955, p. 162).

Scolecite. $CaAl_2Si_3O_{10}.3H_2O$; $Z = 8$; $D = 2{\cdot}27 \pm 0{\cdot}02$. Minor Na_2 for Ca (Hey, 1936).

Stilbite. Approximately $(Ca,Na_2)_4Al_8Si_{28}O_{72}.28H_2O$; $D = 2{\cdot}15 \pm 0{\cdot}02$; to $(Ca,Na_2)_5Al_{10}Si_{26}O_{72}.28H_2O$; $D = 2{\cdot}18 \pm 0{\cdot}02$ (cf. Sekanina and Wyart, 1936). The average water per unit cell for some two dozen representative analyses is 28·7 H_2O as against 24·2 for heulandite. The suggestion of Strunz and Tennyson (1956) that a correct formula should show 24 H_2O as in heulandite and that the two minerals are polymorphs as well as having related (though different) structures, is not therefore accepted.

Thomsonite. $(Ca,Na_2)_{8{\cdot}4}Al_{16{\cdot}8}Si_{23{\cdot}2}O_{80}.24H_2O$; $D \fallingdotseq 2{\cdot}30$ to $(Ca,Na_2)_{10{\cdot}25}Al_{20{\cdot}5}Si_{19{\cdot}5}O_{80}.24H_2O$; $D \fallingdotseq 2{\cdot}38$ (Hey, 1932a). $CaAl_2Si_2O_8.2{\cdot}4H_2O$; $Z = 10$; $D \fallingdotseq 2{\cdot}37$, is a possible synthetic member (Goldsmith, 1952).

Wairakite. $CaAl_2Si_4O_{12}.2H_2O$; $Z = 8$; $Z = 2{\cdot}265$ (Steiner, 1955; Coombs, 1955).

Yugawaralite. Unit cell contents calculated from the data of Sakurai and Hayashi (1952) are approximately $Ca_{3{\cdot}84}(Na,K)_{0{\cdot}34}Al_{7{\cdot}55}Si_{21{\cdot}33}O_{58}{\cdot}15{\cdot}3H_2O$, corresponding roughly to $4CaAl_2Si_5O_{14}.4H_2O$. $D = 2{\cdot}20$.

Appendix 3

Chemical and Physical Data on Heulandite and Prehnite

(A. M. T., D. S. C.)

Chemical analyses and other data on the heulandite and prehnite used in experiments described above are given below.

Heulandite

Locality: Cape Blomidon, Nova Scotia. Colourless crystals.

SiO_2 56·8; Al_2O_3 16·6; Fe_2O_3 tr.; MgO tr.; CaO 5·8; SrO 2·0; Na_2O 1·6; K_2O 0·8;

Li_2O tr.; $H_2O + 110°$ 12·45; $H_2O - 110°$ 3·3; TiO_2 n.f.; P_2O_5 0·01; MnO n.f., CO_2 n.f. Spectrographic analysis: Ag 0·015; Pb 0·015; Sn <0·01; Ba 0·05. Not detected: V, Cd, As, Be, Zn, W, Mo, Ni, Cr, Co, Bi, Sb, B, La, Yt, Ce. Total: 99·44. J. A. Ritchie *anal.*, s. g. 2·23 ± 0·01.

Structural formula: $(Ca_{2\cdot9}Sr_{0\cdot5}Na_{1\cdot5}K_{0\cdot5})Al_{9\cdot2}Si_{26\cdot8}O_{72}.24{\cdot}8H_2O$ in satisfactory agreement with that of Hey and Bannister (1934) and Appendix C above.

Refractive indices variable, α 1·500–1·505 ± 0·001, β 1·500–1·506 ± 0·001, γ 1·506–1·512 ± 0·002.

Prehnite

Locality: Prospect Quarry, New South Wales. Large, transluscent, very pale green botryoidal masses in cavities in dolerite. Average of comparable analyses by A.M.T. and by J. A. Ritchie, Dominion Laboratory, Wellington: SiO_2 43·7; Al_2O_3 24·05; Fe_2O_3 0·93; FeO 0·03; MgO 0·11; CaO 26·85; Na_2O 0·04; K_2O n.f.; Li_2O n.f.; $H_2O + 110°$ 4·54; $H_2O - 110°$ 0·03; TiO_2 tr.; P_2O_5 0·02; MnO n.f.; CO_2 n.f.; Spectrographic analysis (Dominion Laboratory): Ag 0·01; Pb 0·04; SnO 0·01; BaO <0·003. Not detected: V, Cd, etc., as above. Total: 100·36; s. g. 2.93.

Formula on basis of eleven oxygen atoms:
$(Ca_{1\cdot98}Mg_{0\cdot01}Na_{0\cdot01})(Al_{1\cdot95}Fe_{0\cdot05})Si_{3\cdot01}O_{11}.1{\cdot}04H_2O$ in very close agreement with the conventional formula $Ca_2Al_2Si_3O_{10}(OH)_2$. α 1·615 ± 0·001; β 1·624 ± 0·001; γ 1·643 ± 0·002; $\gamma - \alpha$ 0·028; $2V_\gamma$ 69° ± 2° $r > v$ strong.

As is common in prehnite from such environments, and in contrast to the prehnite described in Section 2 above from the New Zealand greywackes, basal sections show complex lamellar twinning, and when thick, anomalous interference tints and incomplete extinction.

References

Ames L. L. and Sand L. B. (1958) Hydrothermal synthesis of wairakite and calcium-mordenite. *Amer. Min.* **43,** 476–480.

Amies A. C. (1950) An intrusion of porphyrite near Waihao Forks, South Canterbury. *Trans. Roy. Soc. N.Z.* **78,** 271–279.

Amies A. C. (1952) Petrological features of the rocks of the Maruwenua district, North Otago. *Trans. Roy. Soc. N.Z.* **79,** 376–385.

Antun P. (1953) Laumontite de Serpont, *Ann. Soc. Géol. Belg.* **77,** B63–71.

Banwell C. J., Cooper E. R., Thompson G. E. K. and McCree K. J. (1957) Physics of the New Zealand thermal area. *Bull. N.2. Dep. Sci. Industr. Res.*

Barrer R. M. (1948) Syntheses and reactions of mordenite. *J. Chem. Soc.* 2158–2163.

Barrer R. M. (1950) Ion-exchange and ion-sieve processes in crystalline zeolites. *J. Chem. Soc.* 2342–2350.

Barrer R. M. and White E. A. D. (1952) Synthetic crystalline sodium aluminosilicates. *J. Chem. Soc.* 1561–1571.

Beattie I. R. (1954) The structure of analcite and ion-exchanged forms of analcite. *Acta Cryst.* **7,** 357–359.

Benson W. N. (1942) The basic igneous rocks of Eastern Otago and their tectonic environment, Part 3. *Trans. Roy. Soc. N.Z.* **72,** 160–185.

Boldyreva A. M. (1953) Authigenic analcime in Upper Permian sediments of the Chkalova and Aktyubinsk districts. *Mém. soc. russe min.* **82,** 291–297; *Chem. Abstr.* **48,** 5030f.

Bradley W. H. (1928) Zeolite beds in the Green River formation. *Science* **67,** 73–74.

Bradley W. H. (1929) The occurrence and origin of analcite and meerschaum beds in the Green River formation of Utah, Colorado and Wyoming. *U.S. Geol. Surv. Prof. Paper* A **158,** 1–7.

Bramlette M. N. and Posnjak E. (1933) Zeolitic alteration of pyroclastics. *Amer. Min.* **18,** 167–171.

Broderick T. M. (1929) Zoning in Michigan copper deposits and its significance. *Econ. Geol.* **24,** 149–162 and 311–326.

Broderick T M. (1931) Fissure vein and lode relations in Michigan copper deposits. *Econ. Geol.* **26,** 840–856.

Brodie J. W. (1953) Stratigraphy and structure of the greywackes and argillites on the south coast of Wellington Peninsula. *N.Z. J. Sci. Tech.* B **34,** 205–226.

Brothers R. N. (1956) The structure and petrography of greywackes near Auckland, New Zealand. *Trans. Roy. Soc. N.Z.* **83,** 465–482.

Brown D. A. (1955) The geology of Siberia Hill and Mount Dasher, North Otago. *Trans. Roy. Soc. N.Z.* **83,** 347–372.

Bur'yanova E. Z. (1954) Analcime sedimentary rocks from Tuva. *Dokl. Akad. Nauk SSSR* **98,** 261–264.

Bur'yanova E. Z. (1956) Authigenic laumontite from Middle Devonian sandstone of Tuva. *Vsesoyuz. Nauch.-Issledovatel. Geol. Inst., Sborn.* **3,** 77–79; *Chem. Abstr.* **51,** 13662c.

Bushinsky G. I. (1950) Mordenite in Jurassic, Cretaceous and Paleocene marine sediments. *Dokl. Akad. Nauk SSSR* **73,** 1271–1274.

Butler B. S. and Burbank N. S. (1929) The copper deposits of Michigan. *U.S. Geol. Surv. Prof. Paper* 144.

Campbell A. S. (1958) *The Hydrothermal Crystallization of Amorphous Silica and the Analcime Albite Phase Boundary.* M.Sc. Thesis, Univ. of Otago, New Zealand.

Campbell J. D. (1955) The Oretian Stage of the New Zealand Triassic System. *Trans. Roy. Soc. N.Z.* **82,** 1033–1047.

Coombs D. S. (1950) The geology of the northern Taringatura hills, Southland. *Trans. Roy. Soc. N.Z.* **78,** 426–448.

Coombs D. S. (1952) Cell size, optical properties and chemical composition of laumontite and leonhardite. With a note on regional occurrences in New Zealand. *Amer. Min.* **37,** 812–830.

Coombs D. S. (1954) The nature and alteration of some Triassic sediments from Southland, New Zealand. *Trans. Roy. Soc. N.Z.* **82,** 65–109.

Coombs D. S (1955) X-ray observations on wairakite and non-cubic analcime. *Miner. Mag.* **30,** 699–708.

Coombs D. S. (1958) Zeolitized tuffs from the Kuttung glacial beds near Seaham, New South Wales. *Austr. J. Sci.* **21,** 18–19.

Cornu F. (1908) Über die Paragenese der Minerale, namentlich die der Zeolithe. *Österr. Z. Berg-Hüttenw.* **56,** 89–93.

Dana J. D. (1892) *System of Mineralogy* (6th Ed.). Paul, Trench, Trübner, London.

Daubrée A. (1879) *Études synthetiques de géologie experimentale.* Paris.

Doelter C. (1921) *Handbuch der Mineralchemie* Vol. II, Pt. 3. Steinkopf, Dresden and Leipzig.

Dzotsenidze G. S. and Skhirtladze N. I. (1953) Analcime horizon in the coal-bearing rocks of the Kutais-Gelat district. *Vop. Petrog. Min. Akad. Nauk SSSR* **1,** 301–310; *Chem. Abstr.* **49,** 7461 g.

Ehlers E. G. (1953) An investigation of the stability relations of the Al-Fe members of the epidote group. *J. Geol.* **61,** 231–251.

Ellis A. J. and Fyfe W. S. (1957) Hydrothermal chemistry. *Rev. Pure Appl. Chem.* **7,** 261–316.

Ellis A. J. (1958) Ph.D. Thesis, University of Otago.

Ellis A. J. and Wilson S. H. (1955) Unpublished work, Dominion Laboratory, Wellington, New Zealand.

Eskola P. (1920) The mineral facies of rocks. *Norsk Geol. Tidsskr.* **6,** 143–194.

Eskola P. (1939) *Die Enstehung der Gesteine* (In Barth T. F. W., Correns C. W. and Eskola, P.). Springer, Berlin.

Fenner C. N. (1936) Bore-hole investigations in Yellowstone Park. *J. Geol.* **44,** 225–315.

Foster W. D. and Feicht F. L. (1946) Mineralogy of concretions from Pittsburgh coal seam, with special reference to analcite. *Amer. Min.* **31,** 357–364.

Fyfe W. S. (1955a) Lower limit of the green-schist facies, *Bull. Geol. Soc. Amer.* **66,** 1649. (Abstract).

Fyfe W. S. (1955b) Results obtained by 1955 and contained in Fyfe, Turner and Verhoogen (1958).

Fyfe W. S., Turner F. J. and Verhoogen J. (1958) *Metamorphic Reactions and Metamorphic Facies.* Geol. Soc. Amer. Memoir No. 73.

Gilbert C. M. (1951) Laumontite from Anchor Bay, Mendocino County, California. *Bull. Geol. Soc. Amer.* **62,** 1517.

Gilbert C. M. and McAndrews M. G. (1948) Authigenic heulandite in sandstone, Santa Cruz County, California. *J. Sediment. Petrol.* **18,** 91–99.

Gill E. D. (1957) Fossil wood replaced by laumontite near Cape Paterson, Victoria. *Proc. Roy. Soc. Victoria* **69,** 33–35.

Goldberg E. D. and Arrhenius G. O. S. (1958) Chemistry of Pacific pelagic sediments. *Geochim. et Cosmochim. Acta* **13,** 153–212.

Goldsmith J. R. (1952) Synthetic soda-free thomsonite. *Miner. Mag.* **29,** 952–954.

Griggs D. T. and Kennedy G. C. (1956) A simple apparatus for high pressures and temperatures. *Amer. J. Sci.* **254,** 722–735.

Gunn B. M. (1956) *The Geology of the Franz Josef–Fox Glacier Region, South Westland.* M.Sc. Thesis, University of Otago.

Harker R. I. (1958) The system $MgO–CO_2–A$ and the effect of inert pressure on certain types of hydrothermal reaction. *Amer. J. Sci.* **256,** 128–138.

Harrington H. J. (1955) The geology of Naseby district, Central Otago. *N.Z. J. Sci. Tech.* B **36,** 581–599.

Harris P. G. and Brindley G. W. (1954) Mordenite as an alteration product of a pitchstone glass. *Amer. Min.* **39,** 819-824.

Hartwig W. (1928) Über die Struktur von Analcim. *Zbl. Miner.* A 380.

Hayashi H. and Sudo T. (1957) Zeolite-bearing bentonites. *Mineral J., Japan* **2,** 196–199.

Heady H. H. (1952) Differential thermal study of Colorado oil shale. *Amer. Min.* **37,** 804–811.

Heald M. T. (1956) Cementation of Triassic arkoses in Connecticut and Massachusetts. *Bull. Geol. Soc. Amer.* **67,** 1133–1154.

Hey M. H. (1932a) Studies on the zeolites. Part II: Thomsonite (including faroelite) and gonnardite. *Miner. Mag.* **23,** 51–125.

Hey M. H. (1932b) Studies on the zeolites. Part III: Natrolite and metanatrolite. *Miner. Mag.* **23,** 243–289.

Hey M. H. (1933) Studies on the zeolites. Part V: Mesolite. *Miner. Mag.* **23,** 421–447.

Hey M. H. (1936) Studies on the zeolites. Part IX: Scolecite and metascolecite. *Miner. Mag.* **24,** 227–253.

Hey M. H. (1955) *An Index of Mineral Species and Varieties* (2nd Ed.). British Museum, London.

Hey M. H. and Bannister F. A. (1933) Studies on the zeolites. Part IV: Ashcroftine (kalithomsonite of S. G. Gordon). *Miner. Mag.* **23,** 305–308.

Hey M. H. and Bannister F. A. (1934) Studies on the zeolites. Part VII: 'Clinoptilolite,' a silica-rich variety of heulandite. *Miner. Mag.* **23,** 556–559.

Hutton C. O. (1937) An occurrence of the mineral pumpellyite in the Lake Wakatipu region, western Otago, New Zealand. *Miner. Mag.* **24,** 529–533.

Hutton C. O. (1940) Metamorphism in the Lake Wakatipu region, western Otago, New Zealand. *N.Z. Dep. Sci. Industr. Res., Mem.* No. 5.

Hutton C. O. (1949a) Notes on the geology of Kapiti Island, Cook Strait, N.Z. Part II: Petrography. *Trans. Roy. Soc. N.Z.* **77,** 465–468.

Hutton C. O. (1949b) Occurrence of leonhardite. *Bull. Geol. Soc. Amer.* **60,** 1939–1940. (Abstract).

Kaley M. E. and Hanson R. F. (1955) Laumontite and leonhardite cement in Miocene sandstone from a well in San Joaquin Valley, California. *Amer. Min.* **40,** 923–925.

Keller W. D. (1951) Analcime in the Popo Agie member of the Chugwater formation. *Science* **115,** 241–242.

Keller W. D. (1952) Analcime in the Popo Agie member of the Chugwater formation. *J. Sediment. Petrol.* **22,** 70–82.

Keller W. D. (1953) Analcime in the Chinle Formation of Utah correlative with the Popo Agie of Wyoming. *J. Sediment. Petrol.* **23,** 10–12.

Kennedy G. C. (1950a) A portion of the system silica-water. *Econ. Geol.* **45,** 629–653.

Kennedy G. C. (1950b) Pressure-volume-temperature relations in water at elevated temperatures and pressures. *Amer. J. Sci.* **248,** 540–564.

Kerr P. F. and Cameron E. N. (1936) Fuller's earth of bentonitic origin from Tehachapi, California. *Amer. Min.* **21,** 230–237.

King E. G. (1955) Low temperature heat capacity and entropy at 298.16°K of analcite, *J. Amer. Chem. Soc.* **77,** 2192–2193.

Koizumi M. and Kiriyama R. (1953) Structural changes of some zeolites due to their thermal dehydrations. *Sci. Rep. Osaka Univ.* No. 2, 67–85.

Koizumi M. and Roy R. (1958) Synthesis and equilibrium stability of the calcium zeolites. *Geol. Soc. Amer.* Abstracts of 1958 Meeting, p. 93.

Kolbin M. F. and Pimburgskayn M. I. (1955) Analcime in sediments of Mt. Bogdo-Ola. *Dokl. Akad. Nauk SSSR* **100,** 155–157.

Kossovskaya A. G. and Shutov V. D. (1955) Changes in the character of fragmental biotite during the process of epigenesis. *Dokl. Akad. Nauk SSSR* **101,** 541–544.

Kossovskaya A. G. and Shutov V. D. (1956) Epigenic formation of epidote and zoisite in Mesozoic and Upper Paleozoic sediments of the western Verkhoyansk Range. *Dokl. Akad. Nauk SSSR* **108,** 139–141.

Kraus O. (1939) Röntgenographische Untersuchungen an Gismondin. *Zbl. Miner.* A 105–109.

Latimer W. M. (1952) *The Oxidation States of the Elements and their Potentials in Aqueous Solutions* (2nd Ed.). Prentice-Hall, New York.

Lillie A. R., Gunn B. M. and Robinson P. (1957) Structural observations in central Alpine region of New Zealand. *Trans. Roy. Soc. N.Z.* **85,** 113–129.

Lillie A. R. and Mason B. H. (1955) Geological reconnaissance of district between Franz Josef Glacier and Copland Valley. *Trans. Roy. Soc. N.Z.* **82,** 1123–1128.

Mackenzie W. S. (1957) The crystalline modifications of $NaAlSi_3O_8$. *Amer. J. Sci.* **255,** 481–516.

Mackie J. B. (1936) A geological traverse from the Waitaki River to Dunstan Peak, Otago. *Trans. Roy. Soc. N.Z.* **66,** 125–142.

McLintock W. F. P. (1915) On the zeolites and associated minerals from the Tertiary lavas around Ben More, Mull. *Trans. Roy. Soc. Edinb.* **51,** I, 1–33.

Marwick J. (1946) The geology of the Te Kuiti Subdivision. *N.Z. Geol. Surv. Bull.* No. 41.

Mason B. (1957) Gonnardite (ranite) from Langesundsfjord. *Norsk Geol. Tidsskr.* **37,** 435–437.

Mason B. and Greenberg S. S. (1953) Zeolites and associated minerals from Southern Brazil. *Ark. Min.* **1,** 519–526.

Meixner H., Hey M. H. and Moss A. A. (1956) Some new occurrences of gonnardite. *Miner. Mag.* **31,** 265–271.

Miyashiro A. and Banno S. (1958) Nature of glaucophanitic metamorphism. *Amer. J. Sci.* **256,** 97–110.

Murray J. and Renard A. F. (1891) Deep sea deposits. *Challenger Rep.* 400–412.

Mutch A. R. (1957) Facies and thickness of the Upper Paleozoic and Triassic sediments of Southland. *Trans. Roy. Soc. N.Z.* **84,** 499–511.

Niggli P., Koenigsberger J. and Parker R. L. (1940) *Die Mineralien der Schweizeralpen.* Wepf, Basel.

Povarennykh A. S. (1954) Problems of the zeolitization of alkaline rocks. *Dokl. Akad. Nauk SSSR* **94,** 761–764.

Reed J. J. (1950) Spilites, serpentinites and associated rocks of the Mossburn district, Southland. *Trans. Roy. Soc. N.Z.* **78,** 106–126.

Reed J. J. (1957) Petrology of the Lower Mesozoic rocks of the Wellington district. *N.Z. Geol. Surv. Bull.* No. 57.

Rengarten N. V. (1940) Authigene analcyme in the Kazanian sandstones of the Kirov region. *Mém. Soc. Russe Min.* Ser. 2., **69,** 50–53.

Rengarten N. V. (1945) A zeolite from the mordenite group in the Upper Cretaceous and Paleocene marine deposits of the eastern slope of the Urals. *Dokl. Akad. Nauk SSSR* **48** 619–622.

Rengarten N. V. (1950) Laumontite and analcime from Lower Jurassic deposits in northern Caucasus. *Dokl. Akad. Nauk SSSR* **70,** 485–488.

Richmond W. E. (1937) Paragenesis of the minerals from Blueberry Mountain, Woburn, Massachusetts. *Amer. Min.* **22,** 290–300.

Robinson P. (1958) *The Structural and Metamorphic Geology of the Brighton-Taieri Mouth Area, East Otago, New Zealand.* M.Sc. thesis, University of Otago.

Roever W. P. de (1955) Some remarks concerning the origin of glaucophane in the north Berkeley hills, California. *Amer. J. Sci.* **253,** 240–244.

Roever W. P. de (1950) Preliminary notes on glaucophane-bearing and other crystalline schists from South East Celebes, and on the origin of glaucophane-bearing rocks. *Koninkl. Ned. Akad. Wet.* **53,** 1455–1465.

Ross C. S. (1928) Sedimentary analcite. *Amer. Min.* **13,** 195–197.

Ross C. S. (1941) Sedimentary analcite. *Amer. Min.* **26,** 627–629.

Ross C. S. (1958) Welded tuff from deep-well cores from Clinch County, Georgia. *Amer. Min.* **43,** 537–545.

Rozendal R. (1957) Analcime in lignite. *Proc. S. Dakota Acad. Sci.* **35,** 39–41; *Chem. Abstr.* **51,** 8590f.

Saha P. (1957) Preliminary report on the system albite-nepheline-water. *Bull. Geol. Soc. Amer.* **68,** 1790. (Abstract).

Sakurai K. (1953) Studies on zeolites from Yugawara Hot Spring, Kanagawa Pref. Japan. I. *Bull. Nat. Sci. Mus. Tokyo* **32,** 83–98.

Sakurai K. and Hayashi A. (1952) "Yugawaralite", a new zeolite. *Sci. Rep. Yokohama Nat. Univ.*, Sec. II, 69–77.

Sand L. B., Roy R. and Osborn E. F. (1957) Stability relations of some minerals in the $Na_2O-Al_2O-SiO_2-H_2O$ system. *Econ. Geol.* **52,** 169–179.

Schaller W. T. (1932) The mordenite-ptilolite group; clinoptilolite, a new species. *Amer. Min.* **17,** 128–134.

Sekanina J. and Wyart J. (1936) Sur la stilbite. *Bull. Soc. Franc. Min.* **59,** 377–383.

Speden I. G. (1956) *The Geology of the Catlins District, South-East Otago.* M.Sc. Thesis, University of Otago.

Staples L. W. and Gard J. A. (1958) The fibrous zeolite erionite: its occurrence, unit cell and possible structure. *Min. Soc. Notice* No. 102 (Abstract).

Steiner A. (1953) Hydrothermal rock alteration at Wairakei, New Zealand. *Econ. Geol.* **48,** 1–13.

Steiner A. (1955a) Hydrothermal rock alteration. *Dep. Sci. Industr. Res. Bull. N.Z.* **117,** 21–26.

Steiner A. (1955b) Wairakite, the calcium analogue of analcime, a new zeolite mineral. *Miner. Mag.* **30,** 691–698.

Steiner A. (1958) Occurrence of wairakite at The Geysers, California. *Amer. Min.* **43,** 781.

Strunz H. (1955) Zur Kristallchemie des wasserreichsten Zeolithes Faujasit. *Naturwissenschaften* **42,** 485–486.

Strunz H. (1956) Die Zeolithe Gmelinit, Chabasit, Levyn (Phakolith, Herschelit, Seebachit, Offretit). *Neus. Jb. Miner., Mh.* **11,** 250–259.

Strunz H. and Tennyson C. (1956) "Polymorphie" in der Gruppe der Blätterzeolithe (Heulandit-Stilbit-Epistilbit; Brewsterit). *Neus Jb. Miner., Mh.* 1–9.

Turner F. J. (1933) The metamorphic and intrusive rocks of southern Westland. *Trans. N.Z. Inst.* **63,** 178–284.

Turner F. J. (1938) Progressive regional metamorphism in southern New Zealand. *Geol. Mag.* **75,** 160–174.

Turner F. J. (1948) Mineralogical and structural evolution of the metamorphic rocks. *Geol. Soc. Amer. Mem.* 30.

Valpy G. W. (1957) *Phase Relations of Some Sodium-Aluminium Silicates.* M.Sc. Thesis, University of Otago, New Zealand.

Vasil'ev V. S. (1954) Mordenite in Mesozoic and Cenozoic sediments of the lower Volga Basin and western Kazakhstan. *Dokl. Akad. Nauk SSSR* **95,** 149–151.

Vasil'ev V. S., Kolbin M. F. and Krasnova V. N. (1956) Zeolites in the Mesozoic and Cenozoic sediments of the Penza area. *Dokl. Akad. Nauk SSSR* **111,** 410–412.

Walker G. P. L. (1951) The amygdale minerals in the Tertiary lavas of Ireland. I. The distribution of chabazite habits and zeolites in the Garron plateau area, County Antrim. *Miner. Mag.* **29,** 773–791.

Walker T. C. and Parsons A. L. (1922) The zeolites of Nova Scotia. *Univ. Toronto Stud. Geol. Ser.* No. 14, 13–73.

Waymouth C., Thornely P. C. and Taylor W. H. (1938) An X-ray examination of mordenite (ptilolite). *Miner. Mag.* **25,** 212–216.

Weed W. H. (1900) Mineral vein formation at Boulder hot springs, Montana. *U.S. Geol. Surv., Twenty-first Ann. Rept.* Pt. 2, 233–255.

Weed W. H. (1904) Economic value of hot springs and hot-spring deposits. *U.S. Geol. Surv. Bull.* **260,** 598–604.

Wellman H. W. (1952) The Permian-Jurassic stratified rocks. *Symposium sur les séries de Gondwana, Proc.* 19e *Congrés Géol. Int., Alger.* 13–24.

Wellman H. W. (1956) Structural outline of New Zealand. *Dep. Sci. Industr. Res. Bull. N.Z.* 121.

Wellman H. W., Grindley G. W. and Munden F. W. (1952) The Alpine schists and the Upper Triassic of Harpers Pass (sheet S52), South Island, New Zealand. *Trans. Roy. Soc. N.Z.* **80,** 213–227.

White D. E. (1955) Thermal springs and epithermal ore deposits. *Econ. Geol.* Fiftieth Anniv. Vol. 99–154.

Whitehouse M. J. (1937) The deuteric mineral sequence in the Enogerra granite, Queensland. *Miner. Mag.* **24,** 538–546.

Williamson J. W. (1939) The geology of the Naseby Subdivision. *N.Z. Geol. Surv. Bull.* No. 39.

Wood B. L. (1953) Paleozoic and Mesozoic stratigraphy and structure in Southland *Rep. Seventh Pacific Science Congress, Christchurch, N.Z.* 106–114

Wood B. L. (1956) The geology of the Gore Subdivision, *N.Z. Geol. Surv. Bull.* No. 53.

Wyart J. and Chatelain P. (1938) Etude cristallographique de la christianite. *Bull. Soc. Franç. Min.* **61,** 121–126.

Yoder H. S. (1950) Stability relations of grossularite. *J. Geol.* **58,** 221–253.

Yoder H. S. (1954) *Carnegie Institution of Washington Year Book.* No. 53, 121–122.

Geochimica et Cosmochimica Acta, 1959, Vol. 17, pp. 108 to 112. Pergamon Press Ltd. Printed in Northern Ireland

Mesure de la teneur en bore-10 des mineraux

G. Allais et H. Curien
Laboratoire de Minéralogie-Cristallographie, de la Faculté des Sciences, Paris

(*Received* 21 *February* 1959)

Résumé—On décrit une méthode d'analyse du ^{10}B, fondée sur ses propriétés d'absorption des neutrons thermiques. La précision de la méthode est de l'ordre de 2%, mais sa mise en oeuvre est simple et rapide. On a d'autre part, constaté l'identité du rapport isotopique $^{10}B/^{11}$ dans cinq minéraux d'origines très diverses.

1. Introduction

Le dosage du bore dans les minéraux par voie chimique exige des manipulations longues et délicates, surtout lorsqu'on s'intéresse à des borosilicates. Il paraît *a priori* plus séduisant de doser directement l'isotope 10 du bore en profitant du fait que sa section efficace d'absorption des neutrons thermiques est très largement supérieure à celles de tous les autres noyaux ordinairement présents dans les minéraux. Cette idée a déjà été exploitée par Green et Martin (1952) qui s'intéressaient aux dosages isotopiques dans BCl_3. Elle nous a été suggérée par le professeur H. Halban. Pour que les dosages du bore-10 fondés sur ce principe puissent être utilisés à la détermination du bore total, il faut évidemment que le rapport isotopique $^{10}B/^{11}B$ reste constant dans tous les échantillons analysés. De nombreux travaux ont déjà été consacrés à la détermination de ce rapport isotopique dans les minéraux. Bentley et Hamer (1958) résument les résultats de ces études (Parwell *et al.*, 1956; Osberghaus, 1950; Panchenkov et Moissev, 1956; Kilpatrick *et al.*, 1952); toutes les mesures faites par spectrographie de masse sur des bores extraits de minéraux d'origines très diverses, n'ont jamais mis en évidence de variations significatives du rapport isotopique $^{10}B/^{11}B$. Les variations possibles semblent être inférieures à quelques $^{0}/_{00}$. Les désaccords entre les mesures absolues de section efficace sur divers standards, effectuées par différentes équipes de physiciens nucléaires, ne sont pas assez systématiques pour qu'on puisse les imputer avec certitude à des variations isotopiques dans le matériel original.

2. Dispositif Experimental

Des neutrons sont émis par une source Ra-α-Be de 1 Curie en rayonnement α, qui émet environ $3 \cdot 10^6$ neutrons par seconde. Cette source S est placée en regard d'un récipent R en plexiglass d'une capacité de 50 cm^3 qui contient la solution boratée à étudier. Au centre de R, est placée une pastille D d'indium qui joue le rôle de détecteur pour les neutrons thermiques. Un support ajusté permet de placer R par rapport à S d'une manière exactement reproductible. L'ensemble est disposé dans un aquarium rempli d'eau. La protection est assurée par une enveloppe de paraffine de 10 cm d'épaisseur. La Fig. 1 donne une idée du montage.

Les neutrons rapides émis par la source sont ralentis par l'eau de l'aquarium.

Ce phénomène de ralentissement a été étudié en détail par Frisch *et al.* (1938). La distance moyenne entre le point où un neutron devient thermique et le point où il est absorbé est en moyenne de 2 cm. Les dimensions adoptées pour le récipient R sont donc telles que le détecteur ne reçoit que des neutrons dont la fin du processus de ralentissement est intervenue dans la solution boratée.

L'indium a une section efficace d'activation de 145 barn pour les neutrons thermiques. Il se désactive en émettant des rayons β et γ avec une période de

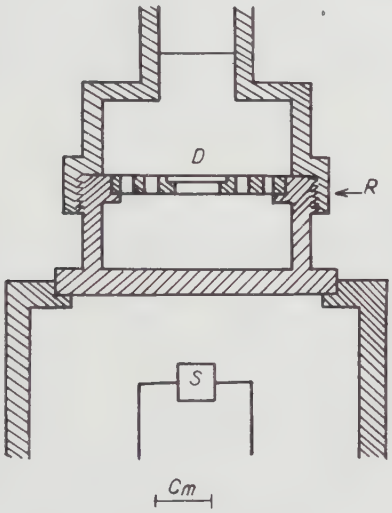

Fig. 1. Dispositif expérimental.

54 minutes. La pastille utilisée comme détecteur a un diamètre de 1 cm et une épaisseur de 0,4 mm. Elle absorbe environ 40% des neutrons thermiques qui la traversent normalement. L'activité de la pastille d'indium est mesurée à l'aide d'un compteur de Geiger-Muller. Pour ce comptage, la pastille D est dégagée vers le haut par dévissage de la partie supérieure du récipient R et elle est placée de manière reproductible en regard de la fenêtre d'un compteur. Une pastille radioactive à longue période, utilisée comme standard pour le contrôle des comptages, peut être substituée au détecteur D en regard du compteur.

L'ensemble des opérations pour une mesure est le suivant: le récipient R est rempli avec la solution boratée à étudier. Il est alors placé sur son support dans l'aquarium où il subit une irradiation aux neutrons pendant deux heures. Il est ensuite vidé, dévissé, lavé et séché, et les comptages commencent 5 minutes après la fin de l'irradiation. Cinq comptages successifs de 10 minutes sont alternés avec autant de comptages sur le standard. L'ordre de grandeur du résultat de chacun des comptages est de 10^4 coups. Le bruit de fond du compteur qui est de l'ordre de 50 coups/minute est mesuré avant et après l'ensemble des comptages.

On caractérise finalement l'activation de l'indium par le rapport Q de la somme des comptages faits sur la pastille d'indium à la somme des comptages faits sur le standard. L'incertitude statistique sur Q est de l'ordre de 1%. Quant le récipient R est rempli d'eau pure, on mesure $Q_0 = 4{,}58$. (Ces chiffres sont évidemment corrigés pour tenir compte de la décroissance de la source dans le temps).

3. Etalonnage et Contrôle de l'Invariance du Rapport Isotopique $^{10}B/^{11}B$ dans quelques Minéraux

L'étalonnage de la méthode a été effectué à l'aide de solutions préparées à partir d'un même borax pris comme référence. Fig. 2 représente les résultats sous la forme d'une courbe donnant Q en fonction de log C. (C étant la concentration en mg de B par cm³). Soit X_0 la teneur isotopique relative en ^{10}B. $X_0 = {}^{10}B/B$, dans ce borax de référence.

Supposons que nous voulions déterminer la teneur isotopique relative X d'une solution boratée, préparée à partir d'un minéral. On va d'abord déterminer, par les procédés chimiques usuels, le titre C en bore de la solution. Puis, par la méthode décrite ci-dessus, on mesure Q. Si X est égal à X_0, la mesure viendra se placer sur

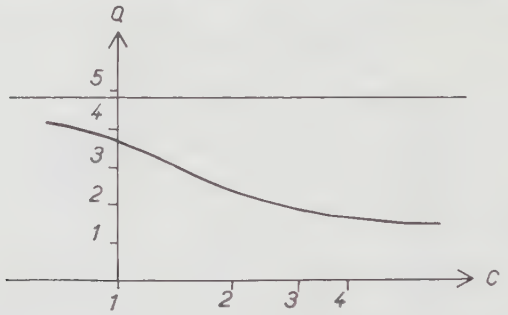

Fig. 2. Courbe d'étalonnage établie à l'aide de solutions d'un borax de référence (echelle logarithmique pour C, mesuré en mg de bore par cm³).

la courbe de la Fig. 2. Sinon, l'écart sera un indice de variation du rapport isotopique par rapport à celui du borax de référence. Déterminons la valeur de C optimum pour détecter un écart $\Delta X = X - X_0$. Cet écart provoque la même variation ΔQ de Q qu'un écart ΔC à la composition C dans la solution de borax-référence si

$$\Delta C \cdot X_0 = C \Delta X \tag{1}$$

On peut alors écrire

$$\Delta Q = \frac{dQ}{dC} \Delta C = \frac{dQ}{dC} C \frac{\Delta X}{X_0} \tag{2}$$

Il en résulte que, pour un ΔX donné, (et petit), le ΔQ observé sera d'autant plus grand que $(dQ/dC) \cdot C$ sera plus grand: il est donc avantageux de choisir, pour ces expériences, la valeur de C correspondant à la tangente d'inflexion de la courbe $Q = f(\log C)$ (Fig. 2). Cette valeur optimum est $C = 2{,}5$ mmg/cm³.

Les discussions précédentes font abstraction des corrections rendues nécessaires par le fait que le ^{10}B n'est pas le seul élément absorbant introduit dans la solution. Les conditions de préparation, de mise en solution ou d'extraction du bore des minéraux à étudier, conduisent à l'introduction d'autres éléments. Les noyaux de ^{11}B bien qu'étant à peu près quatre fois plus nombreux que ceux de ^{10}B, n'apportent à l'absorption des neutrons qu'une contribution négligeable. Le chlore, par contre, avec une section efficace de 32 barn, provoque des effets sensibles qui nous ont amenés à calculer, pour nos mesures, des corrections de l'ordre de 2% (ces

corrections introduisent dans les mesures une incertitude supplémentaire de l'ordre de 0,2%).

Cinq minéraux d'origines très différentes ont fait l'objet d'un test sur le rapport isotopique: une kernite de Californie, une ascharite et une inoïte du Lac Inder (U.R.S.S.). une tourmaline de Madagascar, une datolite des Alpes autrichiennes.

Le Tableau 1 reproduit, dans la colonne 1, les valeurs de Q mesurées sur des solutions boratées préparées à partir de ces divers minéraux. La colonne 2 donne la valeur de Q mesurée sur une solution du borax de référence dont la concentration est égale à celle de la solution préparée à partir du minéral, avec une correction tenant compte de la teneur en chlore de cette dernière.

Tableau 1

Minéral	(1)	(2)
Kernite	2,53	2,54
Ascharite	3,45	3,40
Inoïte	3,34	3,35
Tourmaline	3,89	3,85
Datolite	2,76	2,74

Compte tenu d'une imprécision de l'ordre de 1,5% sur le dosage chimique des solutions. nous ne pouvons conclure, dans aucun des cas étudiés, à un écart du rapport isotopique par rapport à celui pris pour référence.

4. Dosage du Bore dans les Mineraux

Etant ainsi admis que le rapport isotopique $^{10}B/^{11}B$ reste constant quelle que soit l'origine et la nature du minéral, l'appareillage et la méthode décrits ci-dessus peuvent donc être utilisés au dosage du bore dans les minéraux. Il suffit, par les moyens d'attaque classiques, de faire passer en solution (en évitant l'introduction d'une trop grande quantité de chlore dans la solution) tout le bore contenu dans un poids connu d'échantillon. La solution est placée dans le récipient R et la mesure de Q donne, par la courbe d'étalonnage de la Fig. 1, la valeur de la concentration C de la solution, d'où l'on déduit la teneur en bore du minéral. La méthode est rapide (l'ensemble des opérations peut être exécuté en trois heures). Pour une quantité de bore de l'ordre de 100 mg ($C \sim 2$ mg/cm^3), la précision sur Q est de l'ordre de 1% et celle sur la teneur en bore de l'ordre de 2%. Cette précision est donc du même ordre que celle des dosages chimiques. Un des avantages de la méthode que nous proposons est la suppressions des opérations délicates d'extraction et, en particulier, d'élimination complète de la silice dans les borosilicates. D'autre part, dans le cas des borates naturels solubles dans l'eau (ou pour le dosage de liquides organiques), la méthode est d'application immédiate et non destructive.

Remerciements—Nous remercions le Professeur H. Halban qui nous a fait profiter de ses idées et de ses conseils, ainsi que le Dr. Lang et son équipe du Centre d'Etudes Nucléaires de Saclay, qui nous ont très utilement aidés pour les analyses chimiques du bore.

Bibliographie

Bentley P. G. and Hamer A. N. (1958) Boron-10 abundance in nature. *Nature, Lond.* **182,** 1156.

Frisch O. R., Halban H. and Koch J. (1938) On the slowing down and capture of neutrons in hydrogenous substances. *K. Danske Vidensk. Selsk., Math. Fys. Med.* **15,** 10.

Green M. and Martin G. R. (1952) The vapour pressure of isotopic substance. I. Boron trichloride. *Trans. Faraday Soc.* **48,** 416.

Kilpatrick M., Hutchinson C. A., Taylor E. H. and Judson C. M. (1952) *Separation of the Boron Isotopes.* Nat. Nuclear Energy Series Div. III, Vol. V. U.S.A.E.C., Oak Ridge.

Osberghaus O. (1950) Die Isotopenhaüfigkeit des Bors. Massenspektrometrische Untersuchung der Elektronenstossprodukte von BF_3 und BCl_3. *Z. Phys.* **128,** 368.

Panchenkov G. M. et Moissev V. D. (1956) Analyse isotopique au spectrographe de masse des fluorures de bore. *Zh. fiz. khim.* **30,** 1118 (En russe).

Parwell A., v. Ubisch H. and Wickman F. E. (1956) On the variations in the relative abundance of boron isotopes in nature. *Geochim. et Cosmochim. Acta* **10,** 185.

Geochimica et Cosmochimica Acta, 1959, Vol. 17, pp. 113 to 124. Pergamon Press Ltd. Printed in Northern Ireland

The metallic particles of some chondrites

H. C. Urey and Toshiko Mayeda
Enrico Fermi Institute, University of Chicago

(*Received* 15 March 1959)

Gevers, Mendelssohn and Dunne (1945) reported the presence of kamacite and taenite in the Groenewald–Benoni chondrite, and Beck, Stevenson and La Paz (1951) observed them in the La Lande meteorite. Urey (1956) stated that these two phases were present in Holbrook, Beardsley, Richardton and Forest City and that in some cases the two phases occurred in separated pieces of metal. He concluded that they were fragments of larger masses of metal, though no details of the observations were published. This conclusion differs from that of Gevers *et al.*, who expressed the view that the two phases were formed *in situ*. It is the purpose of this paper to describe these metal particles in greater detail for several chondritic meteorites. Great variation in the shapes and composition of the metal particles is observed among different meteorites and usually within a single meteorite sample, commonly within microscopic distances, so that a simple description is quite impossible.

The conclusion of Urey and the present writers is contrary to that of Merrill (1921) who argued that the metal of chondrites is of secondary origin and that it was introduced into the previously agglomerated silicate mass by the reduction of gaseous ferrous chloride by hydrogen gas. He did not etch the polished metal and was unaware of the complicated physical structures of kamacite and taenite which occur in these objects.

Observational Methods

A small sample of a meteorite was placed in a vessel with a side arm which was then evacuated to remove all air. Then thermoplastic liquid was poured over the specimen from the side arm and the vessel was opened to the air, thus forcing the plastic into the specimen. The wet specimen was then placed in a small dish, covered with liquid plastic, which solidified during the course of a day. In this way the particles of the fragile chondrites were held securely in place. With this procedure it was possible to grind and polish the specimens without great masses of crystals falling out of the polished face. The grinding and polishing were done with metallographic lapping disks. Even using this method, some specimens were very fragile and a certain amount of material fell from the polished surface.

After polishing, the specimens were covered for a few seconds with a 2% solution of nitric acid in ethyl alcohol (nital) and then washed with water and alcohol and dried. In this way the metal particles were etched to bring out the characteristic

* Present address: University of California, La Jolla, California, U.S.A.

coloured patterns of kamacite, taenite and plessite as observed in many studies of metal meteorites.

Observations on the specimens so secured were made microscopically and some of the specimens have been photographed. They were viewed entirely in reflected light, since other techniques were found to be inferior to this.

Description of the Types of Metallic Particles

Many varieties of particles have been observed, ranging in size from those so small that they appear as nearly point sources of light to objects about 1 mm in linear dimensions. We were not able to decide the crystal character of the smaller particles but in most other cases we were able to conclude whether the metallic phase was kamacite, taenite or plessite, and troilite was always easily recognized. Kamacite has a white luster, taenite a very slight yellow, troilite is distinctly yellow and commonly cracked. Plessite varies greatly, from a slightly cloudy appearance to a coarsely crystalline character, due to the fact that it is a mixture of kamacite and taenite in which kamacite has crystallized within the massive taenite body. With some experience it is possible to decide in most cases to which general classification the metalic particle belongs.

Kamacite appears in a variety of forms. The larger crystals may be completely clear or they may have Neumann bands. These bands may be quite straight, or curved, or greatly curved and distorted. They may be very faint or sharp, broad or narrow, and in some cases they have broken into short sections, indicating recrystallization following the formation of the bands. Clear kamacite with many small crystals of schreibersite embedded in it are sometimes observed and such kamacite particles are often isolated, with many examples of other types of kamacite within microscopic distances scattered about. In other cases the kamacite has a mottled appearance and in these circumstances it is often difficult to decide whether the mass is polycrystalline kamacite or a mixture of kamacite and taenite. In some samples a micropolycrystalline mass is observed. These masses look like plessite and indeed they may be just this. Such microcrystalline masses sometimes appear to have been shattered with small crystals scattered through some definite small region. The kamacite particles are commonly greatly distorted as though the neighbouring silicate crystals had been pressed into the kamacite. Thus the kamacite appears to be more plastic than the silicates.

Taenite also appears in a variety of ways. Discrete particles with a diffusion border very similar to those in some of the metal meteorites are a common feature of several of the meteorites studied. The interior of these particles is plessite with a variety of modifications, or it may be clear. These particles are commonly completely separated from kamacite and troilite. In other meteorites they are attached to these phases, but usually with much of the periphery, with its characteristic diffusion border, in contact with silicates. The particles are not distorted in the same way nor to as great an extent as the kamacite particles. Usually they appear bent or broken, and thus would seem to be less plastic than kamacite. The taenite particles are small and approximately the same dimensions in all directions. Only rarely do we observe elongated taenite–plessite particles like those commonly found in the octahedrite type of metal meteorite. The taenite particles vary from

20 to 100μ in linear dimensions and appear to be approximately the same size in different meteorites. In many cases there are characteristics which we interpret as a fading of the typical pattern of these particles due to reheating.

Taenite appears also as clear masses, mostly in contact with kamacite or enclosed as crystals in a polycrystalline mass of kamacite. Such polycrystalline masses may have straight or slightly curved crystalline edges, or the boundaries may be quite curved and irregular. The crystal sizes vary from those that can be easily distinguished to smaller sizes, until the interpretation becomes doubtful.

In some meteorites kamacite and taenite are nearly completely separate bodies, while in others most of them are in contact. In some cases, the contact is along one edge with the other edges in contact with silicate and giving the appearance of a partially broken metal mass. In others, the two metal phases appear to be part of one body which became differentiated *in situ*.

Plessite is a mixture of kamacite and taenite and is found on the interior of taenite bodies in metal meteorites. It varies in texture from very fine cloudy material quite unresolved by the microscope to crystals which can be resolved. Recently P. G. Orsini has resolved such plessite with the electron misroscope and finds that it is indeed a mixture of kamacite and taenite. The origin of these structures is quite well understood by the use of the Fe–Ni phase diagram if we assume a very slowly decreasing temperature. The rate of diffusion in taenite is less than in kamacite. As the temperature falls, kamacite appears within the taenite crystals, which were stable at higher temperatures. These kamacite crystals grow by the transfer of iron and nickel between the two phases. Equilibrium requires that the phases be uniform in composition, and hence diffusion through the crystals is necessary. This uniform composition is acquired more easily in kamacite than in taenite. As the temperature falls, diffusion to the surface becomes impossible in taenite and hence crystals of kamacite grow within the taenite. At the edges equilibrium is still maintained and a border high in nickel is formed which remains bright when the specimen is etched. The interior etches in various ways depending on the size of the crystals.

The finest metal particles are widely distributed through the silicate mass. We have wondered whether these are not the result of our grinding and polishing procedures, but they can be seen below the surface of the silicate crystals and for this reason we believe that they are part of the structure. They have been observed within the glass chondrules of Tulia. We are unable to determine whether they are kamacite or taenite and we cannot see any definite plessite interiors within any of these particles.

The chondrules and silicate crystals have not been studied extensively, but some chondrites are glass, and this shows that these chondrules were formed in the melted state and cooled suddenly. Such observations have been made before. Also the presence of maskelynite in Allegan (Merrill, 1921) indicates rapid cooling from high temperatures. As is mentioned below, these facts cause difficulty in understanding the simultaneous presence of plessite within the taenite particles.

The troilite has not been studied in this work. It appears as irregular masses which are greatly distorted by the neighbouring silicates, or often as fine veins running through what appear to have been fine cracks, or as irregular finely-divided

bits throughout the mass. The larger masses in nearly all specimens appear cracked and broken.

Corrosion is evident in some chondrites, but is extensive only in those that have been recorded as "finds". Densmore, for example, appears to contain practically no metal particles. In some "falls" a certain amount of corrosion may be present, but in such small quantity as to suggest a terrestrial origin. In some cases the irregular shape of the kamacite particles seems to indicate that corrosion has been the effective agent in producing this shape. However, if extensive corrosion has produced indentations in the larger particles, it is difficult to understand how smaller kamacite particles have been preserved at all, unless they are extremely high in nickel. Also, these masses intruded into the kamacite particles are crystalline and have the same appearance as the silicates at greater distances. If the materials in contact with the metal are *crystalline*, and have the appearance of the "country rock", we conclude that they are not the products of erosion. It is our conclusion that corrosion in the extraterrestrial environment has been very limited or non-existent.

Detailed Descriptions of Individual Meteorites

(For classifications see Prior's Catalog, 1953)

Abee. Fell, 10 June, 1952, in Canada, achondrite. This meteorite has not been described. It appears to be an intimate mixture of silicates, troilite and polycrystalline kamacite. No chondrules have been observed. The sulphide is a prominent feature. The masses of kamacite are polycrystalline with many irregular crystal boundaries resembling the γ–α transformations sometimes observed in ataxites (see Perry, 1944, Plate 78). No Neumann lines have been observed. These kamacite areas have separate crystals of silicate within the metal areas in section and they seem to extend for a millimetre or more as though they were a continuous phase, appearing broken in section only. The "suspended" silicates are distinctly crystalline with well-formed surfaces. Small amounts of clear taenite of a pinkish colour were observed.

This meteorite does not have a conglomerate structure. Silicates are suspended in numerous cases within the metal and hence melting and crystallization in a very low gravitational field is indicated.

Allegan. Fell in 1899, in Michigan; spherical bronzite chondrite. This stone has a friable structure and many small crystals have fallen out of our polished surfaces. There are many chondrules, all of which are crystalline and are not usually of a smoothly rounded shape. They contain pieces of metal which are often differentiated and belong to the micropolycrystalline type. The periphery of one chondrule contains particles which have a diffusion border and a clear interior with a band between that etches to a dark colour. These chondrules could not have been melted without destroying the taenite patterns, and their structure indicates that they came from some previously differentiated larger body from which they were broken and eroded to these irregularly rounded bodies. For the most part the chondrules contain only very small pieces of metal.

The kamacite occurs as clear masses having mostly straight Neumann lines (Fig. 1). It is commonly in contact with clear taenite of irregular shape, and may follow the edge of the kamacite for short distances as an irregular border. Taenite

Fig. 1. Allegan. This shows an example of straight Neumann lines. K_N, kamacite with Neumann lines.

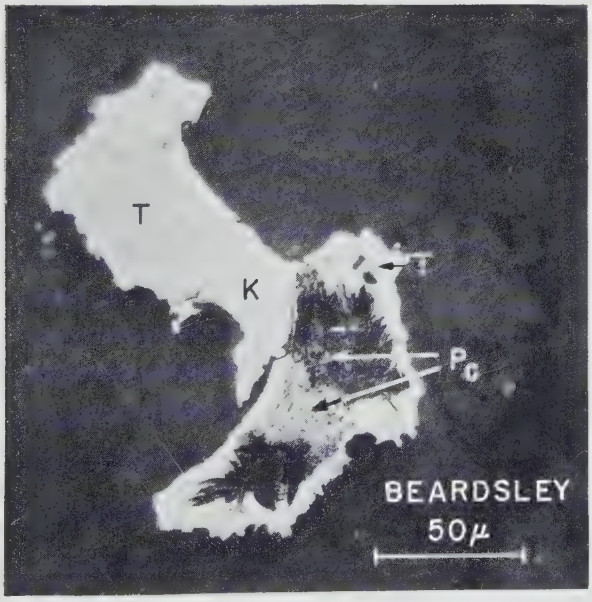

Fig. 2. Beardsley. Kamacite with two types of taenite attached to its sides. One taenite is completely clear whereas the other has a plessite centre. This seems to show different extent of clearing of plessite due to reheating. T, clear taenite; K, kamacite without Neumann lines; T, taenite; P_C, coarse plessite.

is included in some cases in the kamacite as masses with rounded borders but this may be due to the accidental plane of cutting the masses with the bordering taenite. Fine polycrystalline kamacite is present both in the chondrules and in the general silicate mass.

Taenite particles completely separated from the kamacite are common. They have clear diffusion borders and clear interiors with a dark band between. In many cases they are bent and distorted. One was observed adjoining troilite with a very close fit of surfaces, with indistinguishable diffusion borders adjoining the troilite and the silicate. These particles without plessite interiors do not look like the taenite bodies of iron meteorites. Possibly mild heating has dissolved the interior kamacite and only a variation of nickel content remains to give the etching pattern. We have never observed Neumann lines in these bodies and this indicates that their identification as taenite is correct. No corrosion has been observed.

Beardsley. Fell in 1929, in Kansas; grey chondrite. A very great variety of metal particles exists in this meteorite. The massive kamacite may be clear or with Neumann lines. This kamacite in many cases is in contact with clear taenite or with taenite having the diffusion border (Fig. 2). It also occurs in small intermediate and micropolycrystalline particles. Taenite particles with a diffusion border and a coarse plessite interior are very common. They occur alone or in contact with kamacite or sulfide. The plessite has an irregular jagged border. The taenite particles are somewhat larger than those observed in other chondrites (100–200μ). Examples of taenites with both well-preserved and partially dissolved plessite interiors are observed and these seem to grade into a clear taenite. Reheating apparently has caused some recrystallization within these particles.

Bulbous-shaped silicate masses intrude into the kamacite particles but they are crystalline and similar to other crystals in the groundmass and hence they are not regarded as due to corrosion.

Carcote. Found in 1888, in Chile; crystalline bronzite chondrite; some corrosion is observed at the edges of the kamacite. The kamacite is of the large polycrystalline type. It is sometimes clear but prominent Neumann lines are generally present. Clear taenite crystals intermingle with the kamacite crystals (Fig. 3). They are mostly smaller than the larger kamacite crystals and fewer in number, though one area was observed in which the kamacite and taenite were about equal in amount and had crystals of approximately equal size. Hardness tests made on one of such taenite particles showed that it had a Vickers diamond pyramid number of 304 as compared with 209 for the neighbouring kamacite. No small taenite bodies with clear borders and dark interiors are observed, though both fine and coarse plessite without diffusion borders are observed.

Chondrules are broken and crystalline, and contain minute pieces of metal whose crystalline form cannot be identified.

Densmore. Found in 1879, at Kansas; chondrite. The troilite is distributed much as observed in many other meteorites. No metal particles have been clearly identified, although some very small particles ($\sim 1\mu$) may be metal. Certain areas filled with a grey material have shapes suggestive of metal particles. The specimen is apparently badly corroded.

Estacado. Found in 1883, in Texas; crystalline bronzite chondrite. The

Estacado structure is very compact and regular, with the silicate crystals fitting together without cracks between them, and typically fitting tightly against the metal particles. The kamacite particles have very regular boundaries which are straight or nearly so in many examples. The troilite is smooth and sometimes uncracked, which is quite unusual. Kamacite and taenite occur more generally as separate particles than in contact. Neumann lines are rare. The kamacite is mostly polycrystalline in large crystals (100μ). But microcrystalline particles are present, which may be kamacite. Also some polycrystalline kamacite of intermediate-sized crystals is present ($5–10\mu$)(Fig. 4). Clear taenite occurs in contact with kamacite. Also taenite particles with a clear border and a plessite interior are common (Fig. 5). The plessite interior may have a definite and irregular border lying within the taenite particle. Some unusual particles are present. Some kamacite particles have yellowish rounded masses (taenite?) scattered through them. Taenite particles have complicated borders and structures within them (Fig. 5). Some corrosion of the kamacite particles has occurred. For most particles this is very slight or non-existent but others are substantially or apparently wholly replaced. Since this meteorite is a "find", it is very probable that the corrosion is of terrestrial origin.

We believe that this meteorite shows evidence for mild reheating, possibly to 500°C, during which the silicates and iron particles became closely fitted together, and taenite may have precipitated within the kamacite particles.

Forest City. Fell in 1890, in Iowa; brecciated spherical bronzite chondrite. This meteorite is very similar to Allegan. Our preparation exhibits a marked tendency for silicate crystals to be loosened in the grinding and polishing. The troilite contains many cracks. The kamacite is clear for the most part and the Neumann lines are few, and occasionally kamacite particles contain what may be schreibersite though the identification is not certain (Fig 6(b)). In many cases clear taenite is found in intimate contact with kamacite. Separate taenite particles are very common. In most cases they have clear diffusion borders and clear interiors, with a smoky fine plessite band between as observed under our conditions of etching. Some taenite particles are broken with a diffusion border around only part of the periphery. When the particle is partially in contact with the troilite, the diffusion border in some cases is broader along the troilite than it is along the silicate (this differs from the Allegan case). Fig 6(a) shows an unusual taenite particle which may owe its structure to reheating.

The chondrules are crystalline and contain differentiated metal particles of microcrystalline kamacite and probably kamacite and taenite in contact. These metal particles are smaller than those in the main body. The chondrules could not have been formed in the melted state without destroying the metal phases, and, if they were melted, the differentiated metals were formed in the chondrule substance subsequent to the melting process. The chondrules are only roughly spherical in shape. No corrosion was observed.

Gilgoin Station. Found in 1889, in New South Wales; veined white hypersthene chondrite. This meteorite is compact, with silicate and metal particles well fitted together. Corrosion is slight but present. The kamacite has a mottled appearance produced by crystals of irregular shape but with curved boundaries fitted together

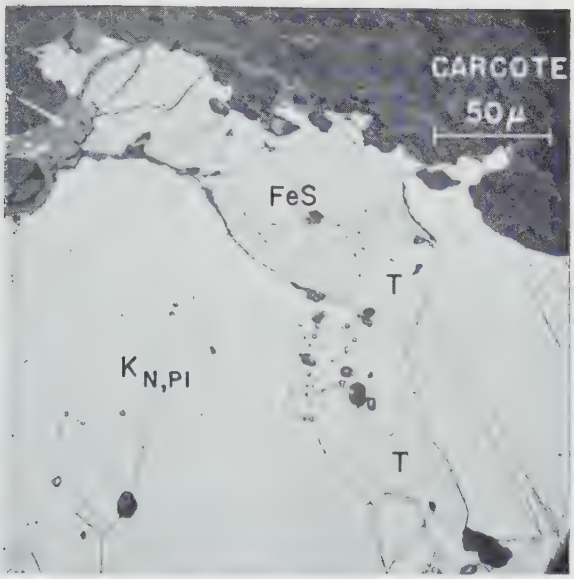

Fig. 3. Carcote. Polycrystalline kamacite with sharp Neumann lines. Kamacite is in contact with some clear taenite and troilite, and edged with greyer vein of corrosion. *T*, taenite; K_{N,P_1}, kamacite with Neumann lines of a coarse polycrystalline form.

Fig. 4. Estacado. Varieties of polycrystalline kamacite within microscopic distances of clear kamacite. Note smooth and compact silicate structure. K_{P_3}, very fine polycrystalline kamacite; K_{P_2}, polycrystalline kamacite of intermediate crystal size; Cor, corrosion.

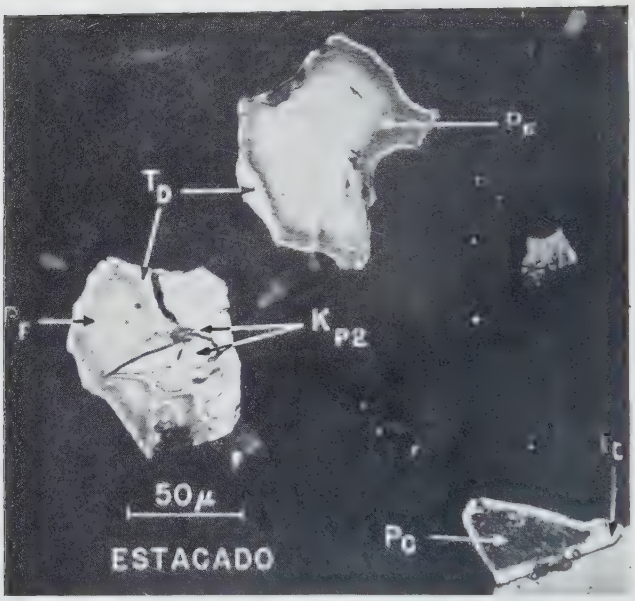

Fig. 5. Estacado. Taenite particles with irregular borders and plessite interiors. P_F, fine-plesite; T_D, taenite diffusion border; P_C, coarse plessite; K_{P2}, polycrystalline kamacite of intermediate degree of fineness.

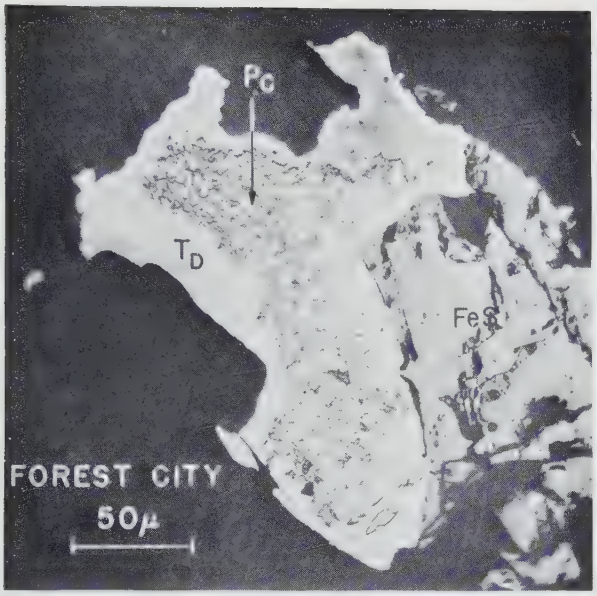

Fig. 6(a). Forest City. Good example of very coarse plessite, P_C. Wider clear taenite region, T_D, along the silicate border is shown in this case.

Fig. 6(b). Forest City. Schreibersite (S) embedded in a section of kamacite. No Neumann lines are observed in this kamacite. K_S, kamacite containing schreibersite.

(Fig. 7). This appearance is more prominent near the edges of the kamacite masses. Inclusions in these metal masses have a slightly yellow colour and may be taenite, although no definite decision in regard to this has been possible. Neumann bands are present in the larger kamacite areas and various stages between coarse Neumann bands in massive kamacite and the polycrystalline kamacite can be found. In a few cases the taenite is clear and attached to kamacite areas. Separate particles of taenite with a diffusion border and plessite interior occur. These are badly disintregrated as though they had been much distorted and broken and possibly heated mildly. They have a clear broken border and fine cloudy plessite next to the border, and a clear interior. Some particles are so mixed up that a regular structure no longer exists and they appear to be mixtures of plessite, kamacite, taenite and troilite.

The kamacite structure suggests that many Neumann lines were first formed and then mild heating caused recrystallization into the polycrystalline kamacite. The appearance of the taenite is not inconsistent with this history.

Holbrook. Fell in 1912, in Arizona; crystalline spherical hypersthene chondrite. Kamacite is present in clear form mostly without Neumann lines up to about 300 μ sizes. They are generally in contact with clear taenite areas. Small pieces of polycrystalline kamacite are present. Some taenite areas in contact with kamacite have very coarse plessite areas in which the kamacite crystals are easily resolved. Some separate metal particles look exactly like these taenite areas. Other particles have clear taenite borders, a coarse pleasite area and a fine plessite interior. None of the small distorted taenite particles with well-defined diffusion border and plessite or clear interior is observed. No corrosion is evident.

Mocs. Fell in 1882, in Transylvania; veined white hypersthene chondrite. The troilite of Mocs is distributed in separate bodies, as in most chondrites, and also in very finely divided form between the silicate crystals and in veins (Fig. 8(c)). These latter distributions are very distinctive. Clear kamacite in large crystals does not occur. Kamacite of intermediate and fine crystal sizes is common. The intermediate or mottled kamacite is commonly in contact with clear or nearly clear taenite. Taenite particles with diffusion borders and plessite interiors are common and are often badly distorted and broken (Fig. 8(d, e, f)). Some taenite particles are sometimes mixed with troilite in complicated ways. One taenite particle of elongated shape and large size (230 μ long broken at the ends and 60 μ wide) with plessite interior and diffusion border was observed in this meteorite (Fig. 8(a)). It is the only taenite particle observed in any meteorite that has the appearance of coming from an octahedrite metal meteorite. The particle is only partly preserved. One end seems to be disintegrated and mixed with polycrystalline kamacite. No corrosion can be detected and no well-formed spherical chondrules can be found. The meteorite in many ways indicates extreme crushing and distortion of all constituents. Fig. 8(b) illustrates an example.

Modoc. Fell in 1905, in Kansas; veined white hypersthene chondrite. The metal particles of Modoc are very complex and variable and there appear to be small amounts of corrosion. Mostly taenite and kamacite are in contact with each other but the taenite particles on the unattached sides have the same appearance as on the attached sides, so that the appearance of being the product of a fragmentation

process is apparent (Fig. 9(b)). The clear kamacite always has Neumann bands and polycrystalline kamacite is mostly of an intermediate fineness, but fine kamacite looking like coarse plessite is present (Fig. 9(e)). The taenite is sometimes clear, and occasionally has a wide diffusion border suggesting an almost clear condition. It occurs with fine and coarse plessite interiors and a diffusion border and also completely enclosed in kamacite, at least in the cross-section (Fig. 9(a)). Many diffusion borders are broken and distorted.

The silicate is not smooth in our prepared section due to crystals falling out during grinding and polishing.

Tulia. Found in 1917, in Texas; polymict brecciated veined crystalline hypersthene chondrite. There is evidence of extensive corrosion. Large kamacite particles (500 μ) are common. They contain Neumann lines which are mostly straight, though some are definitely curved (Fig. 10(b)). A few of these kamacite particles contain needles (lamellae) and irregular small masses of what we believe to be schreibersite, although no analysis for phosphorus have been possible. Some kamacite is coarse polycrystalline and the edges of some of the larger clear particles are also polycrystalline. Clear taenite is found in contact with some kamacite particles. A few separate taenite particles with diffusion border and fine plessite interiors are observed. Fig. 10(a) shows an unusual type of taenite particle.

Glass chondrules are present . Some contain very small metallic particles whose crystal character cannot be determined.

Interpretation of Observations

Certain conclusions stated by one of us (Urey, 1956) previously are shown by the overwhelming evidence to be correct. The metal particles of the chondritic meteorites are fragments of larger masses and could not in many cases have been produced in the localities where they were found. In nearly all chondrites metal particles of widely different character are found near each other but not in relative positions expected for the growth of kamacite and taenite from one parent crystalline mass, as observed in the iron meteorites. Many taenite particles are distorted and the borders are broken and twisted, showing that a very violent process was involved in breaking up these particles. It is necessary that in some object or objects the silicate minerals and the kamacite and taenite were formed by a slow process of cooling to such low temperatures that diffusion was no longer able to maintain uniform concentrations in the taenite. This mass was broken to very small particles and the metal and silicate were reaccumulated into another compact mass which was the immediate parent of these meteorites. Urey (1956) called these the primary and secondary objects and gave reasons for believing that the former were of lunar size and that the latter could be identified with the asteroids. However, there is evidence that some of the displacements of the fragments were very small, even though they were very violent. Thus, Fig. 8(e) shows a displacement of fragments of a taenite particle only a microscopic distance from each other.

Gevers *et al.* (1945) concluded that the metal particles observed in the Groenewald-Benoni chondrite became differentiated *in situ* within the conglomerated silicates because they found that kamacite and taenite were everywhere in contact

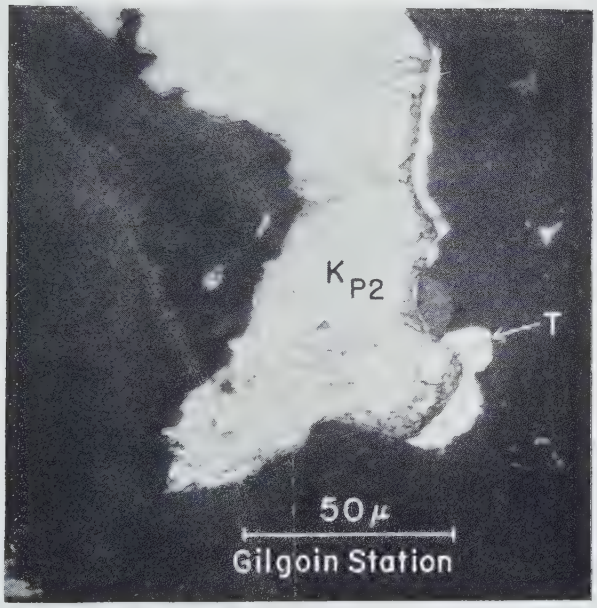

Fig. 7. Gilgoin Station. Mottled looking polycrystalline kamacite, K_{P_2}, with taenite border, T, on one side.

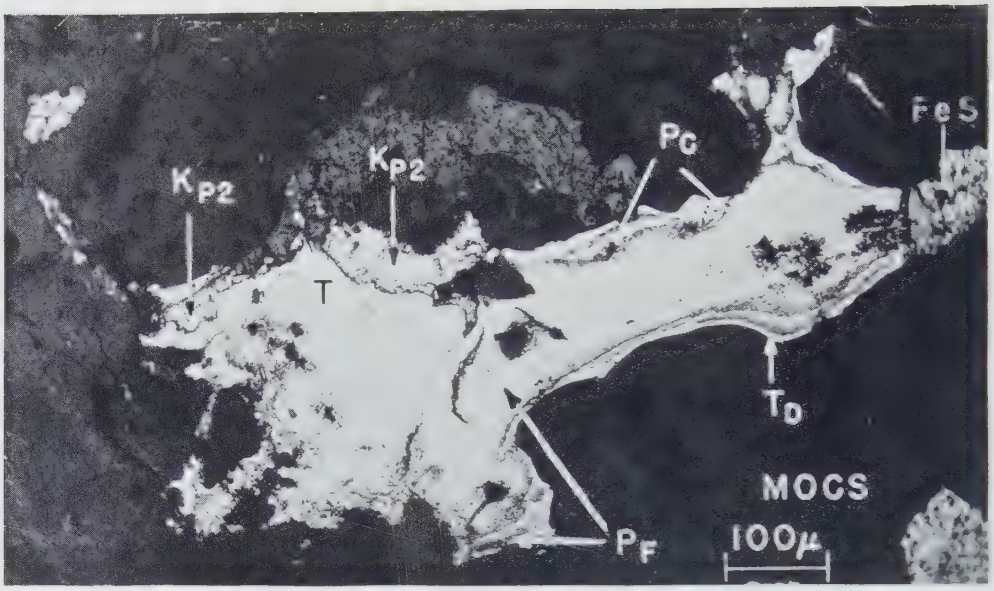

Fig. 8(a). Mocs. Taenite particle which is very similar to that in octahedrite metal meteorite. This taenite particle is of extraordinary size. P_C, coarse plessite, K_{P2}, polycrystalline intermediate kamacite; P_F, fine plessite.

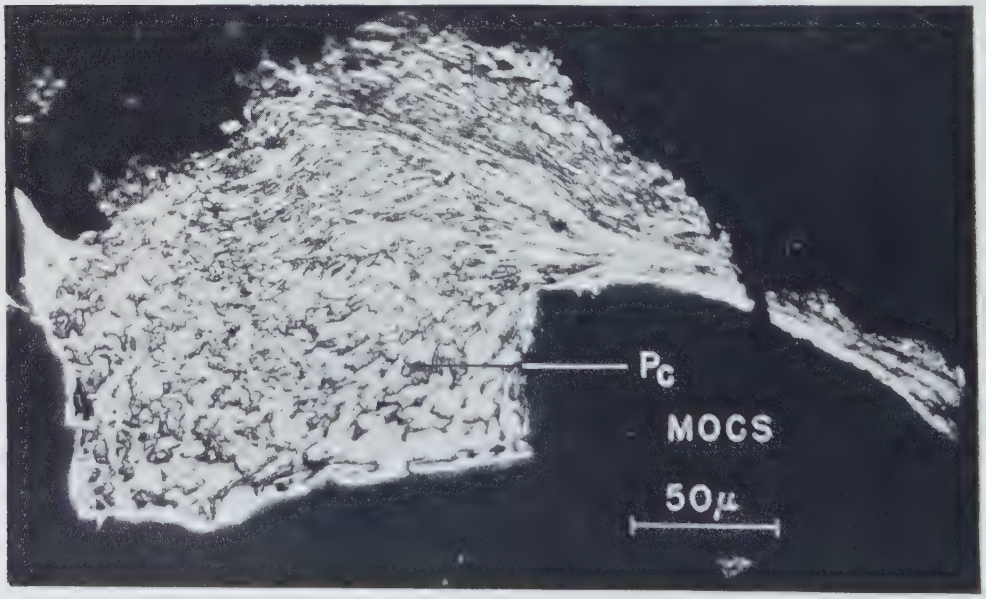

Fig. 8(b). Mocs. Very distorted coarse plessite, P_C. No taenite diffusion border is observed along upper edge

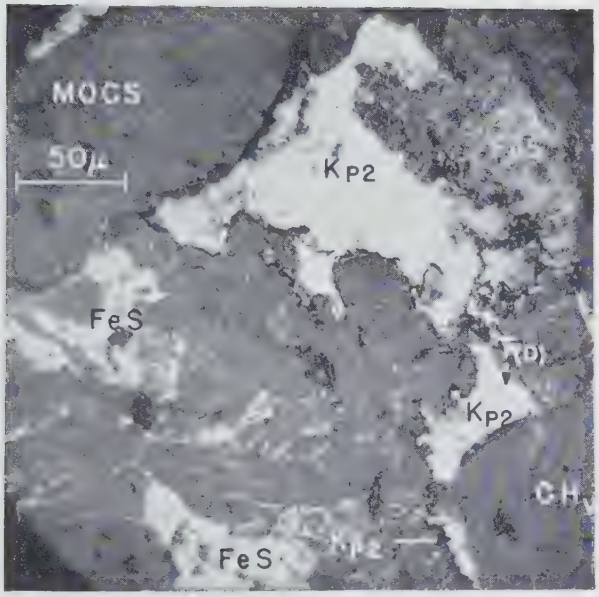

Fig. 8(c). Mocs. Fine net of troilite veins together with pock-marked troilite, FeS, and mottled kamacite, K_{P2}. Note the veined chondrule, CH_V.

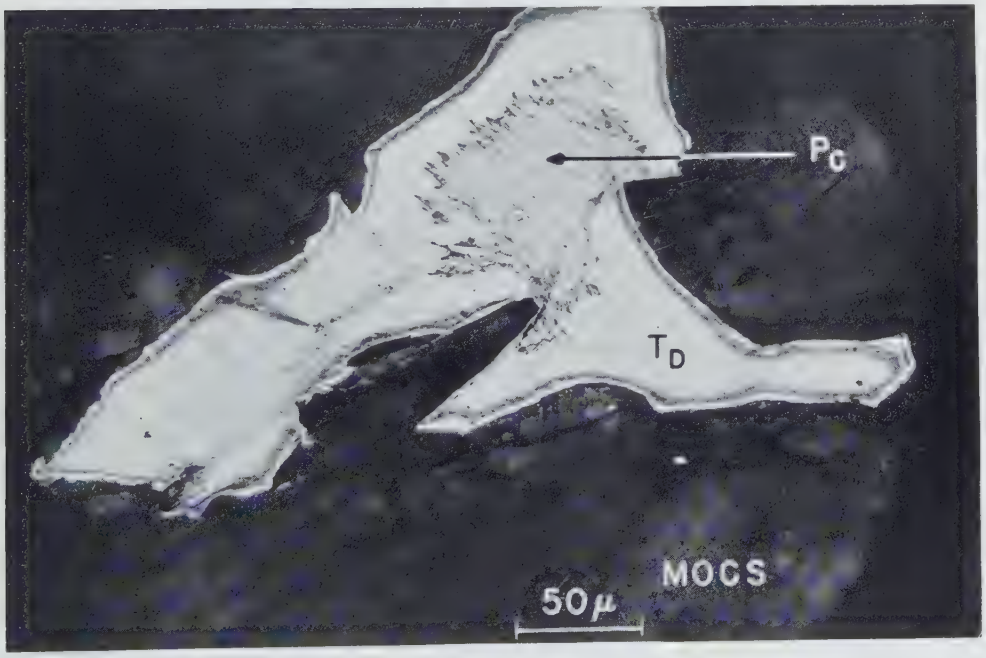

Fig. 8(d) Mocs. Broken taenite particle with jagged border with silicate, one sliver of which intrudes into the metal. Mild heating in situ is indicated by the jagged edge of the interior plessite, P_C.

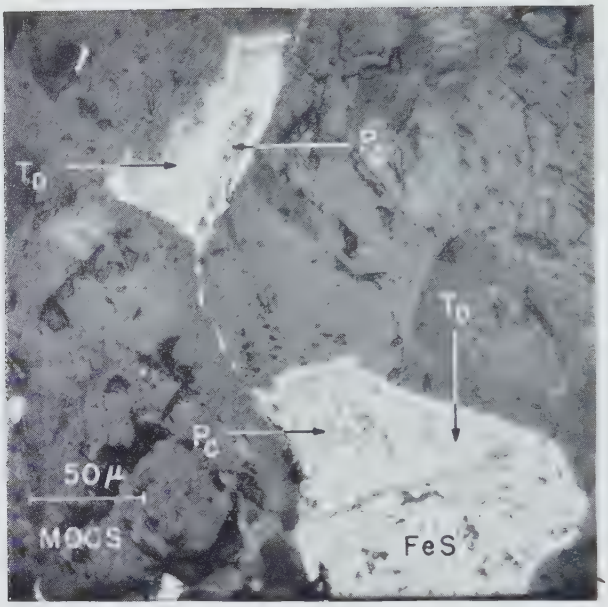

Fig. 8(e). Mocs. These two taenite particles appear to be fragments of a single particle. Note the connecting trace of metal. T_D, taenite diffusion border; P_C, coarse plessite.

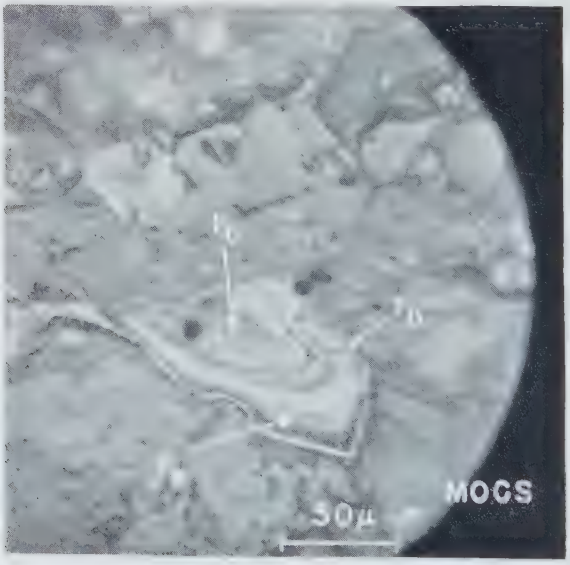

Fig. 8(f). Mocs. Broken taenite showing at least three diffusion zones and broken along the upper edge. P_C, coarse plessite; P_F, fine plessite; T_D, taenite diffusion border.

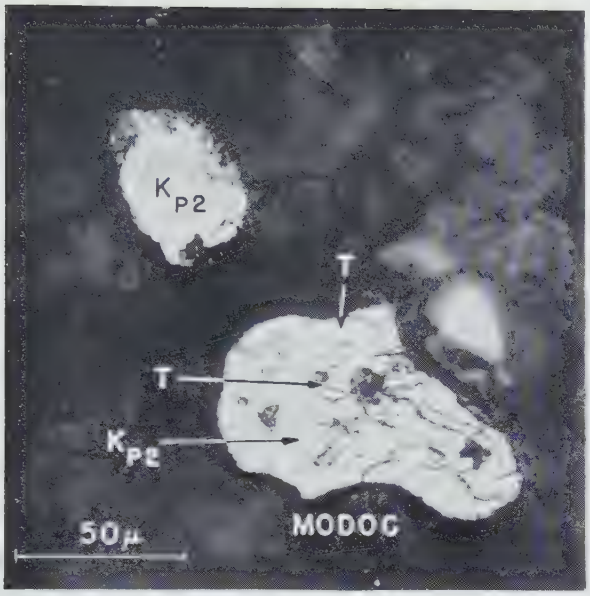

Fig.-9(a). Modoc. Clear taenite intrusions and inclusions in polycrystalline kamacite. This is possibly due to reheating. T, taenite; K_{P_2}, intermediate polycrystalline kamacite.

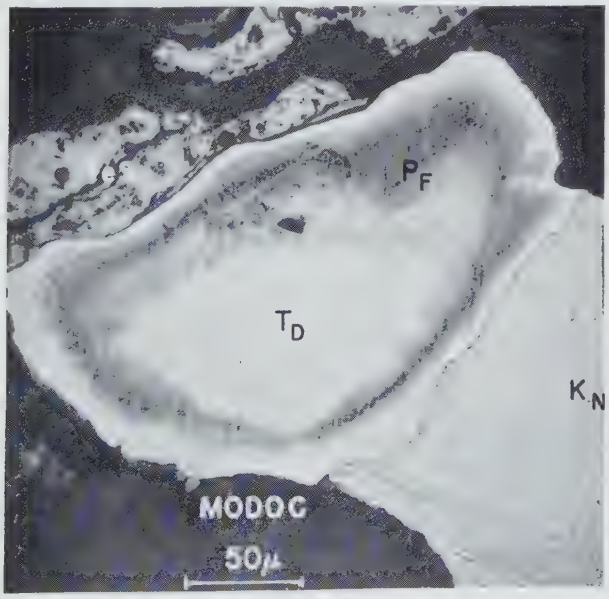

Fig. 9(b). Modoc. Taenite, T_D, attached to both troilite and kamacite with Neumann lines, K_N. Note that the diffusion borders in contact with troilite, kamacite and silicate are are similar.

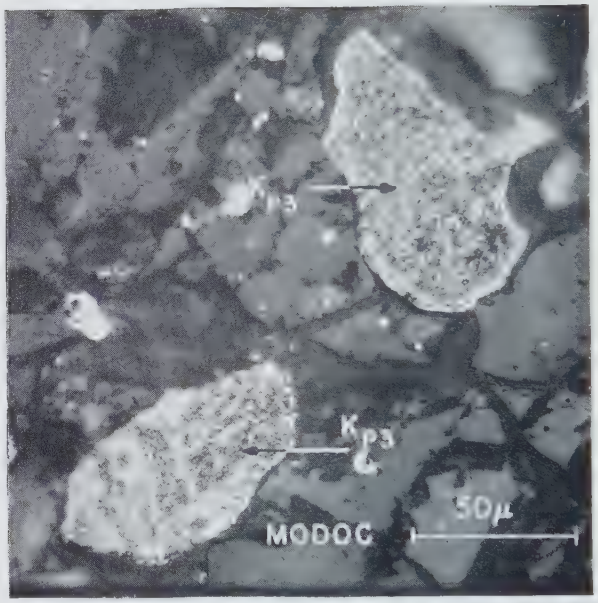

Fig. 9(c). Modoc. Example of fine polycrystalline kamacite, K_{P3}, which is almost identical to some coarse plessite. Note the appearance of a taenite diffusion border around the upper one.

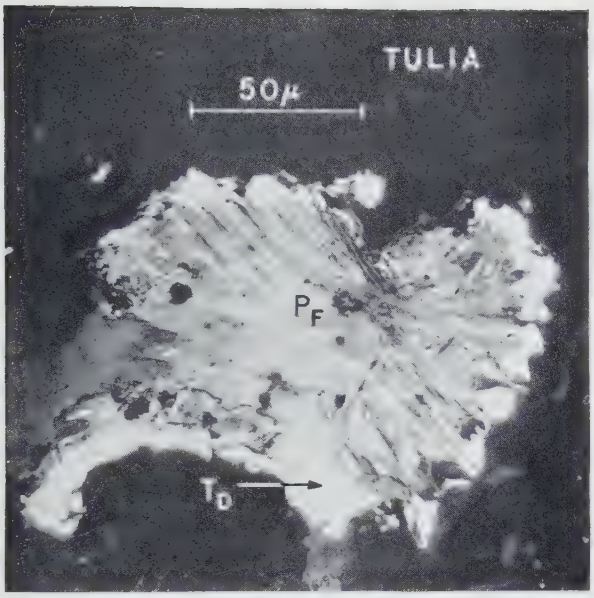

Fig. 10(a). Tulia. Taenite with plessite interior which appears to be recrystallized into needle-like crystals.

Fig. 10(b). Tulia. Example of rather faint and distorted Neumann lines in kamacite. Some corrosion is present.

with each other. We find that this is not universally the case. But their studies show that markedly dissimilar metal fragments are present and it is difficult to understand how these particles became so different unless they differ in iron–nickel ratio or in other chemical composition. This implies some previous physicochemical process in an earlier location where such variations in composition could be acquired. Thus the presence of mono- and polycrystalline kamacite particles reported by them indicates some differences in origin. Our many varieties of both kamacite and taenite particles within very short distances lead to the same conclusion and justify our contention that the metal as well as the silicate crystals originated in the primary objects.

Though certain physical and chemical features of the meteorites must have been established in the primary objects, certain characteristics were acquired in the break-up process and in the secondary objects. Some chondrules, e.g. those of Tulia, are glass and contain undifferentiated metal. At some time they were melted and cooled without crystallization of the silicates. Some metal particles also show evidence of having been reheated. In studying these meteorites the following criteria for reheating have been developed in our thinking: (1) Clear taenite particles occur embedded in kamacite (Fig. 4). We suggest that reheating for a short period caused the plessite to dissolve and rapid cooling prevented its formation again. Carcote contains separate taenite particles having plessite interiors also. See Appendix.

(2) The presence of broad borders and coarse interiors as in Fig. 6(a) suggests that recrystallization of the plessite has occured. Slightly more heating would have caused the pattern to disappear completely.

(3) The presence of polycrystalline kamacite of the intermediate or mottled type (Fig. 7) may be due to reheating of kamacite which has previously has many Neumann lines. Note the clear taenite attached to kamacite in the plate which agrees with criterion (1) above.

(4) The presence of clear taenite attached to kamacite (Fig. 3) indicates a destruction of plessite in the manner suggested under (1) above. The plessite in the interior of the other taenite particle has a ragged border suggestive of a solution process.

(5) The presence of clear taenite within kamacite particles (Fig. 9a) may have been produced by heating kamacite formed at low temperature until it entered the α–γ region of the phase diagram. These criteria are not conclusive, though we know of no other possible explanation of the first of these. Also as mentioned previously, glass chondrules occur which require high temperatures at least for brief periods of time.

It is difficult to estimate the temperature of reheating. The phase diagram requires that the temperatures were all below 910°C, which is the transition temperature for pure iron, and really below 750°C, which is the transition temperature for a 6% nickel alloy with iron. Since structures are mostly preserved, we think the temperatures of reheating may not have been higher than 500°C, though other materials, i.e. the glass chondrules must have been at higher temperatures.

This reheating is easily ascribed to radioactive heating in the secondary objects

but there are reasons for doubting this explanation. Radioactive heating would act over a long period of time. The ages of some of these meteories, using the K–A method, are very great, of the order of 4·4 Æ, and thus the time of heating must have been fairly short, i.e. between the lead–lead ages 4·55 Æ and the K–A ages. (An aeon, symbol Æ, is defined as 10^9 years.) Moreover, in the same meteorite there are particles that seem to have been heated and yet within microscopic distances there are others which do not. This suggests that heating up to temperatures of 500°C occurred during the violent break-up process. The glass chondrules, maskelynite and tridymite, are difficult to explain unless local and limited heating to much higher temperatures occurred, producing a limited number of melted silicates which became mixed with a much larger mass of other material. We are of the opinion that radioactive heating was not the important heating process, though we cannot exclude the possibility that some contribution was made to heating by this method.

Conclusion

A study of the metal particles of eleven chondrites and one achondrite of a unique kind has been made. It is concluded that the metal particles secured their principal characteristics by a slowly cooling process in a primary object. This body was broken up and the materials reaccumulated into a secondary object. Reheating to about 500°C occured during the break-up process. This took place in their history starting some 4·5 Æ ago. A few glass chondrules may owe their origin to heating to high temperatures in very limited volumes.

Abee is an achondrite containing substantial amounts of iron and troilite. It is not a conglomerate and may be a stony iron in which the mixtures of metal and silicate are on a microscopic scale. No evidence of reheating of this object has been found. Crystalline silicates are suspended in the metallic phase, indicating that the body was formed in a low gravitational field.

The observed corrosion in all meteorites studied is probably of terrestrial origin.

Acknowledgements—We are indebted to Professor C. Smith for many constructive suggestions in regard to this study and for making available to us his extensive knowledge of the iron–nickel system, to Mrs. B. Neilson for her help and advice with regard to the observational techniques and to Mr. G. Schmidt of General Atomic for making the hardness tests.

References

Beck C. W., Stevenson R. G. and La Paz L. (1951) *Pop. Astr.* **59,** 88.
Gevers T. W., Mendelssohn E. and Dunne J. C. (1945) *Trans. Geol. Soc. S. Africa* **48,** 83–102.
Merrill G. P. (1921) *Bull. Geol. Soc. Amer.* **32,** 395–416.
Perry S. H. (1944) *N. S. Nat. Museum Bull.* 184.
Prior G. T. and Hey M. H. (1953) *Catalogue of Meteorites.* British Museum.
Urey H. C. (1956) *Astrophys. J.* **124,** 623.

Appendix

The following notations indicate the particles which we have observed. No attempt has been made to indicate relative frequency, for the total number observed were not sufficient to establish such relative frequencies reliably. No attempt has been made to indicate the abundance of each phase.

A survey of each meteorite reveals various metal phases and their combinations. The following system is employed to describe the area under investigation. The notations on chondrules show only obvious cases.

K, clear kamacite.
K_N, kamacite with Neumann lines;
K_{P1}, kamacite with coarse polycrystalline structure;
K_{P2}, kamacite with medium and granular polycrystalline structure;
K_{P3}, kamacite with very fine polycrystalline structure, sometimes indistinguishable from coarse plessite except for the lack of a diffusion border;
K_S, kamacite with schreibersite inclusion;
K_T, kamacite with γ–α transformation structure;
P_C, coarse plessite;
P_F, fine plessite;
T, clear taenite;
T_D, taenite with diffusion border;
FeS, troilite;
S, schreibersite;
CH, chondrules;
CH_M, chondrule with metal bits;
CH_V, chondrule with veins;
$+$ two phases in contact;
$(+)$ two phases in contact, one inside the other.

Abee. K_T, FeS, K + taenite–phosphorus alloy, K_T + FeS. Some unidentified light-coloured phase is present; our analysis is incomplete.

Allegan. K_N, K_N + FeS, $K_N + (T + P_C)$, $K_N + T$, $K_{N,P1} + (T_D + P_F)$, $(K_N + T)$, $K + (T_D + P_F)$, K_{P2}, $K_{P2} + T + P_F$, $K_{P2} + T$, K_{P3}, $K_{P3} + T$, T, $(T_D + P_F)$, $(T + P_C)$, $T_D + P_F$, $(T_D + P_C)$ + FeS, $(T_D + P_F)$ + FeS, $(T_D + P_C)$, $(T_D + P_C)$ + FeS, T + FeS, $(T_D + P_F) + P_F$, FeS, CH, CH_M, CH_V.

Beardsley. Little corrosion. K_N, $K_N + (T_D + P_F)$, $(K_N + T + P_C) + T$ + FeS, $K_{N,P1} + (T + P_C) + T$, K_N + FeS, $K_N + T$, $K_N + T + (T + P_C)$ + FeS, K, K + FeS, $K + T$, $K + T + (T + P_C)$, $K + T + (T + P_C)$ + FeS, $K + T$ + FeS, $(K + T)$ + FeS, $(K_{P2} + T)$ $K_{P2} + T$, K_{P3}, K_{P3} + FeS, $(T_D + P_F + P_C)$ + FeS, $T + P_C$, $T + P_F$ + FeS, $(T + P_C)$ + FeS, $(T + P_F + P_C)$, T + FeS, $T + P_C + (T + P_C + P_F)$, $(T_D + P_C)$, FeS.

Carcote. Some corrosion K_N, $K_{N,P1}$, $K_N + T$, $K_{N,P1}$ + FeS, $K_{N,P1} + T$, $(K_{N,P1}$ + FeS) + T, $K_{N,P1} + (T + P_F) + T$, $K_N + (T_D + P_F + P_C) + K + T$, $K_{N,P1} + (T + P_C)$ + FeS, K, $K + T$, $K + T$ + FeS, K_{P1}, K_{P1} + FeS, $K_{P1} + T$ + FeS, K_{P2}, $K_{P2} + T$, T, $(T + P_F)$, $(T + P_C)$, $(T_D + P_F + P_C)$ + FeS, $T_D + P_C$, $T + (T_D + P_F + P_C)$ + FeS, FeS, CH, CH_M.

Densmore. Very corroded. CH, FeS.

Estacado. Some corrosion. K_N, $K_N + T$ + FeS, $K_N + T$, $K_{N,P1}$, K, $K + (T_D + P_F) + K_{P3}$, $K + (T + P_C)$, $K + T$, $K + (T_D + P_F)$, $(K + T) + (K_{P2} + P_C)$, K_{P1}, $K_{P1} + (T_D + P_F)$, K_{P1} + FeS, K_{P2}, $K_{P2} + T$, $K_{P2} + (T_D + P_F)$, $(K_{P2} + T)$, $K_{P2} + (T_D + P_F)$ + FeS, $(K_{P2} + T) + T$, $K_{P2} + P_C$, K_{P3}, K_{P3} + FeS, $K_{P3} + T$ + FeS, $T_D + P_F$, $(T_D + P_F)$ + FeS, $(T_D + P_F + P_C)$ + FeS, $(T_D + P_F + P_C)$, $(T_D + P_F) + P_C$, $(T_D + P_C)$ + FeS, FeS.

Forest City. K_N, $K_N + T$, $K_N + (T_D + P_F)$, K, K + FeS, $K + T$, $K + (T_D + P_F + P_C)$, K_{P2}, $K_{P2} + (T_D + P_F)$, K_{P2} + FeS, $K_{P2} + T$, $(K_{P2} + T) + T_D$, K_{P3}, K_{P3} + FeS, K_S, $(T_D + P_F)$, $(T_D + P_F) + (T_D + P_F + P_C)$, $(T_D + P_F)$ + FeS, $(T_D + P_F + P_C)$ + FeS, $(T_D + P_C)$ + FeS, FeS, CH_M, CH.

Gilgoin Station. Some corrosion. K_N, K_N + FeS, $K_N + T$, $K_N + (T_D + P_F)$, $(K_N$ + FeS), $(K_N + \text{FeS}) + T$, K, K_{P1}, K_{P2}, $K_{P2} + T$, K_{P2} + FeS, $K_{P2} + T_D$, $K_{P2} + K_{P3}$, $K_{P2} + (T_D + P_F)$, K_{P3}, $K_{P3} + (T_D + P_F)$, T_D, $T_D + (P_C + T_D + P_F)$, T_D + FeS + T, $T_D + P_C$ + FeS, $(T_D + P_F)$, $(T + P_F + P_C)$, $(T_D + P_F) + \text{FeS}$, CH, CH_V, FeS.

Holbrook. K_N, $K_N + T$, $K_N + (T + P_C)$, $K_N + (T + P_C) + T$, K, $K + (T + P_C)$, $K + T$, K + FeS, $K + (T + P_C)$ + FeS, K_{P3}, P_F, $(P_F + P_C)$, $(T_D + P_C)$, $(T + P_C + P_F)$, $(T + P_C + P_F)$ + FeS, $(T + P_F)$, $(T + P_C)$ + FeS, FeS, CH.

Mocs. Little corrosion. K_{P2}, K_{P2} + FeS, $K_{P2} + (T_D + P_F)$, $K_{P2} + (T_D + P_F + P_C)$, $K_{P2} + (T_D + P_C)$, $K_{P2} + T$, $K_{P2} + P_C$, $K_{P2} + (T_D + P_F + P_C)$ + FeS, K_{P3}, K_{P3}

$+ (T_D + P_C)$, $(T_D + P_C) + \mathrm{FeS}$, $(T_D + P_F) + \mathrm{FeS}$ $(T_D + P_F) + \mathrm{FeS}$, $(T_D + P_F)$, $(T_D + P_F + P_C)$, FeS.

Modoc. K, $(K + T + P)$, $K + \mathrm{FeS}$, $(K + \mathrm{FeS}$, K_N, $(K_N + T_D + P_F)$, $K_N + \mathrm{FeS}$, $(K_N + T)$, $K_N + (T_D + P_F)$, $K_N + T$, $K_N + K_{P2} + (T_D + P_F) + (T_D + P_F + P_C)$, $K_N + (T_D + P_F) + \mathrm{FeS}$, K, $(K + T)$, K_{P1}, $K_{P1} + K_{P2}$, $K_{P1} + (T_D + P_F)$, K_{P2}, $(K_{P2} + T)$, $K_{P2} + \mathrm{FeS}$, $K_{P2} + (T_D + P_C)$, $(K_{P2} + T) + T$, $K_{P2} + (T + P_F + P_C)$, $K_{P2} + (T_D + P_F)$, $K_{P2} + (T_D + P_C + P_F) + \mathrm{FeS}$, K_{P3}, $K_{P3} + (T_D + P_F)$, T_D, $(T_D + P_F) + \mathrm{FeS}$, $(T_D + P_F)$, $(T_D + P_C)$, T, $T + \mathrm{FeS}$, FeS.

Tulia. Extensive corrosion. K_N, $K_N + T$, $K + \mathrm{FeS}$, K, $K + \mathrm{FeS}$, $K + T$, $K + (T_D + P_F) + T$, K_{P2}, K_S, $K_S + T$, $(T_D + P_F)$, $T + \mathrm{FeS}$, $(T + P_C)$, FeS, CH, CH_M.

Geochimica et Cosmochimica Acta, 1959, Vol. 17, pp. 125 to 135. Pergamon Press Ltd. Printed in Northern Ireland

Bismuth, thallium and mercury in stone meteorites by activation analysis*

W. D. Ehmann† and J. R. Huizenga
Argonne National Laboratory, Lemont, Illinois

(*Received* 23 *January* 1959)

Abstract—The radiochemical procedures for the assay of bismuth, thallium, and mercury in stone meteorites following neutron activation are described in detail. A Bi^{209} abundance of $2{\cdot}2 \times 10^{-9}$ gramme/gramme meteorite leading to a cosmic abundance of 0·0016 (per 10^6 Si atoms) was determined from the analysis of six stone meteorites. A Tl^{203} abundance of $0{\cdot}40 \times 10^{-9}$ g/g meteorite and a Hg^{202} abundance of 30×10^{-9} g/g meteorite corresponding to cosmic abundances of 0·00030 and 0·023 (per 10^6 Si atoms), respectively, were determined from analysis of five stone meteorites. Implications of these data as pertaining to the life history of meteorites are discussed.

Introduction

The heavy elements Hg, Tl, Pb and Bi are of particular interest to those working in geochemistry and cosmochemistry, since they are the highest atomic number nonradioactive elements in the periodic table. In this work the abundances of three of these, Hg, Tl and Bi, were determined by use of the very sensitive analytical tool of neutron activation.

The advantages and disadvantages of neutron activation analysis have been discussed at length in the literature (Boyd, 1949; Meinke, 1955; Plumb and Lewis, 1955; Jenkins and Smales, 1956), and will not be dealt with in detail here. It is sufficient to say that the two major advantages of the method are its high sensitivity (in this work abundances down to $\sim 10^{-10}$ g/g) and its freedom from contributions to an elemental abundance due to reagent contamination during chemical processing. The latter is of extreme importance for low abundance elements especially in the case of Hg owing to the generally high prevalence of Hg contamination in chemistry laboratories.

Previous data on heavy element abundances in stone meteorites at the time this investigation began were very sparse. Suess and Urey use an interpolated value of 0·284 (Si = 10^6) for the atomic abundance of mercury (Suess and Urey, 1956). They state, however, that all early analyses are suspect because of possible contamination in the laboratory. The Noddack's report the atomic abundance of thallium as 0·108 (Si = 10^6) (Noddack and Noddack, 1934), while Shaw (1952) reports thallium as less than 0·007 (Si = 10^6). El Badry and Kohman (1957) using microchemical techniques found the thallium abundance of the Plainview chondrite to be 0·0005 (Si = 10^6) based on one determination. Suess and Urey adopt 0·144 (Si = 10^6) for the atomic abundance of bismuth based on the work of the Noddacks (Noddack and Noddack, 1934). Recently Reed *et al.* (1958)

* Based on work performed under the auspices of the United States Atomic Energy Commission.
† Permanent address: Department of Chemistry, University of Kentucky, Lexington, Kentucky.

have reported atomic abundances (Si = 10^6) by neutron activation analysis using low level β-counting of 0·00013, 0·027 to 0·178, and $\leq$0·005 for Tl^{203}, Pb^{208} and Bi^{209}, respectively.

Data obtained to date using the neutron activation technique, details of the various procedures, and the general significance of the data are reported in this paper.

Sample and Flux Monitor Preparation

The meteorite samples selected for analysis were obtained wherever possible from the interior of a freshly fractured large individual specimen. In this manner the effects of weathering or other post-fall contamination are minimized. Descriptions of the meteorites used may be found in Prior and Hey (1953). Ideally, dated falls would provide the most useful specimens. However, specimens of dated falls are difficult to obtain and one of the meteorites used in this work, the Plainview chondrite, is a "find" of unknown terrestrial age.

The selected interior sample was pulverized in a steel vibration ball mill. Appropriate precautions were observed at all times to prevent contamination of the samples before irradiation. As a matter of practice, the preparation of the meteorites prior to irradiation was done in the office area of the laboratory, as distinct from the areas in which the later chemistry was done.

The powdered specimen was placed for irradiation in a quartz vial (4 mm internal diameter and 30 mm long), having a ground quartz stopper. Approximately 1 g of meteorite was used for each determination.

Flux monitor packages for each of the elements being determined were wrapped tightly around the vial containing the sample. Each flux monitor package consisted of a "sandwich" of four $\frac{3}{4}$ in. diameter aluminium foils, each 0·00075 in. thick. An aliquot of a standard solution of bismuth, thallium or mercury was evaporated, along with the pipette washings, on one of these foils. Evaporation was accomplished under a heat lamp at a distance of about 2 ft, so that the foil is heated only slightly above room temperature. An identical foil was placed on top of the foil containing the evaporated salt to act as a cover. Another pair of foils, one placed on each side of the flux monitor and its cover, served as monitor blanks.

The sandwich of foils was crimped together tightly and wrapped in ordinary commercial aluminium foil. Each package was also held in its position around the quartz sample vial by a firm wrapping of commercial aluminium foil.

Previous work in this laboratory (Bate *et al.*, 1958) has indicated the absence of self-shadowing effects in the use of physical flux monitors of this type in activation analysis for thorium in stone meteorites. This is reasonable, considering that the known composition of chondrites indicates low abundances of nuclides having very large neutron capture cross-sections and the small physical size of the sample. These investigators also found a 4 per cent per in. flux gradient along the axis of the irradiation can. Therefore the placement of the flux monitor foils directly around and covering the section of the quartz vial containing the sample is an important consideration.

While the validity of neutron activation analysis of the type described has not been vigorously proven for bismuth, thallium and mercury at the concentration

levels in which these elements are found in meteorites, there are no reasons at present to discount the method. The use of flux monitors of the type described to determine the absolute amount of the element in question by means of direct comparison of the flux monitor activity to that found in the sample is the best control available for the accuracy of the activation method.

Irradiation and Counting Procedures

The slow neutron activation of the meteorite samples was carried out in the "Thimble" of the Argonne CP-5 heavy water moderated reactor. The flux density for the positions used was of the order of 3×10^{13} neutrons-cm^{-2}-sec^{-1}. The Cd ratio for In activation (which is related to the ratio of thermal neutrons to fast neutrons) was approximately 10 to 1. The irradiations were usually for a period of from 10 to 15 days.

In this work bismuth was determined by counting the 5·298 MeV α-particles of Po^{210} (138·40 days), the active daughter of Bi^{210}, a 5 day β-emitter produced by an (n, γ) process on 100% natural abundance Bi^{209}. The chemical yield for polonium was determined by use of a "spike" of a known amount of cyclotron produced Po^{208} introduced at the start of the chemistry. The spike also contained small amounts of Po^{209} and Po^{210}. The Po^{210} to Po^{208} ratio for the sample polonium plate was determined by use of an α-ionization chamber connected to a multichannel pulse-height analyser. The sample Po^{210} counting rate was usually 1–5 α-counts/min. A correction was applied for the small amount of Po^{210} in the spike, and the total Po^{210} produced in the irradiation was then calculated. The appropriate decay corrections for the spike were, of course, applied during the course of this work.

The use of α-counting of Po^{210} has at least three major advantages over direct β-counting of Bi^{210}. First, the α-energy, which is easily determined with the α-pulse-height analysis system, provides a firm indentification of the nuclide being counted. Second, less radiochemical purification is necessary owing to the low background of α-emitters formed by the irradiations and the ease of discriminating against impurities by α-energy measurements in a pulse-height analysis. The natural background of the counter in this region was very low. Third, the longer half-life of Po^{210} as compared to Bi^{210} allows a longer "cooling" time for the sample and as a result, less remote handling. Also, decay corrections in processing the data are less severe.

The amount of Po^{210} activity produced in the sample as determined above is compared with the total Po^{210} α-activity of the flux monitor to determine the absolute amount of bismuth in the sample. The foil containing the evaporated bismuth salt, the cover foil and the two blank outside foils were all counted directly without chemistry in a 2π internal sample Bradley-type α-counter. This same counter was used to determine the total counting rate of Po spike added at the start of the chemistry.

A 25 λ aliquot of a standard solution of bismuth nitrate containing 10·31 μg of bismuth per 25 λ was used to prepare the flux monitors. With the usual irradiation time this resulted in a Po^{210} counting rate for the flux monitor of 10,000 to

15,000 α-counts/min in the 2 π Bradley counter. Normally, 75–90 per cent of the activity was found on the flux monitor foil itself with 10–25 per cent found transferred to the cover foil. The blank outside foils always gave a negligible counting rate (1 — 5 α-counts/min) by comparison. The total flux monitor counting rate used was the sum of that of the flux monitor foil and the cover foil.

Thallium was determined by β-counting ($E_{max} = 0{\cdot}765$ MeV) 4·0 year Tl^{204} produced by an (n, γ) reaction on 29·50% natural abundance Tl^{203}. The chemical yield of the thallium was determined by use of 13·95 mg of inert thallium nitrate carrier added at the start of the chemistry. The thallium from both the flux monitors and the samples was counted as a precipitate of TlI. The sample TlI was counted at a geometry of approximately 35 per cent in a low background proportional counter. This counting system used bulk shielding and a ring of anticoincidence tubes to achieve a reproducible background of 1·5 counts/min. The flux monitor TlI was counted under nearly the same geometry conditions with a standard end-window proportional counter having a background of approximately 10 counts/min. A correction was made for the slight difference between the efficiences of the two counters by calibration with a Tl^{204} standard source.

Unlike bismuth, the thallium flux monitors could not be counted directly owing to the very high β-background from the aluminium foils themselves. The flux monitor for thallium was prepared by evaporation of 25 λ of a standard thallium nitrate solution, containing 2·12 μg of Tl per 25 λ, on an aluminium foil. After irradiation the flux monitor foil and its cover were rinsed in portions of warm 1 M H_2SO_4 containing thallium nitrate carrier until additional washings removed no more activity. After reduction with SO_2, TlI was precipitated from this solution in the same manner used for the sample. Washings of the two blank foils from the flux monitor package in a similar manner yielded a negligible counting rate as compared to that from the flux monitor foil and cover. Under the irradiation conditions used, the Tl^{204} flux monitor counting rate was generally from 20,000 to 30,000 β-counts/min on shelf 1 of the standard proportional counter system.

Aluminium absorption curves on the flux monitor Tl^{204} were identical to those for a standard Tl^{204} source. Absorption curves were also taken for the TlI from each meteorite sample and compared to the standard Tl^{204} source. Using the chemical and irradiation procedures of this paper the counting rates obtained for the sample TlI were usually from 3 to 30 counts/min. This allowed a reasonably accurate β-absorption curve to be run in 24–48 hr. In all cases the curve agreed closely with that for the standard source. The absence in all samples of a γ-"tail" on the absorption curve indicated a pure β-emitter, although in the case of the lower activity samples the counting statistics for the points near the range of the Tl^{204} β are necessarily poor. Identical slopes were obtained for all samples over the initial portions of the absorption curve where statistics were good.

Mercury was determined by counting the 279 keV γ-ray associated with the decay of 45·8 day Hg^{203}. Hg^{203} is formed in the neutron irradiation of mercury by an (n, γ) reaction on 29·8% natural abundance Hg^{202}. The chemical yield of mercury was determined by the addition of 15·2 mg of inert mercuric nitrate carrier at the start of the chemistry.

The counting equipment consisted of a 3 in. × 3 in. NaI crystal scintillation

detector coupled to a 200-channel pulse-height analyser. The Hg^{203} γ-ray was identified by both energy calibration and half-life. The counting rate of the mercury samples was about 1000 counts/min. The flux monitor and its cover foil were counted as a unit without chemistry. The spectrum obtained was compared to that obtained by counting the two blank foils from the same package. The foil background in the area of the 279 keV photopeak, as represented by counting the two blank foils, was negligible compared to the Hg^{203} flux monitor foil and its cover. The mercury flux monitor was prepared by the evaporation on a foil of a 25 λ aliquot of a standard solution of mercuric nitrate containing 7·60 μg of mercury per 25 λ. This yielded an integrated counting rate for the flux monitor in the 279 keV photopeak of approximately 50,000 counts/min for a geometry of 3·7 per cent and an irradiation time of about 10 days.

Radiochemical Procedures

Solution and general ion exchange separation. The irradiated meteorite powder was transferred to a small platinum dish containing 5 ml of concentrated H_2SO_4, the Po^{208} spike, and the mercury and thallium carriers. The slurry was warmed under a heat lamp with occasional stirring for from 15 to 20 min. Concentrated HF was then added dropwise with stirring until effervescence ceased. An additional 10 ml of HF were then added, and the mixture was gently heated under a heat lamp at a distance of at least 20 in. until the residue was reduced to a paste. Care was taken to prevent the mixture from going to dryness at any time. Additional HF was added, and the evaporation repeated.

Concentrated HNO_3 (5 ml) was added to the resulting paste, and the slurry was transferred to a glass beaker. A small amount of concentrated HCl was added, and after any evidence for reaction ceased, the solution was made up to 50 ml with 9 M HCl. Usually, the solution at this point was clear. In some cases, however, a very small black deposit settled out on standing. Where this was observed, the residue was treated with aqua regia, diluted with 9 M HCl, and again added to the main portion.

This solution was then introduced into a 20 to 25 ml resin volume anion exchange column. The resin bed was about $\frac{1}{2}$ in. in diameter and 5 in. in length. Dowex 1, X-10, 100 to 200 mesh resin was used in all this work. After introduction of the sample the column was washed successively with 75 ml of 9 M HCl, 75 ml of 0·5 M HCl, and 25 ml of distilled H_2O. This treatment elutes the gross amount of activity from the column, which may now be treated in a "low-level' laboratory (column is $\ll$5 mr/hr at 2 in.).

Polonium chemistry. Polonium is eluted from the column with 75 ml of 1 M H_2SO_4. The eluted solution is brought to boiling and SO_2 bubbled through it to reduce any high valency ions present, which tend to reduce the polonium plating yield.

Polonium is plated directly in two batches from 1 M H_2SO_4 solution on a grease-free silver disk ($1\frac{1}{8}$ in. diameter). A plating time of 3 hr was found to give plating yields in excess of 90 per cent. No potential was necessary to plate polonium on silver. The plate was washed with benzene and acetone and submitted for α-pulse analysis.

Thallium chemistry. Thallium is eluted from the column by reduction of Tl^{3+} to Tl^{1+}. Specifically, the thallium is eluted with 75 ml of 1 M H_2SO_4 freshly saturated with SO_2. Carriers for aluminium, antimony, cadmium, copper, indium, iridium, tellurium and tin (generally in the form of nitrate or chloride solutions) were added to the eluant. The pH of the solution was adjusted to 6·5 with NaOH. The combined precipitates formed were removed by centrifugation and discarded. The supernatant was brought to pH 4 with H_2SO_4, iridium carrier again added, and TlI precipitated by the addition of excess NaI.

The TlI was separated by centrifugation, washed with H_2O, and dissolved in a few drops of aqua regia. Iridium carrier was again added, and the solution was made up to 30–40 ml with 4 M HCl. Several drops of $KMnO_4$ were added to assure oxidation of Tl^{1+} to Tl^{3+}.

The Tl^{3+} was extracted into 25 ml of equilibrated ethyl ether in a separatory funnel. The

ether layer was washed three times with 10 ml portions of 4 M HCl, all aqueous layers being discarded. The ether layer was then evaporated over 10 to 15 ml of 1 M H_2SO_4 containing iridium carrier. Tl^{3+} was reduced to Tl^{1+} with SO_2, and the solution was again scavenged with Al^{3+} carrier at pH 7.

The supernatant from the $Al(OH)_3$ precipitation containing thallium was again treated with NaI to precipitate TlI. The TlI was filtered on a weighted paper, washed with 1 M H_2SO_4, H_2O and ethyl alcohol, dried at 110°C, weighed and mounted for counting. Chemical yields for thallium averaged about 70 per cent.

Mercury chemistry. Mercury was eluted from the column with 75 ml of 4 M HNO_3. The eluant was neutralized to pH 6·5 with solid NaOH and HgS precipitated by addition of H_2S gas. The HgS was separated by centrifugation, washed with H_2O and dissolved in a few drops of aqua regia. Iridium carrier was added, and the solution evaporated with low heat to near dryness to remove excess HNO_3 after addition of 5 ml of concentrated HCl.

The small volume of solution was diluted to 10 ml with H_2O, and mercury was precipitated by the addition of several drops of freshly prepared $SnCl_2$ solution. The mercury precipitate was separated by centrifugation, washed with H_2O, dissolved in aqua regia, and again precipitated as above using iridium carrier and $SnCl_2$.

This final mercury precipitate was again separated and washed and dissolved in several drops of aqua regia. The resulting solution was diluted to 10 ml with H_2O, brought to pH 7 with NaOH and HgS precipitated with H_2S gas.

The HgS was filtered on weighed paper, washed with H_2O and ethyl alcohol, dried at 110°C, weighed and mounted for counting. Chemical yields generally ranged from 50 to 80%, although some early runs resulted in considerably lower yields.

Results and Discussion

The results obtained in this study to date are presented in Table 1 and summarized in Table 2.

It should be noted that sample no. 1 in each case represents an individual sample extracted from the larger meteorite individual and irradiated alone. Samples 2 and 3 represent portions of a separate homogeneous sample from the larger meteorite individual irradiated simultaneously, but with separate flux monitors in the same irradiation can. Therefore, comparison of the results for no. 2 and no. 3 may be looked upon as a measure of the reproducibility of the method, and a comparison of no. 1 to the average of no. 2 and no. 3 as a measure of the homogeneity of the sample. In the case of the Holbrook chondrite two entirely different specimens were used for run no. 1 and no. 2. Run no. 1 was a portion of a small Holbrook pebble. This specimen was found to yield erratic results for several elemental analyses performed in this laboratory. Therefore, the results for Holbrook no. 1, while listed in the tables, are not included in the averages computed. Holbrook no. 2 in contrast was a portion of a large Holbrook fragment and this specimen has given reproducible results in other studies in this laboratory. Therefore, the results of the Holbrook no. 2 specimen are included in the computation of the averages.

The statistical errors due to counting are of the order of 5 per cent for bismuth, 3 per cent for thallium, and 1 per cent for mercury. In general, it was attempted to record a minimum of 10^3 counts of Po^{210}, Tl^{204} and Hg^{203} for each determination. In practice, over 10^4 counts were usually recorded for Hg^{203}, while in some cases less than 10^3 counts for Po^{210} were recorded, owing to demands upon the α-pulse analysis system.

Bismuth. The results obtained for bismuth are reasonably consistent for each

individual meteorite with the exception of the Johnstown and Modoc specimens. Run no. 1 for these specimens exhibits an abundance greater than that for the second irradiation group. There is no experimental reason evident for this discrepancy, and it may be due to a true non-homogeneous distribution of bismuth in these specimens. Johnstown is described by some observers as an achondrite,

Table 1. Bismuth, thallium and mercury content of stone meteorites (10^{-9} g of nuclide/g meteorite)

Sample	No.	Weight irradiated (g)	Bi^{209}	Tl^{203}	Hg^{202}
Beardsley	1	1·2513	2·7	0·57	22
	2	1·2000	3·8	1·4	—
	3	1·2446	3·3	1·3	—
Forest City	1	1·1489	0·18	0·15	24
	2	1·0114	0·50	0·12	—
	3	1·2840	0·15	0·089	—
Holbrook	1	0·6808	(0·49)*	(0·27)*	—
	2	1·1032	2·1	0·35	52
Johnstown	1	1·2614	5·6	0·29	36
	2	1·0245	1·2	0·12	—
	3	1·0343	1·5	0·24	—
Modoc	1	1·4496	3·0	(<1·23)*	—
	2	1·1184	0·07	0·071	—
	3	0·8427	0·33	0·12	—
Plainview	1	1·2994	4·1	—	16
	2	1·0975	3·0	—	—
	3	1·0281	3·8	—	—
Average			2·2	0·40	30

* Omitted from average.

while all the other specimens used are chondrites. In this work the abundances in Johnstown were not significantly different from the major group of chondrites and hence, were included in the average values computed.

It will be noted that the bismuth abundance obtained in this work is significantly less than that adopted by Suess and Urey. This is an interesting result, since it might be expected that element formation by successive neutron capture on a slow time scale would result in a pile-up at bismuth, and hence a relatively high abundance. It is evident that the bismuth abundance is quite relevant to theories of nucleogenesis.

Thallium. the thallium result for Modoc no. 1 is listed as a limit, since a low chemical yield resulted in a high uncertainty. This value is not included in the

averages. The results show some "scatter," which is not unexpected considering the extremely low levels involved. The results for Forest City show quite good internal consistency. Only Beardsley appears to be greatly out of line (almost an order of magnitude greater than Forest City.) Bate *et al.* (1958) found the thorium content of this same Beardsley specimen to be about 25 per cent higher than the average of four other chondrites. It is possible this specimen may have been subjected to post-fall alteration. However, there is no reason to ascribe this result to experimental error, and the Beardsley values are included in the determination of the average. If they were not included, the Tl^{203} abundance average listed in

Table 2. Cosmic abundances of the heavy nuclides Bi^{209}, Tl^{203} and Hg^{202} on the basis of neutron activation analysis on stone meteorites

Nuclide	Abundance (atoms/10^6 Si)	
	Suess and Urey	This work
Bi^{209}	0·144	0·0016
Tl^{203}	0·0319	0·00030
Hg^{202}	0·0846	(0·023)*

* Preliminary result based on five determinations.

Table 1 would be 0·17 rather than 0·40 (10^{-9} g Tl^{203}/g meteorite). This would result in an atomic abundance (Si = 10^6) for Tl^{203} of 0·00013 instead of 0·00030 as listed in Table 2. Both of these values are significantly lower than that listed by Suess and Urey.

Mercury. The results reported here for mercury must be regarded as preliminary, since they are based on only five determinations. Each of the values listed in Table 1 are for a single meteorite sample irradiated alone in an irradiation can. Additional determinations in which two meteorite specimens were irradiated in the same can, as was the case for specimens no. 2 and no. 3, gave variations in the counting rates of the mercury flux monitors from the same can and mercury contents, which were spurious and larger than those reported in Table 1.

A possible explanation may be that the irradiations, in which two meteorite specimens were in the same irradiation can, were exposed to sufficiently different cooling conditions to cause loss of mercuric nitrate by volatilization from the flux monitor foils. There is also an indication that $Hg(NO_3)_2$ may have been physically lost from several of the run no. 2 and no. 3 flux monitors, owing to formation of a flaky non-adhering deposit. This type of deposit did not appear in the preparation of run 1 flux monitors and is not as yet explained. To what extent volatilization may have occurred in the single sample irradiations is unknown, but the consistency of the flux monitor counts and calculated mercury abundances in this group suggests a certain confidence in the values listed in Table 1. Additional work is planned in order to better establish these mercury abundances.

Table 2 summarizes the results of this study and compares them to the literature values accepted by Suess and Urey (1956). In this table the results are in

terms of atomic abundance of the nuclide per 10^6 atoms of Si, using an average Si content of 0·185 by weight in primitive solar non-volatile material. The results of this work are in reasonably good agreement with those of REED *et al.* (1958) for Bi^{209} ($\leq$0·005) and Tl^{203} (0·00013).

These values together with the cosmic abundances of uranium (1·14 $\times$ 10^{-8} g U/g meteorite) reported by HAMAGUCHI *et al.* (1957) and thorium (3·96 $\times$ 10^{-8} g Th/g meteorite) reported by BATE *et al.* (1958) are plotted in Fig. 1.

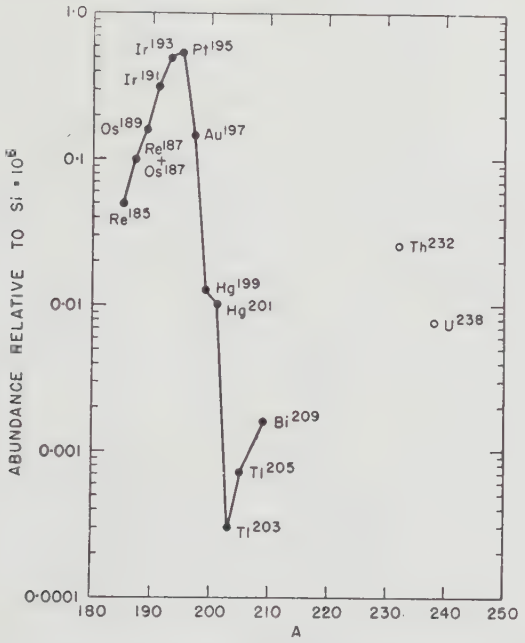

Fig. 1. Cosmic abundances of heavy nuclides based on analyses of chondrites; (●) odd A nuclides; (○) even A nuclides. Re, Os, Ir, Pt and Au, SUESS and UREY (1956); Hg, Tl and Bi, This work; Th, BATE *et al.* (1958); U, HAMAGUCHI *et al.* (1957).

The known abundances of thorium and uranium in chondrites are large compared to the abundances of thallium and bismuth. Processes, such as neutron capture on a fast time scale (BURBIDGE *et al.*, 1957; CAMERON, 1957), which have been invoked to explain the abundances of thorium and uranium, are also expected to make copious amounts of the progenitors of Bi^{209}. The fact that chondrites contain at present only a very small amount of bismuth relative to thorium and uranium strongly suggests that bismuth has been fractionated from these heavier elements sometime in the past.

The longest lived member of the $4n + 1$ radioactive series is Np^{237} which has a half-life of only 2·2 million years. With existing estimates of the time interval between element production and the formation of the solar system (WASSERBURG and HAYDEN, 1955) it is possible that the Bi^{209} progenitors decayed to very low concentrations prior to the formation of the solar system. Fractionation of elements with extremely low concentrations in chondrites such as mercury, thallium, lead, bismuth and indium (SCHINDEWOLF and WAHLGREN, 1958) may have

occurred therefore prior to or during the formation of the solar system (including meteoritic materials). It is interesting to note that present estimates of the lead content in the sun reported by Aller (1957) is a factor of at least 10^4 greater than the thallium and bismuth concentrations of chondrites reported in Table 2. A comparison of the isotopic content of the lead in iron meteorites and stone meteorites like Nuevo Laredo (Patterson, 1955) indicates that the fractionation of lead from thorium and uranium in the meteorites has not been important during their $4{\cdot}5 \times 10^9$ year lifetime. On this basis one would expect the lead in the sun, if its concentration is as high as reported, to have a considerably different isotopic composition from lead in the earth and stone meteorites. This solar lead may possibly have an isotopic composition similar to the lead in iron meteorites, if the fractionation did take place during or prior to the formation of the solar system.

If the process or processes forming the transuranium elements (Burbidge *et al.*, 1957) give an initial yield of Np^{237} (including progenitors decaying by α-emission) which is approximately equal to the initial yield of Th^{232} (including progenitors decaying by α-emission), one calculates from the present bismuth and thorium contents in chondrites and an age of the elements of $6{\cdot}6 \times 10^9$ years that more than 95 per cent of the bismuth has been lost from the chondrites. This figure includes only the bismuth formed from Np^{237} and its progenitors decaying by α-emission and will be considerably larger when the other modes of producing Bi^{209} are included.

Acknowledgements—The assistance of a number of individuals in supplying samples for this work is gratefully acknowledged. The sources of all these meteorites with the exception of the Holbrook no. 2 sample are listed by Bate *et al.* (1958). The Holbrook no. 2 sample was obtained through the courtesy of Dr. U. Schindewolf. We also wish to thank Mr D. J. Henderson for his assistance with the α-pulse-height analyses.

References

Aller L. H. (1957) *The Abundance of the Elements Determined from the Sun and Main-sequence Stars* Chap. 2. Interscience, New York. (Preprint).

Bate G. L., Huizenga J. R. and Potratz H. A. (1958) Thorium in stone meteorites by neutron activation analysis. In press.

Boyd G. E. (1949) Method of activation analysis. *Analyt. Chem.* **21**, 335.

Burbidge E. M., Burbidge G. R., Fowler W. A. and Hoyle F. (1957) Synthesis of the elements in stars. *Rev. Mod. Phys.* **29**, 547–650.

Cameron A. G. W. (1957) *Stellar Evolution, Nuclear Astrophysics, and Nucleogenesis.* Chalk River Laboratory Report No. 41.

El Badry H. and Kohman T. P. (1957) Private communication.

Hamaguchi H., Reed G. W. and Turkevich A. (1957) Uranium and barium in stone meteorites *Geochim. et Cosmochim. Acta* **12**, 337.

Jenkins E. N. and Smales A. A. (1956) Radioactivation analysis. *Quart. Rev. Chem. Soc.* **10**, 83.

Meinke W. W. (1955) Trace-element sensitivity: Comparison of activation analysis with other methods. *Science* **121**, 177.

Noddack I. and Noddack W. (1934) Die geochemischen Verteilungkoeffizunten der Element. *Svensk Kem. Tidskr.* **46**, 173.

Patterson C. C. (1955) The Pb^{207}/Pb^{206} ages of some stone meteorites. *Geochim. et Cosmochim. Acta* **7**, 151.

Patterson C. C., Tilton G. and Inghram M. (1955) Age of the Earth. *Science* **121**, 69.

Plumb R. C. and Lewis J. E. (1955) How to minimize errors in neutron activation analysis. *Nucleonics* **13**, 42.

Prior G. T. and Hey M. H. (1953) *Catalogue of Meteorites* (2nd Ed.). British Museum, London.
Reed G. W., Kigoshi K. and Turkevich A. (1958) Activation analysis for heavy elements in stone meteorites. *Second United Nations International Conference on the Peaceful Uses of Atomic Energy* Paper 953.
Schindewolf U. and Wahlgren M. A. (1958) Private communication.
Shaw D. M. (1952) The geochemistry of Tl. *Geochim. et Cosmochim. Acta* **2**, 118.
Suess H. E. and Urey H. C. (1956) Abundances of the elements. *Rev. Mod. Phys.* **28**, 53.
Wasserburg G. J. and Hayden R. J. (1955) Time interval between nucleogenesis and the formation of the meteorites. *Nature, Lond.* **176**, 130.

Geochimica et Cosmochimica Acta, 1959, Vol. 17, pp. 136 to 147. Pergamon Press Ltd. Printed in Northern Ireland

Data of rock analyses—VI

Bibliography and index of rock analyses in the periodical and serial literature of Scotland*

Mary Vogt Woodland
U.S. Geological Survey, Washington 25, D.C.

(*Received* 24 *November* 1958)

While Hutton fortified his convictions by constant appeals to the rocks themselves, his disciple Hall tested their truth in the laboratory. It is the boast of Scotland to have led the way in the application of chemical and physical experiment to the elucidation of geological history.
Archibald Geikie, 1882

As the geological literature published in Great Britain is replete with chemical analyses of igneous and metamorphic rocks, the bibliographic data are being published in several parts. This part, dealing with the analyses contained in the periodical and serial publications of Scotland from 1914 through 1953, will be followed by one for the Republic of Ireland and Northern Ireland and another for England and Wales.

No analysis of a rock from an English or Welsh locality appears in the Scottish literature that has been examined but the converse is certainly not true. Many analyses of rocks from Scotland appear first in journals published in England. In the course of the literature examination, therefore, it has been found that quite a few analyses given in the Scottish references are actually quotations from earlier English publications. As far as can be ascertained, the analyses here recorded and indexed were first published in the Scottish literature; analyses that were first published in the English literature are not listed here but will appear in a later part.

Part VI includes a list of fourteen periodicals and serials published in Scotland, an annotated bibliography of eighty-four references taken from five of these publications between 1914 and 1953, a geographic index to the eleven countries or areas represented, and a rock-name index to the 397 analyses contained in the references. In the geographic index, Scotland is subdivided into counties.

Dr. P. A. Sabine and Miss Eileen Guppy of the Geological Survey of Great Britain and Dr. A. G. MacGregor of the Scottish Office of the Survey have read the manuscript and contributed valuable suggestions. Our appreciation of this help is gratefully acknowledged.

A list of the previously published parts of the "Data of rock analyses" series is given on page 147.

Periodical and Serial Literature

Dumfriesshire and Galloway Natural History and Antiquarian Society, Transactions and Journal of Proceedings (1862–).

Edinburgh Geological Society, Transactions (1868–).

* Publication authorized by the Director, U.S. Geological Survey.

Geological Society of Glasgow, Transactions (1860–).
Glasgow Naturalist (1909–).
Glasgow University, Geological Department, Papers. Reprints from other periodicals. (1914–).
Glasgow University, Hunterian Museum, Geological Department, Monograph (1925–).
Mining Institute of Scotland, Transactions (1879–).
Paisley Naturalists' Society, Transactions (1912–1934).
Perthshire Society of Natural Science, Proceedings and Transactions (1880–1914).
Royal Philosophical Society of Glasgow, Proceedings (1814–1952).
Royal Society of Edinburgh, Proceedings (1832–).
——, Transactions (1783–).
Scotland Geological Survey Memoir (1869–).
Scottish Geographical Magazine (1885–).

Bibliography

Allan, Douglas A. (1924) The igneous geology of the Burntisland district: Roy. Soc. Edinburgh Tr. **53,** Pt. 3, 479–501. *Scotland:* 2; olivine dolerite, basalt.

Anderson, J. Graham C. (1935) The marginal intrusions of Ben Nevis; the Coillè Lianachain complex; and the Ben Nevis dyke swarm: Geol. Soc. Glasgow Tr. **19,** Pt. 2, 225–269. *Scotland:* 5; porphyritic granite, granodiorite, quartz diorite.

Anderson, J. Graham C. and George W. Tyrrell (1936) Xenolithic minor intrusions in the Loch Lomond district: Geol. Soc. Glasgow Tr. **19,** Pt. 3, 373–384. *Scotland:* 1 granite.

Bailey, Edward B. *et al.* (1916) The geology of Ben Nevis and Glen Coe, and the surrounding country: Scotland Geol. Surv. Mem., 247 p. *Scotland:* 14; quartz porphyry (alsbachite?), rhyolite, hornblende porphyrite, biotite hornblende porphyrite, hornblende augite malachite, hornblende andesite, banatite-porphyrite, monzonite, pyroxene andesite, metamorphic limestone.

Bisset, Charles B. (1934a) A contribution to the study of some granites near Aberdeen: Edinburgh Geol. Soc. Tr. **13,** Pt. 1, 72–88. *Scotland:* 3; porphyritic granite, quartz biotite diorite, dioritic xenolith.

Bisset, Charles B. (1934b) Some minor intrusions in south-central Aberdeenshire: Edinburgh Geol. Soc. Tr. **13,** Pt. 1, 133–147. *Scotland:* 4; acid kersantite, spessartite (?)-lamprophyre, odinite.

Brown, Howard J. W. (1929) Dykes and associated intrusions of the Island of Bute: Geol. Soc. Glasgow Tr. **18,** Pt. 3, 388–419. *Scotland:* 2; quartz dolerite, olivine tholeiite.

Buist, David S. (1952) A contribution to the petrochemistry and petrogenesis of the composite sill of South Bute: Edinburgh Geol. Soc. Tr. **15,** 52–68. *Scotland:* 5; dolerite, olivine-bearing dolerite, pitchstone porphyry.

Campbell, Robert and James W. Lunn (1927) The tholeiites and dolerites of the Dalmahoy syncline: Roy. Soc. Edinburgh Tr. **55,** Pt. 2, 489–505. *Scotland:* 2; tholeiite, basalt.

Campbell, Robert, T. Cuthbert Day and Andrew G. Stenhouse (1932) The Braefoot Outer Sill, Fife: Part I. The Braefoot promontory: Edinburgh Geol. Soc. Tr. **12,** Pt. 4, 342–375. *Scotland:* 9; olivine basalt, teschenite, chlorophaeite dolerite-pegmatite, chloritized dolerite-pegmatite, dolerite, basalt, microsyenite, hornblende teschenite.

Campbell, Robert, T. Cuthbert Day and Andrew G. Stenhouse (1934) The Braefoot Outer Sill, Fife: Part II. (a) Braefoot promontory to Bouprie; (b) Hallcraig promontory; (c) Long Craig Island; (d) Haystack Island; (e) Donibristle: Edinburgh Geol. Soc. Tr. **13,** Pt. 1, 148–173. *Scotland:* 2; teschenite, picroteschenite.

Clark, Robin H. (1952) The significance of flow structure in the microporphyritic ophitic basalts of Arthur's Seat: Edinburgh Geol. Soc. Tr. **15,** 69–83. *Scotland:* 5 microporphyritic basalt.

Cockburn, Alexander M. (1935) The geology of St. Kilda: Roy. Soc. Edinburgh Tr. **58,** Pt. 2, 511–547. *Scotland:* 10; eucrite, gabbro, granophyre, pitchstone, olivine dolerite, dolerite, basalt.

Cockburn, Alexander M. (1952) Minor intrusions of the Pentland Hills: Edinburgh Geol. Soc. Tr. **15,** 84–99. *Scotland:* 2; olivine dolerite, andesine dolerite.

Davidson, Charles F. (1935) The Tertiary geology of Raasay, Inner Hebrides: Roy. Soc. Edinburgh Tr. **58,** Pt. 2, 375–407. *Scotland:* 4; gabbroid teschenite, riebeckite granophyre, peridotite, andesitic pitchstone.

Davidson, Charles F. (1933) The Archean rocks of the Rodil district, South Harris, Outer Hebrides: Roy. Soc. Edinburgh Tr. **61,** Pt. 1, 71–112. *Scotland:* 7; metamorphic dolomitic limestone, edenite saxonite-gneiss, anorthosite-gneiss, saussuritized anorthosite-gneiss, biotite andesine granulite, eclogite.

Davies, L. Merson (1936) The geology of Inchkeith: Roy. Soc. Edinburgh Tr. **58,** Pt. 3, 753–786. *Scotland:* 2; teschenite, analcite-bearing basalt.

Day, T. Cuthbert (1923) Chemical analyses of the dolerite and hornfels of Auchinoon: Edinburgh Geol. Soc. Tr. **11,** Pt. 2, 128–130. *Scotland:* 7; dolerite, hornfels.

Day, T. Cuthbert (1925) The Leithies, North Berwick, a small laccolite with unusual intrusive phenomena: Edinburgh Geol. Soc. Tr. **11,** Pt. 3, 300–307. *Scotland:* 2 monchiquite.

Day, T. Cuthbert (1928a) The volcanic vents on the shore between North Berwick and Tantallon Castle: Edinburgh Geol. Soc. Tr. **12,** Pt. 1, 41–52. *Scotland:* 2; monchiquite, basalt.

Day, T. Cuthbert (1928b) Chemical analyses of quartz-dolerites and segregation veins at Hound Point, North Queensferry, and Inverkeithing: Edinburgh Geol. Soc. Tr. **12,** Pt. 1, 80–86. (Analysis corrections in Edinburgh Geol. Soc. Tr. **12,** Pt. 4, 390, 1932). *Scotland:* 11; quartz dolerite, quartzite, segregation vein.

Day, T. Cuthbert and Edward B. Bailey (1928c) Bombs of nepheline-basanite in the Partan Craig vent, North Berwick: Edinburgh Geol. Soc. Tr. **12,** Pt. 1, 87–89. *Scotland:* 1 nepheline basanite.

Day, T. Cuthbert (1928d) Metasomatism in basalt near Eel Burn, North Berwick: Edinburgh Geol Soc. Tr. **12,** Pt. 1, 117–121. *Scotland:* 3 basalt.

Day, T. Cuthbert (1930a) Chemical analyses of white trap from Dalmeny, Granton, Weak Law, and North Berwick: Edinburgh Geol. Soc. Tr. **12,** Pt. 2, 189–194. *Scotland:* 10; white trap, dolerite.

Day, T. Cuthbert (1930b) Volcanic vents on the coast, from Tantallon Castle eastwards to Peffer sands, and at Whitberry Point: Edinburgh Geol. Soc. Tr. **12,** Pt. 2, 213–233. *Scotland:* 4 basalt.

Day, T. Cuthbert (1930c) Chemical analyses of phonolites from Traprain Law, the Bass Rock, and North Berwick Law: Edinburgh Geol. Soc. Tr. **12,** Pt. 2, 234–235. *Scotland:* 4 phonolite.

Day, T. Cuthbert and Andrew G. Stenhouse (1930d) Notes on the Inchcolm anticline: Edinburgh Geol. Soc. Tr. **12,** Pt. 2, 236–251. *Scotland:* 7; picrite, teschenite, olivine basalt, metamorphosed limestone.

Day, T. Cuthbert (1930e) Two large xenoliths within the phonolite of Traprain Law: Edinburgh Geol. Soc. Tr. **12,** Pt. 2, 252–255. *Scotland:* 3; phonolite, shale xenolith, sandstone xenolith.

Day, T. Cuthbert (1930f) An igneous dyke in the quartz-banakite of Bangly quarry near Haddington: Edinburgh Geol. Soc. Tr. **12,** Pt. 2, 256–259. *Scotland:* 3; quartz banakite, trachybasalt.

Day, T. Cuthbert (1930g) The intrusive rock of Frances Craig and the teschenite of Ravensheugh: Edinburgh Geol. Soc. Tr. **12,** Pt. 2, 260–262. *Scotland:* 2 teschenite.

Day, T. Cuthbert (1930h) Chemical analyses of thirteen igneous rocks of East Lothian: Edinburgh Geol. Soc. Tr. **12,** Pt. 2, 263–266. *Scotland:* 13; teschenite, white trap, monchiquitic basalt, basalt, essexite, mugearite, trachyte.

Day, T. Cuthbert (1932a) The teschenite of Point Garry, North Berwick: Edinburgh Geol. Soc. Tr. **12,** Pt. 4, 334–337. *Scotland:* 6; teschenite, sandstone xenolith, sandy ash, ash.

Day, T. Cuthbert (1932b) Large sandstone xenolith within the phonolite of Traprain Law: Edinburgh Geol. Soc. Tr. **12,** Pt. 4, 338–341. *Scotland:* 4 sandstone xenolith.

Day, T. Cuthbert (1932c) Volcanic vents at Longskelly Rocks and at Yellow Craig Plantation, west of North Berwick: Edinburgh Geol. Soc. Tr. **12,** Pt. 4, 376–381. *Scotland:* 3; mugearite, basalt.

Day, T. Cuthbert (1934) An intrusive junction between Jurassic sandstones and Tertiary granite, southeast of Dunan, Isle of Skye: Edinburgh Geol. Soc. Tr. **13,** Pt. 1, 57–60. *Scotland:* 6; granite, granite-sandstone mixture, metamorphosed sandstone.

Day, T. Cuthbert (1936) The presence of iron oxide and dolomite in the trachyte lavas on the foreshore at Weak Law: Edinburgh Geol. Soc. Tr. **13,** Pt. 3, 311–316. *Scotland:* 2 trachyte.

Drever, Harold I. (1940) The geology of Ardgour, Argyllshire: Roy. Soc. Edinburgh Tr. **60,** Pt. 1, 141–170. *Scotland:* 3; diorite-gneiss (epidiorite), sillimanite gneiss.

Drever, Harold I. and David F. Livingstone (1948) Some basaltic rocks from West Greenland: Roy. Soc. Edinburgh Proc., sec. B, **63,** Pt. 2, 97–114. *Greenland:* 3; picrite-basalt, olivine basalt, tholeiitic basalt.

Finlay, Thomas M. (1930) The Old Red Sandstone of Shetland. Part II. Northwestern area: Roy. Soc. Edinburgh Tr. **56,** Pt. 3, 671–695. *Scotland:* 3 granite.

Harris, John W. (1928) The intrusive igneous rocks of the Dundee district: Edinburgh Geol. Soc. Tr. **12,** Pt. 1, 53–68. *Scotland:* 5; oligoclase biotite porphyrite, hypersthene augite andesite, augite porphyrite, hypersthene quartz dolerite.

Harrison, John V. (1916) Notes on the geology of the East Kilsyth Hills: Geol. Soc. Glasgow Tr. **15,** Pt. 3, 315–333. *Scotland:* 1 basalt.

Holmes, Arthur (1945) The kalsilite-bearing lavas of Kabirenge and Lyakauli, southwest Uganda. Part II. Petrology: Roy. Soc. Edinburgh Tr. **61,** Pt. 2, 359–379. *Uganda:* 10; kalsilite katungite, katungite, mafurite, kalsilite ugandite, melilite mafurite, kalsilite melilite ugandite, transfused granitic xenolith, pyroxenite xenolith, biotite peridotite xenolith, glimmerite xenolith.

Holmes, Arthur (1952) The potash ankaratrite-melaleucitite lavas of Nabugando and Mbuga craters, southwest Uganda: Edinburgh Geol. Soc. Tr. **15,** 187–213. *Uganda:* 13, leucite ankaratrite, potash ankaratrite, olivine melaleucitite, melaleucitite, biotite pyroxenite.

Hutchison, Arthur G. (1933) The metamorphism of the Deeside limestone, Aberdeenshire: Roy. Soc. Edinburgh Tr. **57,** Pt. 2, 557–592. *Scotland:* 4; biotite-free hornfels, grossularite vesuvianite diopside rock (hornfels), diopside band (in hornfels), hornblende schist.

King, Basil C. (1953) Structure and igneous activity in the Creag Strollamus area of Skye: Roy. Soc. Edinburgh Tr. **62,** Pt. 2, 357–402. *Scotland:* 10; basalt, porphyritic basalt, amphibolized basalt, gabbro, acidified gabbro.

Leitch, P. Arthur and Alexander Scott (1917) Notes on the intrusive rocks of west Renfrewshire: Geol. Soc. Glasgow Tr. **16,** Pt. 2, 275–289. *Scotland:* 1 quartz keratophyre.

Lunn, James W. (1928) The intrusion of Binny Craig, West Lothian: Edinburgh Geol. Soc. Tr. **12,** Pt. 1, 74–79. *Scotland:* 1 basalt.

McCallien, William J. (1927) Preliminary account of the post-Dalradian geology of Kintyre: Geol. Soc. Glasgow Tr. **18,** Pt. 1, 40–126. *Scotland:* 6; orthophyre, trachyandesite, monchiquite, basalt.

Nockolds, Stephen R. and Robert L. Mitchell (1948) The geochemistry of some Caledonian plutonic rocks; a study in the relationship between the major and trace elements of igneous rocks and their minerals: Roy. Soc. Edinburgh Tr. **61,** Pt. 2, 533–575. *Scotland:* 4; granite, muscovite biotite adamellite, pyroxene mica diorite, porphyrite.

Pallister, John W. (1952) The Birrenswark lavas, Dumfriesshire: Edinburgh Geol. Soc. Tr. **14,** Pt. 3, 336–348. *Scotland:* 4; basalt, calcified basalt.

Patterson, Edward M. (1946) The teschenite-picrite sill of Saltcoats, Ayrshire: Geol. Soc. Glasgow Tr. **21,** Pt. 1, 1–28. *Scotland:* 2; biotite teschenite, potash lugarite.

Peacock, Martin A. (1925) A contribution to the petrography of Iceland; being a description of the MacKenzie Collection of 1810: Geol. Soc. Glasgow Tr. **17,** Pt. 2, 271–333. *Iceland:* 7; basalt, picrite-basalt, olivine trachybasalt, rhyolite, soda trachyte, palagonite rock.

Read, Herbert H. (1923) The geology of the country round Banff, Huntly and Turriff: Scotland Geol. Surv. Mem., 240 p. *Scotland:* 2; contaminated norite, hornfelsed phyllite xenolith.

Read, Herbert H. *et al.* (1926) The geology of Strath Oykell and lower Loch Shin: Scotland Geol. Surv. Mem., 220 p. *Scotland:* 11; perthosite, pulaskite, basic pulaskite, shonkinite, epidioritic rock, epidioritic hornblendite, melanite syenite, granulite, pelitic schist, weathered minette.

Read, Herbert H. (1927) The igneous and metamorphic history of Cromar, Deeside, Aberdeenshire: Roy. Soc. Edinburgh Tr. **55,** Pt. 2, 317–353. *Scotland:* 6; microaugen orthoclase oligoclase biotite gneiss, oligoclase biotite gneiss, oligoclase porphyroblast schist, granite.

Reynolds, Doris L. (1951) The geology of Slieve Gullion, Foughill and Carrickcarnan; an actualistic interpretation of a Tertiary gabbro-granophyre complex: Roy. Soc. Edinburgh Tr. **62,** Pt. 1, 85–142. *Northern Ireland:* 16; hypersthene dolerite, feldspar-phyric dolerite, hornblende granodiorite, granodiorite, adamellite, microgranite, granophyre, olivine gabbro, aplitic microgranite, porphyritic granophyre; *Republic of Ireland:* 3; olivine gabbro, quartz dolerite, olivine dolerite.

Reynolds, Doris L. (1952) Partially fused plagioclases in the rocks of Slieve Gullion: Edinburgh Geol. Soc. Tr. **15,** 280–296. *Northern Ireland:* 1 feldspar-phyric dolerite xenolith.

Richey, James E. *et al.* (1930a) The geology of Ardnamurchan, northwest Mull and Coll: Scotland Geol. Surv. Mem., 393 p. *Scotland:* 13; quartz dolerite, inninmorite-pitchstone, augite granophyre, biotite eucrite, hypersthene gabbro, gabbro, porphyritic dolerite, quartz gabbro, biotite gabbro, tonalite, quartz monzonite.

Richey, James E. *et al.* (1930b) The geology of North Ayrshire: Scotland Geol. Surv. Mem., 417 p. *Scotland:* 5; hornblende biotite granodiorite, contact-altered porphyrite, contact-altered diorite, contact-altered hypersthene quartz diorite, metamorphosed sandstone.

Robson, Douglas A. (1948) The Old Red Sandstone volcanic suite of eastern Forfarshire: Edinburgh Geol. Soc. Tr. **14,** Pt. 2, 128–140. *Scotland:* 5; olivine basalt, basalt, andesite-basalt, andesite.

Rutledge, Harold (1952) A petrological note on a composite sill. The Dasses, Arthur's Seat: Edinburgh Geol. Soc. Tr. **14,** Pt. 3, 379–388. *Scotland:* 4; basalt, olivine basalt.

Skiba, Wladyslaw (1952) The contact phenomena on the northwest of the Crossdoney complex, Co. Cavan: Edinburgh Geol. Soc. Tr. **15,** 322–345. *Republic of Ireland:* 5; amphibole biotite plagioclase hornfels, biotite hornblende diorite, porphyritic granodiorite, plagioclase biotite hornfels, hornfelso-tonalite.

Smellie, William R. (1915) The Tertiary composite sill of south Bute: Geol. Soc. Glasgow Tr. **15,** Pt. 2, 121–139. *Scotland:* 1 bostonite.

Smellie, William R. (1916) The igneous rocks of Bute: Geol. Soc. Glasgow Tr. **15,** Pt. 3, 334–373. *Scotland:* 3; mugearite, bostonite, quartz dolerite.

Swift, William H. (1952) The geology of Chishanya, Buhera district, Southern Rhodesia: Edinburgh Geol. Soc. Tr. **15,** 346–359. *Southern Rhodesia:* 11; gneissic granite, leucocratic syenite, melanocratic syenite, nepheline syenite, phonolite, melanocratic ijolite (melteigite), nepheline basalt (olivine nephelinite), carbonatite, leucocratic ijolite (urtite), ijolite.

Tomkeieff, Sergei I. (1945) Petrology of the Carboniferous igneous rocks of the Tweed basin: Edinburgh Geol. Soc. Tr. **14,** Pt. 1, 53–75. *Scotland:* 5; olivine basalt, olivine dolerite.

Tomkeieff, Sergei I. (1952a) Nepheline-basanite of Southdean, Roxburghshire: Edinburgh Geol. Soc. Tr. **14,** Pt. 3, 349–359. *Scotland:* 1 nepheline basanite.

Tomkeieff, Sergei I. (1952b) Analcite trachybasalt inclusions in the phonolite of Traprain Law: Edinburgh Geol. Soc. Tr. **15,** 360–373. *Scotland:* 1 analcite hornblende trachybasalt xenolith.

Tyrrell, George W. (1916) A contribution to the petrography of Benguella, based on a rock collection made by Professor J. W. Gregory: Roy. Soc. Edinburgh Tr. **51,** Pt. 3, 537–560. *Angola:* 2; rhyolite-tuff, shonkinite.

Tyrrell, George W. (1926a) The petrography of Jan Mayen: Roy. Soc. Edinburgh Tr. **54,** Pt. 3, 747–765. *Jan Mayen:* 7; quartz trachyte, trachyandesite, olivine trachybasalt, basanitoid olivine trachybasalt, ankaramite (ultrabasic olivine basalt), doleritic basalt; *Iceland:* 1 trachyandesite.

Tyrrell, George W. and Martin A. Peacock (1926b) The petrology of Iceland: Roy. Soc. Edinburgh Tr. **55,** Pt. 1, 51–76. *Iceland:* 2; sideromelane-tuff, palagonite rock.

Tyrrell, George W. (1928a) A further contribution to the petrography of the late Paleozoic igneous suite of the west of Scotland: Geol. Soc. Glasgow Tr. **18,** Pt. 2, 259–294. *Scotland:* 4; olivine basalt, analcite basanite, nepheline basalt, bekinkinite.

Tyrrell, George W. (1928b) The geology of Arran: Scotland Geol. Surv. Mem., 292 p. *Scotland:* 4; aplitic rock, crinanite, olivine tholeiite.

Tyrrell, George W. and Kenneth S. Sandford (1933) Geology and petrology of the dolerites of Spitsbergen: Roy. Soc. Edinburgh Proc. **53,** Pt. 3, 284–321. *Spitsbergen:* 2 quartz olivine dolerite.

Tyrrell, George W. (1948) A boring through the Lugar sill: Geol. Soc. Glasgow Tr. **21,** Pt. 2, 157–202. *Scotland:* 3; potash alkali syenite, melanocratic olivine theralite, picroteschenite.

Tyrrell, George W. (1949) Petrography of igneous rocks from the Vatnajökull region, Iceland, collected by Mr. F. W. Anderson: Roy. Soc. Edinburgh Tr. **61,** Pt. 3, 793–801. *Iceland:* 8; basalt, olivine gabbro, bytownite gabbro (eucrite), gabbro-peridotite, albite granophyre, magnetite granite.

Walker, Frederick (1925) Four granitic intrusions in southeastern Scotland: Edinburgh Geol. Soc. Tr. **11,** Pt. 3, 357–365. *Scotland:* 2; porphyritic biotite hornblende granodiorite, augite biotite quartz diorite.

Walker, Frederick (1927) The igneous geology of Ardsheal Hill, Argyllshire: Roy. Soc. Edinburgh Tr. **55,** Pt. 1, 147–157. *Scotland:* 3; orthoclase olivine basalt, appinite, hornblende porphyrite.

Walker, Frederick and J. Irving (1928) The igneous intrusions between St. Andrews and Loch Leven: Roy. Soc. Edinburgh Tr. **56,** Pt. 1, 1–17. *Scotland:* 2; analcitized quartz dolerite, teschenite.

Walker, Frederick (1931) The dolerite isles of the North Minch: Roy. Soc. Edinburgh Tr. **56,** Pt. 3, 753–766. *Scotland:* 2; olivine dolerite, pegmatite.

Walker, Frederick (1932) Differentiation in the sills of northern Trotternish (Skye): Roy. Soc. Edinburgh Tr. **57,** Pt. 1, 241–257. *Scotland:* 4; olivine dolerite, picrite, teschenite.

Walker, Frederick (1936a) The geology of the Isle of May: Edinburgh Geol. Soc. Tr. **13,** Pt. 3, 275–285. *Scotland:* 1 teschenite.

Walker, Frederick and Charles F. Davidson (1936b) A contribution to the geology of the Faeroes: Roy. Soc. Edinburgh Tr. **58,** Pt. 3, 869–897. *Faeroe Islands:* 3; basalt, olivine dolerite, ultramafic olivine basalt.

Walker, Frederick (1952) Differentiation in a quartz-dolerite sill at Northfield quarry, Stirlingshire: Edinburgh Geol. Soc. Tr. **15,** 393–405. *Scotland:* 5; felsite, granophyric dolerite, dolerite.

Geographic Index

The localities of the igneous and metamorphic rocks for which chemical analyses are published in the Scottish scientific periodical and serial literature between 1914 and 1953 are listed below alphabetically by country and in the case of Scotland by county. For each country and county the appropriate author and year of publication cited in the bibliography are given, as well as the total number of analyses for that country or county.

ANGOLA 2
Tyrrell 1916
FAEROE ISLANDS 3
Walker and Davidson 1936b
GREENLAND 3
Drever and Livingstone 1948
ICELAND 18
Peacock 1925
Tyrrell 1926a, 1949
Tyrrell and Peacock 1926b
IRELAND, REPUBLIC OF 8
Reynolds 1951
Skiba 1952
JAN MAYEN 7
Tyrrell 1926a
NORTHERN IRELAND 17
Reynolds 1951, 1952
SCOTLAND 303
ABERDEEN 19
Bisset 1934a, 1934b
SCOTLAND—*contd.*
Hutchison 1933
Read 1923, 1927
ANGUS 5
Robson 1948
ARGYLL 39
Anderson and Tyrrell 1936
Bailey 1916
Drever 1940
McCallien 1927
Richey 1930a
Walker 1927
AYR 14
Patterson 1946
Richey 1930b
Tyrrell 1928a, 1948
BERWICK 1
Tomkeieff 1945
BUTE 15
Brown 1929

SCOTLAND—*contd.*
Buist 1952
Smellie 1915, 1916
Tyrrell 1928b
DUMFRIES 4
Pallister 1952
EAST LOTHIAN 61
Day 1925, 1928a, 1928d, 1930a, 1930b, 1930c, 1930e, 1930f, 1930g, 1930h, 1932a, 1932b, 1932c, 1936
Day and Bailey 1928c
Tomkeieff 1952b
Walker 1925
FIFE 31
Allan 1924
Campbell, Day and Stenhouse 1932, 1934
Davies 1936
Day 1928b
Day and Stenhouse 1930d
Walker 1936a
Walker and Irving 1928
FORFAR see ANGUS
HADDINGTON see EAST LOTHIAN
INVERNESS 51
Anderson 1935
Bailey 1916
Cockburn 1935
Davidson 1935, 1943
Day 1934
King 1953
Nockolds and Mitchell 1948
Walker 1931, 1932
KIRKCUDBRIGHT 1
Nockolds and Mitchell 1948
SCOTLAND—*contd.*
MIDLOTHIAN 28
Campbell and Lunn 1927
Clark 1952
Cockburn 1952
Day 1923, 1928b, 1930a
Rutledge 1952
PEEBLES 1
Cockburn 1952
PERTH 6
Harris 1928
Nockolds and Mitchell 1948
RENFREW 1
Leitch and Scott 1917
ROSS AND CROMARTY 4
Read 1926
ROXBURGH 5
Tomkeieff 1945, 1952a
SHETLAND 3
Finlay 1930
STIRLING 6
Harrison 1916
Walker 1952
SUTHERLAND 7
Read 1926
WEST LOTHIAN 1
Lunn 1928
SOUTHERN RHODESIA 11
Swift 1952
SPITSBERGEN 2
Tyrrell and Sandford 1933
UGANDA 23
Holmes 1945, 1952

Rock Name Index

Adamellite
muscovite biotite — Reynolds 1951
Alsbachite (?) — Nockolds and Mitchell 1948
Andesite — Bailey 1916
hornblende — Robson 1948
hypersthene augite — Bailey 1916
pyroxene — Harris 1928
Andesite–basalt — Bailey 1916
Ankaramite — Robson 1948
Ankaratrite — Tyrrell 1926a
leucite
potash — Holmes 1952
Anorthosite–gneiss — Holmes 1952
saussuritized — Davidson 1943
Aplitic rock — Davidson 1943
Appinite — Tyrrell 1928b
Ash — Walker 1927
sandy — Day 1932a
Day 1932a

Banakite, quartz	Day 1930f
Banatite–porphyrite	Bailey 1916
Basalt	Allan 1924; Campbell and Lunn 1927; Campbell, Day and Stenhouse 1932; Cockburn 1935; Day 1928a, 1928d, 1930b, 1930h, 1932c; Harrison 1916; King 1953; Lunn 1928; McCallien 1927; Pallister 1952; Peacock 1925; Robson 1948; Rutledge 1952; Tyrrell 1949; Walker and Davidson 1936b.
amphibolized	King 1953
analcite-bearing	Davies 1936
andesite-	Robson 1948
calcified	Pallister 1952
doleritic	Tyrrell 1926a
microporphyritic	Clark 1952
monchiquitic	Day 1930h
nepheline	Tyrrell 1928a; Swift 1952
olivine	Campbell, Day and Stenhouse 1932; Day and Stenhouse 1930d; Drever and Livingstone 1948; Robson 1948; Rutledge 1952; Tomkeieff 1945; Tyrrell 1928a; Walker and Davidson 1936b
orthoclase olivine	Walker 1927
picrite	Drever and Livingstone 1948; Peacock 1925
porphyritic	King 1953
tholeiitic	Drever and Livingstone 1948
ultrabasic olivine	Tyrrell 1926a
ultramafic olivine	Walker and Davidson 1936b
Basanite	
analcite	Tyrrell 1928a
nepheline	Day and Bailey 1928c; Tomkeieff 1952
Bekinkinite	Tyrrell 1928a
Bostonite	Smellie 1915, 1916
Carbonatite	Swift 1952
Crinanite	Tyrrell 1928b
Diopside band (in hornfels)	Hutchinson 1933
Diorite	
augite biotite quartz	Walker 1925
biotite hornblende	Skiba 1952
contact-altered	Richey 1930b
contact-altered hypersthene quartz	Richey 1930b
pyroxene mica	Nockolds and Mitchell 1948
quartz	Anderson 1935
quartz biotite	Bisset 1934a
Diorite-gneiss	Drever 1940
Dioritic xenolith	Bisset 1934a
Dolerite	Buist 1952; Campbell, Day and Stenhouse 1932; Cockburn 1935; Day 1923, 1930a; Walker 1952
andesine	Cockburn 1952
analcitized quartz	Walker and Irving 1928
feldspar–phyric	Reynolds 1951
granophyric	Walker 1952
hypersthene	Reynolds 1951
hypersthene quartz	Harris 1928
olivine	Allan 1924; Cockburn 1935, 1952; Reynolds 1951; Tomkeieff 1945; Walker 1931, 1932; Walker and Davidson 1936b

olivine-bearing	Buist 1952
porphyritic	Richey 1930a
quartz	Brown 1929; Day 1928b; Reynolds 1951; Richey 1930a; Smellie 1916
quartz olivine	Tyrrell and Sandford 1933
Dolerite xenolith,	Reynolds 1952
feldspar-phyric	
Dolerite–pegmatite	
chloritized	Campbell, Day and Stenhouse 1932
chlorophaeite	Campbell, Day and Stenhouse 1932
Eclogite	Davidson 1943
Edenite bronzite olivine rock	Davidson 1943
Epidiorite	Drever 1940
Epidioritic rock	Read 1926
Essexite	Day 1930h
Eucrite	Cockburn 1935; Tyrrell 1949
biotite	Richey 1930a
Felsite	Walker 1952
Gabbro	Cockburn 1935; King 1953; Richey 1930a
acidified	King 1953
biotite	Richey 1930a
bytownite	Tyrrell 1949
hypersthene	Richey 1930a
olivine	Reynolds 1951; Tyrrell 1949
quartz	Richey 1930a
Gabbro–peridotite	Tyrrell 1949
Glimmerite xenolith	Holmes 1945
Gneiss	
anorthosite-	Davidson 1943
diorite-	Drever 1940
edenite saxonite-	Davidson 1943
microaugen orthoclase oligoclase biotite	Read 1927
oligoclase biotite	Read 1927
saussuritized anorthosite-	Davidson 1943
sillimanite	Drever 1940
Granite	Anderson and Tyrrell 1936; Day 1934; Finlay 1930; Nockolds and Mitchell 1948; Read 1927
aplitic micro-	Reynolds 1951
gneissic	Swift 1952
magnetite	Tyrrell 1949
micro-	Reynolds 1951
porphyritic	Anderson 1935; Bisset 1934a
Granite–sandstone mixture	Day 1934
Granitic xenolith, transfused	Holmes 1945
Granodiorite	Anderson 1935; Reynolds 1951
hornblende	Reynolds 1951
hornblende biotite	Richey 1930b
porphyritic	Skiba 1952
porphyritic biotite hornblende	Walker 1925
Granophyre	Cockburn 1935; Reynolds 1951
albite	Tyrrell 1949
augite	Richey 1930a
porphyritic	Reynolds 1951
riebeckite	Davidson 1935

Granulite	Read 1926
biotite andesine	Davidson 1943
Grossularite vesuvianite diopside rock	Hutchison 1933
Hornblendite, epidioritic	Read 1926
Hornfels	Day 1923; Hutchinson 1933
amphibole biotite plagioclase	Skiba 1952
biotite-free	Hutchison 1933
plagioclase biotite	Skiba 1952
Ijolite	Swift 1952
leucocratic	Swift 1952
melanocratic	Swift 1952
Inninmorite–pitchstone	Richey 1930a
Katungite	Holmes 1945
kalsilite	Holmes 1945
Keratophyre, quartz	Leitch and Scott 1917
Kersantite, acid	Bisset 1934b
Lamprophyre, spessartite (?)-	Bisset 1934b
Lugarite, potash	Patterson 1946
Mafurite	Holmes 1945
melilite	Holmes 1945
Malchite, hornblende augite	Bailey 1916
Melaleucitite	Holmes 1952
olivine	Holmes 1952
Melteigite	Swift 1952
Metamorphosed limestone	Bailey 1916; Day and Stenhouse 1930d
Metamorphosed dolomitic limestone	Davidson 1943
Metamorphosed sandstone	Day 1934; Richey 1930b
Microgranite	Reynolds 1951
aplitic	Reynolds 1951
Microsyenite	Campbell, Day and Stenhouse 1932
Minette, weathered	Read 1926
Monchiquite	Day 1925, 1928a; McCallien 1927
Monzonite	Bailey 1916
quartz	Richey 1930a
Mugearite	Day 1930h, 1932c; Smellie 1916
Nephelinite, olivine	Swift 1952
Norite, contaminated	Read 1923
Odinite	Bisset 1934b
Orthophyre	McCallien 1927
Palagonite rock	Peacock 1925; Tyrrell and Peacock 1926b
Pegmatite	Walker 1931
chloritized dolerite-	Campbell, Day and Stenhouse 1932
chlorophaeite dolerite-	Campbell, Day and Stenhouse 1932
Peridotite	Davidson 1935
biotite (xenolith)	Holmes 1945
gabbro-	Tyrrell 1949
Perthosite	Read 1926
Phonolite	Day 1930c, 1930e; Swift 1952
Picrite	Day and Stenhouse 1930d; Walker 1932
Picrite-basalt	Drever and Livingstone 1948; Peacock 1925
Picroteschenite	Campbell, Day and Stenhouse 1934; Tyrrell 1948
Pitchstone	Cockburn 1935
andesitic	Davidson 1935
inninmorite-	Richey 1930a

Pitchstone porphyry	Buist 1952
Porphyrite	Nockolds and Mitchell 1948
augite	Harris 1928
banatite-	Bailey 1916
biotite hornblende	Bailey 1916
contact-altered	Richey 1930b
hornblende	Bailey 1916; Walker 1927
oligoclase biotite	Harris 1928
Porphyry	
pitchstone	Buist 1952
quartz	Bailey 1916
Pulaskite	Read 1926
basic	Read 1926
Pyroxenite, biotite	Holmes 1952
Pyroxenite xenolith	Holmes 1945
Quartzite	Day 1928b
Rhyolite	Bailey 1916; Peacock 1925
Rhyolite-tuff	Tyrrell 1916
Sandstone xenolith	Day 1930e; 1932a; 1932b
Saxonite–gneiss, edenite	Davidson 1943
Schist	
hornblende	Hutchison 1933
oligoclase porphyroblast	Read 1927
pelitic	Read 1926
Segregation vein	Day 1928b
Shale xenolith	Day 1930e
Shonkinite	Read 1926; Tyrrell 1916
Sideromelane-tuff	Tyrrell and Peacock 1926b
Spessartite (?)-lamprophyre	Bisset 1934b
Syenite	
leucocratic	Swift 1952
melanite	Read 1926
melanocratic	Swift 1952
micro-	Campbell, Day and Stenhouse 1932
nepheline	Swift 1952
potash alkali	Tyrrell 1948
Teschenite	Campbell, Day and Stenhouse 1932, 1934; Davies 1936; Day and Stenhouse 1930d; Day 1930g, 1930h, 1932a; Walker and Irving 1928; Walker 1932, 1936a
biotite	Patterson 1946
gabbroid	Davidson 1935
hornblende	Campbell, Day and Stenhouse 1932
Theralite, melanocratic olivine	Tyrrell 1948
Tholeiite	Campbell and Lunn 1927
olivine	Brown 1929; Tyrrell 1928b
Tonalite	Richey 1930a
hornfels	Skiba 1952
Trachyandesite	McCallien 1927; Tyrrell 1926a
Trachybasalt	Day 1930f
analcite hornblende (xenolith)	Tomkieff 1952b
basanitoid olivine	Tyrrell 1926a
olivine	Peacock 1925; Tyrrell 1926a

Trachyte	Day 1930h, 1936
quartz	Tyrrell 1926a
soda	Peacock 1925
Trap, white	Day 1930a, 1930h
Tuff	
rhyolite-	Tyrrell 1916
sideromelane-	Tyrrell and Peacock 1926b
Ugandite	
kalsilite	Holmes 1945
kalsilite melilite	Holmes 1945
Urtite	Swift 1952
White trap	Day 1930a, 1930h
Xenolith	
analcite hornblende trachybasalt	Tomkeieff 1952b
biotite peridotite	Holmes 1945
dioritic	Bisset 1934a
feldspar–phyric dolerite	Reynolds 1952
glimmerite	Holmes 1945
hornfelsed phyllite	Read 1923
pyroxenite	Holmes 1945
sandstone	Day 1930e, 1932a, 1932b
shale	Day 1930e
transfused granitic	Holmes 1945

List of Published Parts of the Series

Marjorie Hooker (1956) Data of rock analyses: African periodical and serial literature, Part I. *Geochim. et Cosmochim. Acta* **9,**

Marjorie Hooker (1956) Data of rock analyses: Bibliography and index of rock analyses in the African periodical and serial literature, Part II. *Geochim. et Cosmochim. Acta* **9,** 190–213, Supp., **11,** Nos. 1–2, 138.

Marjorie Hooker (1957) Data of rock analyses: New Zealand periodical and serial literature. Bibliography and index of rock analyses, Part III. *Geochim. et Cosmochim. Acta* **11,** 130–138.

Marjorie Hooker (1958) Data of rock analyses: Icelandic periodical and serial literature. Bibliography of rock analyses, Part IV. *Geochim. et Cosmochim. Acta* **15,** 30–31.

Marjorie Hooker (1959) Data of rock analyses: Australian periodical and serial literature. Bibliography and index of rock analyses, Part V. *Geochim. et Cosmochim. Acta* **15,** No., 342–369.

Geochimica et Cosmochimica Acta, 1959, Vol. 17, pp. 148 to 156. Pergamon Press Ltd. Printed in Northern Ireland.

LETTERS TO THE EDITOR

Synthesis of häggite

In a recent paper (Pommer, 1957) I reported the synthesis of a new hydrated tervalent–quadrivalent mixed vanadium oxide mineral by reduction of a quinquevalent vanadium solution by wood at 150°C at pH 2. This mineral from a natural occurrence, has now been named häggite by Evans and Mrose (1958).

U.S. Geological Survey
Washington 25, D.C.

A. M. Pommer

References

Evans H. T., Jr. and Mrose M. E. (1958) The crystal structure of three new vanadium oxides. *Acta Cryst.* **11**, 56–57.

Pommer A. M. (1957) Reduction of quinquevalent vanadium solutions by wood or lignite. *Geochim. et Cosmochim. Acta* **13**, 26.

Cosmogenic potassium-40 in iron meteorites

The radioactivity of potassium isolated from three samples of iron meteorite has been measured using a low-level β-counter. In addition to the normal activity of potassium-40, an excess corresponding to 1–3 . 10^{-10}g K^{40}/g was expected due to cosmic ray bombardment.

A number of investigators have reported so-called cosmogenic stable and radioactive nuclides in meteorites. The spallation cross-section of iron for the production of K^{40} is appreciable in in the BeV region (up to 10 mbarns). Thus we expect that meteorites having a high content of He^3 (5.10^{-6}cm^3/g, for example) should contain perhaps 3.10^{-10}g K^{40}/g. The natural potassium content of iron meteorites is quite low, often less than 0·1 p.p.m. (Stoenner and Zaehringer, 1958). Thus cosmogenic K^{40} should greatly exceed the natural K^{40} in such meteorites, if the isotopic composition is the same as terrestrial (Suess, 1938; Schumb *et al.*, 1941; Nier, 1950). This situation favours the determination of excess K^{40}, even if some contamination of natural potassium occurs in chemical processing.

This experiment was performed in connexion with a separation of other cosmogenic radioactive nuclides, Be^{10}, Al^{26} and Mn^{53}, at this laboratory (Shedlovsky, 1959). The samples were originally dissolved in aqua regia. In one case (Grant) 1 mg of purified caesium carrier was added along with the other carriers. Iron, cobalt, copper and other elements were removed by ether extraction and anion exchange with 1 l. column of a Dowex 1 in the chloride form using 9 M hydrochloric acid sample solution. After concentration, to about 500 cm^3 the solutions were neutralized with ammonia in the presence of hydrogen peroxide to collect the above nuclides with their carriers.

The filtrates, which were supplied to the writer, contained about 3 moles of ammonium chloride and 0·7 moles of nickel-ammine chloride from each 500 g of original sample. The solution was diluted to 3 l. and was passed through 2 l. of a Dowex 50 column in the ammonium form. The eluent for potassium and caesium was 6 l. of ammoniacal 1 M ammonium acetate solution (Honda, 1955). The effluents were evaporated and both elements were precipitated with tetraphenylborate in the presence of EDTA (Sporek, 1956; Schall, 1957). The final separation of alkaline metals was made by cation exchange using 10 cm^3 of a Dowex 50 column in the hydrogen form and 1 M hydrochloric acid as the eluent. Chemical yield for the Grant meteorite was estimated from the caesium recovery. Most of the potassium found must have

been due to laboratory contamination. After first counting, the samples were dissolved in acetone–water mixture and passed through 10 cm^3 of the cation exchange column.

Copper sulphide and iron hydroxide scavengings were performed with potassium fraction of 1 M hydrochloric acid effluents. Finally the tetraphenylborate was recovered as the recycle sample. The sample, $KB(C_6H_5)_4$, was counted in about 30 per cent geometry in a thin walled cylindrical low level β-counter (SUGIHARA *et al.*, 1953). Counter background was 0·17 counts/min during this work. The amount of excess potassium activity was estimated by comparison with a laboratory potassium sample of the same size (Table 1). The counting data are tabulated

Table 1. Potassium-40 activity in iron meteorites

Sample name*	Weight treated (g)	Weight of potassium collected (mg)	Weight of potassium counted (mg)	Net counting rate (counts/min)	Specific activity of potassium (counts/min per mg)	Excess† K^{40} in meteorite (disintegration/min/kg of meteorite)
Grant	460	1·58	1·53	1·20 ± 0·04	0·78 ± 0·03	4·9 ± 0·5
recycle			1·33	0·99 ± 0·07	0·74 ± 0·05	4·3 ± 0·8
Williamstown	170	1·08	1·02	0·69 ± 0·03	0·68 ± 0·03	6·4 ± 1·0
recycle			0·57	0·33 ± 0·02	0·58 ± 0·04	3·5 ± 1·2
Odessa	1100	5·56	4·29	2·43 ± 0·10	0·57 ± 0·02	2·4 ± 0·7
Reagent $KB(C_6H_5)_4$			1·96	0·90 ± 0·04	0·46 ± 0·02	—
Reagent $KB(C_6H_5)_4$			1·11	0·53 ± 0·02	0·48 ± 0·02	—

* Detailed description of the samples will be made in another paper (SHEDLOVSKY, 1959). The He^3 content of Grant is given as 6.10^{-6} cm^3/g by HOFFMAN and NIER (1958); that of Williamstown is the same according to unpublished work by other investigators.

† Chemical yield: 85 per cent for Grant; assumed as 80 per cent for others.

in counts/min above background. The data were consistent with our expectations.

The high contamination observed in these experiments can certainly be reduced. By using smaller samples and a simpler chemical procedure, we have already reduced it to 2 p.p.m. K. Mass spectrometric methods should be superior for this sort of measurement and Dr. G. J. WASSERBURG has undertaken to make such measurements on our samples.

The half-life of K^{40} falls in an especially interesting range for the study of past variations of cosmic radiation intensity and of bombardment time in space. By comparison with the stable nuclides and radioactive species of relatively short half-life much useful information should be obtained.

Acknowledgement—The writer wishes to thank Professor J. R. ARNOLD for instruction and encouragement throughout this work and Mr. J. SHEDLOVSKY for collaboration in these experiments. This research was supported by the Office of Ordnance Research, U.S. Army.

Note added in proof—Dr. WASSERBURG has reported that the ratios of K^{40} to K^{41} and K^{39} in our Grant and Williamstown samples are higher than in reagent potassium by factors of 1·36 and 1·17 respectively, in agreement with the above results.

MASATAKE HONDA

School of Science and Engineering
University of California
La Jolla, California

REFERENCES

HOFFMAN J. H. and NIER A. O. (1958) Production of helium in iron meteorites by the action of cosmic rays. *Phys. Rev.* **112,** 2112.

HONDA M. (1955) Ion-exchange separation of transition elements. *Japan Analyst* **4,** 384

Nier A. O. (1950) A redetermination of the relative abundances of the isotopes of carbon, nitrogen, argon and potassium. *Phys. Rev.* **77**, 789.

Schall E. D. (1957) Volumetric determination of potassium. *Analyt. Chem.* **29**, 1044.

Schumb W. C., Evans R. D. and Leaders W. M. (1941) Radioactive determination of the relative abundance of the isotope K^{40} in terrestrial and meteoritic potassium. *J. Amer. Chem. Soc.* **63**, 1203.

Shedlovsky J. (1959) Thesis. To be published.

Stoker K. F. (1956) Gravimetric determination of potassium in sea water as potassium tetraphenylboron salt. *Analyst* **81**, 540.

Stoffner R. W. and Zähringer J. (1958) Potassium-argon age of iron meteorites. *Geochim. et Cosmochim. Acta* **15**, 40.

Suess H. (1938) Remarks on the meteorite problem: The radioactivity of potassium as a means to determination of the relative ages of the elements. *Naturwissenschaften* **26**, 411.

Suess H. (1939) The radioactivity of potassium as a means for determination of the relative age of elements in meteorites. *Naturwissenschaften* **27**, 702.

Sugihara T. T., Wolfgang R. L. and Libby W. F. (1953) Large thin wall Geiger counter. *Rev. Sci. Instrum.* **24**, 511.

Moldavites and similar tektites from Georgia, U.S.A.

Recently evidence has been uncovered by Barnes and Bruce (1959) that indicates conclusively that tektites are found in Dodge County and Irwin County, Georgia. Two tektites were purchased by the U.S. National Museum in 1938 which were found in the northern part of Dodge County near Empire, Georgia (Henderson, 1957). The writer earlier examined these specimens and stated "both these tektites are flattened ellipsoids similar in form and color to

Table 1. Some physical constants of selected tektites

Tektite	Locality	Density	N_D	Magnetic susceptibility ($\times 10^{-6}$ e.m.u./g)	Fe^{2+} band maximum (cm^{-1})
Moldavite	Lhenice, Bohemia*	2·343*	1·487*		8·11†
Moldavites	Bohemia	2·3348‡, 2·3985‡, 2·3733 (20°C)‡		2·3, 3·0§	
	Vrabsi (U.S. Museum No. 54096)	2·349‡			
	Moldavia (U.S. Museum No. 86240)	2·381‡			
Tektites	Georgia (U.S. Museum No. 1396‡§)	2·33–2·36**	1·482–1·485**	3·6§	8·40†
Bediasites	Texas	2·397*, 2·357*	1·502*, 1·492*	4·2, 5·0, 5·2	
			1·49065 (26·5°C)†	5·4, 5·4, 6·5§	11·11†
Australites	Nullarbor Plain‡ Western Australia	2·4549‡, 2·4477 (20°C)‡	1·50855 (27·2°C)†	5·8, 5·9, 6·0 6·2, 6·9§	18·33†

* Barnes (1940).
† Cohen (1958).
‡ Hammond (1950).
§ Senftle and Thorpe (1959).
** Henderson (1959).

some moldavites" (Cohen, 1958). The absorption spectrum was found to be similar to moldavites, and the ferrous band had an absorption coefficient of 8·40 cm^{-1} compared to 8·11 cm^{-1} for a moldavite (Cohen, 1958). Thin-section examination of the Georgia tektite showed the same inhomogeneities and lechatelierite inclusions as found in moldavites. The writer then stated, "One is inclined to regard the Empire, Georgia, tektites as moldavites until concrete evidence of their locality and the stratum in which they are found is forthcoming" (Cohen, 1958). Since the above statement was made, Barnes and Bruce (1959) by diligent search have

unearthed evidence that eight tektites have been found in two areas in Georgia separated by about 50 miles. One from Irwin County weighs 17·797 g (Furcron, 1959). Henderson (1959) has recently measured the density and index of refraction of two specimens and finds that the former ranges between 2·33 and 2·36, while the latter ranges between 1·482 and 1·485.

The published densities and indices of refraction of several tektites are given in Table 1. Upon examination of this table one concludes that the Georgia tektites are quite similar to moldavites in density, index of refraction, magnetic susceptibility, and ferrous iron content, in addition to shape, internal structure, external texture and appearance. The ferrous content, of course, determines the intensity of the green colour seen in the glasses in transmitted light. Then, upon comparing the Georgia tektites with the Texas tektites, one finds that the agreement

Table 2. Emission analyses of minor constituents in selected tektites (p.p.m.)
(absolute values one-half to twice the stated values)

Metal	Moldavite*	Moldavite†	Georgia Tektite‡	Bediasite§	Australite**
Ag	<1	<1	<1	<1	<1
Co	8	8	10	10	10
Cr	30	30	30	40	165
Li	650	650	65	100	650
Mn	650	650	650	650	650
Ni	10	20	10	20	30
Rb	900	1000	600	500	800
Sr	550	550	550	550	550
Ti	>1000	>1000	>1000	>1000	>1000
V	20	20	30	40	50
Zr	550	550	550	550	550

* Obtained from H. H. Nininger.
† Courtesy, Dr. P. C. Zwaan, Rijksmuseum van Geologie en Mineralogie, Leiden, Holland.
‡ Courtesy, E. P. Henderson.
§ Courtesy, V. E. Barnes.
** Courtesy of T. P. Kohman, Carnegie Institute of Technology; composite of two specimens.

is still fairly good. The indices of refraction and magnetic susceptibilities of bediasites are, in general, slightly higher, which is indicative of the slightly higher iron content. The australites differ markedly from the moldavites and Georgia tektites listed, having higher densities, index of refraction, and ferrous iron content and, thus, are more deeply coloured. The magnetic susceptibility values, however, are similar to the bediasites and Barnes (1940) has shown overlap of indexes of refraction and density.

At this juncture it is desirable to compare the trace impurity contents of these four materials. Table 2 contains comparative emission analyses of the trace impurity contents of two moldavites, a Georgia tektite, a bediasite, and an australite. It is to be noted that the two moldavites, although obtained from different sources, give very close comparative analyses, indicating both the precision of the work and the similarity of the trace impurity contents of moldavites. The elements showing the greatest variation among the samples tested are chromium, lithium, nickel, rubidium and vanadium. If one intercompares these elements, it is found that the Georgia tektites are somewhat closer to bediasites than moldavites, while the australite is much higher in chromium and slightly higher in nickel and in vanadium than the other tektites.

Let us now consider the strata in which these materials are found:

The australites are apparently the most recent tektites, being found on the desert surface still containing delicate surface features absent in all other tektites and are dated by the K-A method, as $0{\cdot}8 \pm 0{\cdot}2 \times 10^6$ years (Reynolds and Ford). *They cover a large portion of the Australian continent.*

The moldavites are found in two areas in Czechoslovakia (Moravia and Bohemia). In one area they are found in quartz gravels of an ancient river system, from 50 to 100 m above the present flood plain (Barnes, 1940). Janoschek (Barnes, 1940) considers that the moldavites are middle Miocene in age. Ehmann and Kohman (1958) give age limits for time of fall of moldavites, based on the Al^{26} activity level, as $>0{\cdot}8 \times 10^6$ years and Be^{10} level as $>3 \times 10^6$ years.

The Georgia tektites are found on the surface and in stream deposits on the Hawthorn formation (Cooke, 1943) which is 300 ft thick in Georgia. This formation is of middle or lower Miocene age and extends into Florida (Cooke and Mossom, 1929).

The bediasites of Texas, according to Barnes (1940), are in gravel-bearing soil *overlying* rocks of Eocene age. The Al^{26} activity level gives an age limit of $>1{\cdot}2 \times 10^6$ years for bediasites (Ehmann and Kohman, 1958).

It is impossible to determine from known geological considerations whether the moldavites, Georgia tektites and bediasites are *one and the same* widespread tektite fall of hemispheric proportions and not enough dating work has as yet been done for definite conclusions to be reached. However, trace analyses and physical properties indicate that there is a close similarity among these three local finds with the ferrous iron contents and physical features indicating closer similarity between moldavites and Georgia tektites. One may seriously consider that tektite falls other than the Australian one are very widespread in distribution. As new discoveries of locale and possibly geological strata are brought to light, intercomparisons with earlier finds are increasingly necessary. Of course, widespread distribution would greatly strengthen the postulate for a lunar origin of tektites. While the great bulk of igneous rocks do not compare with tektites in composition, there are igneous compositions that do (Barnes, 1940 and Mason, 1959); and one would be too hasty to conclude that tektites *must* come from melting of sedimentary or metamorphic materials.

Acknowledgements—The writer desires to acknowledge the emission analyses of Mr. E. R. Shuster, Jr. of the Physicochemical Section of this Laboratory and the personal communications from V. E. Barnes of The University of Texas, A. S. Furcron of the Department of Mines, Mining and Geology of Georgia, and E. P. Henderson of the U.S. National Museum. F. E. Senftle of the U.S. Geological Survey and A. Thorpe of Howard University are thanked for allowing me to quote from their manuscript containing the magnetic susceptibility data.

A. J. Cohen*

Mellon Institute
Pittsburgh 13, *Pennsylvania*

References

Barnes V. E. (1940) North American tektites. *Univ. Texas Publ.* No. 3945, 477.

Barnes V. E. and Bruce G. A. (1959) Tektites in Georgia. *GeoTimes* **3**, No. 7, 18; and Personal communication.

Cohen A. J. (1958) The absorption spectra of tektites and other natural glasses. *Geochim. et Cosmochim. Acta* **14**, 279.

Cooke C. W. (1943) Geology of coastal plain of Georgia. *U.S. Geol. Survey.* Bull. 941.

Cooke C. W. and Mossom S. (1929) Geology of Florida. *Twentieth Annual Report of the Florida State Geological Survey* p. 77.

Ehmann W. D. and Kohman T. P. (1958) Cosmic-ray-induced radioactivities in meteorites—II Al^{26}, Be^{10}, Co^{60}, aerolites, siderites and tektites. *Geochim. et Cosmochim. Acta* **14**, 364.

Furcron A. S. (1959) Personal communication.

Hammond C. R. (1950) The chemical composition and some physical characteristics of tektites. *Contr. Meteorit. Soc.: Pop. Astr.* **58**, 345.

Henderson E. P. (1957) Personal communication.

Henderson E. P. (1959) Personal communication.

* Pittsburgh Plate Glass Company Project.

Mason B. (1949) Chemical composition of tektites. *Nature, Lond.* **183**, 254.
Reynolds J. H. and Ford G. C. (1959) *Bull. Amer. Phys. Soc.* **4**, 140, Paper D3.
Senftle F. E. and Thorpe A. (1959) Magnetic susceptibility of tektites and some terrestrial glasses. *Geochim. et Cosmochim. Acta.* In press.

Age of the Fen carbonatite (Norway) and its relation to the intrusives of the Oslo Region*

The Fen area covers only a little more than 3 miles^2 of the province of Telemark in southern Norway, about 70 miles south-west of Oslo. For centuries it was an iron mining centre, but in modern times the area has attracted much attention from geologists largely as a result of the now classic work of Brøgger (1921) who studied and described the remarkable series of carbonatites and alkalic rocks that compose the area. More recently, the discovery and development of niobium deposits in the carbonatite near Søve (Bjørlykke, 1955) again focused attention on this spot. A comparison of many carbonatites throughout the world is given in a review by Pecora (1956), in which the Fen area is listed as No. 1.

Brøgger originally thought that the carbonatites at Fen were the product of magmatic crystallization and that the invading magma was enriched in carbonate by digesting limestone. He mapped several massive limestones in the Oslo region. Some recent students of the Fen area believe that the carbonatites are a product of extensive contact metamorphism of limestones by intrusives of the Oslo region (Svinndal, written communication; Bjørlykke, 1955). Others postulate magmatic processes as dominant genetic factors (Sæther, 1948, 1950, 1957). Tomkeieff (1958) is of the opinion that the Fen rocks are differentiates of the basic magma of the Oslo intrusives. The distance from the Fen area to the nearest boundary of the Oslo region is only about 8 miles. Of the recent authors, only Sæther does not assume any necessary connexion between the intrusives of Fen and the rocks of the Oslo region.

The concept of the Fen area as a contemporary outlier was first formulated by Goldschmidt (see Brøgger, 1921) and was followed by Brøgger for a long time. However, he gradually became convinced that the Fen rocks could not be comagmatic with the Oslo intrusives and that they must represent an altogether separate intrusive event, probably older than the Oslo rocks. He wrote:

> Erst während des Druckens der Abhandlung wurde es mir aber nach und nach einleuchtend, dass die Auffassung des Fengebietes als ein 'outlier' des postsilurischen Kristianiagebietes weniger wahrscheinlich ist, und *ich habe schliesslich die Annahme eines jotnischen oder eokambrischen Alters desselben mehr berechtigt gefunden.*

(Brøgger, 1921, p.x). It is with pleasure that the present writers report that Brøgger's inspired estimate of the age of the Fen carbonatite essentially agrees with the results of the present measurements.

The first confirmation came from Sæther (1957), although the methods available to him were only semiquantitative. Using the Geiger–Müller counter, optical spectrograph and dithizone colorimetry, Sæther made preliminary measurements of the Th/Pb age of columbite, koppite and zircon from the Fen area. He concludes that the probable age of these minerals is 400–600 million years.

We have now made K/Ar age measurements on large (1 cm) euhedral biotite crystals from the Søve mine in the Fen area and on impure biotite from the granite of Drammen in the Oslo region. We have also measured isotopic U/Pb on zircon from the Oslo nordmarkite. The Søve biotite is clear, unaltered and free of inclusions, and thus ideally suited for reliable age determination, but the material currently available to us from the Oslo rocks is partly chloritized and hence not as good as it could be. Nevertheless, our results show clearly that the Fen rocks are very much older than the Oslo intrusives and could not be temporally related to them.

---

* Publication authorized by the Director, U.S. Geological Survey.

Table 1. Age of rocks from the Fen area and the Oslo region.
(Ages are calculated with the constants quoted by ALDRICH *et al.*, 1958)

Rock	K/Ar age (million years)	U^{238}/Pb^{206} age (million years)	Th^{232}/U^{208} age (million years)
Biotite from the carbonatite, Søve mine, Fen area, 59°10·7′N, 1°20·6′W of Oslo.	565		
Biotite from a porphyritic granite, road cut near Skoglyst, Drammen, 59°44·08′N, 0°33·3′W of Oslo.	259		
Zircon from the Oslo nordmarkite, Trondheimsveien, large new road cut near Oslo city limit, 59°58·65′N, 0°12·47′E of Oslo.		259	(216)

Both the Drammen granite and the Oslo nordmarkite are definitely Permian or younger (HOLTEDAHL, 1953). The Drammen granite is usually considered to be younger than the Oslo nordmarkite, but both rocks intrude basalts and rhomb-porphyry lavas which are interbedded with fossiliferous lake deposits of Lower Permian age, correlative with the German *Rotliegendes*. The nordmarkite also intrudes non-fossiliferous sandstones and conglomerates correlated with the lake sediments. We have studied these intrusive rocks because of their importance in the geologic time scale.

Our age results are shown in Table 1 and the analytical data follow in Table 2. Judging by the excellent quality and high potassium content of the Søve biotite, we believe that our measurement of 565 million years is close to the true age of the Fen intrusion. Our number might be lower than the true age, but not higher. The mica separated from the Drammen granite was partly chloritized. Methods for purifying chloritized mica are available (FAUL and DAVIS, in press), but the amount of rock at our disposal was too small to permit a really clean concentrate. For that reason we prefer to view the 259 million year figure as a minimum age of the Drammen granite. Agreement with the zircon age of the nordmarkite is good but may be accidental, for the zircon age is in itself a minimum figure. MAYNE *et al.* (1959) give 308 million years as the age the "Oslo alkali suite", measured by the K/Ar method on biotite.

Table 2. Analytical data
(Brackets indicate replicate analyses; all errors shown are estimated standard deviations.)

	K (%)*	Radiogenic Ar^{40} (p.p.m.)†	Radiogenic Ar^{40} / Total Ar^{40}
Fen biotite	8·28 ± 0·06	0·389 ± 0·004 0·389 ± 0·004	0·87 0·92
Drammen biotite	4·03 ± 0·04	0·080 ± 0·001	0·77
Oslo zircon†:	U: 363 ± 4, 368 ± 4 p.p.m, Th: 388 ± 4, 396 ± 4 p.p.m, Pb: 21·9 ± 0·5, 20·9 ± 0·5 p.p.m.		
	204/206: 0·0040, 207/206: 0·113, 208/206: 0·428		

* Flame-photometer analyses by P. L. D. ELMORE.
† Isotope-dilution analyses by H. FAUL.

We report only the U/Pb and the Th/Pb ages for the Oslo zircon, and we believe that the the U/Pb age (259 million years) is closer to the truth. The lead content is low (21 p.p.m.) and about 10 per cent of the lead found was non-radiogenic. How much of this non-radiogenic lead represents original lead in the zircon and how much is due to laboratory contamination we do not know. Calculation of a Pb/Pb age would be of little use here. The value depends greatly on the choice of a ratio for the common-lead correction. With one ratio ("Patterson lab. lead", 1 : 18·5 : 15·6 : 38·4) the Pb/Pb "age" would be 400 million years, but the estimated standard deviation is +100–180 million years. The Th/Pb "age" is characteristically low (Tilton *et al.*, 1957; Faul, 1957).

Bowen (1924) suggested that the carbonate of the Fen area differentially replaced earlier existing minerals of the igneous rocks around it. Hence, it could be argued that the biotite we have analysed might be older than the carbonatite intrusion. Bowen's thin sections do not show mica, although biotite is common in the damtjernite within the Fen area. The damtjernite, however, is considered to be the youngest rock in the area. The euhedral shape, large size and unaltered condition of our biotite from the carbonatite strongly suggest that the carbonatite and the biotite crystallized roughly at the same time.

The research reported here is a reconnaissance. Many more samples must be collected and additional analyses made, particularly by the Rb/Sr method. It would be some time before we could undertake a more thorough study. Therefore, we report the data in their present rough form, with the thought that they might be of value in further geological and geochemical studies of this important area.

Acknowledgements—We are greatly indebted to Dr. H. Bjørlykke, Dr. T. Gjelsvik, and T. Siggerud of the Norwegian Geological Survey, and to S. Svinndal of the A/S Norsk Bergwerk for their guidance in the field and many helpful discussions. Professor M. Rutten and R. O. van Everdingen of the University of Utrecht (Holland) kindly collected the biotite-bearing rock from Drammen. The senior writer is grateful to the Geophysical Laboratory an the Department of Terrestrial Magnetism of the Carnegie Institution of Washington for much assistance and the use of facilities for U, Th and Pb analysis. The United States Educational Foundation in Norway (Fulbright Program) supported the senior writer's field work in Norway in 1955.

U.S. Geological Survey
Washington 25, *D.C.*

H. Faul
P. L. D. Elmore
W. W. Brannock

References

Aldrich L. T., Wetherill G. W., Davis G. L. and Tilton G. R. (1958) Radioactive ages of micas from granitic rocks by Rb-Sr and K-A methods. *Trans. Amer. Geophys. Un.* **39,** No. 6, 1125.

Bjørlykke H. (1955) The niobium deposits at Søve, Southern Norway. *Mining J.* (*London*) **224,** No. 6243, 412–413.

Bowen N. L. (1924) The Fen Area in Telemark, Norway. *Amer. J. Sci.* **8,** Ser. 5, 1–11.

Brøgger W. C. (1921) Die Eruptivgesteine des Kristianiagebietes—IV. Das Fengebiet in Telemark Norwegen (Eruptive rocks of the Oslo region—IV. The Fen Area in Telemark, Norway). *Vidensk. Skr., Mat.-Naturv. Kl.* No. 9, 1920, 408.

Faul H. (1957) Study of a point in the fossil time scale. *Carnegie Inst. Washington. Year Book* 56 pp. 168–170.

Faul H. and Davis G. L. (1959) Mineral separation with asymmetric vibrators. *Amer. Min.* In press.

Holtedahl O. (1953) Norg. geologi. *Norg. Geol. Unders.* **164,** 1118.

Mayne K. I., Lambert R. St. J. and York D. (1959) The geological time scale. *Nature, Lond.* **183,** 212–214.

Pecora W. T. (1956) Carbonatites: A review. *Bull. Geol. Soc. Amer.* **67,** 1537–1556.

Sæther E. (1948) Foreløpig meddelelse om resultat av undersøkelser i Fensfeltet (Preliminary report of surveys in the Fen Area). *Norsk Geol. Tidsskr.* **27,** 66–73.

Sæther E. (1950) On the genesis of peralkaline rock provinces. *Int. Geol. Congr. (Lond.) Rep.* Pt. II, 123–130.

Sæther E. (1957) The alkaline rock province of the Fen Area in Southern Norway. *K. Norsk Vidensk. Selsk. Skr.* **1,** 150.

Tilton G. R., Davis G. L., Wetherill G. W. and Aldrich L. T. (1957) Isotopic ages of zircon from granites and pegmatites. *Trans. Amer. Geophys. Un.* **38,** 360–371.

Tomkeieff S. I. (1958) The petrochemistry of the Oslo-Fen petrographical province. *Geochim. et Cosmochim. Acta* **14,** 165. (Abstract).

Note added in proof—A small piece of *EX* diamond drill core from the Cappelen deposit, Søve mine (hole C43, 94·5 m down) was given to the writer by Mr. Svinndal. The carbonatite core contained a streak of large (2 mm) euhedral zircon crystals. A lead–alpha (Larsen) age determination on the zircon gives a value of 530 $\pm$ 50 million years. The alpha activity was determined by the thick-source technique as 277·5 α/mg-h by T. W. Stern. The lead was measured by a newly-developed spectrographic method, using synthetic zircon containing lead as a standard, by H. J. Rose, Jr. The new method is carefully monitored by isotope dilution analyses and gives a lead value of 62 p.p.m.

Geochimica et Cosmochimica Acta, 1959, Vol. 17, pp. 157. Pergamon Press Ltd.—Printed in Northern Ireland

NEWS AND NOTES

Eighth National Clay Conference

On October 12, 13, and 14, 1959, the Eighth National Clay Conference will be held on the University of Oklahoma campus at Norman, Oklahoma under the auspices of the Clay Minerals Committee of the National Academy of Sciences—National Research Council.

A field trip will be arranged for either Sunday, October 11 or Thursday, October 15, probably to the Wichita Mountains in southwest Oklahoma to visit clay occurrences of geological interest.

Two symposia of invited papers will be held on the subjects of "Clay-Water Systems" and "Clay Mineral-Geochemical Prospecting Methods." In addition to these special symposia there will be general sessions of contributed papers. All those having contributions should contact Professor C. G. Dodd, Chairman, Eight National Clay Conference, University of Oklahoma, Norman, Oklahoma. The title and a letter of intent should be sent in by June 15, and a 250 word abstract by July 1.

Further information and a preliminary announcement of the Conference may be obtained by writing Professor Dodd.

Organic Geochemistry Section of the Geochemical Society

A group of organic and petroleum geochemists plan to organize an Organic Geochemistry Section within The Geochemical Society. The purpose of this section is to offer a common forum for research workers who are active in the various fields of organic and petroleum geochemistry. Recent advances in these fields indicate the desirability of the exchange of ideas and of their coordination with modern concepts of inorganic geochemistry and geology. The interest shown by earth scientists in The General Petroleum Geochemistry Symposium, which was held recently at Fordham University, supports this view.

Plans are being made to organize the Organic Geochemistry Section at the 1959 annual meetings of the Geological Society of America and The Geochemical Society in Pittsburgh, Pennsylvania, November 2–4. Information regarding this section may be obtained from the members of the Interim Executive Committee, who are listed below. The members of this committee invite suggestions and comments regarding this matter. It would be helpful if interested individuals could, in advance of the annual meeting, signify their intention to affiliate with the Section whether or not they plan to attend the meeting.

The only requirements for affiliation with the Section are membership in the Geochemical Society and an interest in organic geochemistry. Membership in the society is open to individuals who have a bachelor's degree or its equivalent in a natural science and an interest in applying that science to geologic problems. Dues are $2.00 per year. Application blanks can be obtained from the Secretary, Professor Konrad B. Krauskopf, Department of Geology, Stanford University, California.

Edward G. Baker
Esso Research and Engineering Co.
P.O. Box 51
Linden, New Jersey

Earl Ingerson
Department of Geology
The University of Texas
Austin 12, Texas

Bartholomew Nagy, Chairman
Department of Chemistry
Fordham University
New York 58, New York

Paul A. Witherspoon
Department of Petroleum Engineering
University of California
Berkeley 4, California

Geochimica et Cosmochimica Acta, 1959, Vol. 17, p. 158. Pergamon Press Ltd. Printed in Northern Ireland

ERRATUM

H. H. Le Riche: The distribution of certain trace elements in the Lower Lias of Southern England

Geochim. et Cosmochim. Acta **16,** 101–122.

The following correction should be made:

Trueman, A. E. (1922). The Liassic rocks of Glamorgan. *Proc. Geol. Assoc.* **33,** 245.

Geochimica et Cosmochimica Acta, 1959, Vol. 17, pp. 159 to 160. Pergamon Press Ltd. Printed in Northern Ireland

PAPERS TO BE PUBLISHED IN FUTURE ISSUES

F. A. PANETH *et al.*; Der Meteorit von Breitscheid, I–IV

N. YAMAGATA, Y. MURAKAMI and T. TORII: Biogeochemical investigation in a serpentine–chromite ore district

K. S. HEIER and S. R. TAYLOR: Distribution of Ca, Sr and Ba in Southern Norwegian pre-Cambrian alkali feldspars

J. D. GRACE and T. F. BATES: Determination of uranium equilibrium in rocks using alpha and fission fragment radiography

J. M. WHITFIELD, J. J. W. ROGERS and J. A. S. ADAMS: The relationship between the petrology and the thorium and uranium contents of some granitic rocks

U. SCHINDEWOLF and M. WAHLGREN: The rhodium, silver and indium content of some chondritic meteorites

J. M. WHITFIELD, J. J. W. ROGERS and M. C. MCEWEN: Relationships among textural properties and modal compositions of some granite rocks

F. E. SENFTLE and A. THORPE: Magnetic susceptibility of tektites and some other glasses

C. E. ADAMS, N. H. FARLOW and W. R. SCHELL: The compositions, structures and origins of radioactive fallout particles

E-an ZEN: Carbonate equilibria in the open ocean and their bearing on the interpretation of ancient carbonate rocks

H. FECHTIG, W. GENTNER und G. KISTNER: Räumliche Verteilung der Edelgasisotope im Eisenmeteoriten Treysa

A. P. TUDGE: A method of analysis of oxygen isotopes in orthophosphate—its use in the measurement of paleo temperatures

R. E. MARINGER and G. K. MANNING: Aerodynamic heating of the Grant meteorite

M. S. CROWLEY and R. ROY: The effect of formation pressures on sheet structures, a possible case of Al–Si ordering

G. L. BATE, H. A. POTRATZ and J. R. HUIZENGA: Scandium, chromium and europium in stone meteorites by simultaneous neutron activation analysis

J. R. MERRILL, E. F. X. LYDEN, M. HONDA and J. R. ARNOLD: The sedimentary geochemistry of the beryllium isotopes

H. G. F. WINKLER und H. VON PLATEN: Experimentelle Gesteinsmetamorphose—III. Ultrametamorphase kalkhaltiger Tone

E. A. VINCENT and J. H. CROCKET: Studies in geochemistry of gold—I. The distribution of gold in rocks and minerals of the Skaergaard intrusion

E. A. VINCENT and J. H. CROCKET: Studies in the geochemistry of gold—II. The gold content of some basic and ultrabasic rocks and stony meteorites

F. A. PANETH: The discovery and the earliest reproductions of the Widmanstätten figures

E. J. CATANZARO and P. W. GAST: Isotopic composition of lead in pegmatitic feldspars

E. L. FIREMAN and J. DEFELICE: Argon-39 and tritium in meteorites

P. E. Brown and B. J. Rushton: Some chemical data on the Mourne mountain granite G2

K. H. Wedepohl: Spurenanalytische Untersuchungen an Tiefseetonen aus dem Atlantik

H. Hamagushi, R. Kuroda and H. Ishikawa: The distribution of minor elements in the rocks of Sakura-jima volcano

P. M. Hurley, H. W. Fairburn, W. H. Pinson and G. Faure: K–A and Rb–Sr minimum ages for the Pennsylvanian section in the Narragansett basin

K. Krejci-Graf und F. E. Wickman: Ein geochemisches Profil durch den Lias alpha

A. T. Wilson and G. J. Fergusson: Origin of terrestrial tritium

W. G. Ernst: The stability relations of magnesioriebeckite

R. E. Maringer: Ablation deposits on iron meteorites

P. W. Gast: Alkali metals in stone meteorites

INFORMATION FOR CONTRIBUTORS

I. GENERAL

1. Papers on geochemistry should be submitted to the appropriate Executive Editor (*Papers on cosmochemistry should be sent to Prof. W. A. Wahl*). Papers submitted for publication will naturally be judged from the standpoint of scientific originality and novelty. Technical details of apparatus used in scientific investigation can, however, be presented in brief notes. Critical comments or preliminary results requiring early publication should be submitted as letters to the editors. Where possible, letters should be confined to 500 words. The preparation of progress reports and review articles will be invited by the editors from time to time. The journal appears as independent and complete numbers, which are combined into volumes of about 300 pages.

2. Only papers which have not been previously published can be accepted. Authors must agree not to publish elsewhere a paper submitted to and accepted by *Geochimica et Cosmochimica Acta*.

3. Fifty reprints of each paper are provided free. Additional copies can be purchased if ordered at the time the first proofs are returned. A reprint order form will accompany first proofs.

II. SCRIPT REQUIREMENTS

1. Scripts must be written in one of the three official languages—English, French or German.

2. The script should be typed (not a carbon copy). The text must be ready for printing and should be carefully checked for errors. Authors will receive proofs for correction.

3. Illustrations should accompany the script, mounted on separate sheets. Line diagrams that require to be redrawn should include all relevant details. Half-tone illustrations should be restricted to the minimum necessary. Photographs should be enlarged sufficiently to permit their clear reproduction, and if words or numbers appear on them, two copies should be sent, one clearly printed and the other without inscription. All illustrations should be provided with descriptive legends, which should be given on a separate sheet. Any lettering on diagrams—other than Greek letters, symbols, etc.—should be stencilled and should be sufficiently large and bold to permit reproduction when the diagram has been reduced to a size suitable for inclusion in the journal.

4. References in the text should be given by quoting the author's name and year of publication, i.e. AHRENS (1952). **Full references should be listed at the end of each paper, in alphabetical order, in the following manner:**

AHRENS, L. H. (1952) The use of ionization potentials—I. Ionic radii of the elements. *Geochim. et Cosmochim. Acta* **2**, 155–169.

and should include the full title of the article, standard abbreviated title of the journal, year, volume, number and inclusive page numbers.

5. The text of articles submitted should be concise and in a readily understandable style. The technical description of the methods used should only be given in detail when such methods are new. The essential contents of each paper should be briefly recapitulated in an abstract in English. Such an abstract, may, however, be submitted by the author in the language of the original typescript for translation into English by the editorial staff.

6. To conserve space, authors are requested to mark less important portions of the paper (such as description of methods, record of experimental results, etc.) for printing in smaller type.

7. Indices of refraction should be denoted by the symbols α, β, γ, ω, ε, n, and vibration directions by X, Y, Z, O and E.

Pergamon Press are also publishers of the following Journals:

JOURNAL OF NUCLEAR ENERGY (*including* THE SOVIET JOURNAL OF ATOMIC ENERGY*). PART A: REACTOR SCIENCE; PART B: REACTOR TECHNOLOGY
HEALTH PHYSICS (*The Official Journal of the Health Physics Society*)
JOURNAL OF INORGANIC AND NUCLEAR CHEMISTRY
TETRAHEDRON (*The International Journal of Organic Chemistry*)
TALANTA (*An International Journal of Analytical Chemistry*)
INTERNATIONAL JOURNAL OF APPLIED RADIATION AND ISOTOPES
BIOCHEMICAL PHARMACOLOGY
ARCHIVES OF ORAL BIOLOGY
* BIOPHYSICS
* JOURNAL OF MICROBIOLOGY, EPIDEMOLOGY AND IMMUNOBIOLOGY
* PROBLEMS OF HEMATOLOGY AND BLOOD TRANSFUSION
* PROBLEMS OF VIROLOGY
* PROBLEMS OF ONCOLOGY
* SECHENOV PHYSIOLOGICAL JOURNAL OF THE U.S.S.R.
* PAVLOV JOURNAL OF HIGHER NERVOUS ACTIVITY
* ELECTRIC TECHNOLOGY, U.S.S.R.
* RADIO ENGINEERING
* RADIO ENGINEERING AND ELECTRONICS
* TELECOMMUNICATIONS
* PHYSICS OF METALS AND METALLOGRAPHY
* THE ABSTRACTS JOURNAL OF METALLURGY
* APPLIED MATHEMATICS AND MECHANICS
CHEMICAL ENGINEERING SCIENCE
JOURNAL OF ATMOSPHERIC AND TERRESTRIAL PHYSICS
PLANETARY AND SPACE SCIENCE
BULLETIN GÉODÉSIQUE
ANNALS OF THE INTERNATIONAL GEOPHYSICAL YEAR
SPECTROCHIMICA ACTA
JOURNAL OF THE MECHANICS AND PHYSICS OF SOLIDS
ACTA METALLURGICA
(*for the Board of Governors of Acta Metallurgica*)
INTERNATIONAL JOURNAL OF THE PHYSICS AND CHEMISTRY OF SOLIDS
DEEP-SEA RESEARCH
JOURNAL OF NEUROCHEMISTRY
JOURNAL OF PSYCHOSOMATIC RESEARCH
JOURNAL OF INSECT PHYSIOLOGY
INTERNATIONAL JOURNAL OF AIR POLLUTION
INTERNATIONAL ABSTRACTS OF BIOLOGICAL SCIENCES (*for Biological and Medical Abstracts Ltd.*)
RHEOLOGY ABSTRACTS
VACUUM
OPERATIONAL RESEARCH QUARTERLY
ANNALS OF OCCUPATIONAL HYGIENE
ELECTROCHIMICA ACTA

* *Translations of Russian journals published on behalf of the Pergamon Institute, a non-profit-making foundation*

Leaflets giving further details and subscription rates of each of these journals are available on request

16Nov1959R

26Apr'65F

THE GEOCHEMICAL SOCIETY

OFFICERS

J. Frank Schairer, President
Tom F. W. Barth, Vice-President
Konrad B. Krausfopf, Secretary
George T. Faust, Treasurer

COUNCILLORS

John A. S. Adams, 1957–1959
Alfred O. Nier, 1957–1959
E. F. Osborn, 1958–1960
H. G. Thode, 1958–1960
Albert E. J. Engel, 1959–1961
Friedrich G. Hontermans, 1959–1961

REGIONAL VICE-PRESIDENTS

Louis H. Ahrens
Rui Ribeiro Franco
Ing. Georges Ordoñez
C. W. Correns
William S. Fyfe
Ken Sugawara

COMMITTEES

Auditing Committee:

Joseph J. Tregoning, Chairman
William L. Hill
C. R. Nasser

Constitution and By-Laws Committee:

Michael Fleischer, Chairman
Julian R. Goldsmith
Denis M. Shaw

Education Committee:

H. D. Holland, Chairman
J. A. S. Adams
D. M. Henderson
Kurt E. Lowe
G. D. Nicholls
Hans P. Eugster

Membership Committee:

R. M. Garrels, Chairman
Harvey C. Diebl
Chester B. Slawson
James E. Slosson
Irving Breger

Nominating Committee:

Wm. T. Pecora, Chairman
T. G. Sahama
C. E. Tilley
G. Tunell

Programme Committee:

H. T. Evans, Chairman
Gordon J. F. MacDonald
H. E. Lowenstam

Publications Committee:

E. W. Heinrich, Chairman
Julian R. Goldsmith
John C. Maxwell
N. W. Rakestraw
S. C. Robinson
L. R. Wager
Earl Ingerson

Research Committee:

C. G. Dodd, Chairman
W. F. Bradley
R. A. Rowland
T. G. Thompson

Russian Translations Committee:

Earl Ingerson

Standards Committee:

Alvin Van Valkenberg, Chairman
Michael Fleischer
Loren Stieff
George Switzer
George Tilton

Tellers Committee:

Charles Meyer, Chairman
Henry R. Cornwall
Colin O. Hutton